GENE EXPRESSION PROFILE OF CELLS IN SUCCESSIVE STAGES OF THE CORNEAL STEM CELL LINEAGE.

by

ANDREAS BALLIS
PH.D

University of Cardiff, UK. 2006

ProQuest LLC
789 East Eisenhower Parkway
P.O. Box 1346
Ann Arbor, MI 48106-1346

Declaration

This work has not previously been accepted in substance for any degree and is not being concurrently submitted in candidature for any degree

Signed..... **(candidate)**
Date.....13/07/2006.....

Statement 1

This thesis is the result of my own investigations, except where otherwise stated. Other sources are acknowledged by footnotes giving explicit references. A bibliography is appended.

Signed..... **(candidate)**
Date.....13/07/2006.....

Statement 2

I hereby give consent for my thesis, if accepted, to be available for photocopying and for inter-library loan, and for the title and summary to be made available to outside organisations

Signed..... **(candidate)**
Date.....13/07/2006.....

Dedicated to my Family

"In the world of knowledge the idea of the good appears last of all, and is seen only with effort"

Socrates. 470BC- 399BC *Athens*

Acknowledgements.

First and foremost I would like to thank my parents, Charalambos and Eleni and my sister Natasa for their continuous support throughout my life and especially during these last few years, at every level, often with the heartbreaking sacrifice of their own well being.

I would also like to thank my supervisors Prof. Mike Boulton and Dr. Julie Albon for having carefully and patiently guided me in my first steps of my life as a scientist, with their never ending support and belief in me and this study.

A special thank goes to Dr. James Sidaway and the people in the molecular toxicogenomics department in Astra-Zeneca for being supportive, providing their facilities and help and participating in the costs of these studies.

I am also thankful to Prof. Alan Clarke and Doctors Owen Sansom and James Matthews for freely allowing me to use their Laser facilities and opening their lab doors for me, even in the weekends.

My deepest appreciation is given to Sir Martin Evans for his will to consider my approaches and offer his valuable comments.

Last but not least I thank all my Friends for being there when it was important.

Abstract

In this study the complete transcriptome of groups of cells at specific successive stages of the complete corneal stem cell hierarchy was revealed.

The cornea presents a linear differential distribution of each type of cell of this hierarchy, with stem cells, transient amplifying cells and mature cells residing predominantly in the basal limbal, peripheral and central corneal epithelium respectively.

In order to realise the complete set of genes that are up or down regulated at each stage of the corneal stem cell lineage, a Laser Micro-dissection and pressure Catapulting method was optimised, that allows for isolation of the desired type of cell from the specific areas they predominate, in a manner that would not challenge the integrity of their mRNA, as determined by 3'-5' relative ratios, estimated by semi-quantitative RT-PCR.

To analyse the relative abundance of every gene in each of the cell types that were isolated, a linear amplification of mRNA method had to be optimised, as determined by comparing the relative abundances of specific endogenous and exogenous gene transcripts before and after the amplification reaction, using high density oligonucleotide arrays.

In order to amplify the mRNA in such a manner and to such a degree that it could be analysed by high density oligonucleotide arrays an *in-vitro transcription* based amplification method was employed and optimised. The method entailed the generation of double stranded cDNA reverse transcripts carrying the T7 RNA polymerase promoter and subsequent in-vitro transcription that yielded large amounts of linearly amplified mRNA (aRNA)

.

The midfield of data that was produced was analysed by appropriate mathematical methods such as Robust Multiarray Analysis and in order to obtain a set of genes that are up or down regulated specifically in each cell type.

Principal Component analysis confirmed the validity of the hypothesis that the variance in gene expression arose from the fact that different types of cells were analysed

The results were validated by semi-quantitative RT-PCR analysis, which confirmed the sensitivity of the arrays.

Additionally several protein targets that were indicated by the array analysis were studied by immunohistochemical methods.

The putative differential mechanisms regulating corneal epithelial stem and well as transient amplifying cell fate and corneal homeostasis are discussed.

The results of this study are likely to augment the efforts of understanding corneal epithelial stem cells and possibly other adult stem cells and thereby assist in future research and therapeutic interventions involving stem cells.

Table of contents

List of Figures

List of Tables

Chapter 1

Introduction

This is detailed documentation of some aspects that involve the study of the limbal-corneal epithelial relationship with respect to corneal epithelial stem cells under the scope of paradigms from stem cells of other tissues as well. Initially a detailed description of the ocular anatomical regions of interest is given and then the introduction proceeds to understand the given knowledge about stem cells. Then it describes the technologies that facilitated the transcriptional study of stem cells, transient amplifying cells and differentiated cells of the cornea.

1.1 Ocular Surface Anatomy

The term ocular surface was coined by Thoft and Friend in 1977 and covered all of the components of the lids, conjunctiva and globe as well as their dynamic interaction which contributes to the maintenance of the normal local environment. The notion of this degree of interaction justifies the need to consider the limbus and the conjunctiva, together with the tear film, as essential when setting off to describe the corneal anatomy, structure and function.

1.1.1 The Cornea.

The cornea is a non-vascularised, very specialized tissue that is composed of an anterior stratified squamous non-keratinized epithelium, an inner connective tissue stroma and a posterior low cuboidal endothelium.

It is located on the front portion of the eye that functions to maintain transparency to admit and refract light. Being transparent only I% of incident light is reflected. The refractive index of the cornea is 1.376, although that changes with ageing. In conjunction with the power of the crystalline lens, the cornea actually reconfigures light rays to bring these rays into focus on the retina.

The cornea measures approximately 12 mm in the horizontal plane and 11 mm in the vertical plane. The thickness of the cornea is approximately 520µm at the apex and thickens to around 670µm in the periphery. Peripherally the cornea borders with the sclera at the region called the corneal sulcus. The central 4-5 mm zone of the cornea has more curvature than the peripheral zone which is more flattened. It is the shape of the cornea, convex externally and concave on its internal curve which creates its refractive power. the external curve is a convex (plus) lens with the power of approximately +48.8 dioptres and the internal curve is a negative, concave lens with a power of -5.8 dioptres yielding a net power of 43 dioptres of light bending power.

The cornea is comprised of five discretely differentiated layers:

Epithelium (EP)

Bowman's layer (BL)

Stroma (referred to as subcutanea propria)

Descemet's membrane

Endothelium

Figure 1. 1 A cross-section of human corneal epithelium, depicting the epithelial layer (EP), Bowman's layer (BL), stromal-substantia propria-(SP), Descemet's membrane (DM) and endothelium (En).

A detailed description of each layer is given in the following paragraphs.

1.1.1.1 Epithelium

The epithelium is located in the anterior of the corneal structure and it is the most external structure of it, only followed by the tear film. It consists of 5-6 layers of cells, with three cell types present (Hogan et al. 1971; Kenyon 1979) namely, the squamous cells, the wing cells, the basal cells.

The squamous cells: compose the two superficial layers of flattened polygonal epithelial cells. These are the most differentiated cells of the corneal epithelium. The have relatively low metabolic rate and proliferative activity. These cells have microvilli, tiny projections on their surface that are intruding the mucin glycocalyx of the tear film contributing to the stability of the latter.

The wing cells form two or three layers of compact, interdigitating polygonal cells located posterior to the squamous cell layers. They are less flattened than the squamous epithelial cells, a characteristic that is being lost in cells as we proceed towards the basal lamina. The nuclei of these cells, as well as those of the squamous epithelial cells, are oval instead of spherical shaped, which is a characteristic of the nuclei found in the underlying basal cells. In general as we proceed above the basal cell layer a greater degree of squamous, epithelial, differentiation is phenotypically observed.

The basal cells form a single layer in between the basement membrane (basal lamina) and the wing cell layers. They are cuboidal or cylindrical in form with varying heights, around 15μm, and rounded heads facing the wing cells, of 10μm diameter (Saude, T., 1993, *Ocular anatomy and physiology*, Blackwell

Publishing, Oxford). Basal cells have a higher metabolic, synthetic and proliferative activity. They adhere to the underlying basal membrane.

Basal cell and the Basal Membrane (adhesion of the epithelium to the stroma).

The adhesion of the epithelial cells on their basement membrane (BM) is not only interesting structurally. There is a function-based relationship of the basement cells and their membrane to a higher level than simple anchorage. BM composition influences cell behaviour and one of the components of the induced behaviour is, in turn, the development of a secretory pattern aimed at preserving the composition of the inducing BM (Wolosin et al.,2000). This implies that the BM could act as an active differentiation reference to the cells that travel on it, created by the cells that exist there already.

Basal cells attach themselves on the basement membrane and the stroma by employing the adhesion complex. Hemidesmosomes (HD) occupy 28% of the basement membrane in the central cornea (Gipson 1989). The hemidesmosome acts as a cell to substrate adhesion junction. On the outside of the cell membrane, opposite the electron dense cytoplasmic plaque of a hemidesmosome runs another thin electron dense line parallel to the cell membrane. From it fine anchoring filaments intrude the lamina lucida and insert in the electron dense zone of the BM and surpass the BM (Gipson, Spurr-Michaud & Tisdale 1987). These anchoring fibrils are cross banded and have type VII collagen as a component (Sakai et al. 1986). The helical domains of type VII collagen molecules associate to form the cross-banded

"arm" of the fibril where the globular domain of these molecules associate in the BM at the hemidesmosome and also some of them at areas in the anterior 1-2μm of Bowman's layer, termed anchoring plaques. So collagen type VII helical domains build a network that surrounds collagen type I fibres, holding the epithelium and the basement membrane bound to the stroma (Smolin & Thoft 1987).

Desmosomes, Gap junctions, and tight junctions in the corneal epithelium.

Desmosomes are present in the squamous epithelial layers as well as throughout all the epithelial layers of the cornea, especially in the interdigitating cell borders of the wing cells (Gipson & Sugrue1994). Gap junctions are also present all over the corneal epithelium. However different connexins are present in different layers. More specifically Cx43 (connexin of 43kD) is only found in basal cells where Cx50 is present in all cell types (Dong et al. 1994). Tight junctions are also present in the lateral membranes of the apical cells (i.e. mainly squamous, and some wing cells, Gipson and Sugrue1994).

1.1.1.2. Bowman's layer.

It is a modified region of the anterior stroma also called anterior limiting lamina. It is an acellular zone that is composed of randomly interplexed collagen fibrils and proteoglycans. The layer is 12μm thick and it is associated

with the basal membrane in the fashion described above. Collagen type VII fibrils which extend from the anchoring filaments of the hemidesmosome are interwoven with the type I collagen fibres.

1.1.1.3. Substantia propria or corneal stroma.

The corneal stroma is a dense connective tissue of remarkable regularity. It makes up the vast majority of the cornea and consists predominantly of: 2μm thick flattened collagenous lamellae (200-250 layers) orientated parallel to the corneal surface and continuous with the sclera at the limbus. Between the lamellae lie extremely flattened, modified fibroblasts known as keratocytes. These cells are stellate in shape with thin cytoplasmic extensions containing few distinctive organelles. The collagenous lamellae form a highly organised orthogonal ply, adjacent lamellae being orientated at right angles, with the exception of the anterior third in which the lamellae display a more oblique orientation.

The collagen fibrils are predominantly of Type I (30nm diameter, 64-70nm banding) with some type III, V and VI. The transparency of the cornea is highly dependent upon the regular spacing of the collagen fibres (interfibrillary distance) which in turn is regulated by glucosaminoglycans (GAG) and proteoglycans forming bridges between the collagen fibrils. The GAGs in the human cornea are predominantly keratan sulphate and chondroitin (dermatan) sulphates. The corneal stroma normally contains no blood or lymphatic

vessels but sensory nerve fibres are present in the anterior layers 'en route' to the epithelium.

1.1.1.4. Descemet's Membrane.

This is a thin, homogenous, discrete, PAS-positive layer between the posterior stroma and the endothelium, from which it can become detached. It is 8-12μm in thickness and represents the modified basement membrane of the corneal endothelium. It consists of two parts, an anterior third which is banded and a homogenous or non-banded posterior two-thirds.

It is rich in basement membrane glycoproteins, laminin and type IV collagen. The anterior banded region is reported to contain type VIII collagen. Types V and VI collagen may be involved in maintaining adherence at the interface of Descemet's membrane with the most posterior lamellae of the stroma. Descemet's membrane is continuous peripherally with the cortical zone of the trabeculae in the trabecular meshwork.

Microscopic wart-like protuberances (Hassal-Henle bodies or peripheral guttatae) containing 'long banded (100nm)' deposits of unknown nature appear in the periphery of Descemet's membrane with age. It is frequently thickened at its peripheral termination (Schwalbe's line at the anterior limit of the trabecular meshwork). If disrupted Descemet's membrane tends to curl inwards towards the anterior chamber.

1.1.1.5 Corneal Endothelium.

Fluid is constantly being lost via evaporation at the ocular surface, a fact illustrated by increased corneal thickness after a night of lid closure and if an impermeable lens is placed over the epithelium.

The corneal endothelium, a simple squamous epithelium on the posterior surface of the cornea, has a critical role in maintaining corneal hydration and thus transparency. The endothelial cells rest upon Descemet's membrane and form regular an uninterrupted polygonal or hexagonal array or mosaic which can be clearly seen in vivo with the aid of specular microscopy, which is also used to assess cell density (see below). The cells are 5-6μm in height and 18-20μm in diameter (250μm surface area). Their lateral surfaces are highly interdigitated and possess apical junctional complexes which together with the cytoplasmic organelles, such as very large numbers of mitochondria, are indicative of their crucial role in active fluid transport.

The endothelium in the normal human cornea has low regenerative capacity and lost cells are quickly replaced by spreading of adjacent cells. There are approximately 350,000 cells per cornea (approximately 3-4000 cells/mm2 at birth, falling to 2,500/mm2 in mid-age and 2000/mm2 in old age. Consequently, with age the dense regular hexagonal arrangement typical of young corneas is replaced by fewer cells of more heterogeneous sizes and shapes. An endothelial cell density of below 800/mm2 induces oedema (swelling) of the stroma, with resultant loss of transparency and general

corneal damage. A density of below 1500/mm2 is considered too low for consideration for corneal transplantation.

1.1.1.6. The nerve supply of the cornea.

The cornea is richly supplied by sensory fibres derived from the ophthalmic division of the trigeminal nerve, mainly via the long ciliary nerves. Branches radiate into the anterior corneal stroma from an annular plexus near the limbus, whereupon they lose their myelin sheaths and form a sub epithelial plexus from which fine axons, devoid of Schwann cells, pierce Bowman's layer to form a terminal intraepithelial plexus. (Muller, 96-97) There are apparently no specialised end-organs associated with these terminal axons which are sensitive to pain and temperature.

1.2 Stem Cells

Firstly it has to be clarified that the theory of stem cells is under development. Several definitions of stem cells exist. Pinpointing though to a single property that is the minimum essential to characterise a cell as a stem cell opinions deviate from each other.

It is therefore very important to carefully consider stem cell characteristics under the notion that a complete stem cell law has not been understood yet. There are fundamental questions that remain to be answered as it will be discussed in this section. As a result stem cells are defined by their abilities functional characteristics. This by itself is posing as a difficulty because some of those functional attributes cannot be clearly assigned unless the cell gets experimentally manipulated, something that potentially changes the very same characteristics and/or b) the fact that it is not clear for many tissues if there is a single or multiple sources of stem cells.

As it arises by the body of research on this field, stem cells were defined, by Potten and Loeffler in 1990, as undifferentiated cells capable of,

(a) proliferation,

(b) self-maintenance,

(c) the production of a large number of differentiated, functional progeny,

(d) regenerating the tissue after injury, and

(e) a flexibility in the use of these options (see, Lajtha, 1967, *1979a, b, c*; Steel, 1977; Potten and Lajtha, 1982; Potten 1983a, Wright and Alison, 1984; Potten and Morris, 1988; Hall and Watt, 1989; Potten and Loeffler, 1990).

Generally stem cell theory was generated by the need to explain in which way a single cell manages to produce a complete multicellular mechanism that organises in a complex set of tissues and organs that in addition would need to be self-renewing. It was later understood that in renewing tissues there are very few cells that posses the ability to produce large amounts of cells which then in turn would differentiate to the desired cell types required to maintain tissue homeostasis upon a physiological state and in wound healing.

Early studies in the 50s by histologists such as Leblond inferred the existence of pluripotent progenitor cells, or stem cells (Leblond et al. 1956). In normal bone marrow transplantation experiments in irradiated mice, it was observed that there were spleen colony forming cell that were derived from bone marrow cells and one cell was creating each colony (Till and McCulloch 1961). Siminovitch, McCulloch and Till (1963) assayed the capacity of individulal spleen colonies to form new colonies and suggested the defining property of stem cells is the capacity to self-renew upon division and produce a stem cell and a cell that would differentiate and enter a series of divisions leading to a terminal one.

In the epithelium, fundamental studies on tissue architecture and mitosis from 1970 by Mackenzie were showing that cell division does not occur randomly in the basal layers of squames but occurs mainly at the base of the junctional region of the overlying squames. This has then opened the question of why such an order was there. The work of Christophers (1970, 1971a, *b, c)* had

shown that the basal cells directly beneath the column produce the superficial cells forming that column.

These findings finally led to the concept of the epidermal proliferation unit (EPU) (Potten, 1974; Allen and Potten, 1974; Mackenzie, 1975) wherein a single stem cell and its progeny amplifying cells and differentiated cells formed a distinct spatial unit in murine epidermis. This concept was fundamental in establishing a system of thought about epithelial stem cell that together with the earlier findings of Till and McCulloch (1963) led to the definition of a stem cell by Lajtha in 1979 (Lajtha 1979) that was revised by Barrandon (2003) as well as Potten's in his revised theory of cellular hierarchies (Potten and Booth 2002).

It is not completely understood today, how an adult organism ends up having such a hierarchy. At present there is intensive research on the way the differentiation options open to cells derived from embryonic stem cells are modulated during development through to the adult (Potten and Booth 2002).

Although stem cells of various tissues must employ different capabilities to maintain a tissue self-maintenance or self-renewal remains the defining propery of a stem cell.

The following section introduces studies on adult or somatic stem cells and the characteristic properties they assume in order to fulfil the task of maintaining a tissue.

1.2.1 Adult stem cell characteristics and implications to the cornea.

1.2.1.1 Very Large division potential.

It remains unclear whether stem cells have a limited or unlimited division potential or whether their numbers and functional competence in replenishing tissues deteriorates (Potten & Booth 2002). One characteristic that is necessary for adult stem cells though would by definition to have the potential to divide at least as many times as needed for replenishing particular tissue for the life span of an animal.

In the lympho-hematopoietic system the number of HSC increases several fold with old age as measured by flow-cytometric phenotype (Morrison et al. 1996; Sudo et al. 2000) as well as cobblestone area forming cell assay (de Haan & Van Zant 1999). However their capacity to home in new bone marrow in transplantation experiments decreases with age (Morrison et al 1996). Additionally prolonged challenging of the hematopoietic system with hydroxyurea shows no decline in HSC regenerative capacity (Ross, Andreson and Micklem 1982). Therefore we can suggest that in the hematopoietic system the capacity of stem cells to self renew is not affected by age but the quality of their progeny is deteriorating.

Stem cells in the epidermal proliferative unit divide about 140 times in the life of a mouse (revised by Potten 2004) whereas those in the gut can divide probably about 1000 times in mice and 5000-6000 times in humans

(Marshman et al 1988). In the cornea it is not yet clear how many times a label retaining cell of the basal limbus divides. Labelling studies were performed on SENCAR mice show a cycling time of label retaining cells is 4-8 weeks (Cotsarelis et al. 1989; Lehrer et al.1998). This would indicate that they would need to divide from around 10-21 times for a SENCAR mouse that lives for 85 weeks. Probably in order to overcome the hurdle that long periods of treatment with radiolabelled (tritiated thymidine) or teratogenic (Brdu) DNA derivatives could potentially kill mice researchers chosen a model that is hyperproliferative in epithelial cells (SENCAR mouse) so that the results could be visualised before mice die. The problem is that SENCAR (sensitive for carcinogenesis) are prone to skin tumours (source National Cancer Institutes at Federic). Retinoic acid has been shown to affect their tumorigenicity in skin epithelium of SENCAR mice from as early as 1989 (De Luca et al 1989). Retinoic acid has been also shown to be one of the potential modulators of proliferative activity and differentiation of corneal epithelial stem cells (Kruse and Tseng 1994). Additionally it has been shown for keratinocyte stem cells (Popova et al. 2004) as well as for hematopoietic (Haan et al. 1997) and liver stem cells (Kolesnichenko and Popova. 1979) that genetically distinct mouse strains have difference in the frequency of clonogenic stem cells and that this is associated with the strain life span. SENCAR mice have lower life span than other strains like C57BL/6 (Storer 1966; Goodrick 1975; Festing & Blackmore 1971) although it has to be considered that those studies are based on clonogenic ability and not label retaining.

Therefore labelling studies on SENCAR mice although might not reflect completely on the reality of cycling times (or strategies) of other mice or extrapolated to humans and other species they provide the fundamental evidence that in the cornea there are ancestral cells that do not divide from 4-8 weeks after birth (Cotsarelis et al. 1989; Lehrer et al. 1998). The studies are discussed in detail bellow.

What is interesting is that if the property of self renewal does not decline with the number of total generations of stem cells, given that corneal epithelial stem cells divide only a few times compared to epithelial stem cells in other locations than they could have less accumulated damage, might be more closely related to their embryonic ancestoral cells, while being able to produce a large number of progeny, making them attractive for clinical use.

1.2.1.2 Label Retaining Studies on stem cells in perspective.

Insights of the location of stem cells in tissues have come from label retaining and cell kinetic studies. Label retaining studies are based upon empirical observation that DNA precursors such as tritiated thymidine (H^3-T) and Bromodeoxyuridine (Brdu) which are incorporated in cells during development persist in DNA of a few adult cells. It was assumed therefore that the label retaining cells because they haven't divided many times they have a closer

relationship with ancestral cells of the developing organism. Studies like these on interfolicullar epidermis stem cells (Bickenbach 1981; Morris et al. 1985; Bickenbach et al. 1986) agreed with cell kinetic studies on the location of stem cells (Potten et al. 1982; Morris et al. 1985; Morris and Potten 1994).

In the cornea there is strong evidence that cells in the basal limbus of 5-6 week old mice can retain label for 4-8 weeks. It has been demonstrated that, in wild-type mice, development of the corneal epithelium, with activation of LSCs and centripetal streaming of their progeny into the cornea, is not completed before the 10th postnatal week in a study using *LacZ*$^{+}$- *LacZ*$^{-}$ mouse chimeras (Collison 2002). Therefore there are indications that, in the cornea, there could be epithelial cells of a developmentally primitive character that home in the basal limbus only and they then divide very infrequently for 9-14 weeks postnatally. Therefore for a minimum of 4 weeks after the complete maturation of developmental events for the corneal epithelium in physiological conditions, there are label retaining cells. Therefore it can be hypothesised with some caution that those cells are indeed label retaining cells that were there before the maturation of developmental events.

It was also observed in those label retaining studies that 50% of those label-retaining stem cells are recruited to proliferate in the case of central corneal wounding (Lehrer et al. 1998)

Since usually the cycle times of stem cells is longer than the cycle time of more mature cells, it is often stated that most of epithelial adult stem cells are

thought to be in a G_o phase (Potten and Booth 2002). On the other hand, when researchers induce wounding conditions in the cornea this cycle time is reduced from 4 weeks or more to 24 hours (Lehrer et al. 1998). Moreover 50% of those slow cycling cells are induced to incorporate the second dye in 24h (Lehrer et al.1998). Starting with a label retaining quantity of 1 in the end of 24h post central wounding this quantity was 1.5. This indicates that only half of the label retaining cells responded to the wound. This might entail that there are two qualitative different states of stem cells in the limbus one being more responsive to immediate crisis than the other. It is not known what the destiny of the double labelled cells was. More specifically, one could ask, do some of them or all of them revert to a slow cycling mode? Perhaps some answer can be deduced if we consider the corneal epithelium as a hierarchical and dynamic system.

There is no experimental evidence in the case of the cornea that it is the LRC only that is kept undifferentiated and has the capacity of very large division potential. The situation is being further perplexed by the lack of a reconstitution assay due to model limitations. If anything research is showing that nearly all the basal layer cells are undifferentiated as defined by differentiation markers (Schermer et al. 1986; Kurpakus et al. 1990; Kiritoshi et al. 1991; Liu et al. 1993; Kurpakus et al. 1994; Matic et al. 1997).

So far it has not been shown that long term reconstitution or clonogenicity is ascribed uniquely to the single cell entity which is slow cycling and label retaining. Studies by Claudinot (2005) show that epithelial stem cells from the

whisker follicle of rats there are many more stem cells than could be anticipated from label-retaining experiments. These stem cells were showing clonogenic ability and could reconstitute the complete follicle after more than 140 doublings in culture. The study calculated that there are more stem cells than previously anticipated by label retaining experiments. In particular that there are enough stem cells in a single rat whisker to maintain the follicle for more than 50 years. Why there are so many stem cells is still a matter of research, but this demonstrates further that there is a bimodal state of stem cells, with a few cells being the label retaining ones.

In the corneal label retaining experiments it was impossible to see if the double labelled and single labelled cells in the limbus have the same clonogenicity or capacity to reconstitute the corneal epithelium, due to the model limitations. It would be however possible to see if the double labelled cells of the limbus revert back to slow cycling and long term reconstitute the lineage leading to tissue formation if some corneas were chased for more weeks.

The last consideration for label retaining studies comes from the Cairns selective DNA strand segregation hypothesis suggested for stem cells (Cairns 1975; Potten et al. 1978). Simply if we take the case of interfolicullar epidermis stem cells which are thought to have an average cycling time of 8 days (Potten and Booth 2002) as an example, then in label retaining studies on 8 week old or 11 week old mice (Potten et al. 1982; Morris et al. 1985; Morris and Potten 1994) the stem cells are expected to have divided at least 8

times. Dilution by division though is normally expected to have the dye diluted to sub-threshold levels after 5 divisions. Then why are there any label retaining cells there? The selective DNA strand hypothesis explains this by stating that slow cycling stem cells keep their original strand of DNA after each replication. So far there it was demonstrated that label retaining cells in the crypt of the small intestine do indeed retain their template DNA (3HTdR) and pass the newly synthesized strands marked with 5-bromo-deoxyuridine (5BrdU) to their progeny (Potten et al. 2002). Additionally a very recent study demonstrated that in the mouse mammary gland, label-retaining epithelial cells divide asymmetrically and retain their template DNA strands (Smith 2005)

1.2.1.3 Non-label-retaining cells could be stem cells.

What is very intriguing is that those label retaining as well as studies on retaining of radiolabelled carcinogens show that slow cycling LRCs retain the carcinogens used as labels. If label LRCs are the sole master copies of a particular tissue, this indicate a very insufficient mechanism to build an organism. How can a Go quiescent cell be correcting itself continuously since we detect carcinogens for months in the slow cycling cells especially if it keeps the original DNA strand? All of these facts pinpoint again to the possibility that loss of stem cell functional capability (or differentiation) does not occur at the level of the division of the slow cycling stem cell, but it could be gradual. If this is true there might be a gradual loss of "stemness" as we go

down the lineage, diluting factors all the time making a cell down the lineage non-clonogenic (i.e. a TA cell)

Studies by Balpain in 2004 have shown that two subpopulations of cells exist within the hair follicle stem cell niche. Despite expressing differentiation markers, clonal populations of suprabasal bulge region cells can regenerate skin and hair follicles as well as a new stem cell niche (Balpain et al. 2004). The findings suggest that early lineage commitments of epithelial cells in the hair follicle may be reversible or that the first generations of cells coming from the ancestral slow-cycling stem cell might not really be TA cells but indeed stem cells as well.

This kind of strategy would fit well in reducing the chances of accumulated damage in the early lineage cells that would reconstitute a self-renewing tissue. This is because if a slow cycling cell out of the stem cell pool is damaged then its progeny will have to compete with not only the first ancestral slow cycling pool stem cells but also with stem cells of their first or second generation.

More evidence of such a strategy comes from closely inspecting the proliferation rates of slow cycling- label retaining ancestral stem cells to those of TA cells. Studying the situation in the limbus the following thought experiment can be devised:

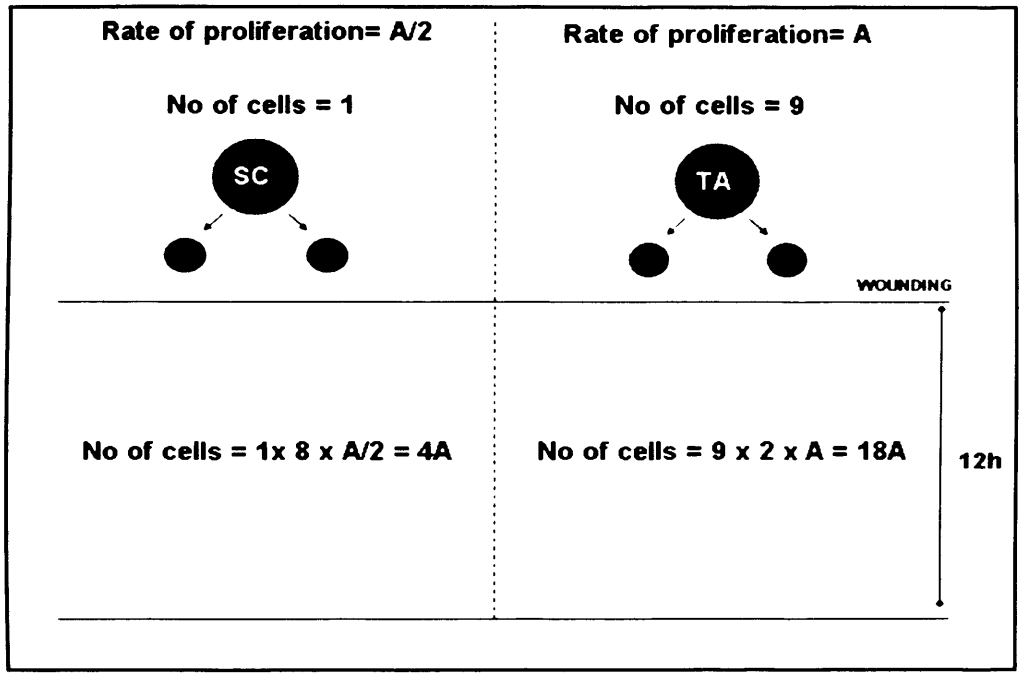

Figure 1. 2 Thought experiment based on today's research on the basal limbus. The ratio of progeny of the ancestral slow cycling stem cell to those of a TA cell in the limbus (1/9) doubles 12 hours post-central cornea wounding).

Considering that:

- label retaining stem cells residing in the limbus increase their rate of proliferation by an eight- to nine fold compared to a twofold increase in TA cells 12h post central epithelial injury(Cotsarelis et al., 1989)
- 50% of those label-retaining stem cells are recruited to proliferate in the case of central corneal wounding (Lehrer et al. 1998)

- stem cells are believed to have half the proliferation rate of TA cells (skin and gut stem cells have half of the proliferation rate of their TA counterparts) (Potten and Booth 2002),

- Slow cycling limbal basal stem cells are about 10% of the total limbal basal cells. (Cotsarelis, 1989; Lavker et al., 1991)

- TA cell of the peripheral cornea increase their number and double the rate of cell divisions.

Then the following conclusions arise:

The ratio of the progeny of limbal stem cells to this of the TA cells doubles after wounding (see figure from 1/9 it goes to 2/9). Indeed in stochastic terms this is only possible if one of the two types of cells does not divide. But the question is if both of these types of cells are stem cells. Perhaps this can be explained by clonal analysis assays.

In proliferative potential clonogenic assays in the limbus (Pellegrini et.al. 1999), where the Barrandon & Green holoclones-meroclone-paraclone assay (1987) was employed to evaluate the stem cell content of the cornea, it was observed that clonogenic cell were only present in the limbus, and that from the 58 limbal clones that were investigated 11 were holoclones 39 Meroclones and 8 paraclones. These findings indicate that the percentage of stem cells

(almost 20%) in the basal limbus is a much higher than it was anticipated by label retaining studies (10%) (Cotsarelis, 1989; Lavker et al. 1991). The ratio of stem cell content evaluated by the two methods is very close to 2. However, it must be stated that clonogenic studies were conducted in humans whereas label retaining in mice. This offers more to the argument that there are two qualitative different sets of stem cells since one has the property to retain label and the other does not.

It remains unclear if these two sets reflect two different states of stem cells and if those states are reversible.This remains a fundamental question in stem cell biology today.

1.2.1.4 Ability to long term reconstitute a tissue.

The ability of stem cells to long term reconstitute a tissue is perhaps their fundamental property since we do not much about stem cell hierarchies or control mechanisms. Hematopoietic stem cell transplantation has been now established as a standard clinical procedure to treat hematological disorders as well as sustain blood cell levels to a point that allows for chemotherapy (reviewed by Weissman 2001). Studies on human keratinocytes that have been genetically altered by adding the b-galactosidase gene reconstituted long term the epidermis of athymic mice (Mackenzie 1997; Kolodka et al. 1998). Newborn mouse keratinocytes can generate epidermis, hair, sebaceous glands if first combined with newborn dermal fibroblasts and then grafted to the back of a nude mouse, lacking hair because of a matrix

transcription factor is knocked out (Nehls et al. 1994; Segre et al. 1995), at a site where the skin has been surgically removed (Lichti et al. 1993; Weinberg et al. 1993). Both stem cell populations distinguished in the hair follicle were able to reconstitute the epidermis, hair, sebaceous glands in such mice (Balpain et al. 2004). However the contribution of these two populations in the maintenance of the epithelial proliferative unit (EPU) is under debate (Gambardella and Barrandon 2003), since gene tagged interfolicullar stem cells have been shown to be able by themselves to maintain the EPU and self-renew for months without any contribution from the follicle.

In the cornea there is also a great amount of evidence that stem cells that reside in the limbus are able to reconstitute the tissue long term. Autologous or homologous transplantation of limbal tissue is required to regenerate a viable cornea and restore visual function (Kenyon and Tseng 1989; Kruse and Reinhard 2001). Additionally ex-vivo expanded stem cells for the purposes of transplantation on amniotic membranes and other substrates have been developed (Lindberg et al. 1993; Pellegrini et al. 1997; Schwab et al. 2000; Koizumi et al, 2001; Tseng et al. 2002) Grueterish et al. 2002). Further evidence that corneal stem cells are responsible for the long term maintenance of a functional cornea comes from cases of limbal stem cell deficiency whether iatrogenic or pathogenic, which are characterised by constitution of the cornea by conjunctival epithelium, chronic inflammation, recurrent erosions and persistent ulcer, destruction of the basement membrane and fibrous tissue ingrowth leading to severe functional impairment (Puangsricharern and Tseng 1995; Holland and Schwartz 1996). Abnormal

corneal epithelial wound healing after removal of the limbal epithelium (Chen and Tseng 1990, 1991; Huang and Tseng 1991) also gives further proof that the corneal epithelium is maintained throughout life from cells of the limbal epithelium.

Caution must be given though to the fact that the cellular hierarchy that stem cells adopt has not been resolved yet for the cornea and there are no markers that would distinguish between cells at different stages of that hierarchy. Thus we cannot claim if the slow cycling cells of the basal limbus are the only cells that are responsible for that maintenance.

1.2.1.5 Poor Differentiation

Stemness does not include further differentiation as a necessary property. The cytoplasm of SC is primitive with few or no differentiation products. Limbal stem cells appear phenotypically more primitive being small and round (Lavker et al. 1991)

In the cornea, cytokeratin 3 (CK3) was observed in all layers of the corneal epithelium, but only the suprabasal layers of the limbus (Schermer et al. 1986). Then further evidence of a population of least differentiated cells in the corneal basal limbus came from the cornea specific cytokeratin 12 which was also shown to be expressed throughout the corneal and limbal epithelium except the basal limbus (Chaloin-Dufau et al. 1990; Kurpakus et al. 1990; Wu et al. 1994).

1.2.1.6 Clonogenicity of corneal epithelial stem cells.

One characteristic that is often attributed to stem cells due to their great division potential is clonogenicity. Limbal basal cells exhibit a higher proliferative potential in culture than central corneal epithelial cells (Friend and Thoft 1987, 1988). Pellegrini isolated limbal basal cells that formed holoclones that could produce more holoclones (Pellegrini et al. 2001), indicative of stem cell self renewal according to Barrandon and Green (1987)..

1.2.2 The differentiation pattern of the cornea and the lack of specific molecular markers for limbal stem cells

1.2.2.1 Cytoskeletal proteins

Cytokeratins or keratins are a group of cytoskeletal proteins that form intermediate filaments in epithelial cells and are expressed in distinct patterns during epithelial development and differentiation (Schlotzer-Schrehardt and Kruse 2005)

The subfamily comprises at least 20 different polypeptides, which are expressed in paired combinations of acidic and basic molecules according to the type of epithelium and its state of differentiation (Sun et al., 1984). Among numerous other keratins which are also present in a variety of other cell types,

keratins (K) 3 and 12 are specifically expressed in corneal epithelial cells and are regarded as markers of corneal epithelial differentiation (Rodrigues et al., 1987; Kasper et al., 1988; Liu et al., 1993).

As briefly discussed earlier, immunohistochemistry studies of the cornea show that epithelial cells in the basal layer of the limbus are devoid of these two corneal specific keratins, emphasising their undifferentiated nature (Schermer et al. 1986; Kurpakus et al. 1990, 1994; Wiley et al. 1991; Wu et al. 1994; Zhao et al. 2002; Chen et al. 2004).

Additionally monoclonal antibody Mab AE1, which recognizes several acidic keratins, was complementary, reacts with the basal limbal layers of the limbus, but not those of peripheral or central epithelium (Wiley et al., 1991). The appearance of the K3/K12 keratin pair during migration from the limbal to the corneal stroma has been interpreted as differentiation of SC into TAC (Grueterich et al., 2003).

Epidermal stem cells express K14 as shown by Bickenbach (in Turksen K, editor. Epidermal cells methods and protocols. Ontario: Humana Press; 2004, p97-102). Most of the undifferentiated cells in stratified epithelia amongst them basal cells of both corneal and limbal epithelia have been shown to express the keratin pair K5/K14 in humans (Kurpakus et al. 1994; Barnard et al. 2001; Hsueh et al. 2004). In rabbits though K14 positive cells exist in the basal and suprabasal layers of the limbal epithelium and not in the peripheral and central corneal epithelium (Wang et al., 2003).

The expression pattern of K14 in the mouse cornea has not been determined yet. What would be expected for K14 is that it would be expressed both by stem cells and TA cells, as understood from all the other studies to now.

Components of intermediate cell filaments like Keratin 19 and vimentin have been localized to the human and murine basal limbal epithelium (Kasper et al., 1988, 1992; Lauweryns et al., 1993b). K 19 is regarded as a marker of proliferating keratinocytes in the skin and has been used to localize epidermal SC in hair follicles (Michel et al., 1996). Cells expressing both of these intermediate cell filament components (K19 and vimentin) have been found to be identical with label-retaining cells (Kasper, 1992).

In humans, immunohistochemistry of corneoscleral rims, shows K14 and K19 to be localized in basal limbal cells and K14 reactivity was stronger than K19 (Barnard et al. 2001) showed strong immunoreactivity for,

In another study however, although K19 was more expressed more in basal limbal epithelial cells than in the suprabasal cells it was also observed to be expressed in most corneal epithelial cells (Chen et al., 2004).

Other keratins that were expressed in the limbal epithelium of guinea pig and mouse eyes include K4 and K13, whereas K17 was not detected (Kasper, 1992).

Further studies from Schlotzer-Schrehardt and. Kruse (2005) confirm that human limbal basal cells express K5/K14, K19, and vimentin and do not express K3/K12. The staining pattern though appeared in clusters of unstained limbal basal cells. K19 and vimentin stained cells co-localised more intensely in basal cells of limbal-peripheral margin. With respect to the K5/K14 pair they also found it expressed in some suprabasal cells of the limbal epithelium, in all basal cells of the conjunctival epithelium and occasionally in individual basal cells of the peripheral cornea.

These findings suggest that in humans the K5/14 pair and K19 are not specific for limbal stem cells, whereas vimentin seemed to localize specifically to TC along the corneal limbal borderline.

1.2.2.2. Cytosolic proteins

Cell-cycle associated proteins, such as cyclins D, E, and A, have been identified as shown to preferentially localized to human basal limbal epithelial cells (Joyce et al., 1996). In the same study, nearly all limbal basal cells showed positive cytoplasmic rather than the nuclear staining characteristic of actively cycling cells whereas Ki67 (a marker for actively cycling cells), was only observed in few basal cells at the limbus. It has to be noted that these findings contradict the notion that a quiescent G_0 population is the true stem cell population only. This notion is further questioned by the findings of

Bickenbach (2004) which shown that while the majority of epithelial SC reside in the G1 phase of the cell cycle, they are not held out of the cell cycle, and that that they express proliferating genes and the mitotic cyclin B1 protein.

Cytosolic proteins that are highly expressed in basal limbal cells include Cytochrome oxidase (Hayashi and Kenyon, 1988), Na/K-ATPase (Lutjen-Drecoll et al. 1982), and carbonic anhydrase (Steuhl & Thiel, 1987), indicating increased metabolic activity. Apparently both aldehyde dehydrogenase (ALDH) and transketolase are expressed in the peripheral and central corneal epithelium but aldehyde dehydrogenase is absent and transketolase is expressed (TKT) in low levels in the murine limbus (Guo et al. 1997; Kays & Piatigorsky 1997).

The glycolytic enzyme a-enolase (Pancholi, 2001) was expressed by both basal and suprabasal epithelial cells at the limbus and occasionally by basal peripheral epithelial cells (Chen et al., 2004), as well as in the conjunctival epithelium. The above study confirmed earlier data that indicated alpha-enolase was expressed preferentially from human, rat and rabbit limbal basal cells as determined by immunohistochemistry and was a suggested marker of limbal SC (Zieske et al. 1992 a, b, Zieske 1994; Zhao et al. 2002). Finally, it seems that the enzyme is over-expressed when cells migrate from limbal basal to peripheral compartment after non-penetrative wounding (Chung et al. 1995).

Therefore evidence remains controversial as to whether a-enolase can be used as a stem cell marker because the expression of the enzyme is very

dynamic rendering difficult the use of it to segregate cells at the early steps of the corneal epithelial lineage.

Protein kinase C (PKC) is a very important family of enzymes in asymmetric cell division because of its role in positioning Numa-Dynactin and LGN-Par3-Inscrutable crescents on the apical side of the membrane of dividing basal epithelial cells and therefore in proliferative to differentiation state transition (Lechler and Fuchs 2005). Members of this family, like PKC-gamma and alpha are expressed in proliferative basal cells of human limbus but not the cornea., (Tseng and Li 1996). Differential expression of the atypical members of the PKC family can offer insight into potentialy different mechanisms of asymmetric cell division of the limbal and peripheral corneal epithelium.

Metallothioneins, which are cysteine-rich metal-binding intracellular proteins, have been linked to cell proliferation and have been shown to be strongly expressed by basal limbal cells of human corneas (Lauweryns et al., 1993b, Schlotzer-Schrehardt and Kruse 2005), but some researchers found it immunolocalising to suprabasal epithelial cells at the limbus in a mosaic-like pattern and to basal cells in the peripheral corneal epithelium and usually superficial cells labeled more strongly (Schlotzer-Schrehardt & Kruse 2005).

This kind of pattern could be indicative of the asymmetric localization of mRNA species during asymmetric cell division, with earlier cells excluding that RNA to later ones. The pattern although interesting because if asymmetric

localization of its mRNA is true it will be a cell fate determinant, it is more likely that it will participate maybe in lineages from TA cell onwards.

Protein S100A12, which is involved in Ca^{+2} dependent signal transduction processes in differentiated cells as well as the calcium-linked protein (CLED), associated with early epithelial differentiation, are both expressed in corneal epithelial basal cells but not in limbal basal cells (Sun et al., 2000; Lavker et al., 2004). This does not in any way mean that Ca^{+2} dependent mechanisms are not there in stem cells since embryonic, neural and hematopoietic stem cells express other S100A proteins (Ivanova et al. 2002; Ramalho-Santos 2002)

1.2.2.3 Nuclear proteins

There is a big controversy surrounding the transcription factor p63. This factor is a p53 homologue and it is known to be involved in tumour suppression and morphogenesis. It is expressed in basal cells of stratified epithelia and it is essential for the epithelial development and differentiation (Yang et al 1998; Yang et al 2000).

Studies in the cornea led to the proposition that p63 is as a nuclear stem cell marker (Pellegrini et al., 2001). In that study P63-positive cells were interspersed with patches of p63-negative cells at the basal limbus. In vitro

experiments in the same study showed elevated expression in holoclones than in paraclones which did not contain detectable p63 as determined by Western Blotting.

In the same study most cells expressing p63 in the limbal basal layer were proliferative as determined by presence of nuclear antigen (PCNA), a specific marker of proliferating cells. Some PCNA expressing cells did not produce p63 and these cells were almost always located next to p63-positive cells.

Another study has shown predominant nuclear immunolocalisation of p63 in the nuclei of the limbal epithelial basal cells interspersed with patches of p63-negative cells (Chen et al. 2004).
The presence of p63 not only in the limbal region but also among most of the basal cells of the peripheral and central corneal epithelium was indicated in human frozen and formalin-fixed specimens (Dua et al. 2003).

In Brd-U pulse labeling studies in murine corneas p63 expression was observed throughout the corneal epithelium with highest levels in near-central proliferative cells (Moore et al. 2002).

Aging animals have higher levels of p63 in the basal epithelial cells in the peripheral cornea than in the limbus (Hsueh et al. 2004).

Before explaining the potential meaning of those findings it has to be noted that most of these studies use the 4A4 clone of monoclonal antibody which

does not discriminate between isoforms. The dependence of p63 staining on the technical procedure has also been suggested by Hsueh et al. (2004) when by using an antigen retrieval method demonstrated an elevated immunoreactivity of p63-positive cells.

Firstly even if p63 was a marker of epithelial stem cells the significance of it in selecting for those cells would be perhaps not very great considering that it is a transcription factor. Any intervention in the tissue could potentially change the levels of that factor. Fluorescent constructs can be a potential solution, but they have to be used in a way that will not affect the behavior of that transcription factor.

However it is more important to look at p63 for what it really is and what it does rather than a marker. P63 selective inducible knockout with the cre-lox system, which circumvents the problem of epithelial defects and lethality in development (Yang et al 1998), fail to divide their epithelial cells asymmetrically (Lechrer & Fuchs 2005). Perhaps this explains the lethality of knockout mice since asymmetric cell division is needed to create cells of different lineages during embryonic development. The role in asymmetric cell division is also supported by studies on holoclones and paraclones (Pellegrini et al. 2001). Of course asymmetric cell division dictates that the cell must be dividing, thus it is not surprising that it is co-expressed with markers of proliferation. Maybe the evidence that p63 has a decisive role in asymmetric cell division is more important than the fact that it is not a marker for stem

cells. Since it is likely to be a key factor in the asymmetric cell division of epithelial cells it would be very interesting to study p63 in that context.

Rambhatla L, Bohn SA and Stadler (2001) recently proposed that a major barrier to the growth of adult stem cells in culture is their intrinsic asymmetric cell kinetics. Given the significance of p53 in the regulation of asymmetric cell kinetics (Sherley et al. 1995 a & b) the significance of p63 as a potential regulator of such kinetics in-vitro overshadows the fact that it is not a stem cell marker because by modulating p63 activity in culture we might be able to expand those cells.

1.2.2.4 Transporters.

Stem cells from bone marrow, skeletal muscle, and other tissues can be isolated based on their ability to exclude the vital dye Hoechst 33342 (bis-benzimide), which defines a 'side-population (SP)' phenotype (Goodell et al. 2004).

This exclusion phenomenon is mediated by several ATP binding cassette (ABC) class of transporters in general like ABCB1, also called MDR1, multidrug resistant 1. ABCB1 has been proposed as a neural stem/progenitor cells marker (Islam et al. 2005). ABCG2, also called breast cancer resistant protein 1 (BCRP1) is also a member of the ATP binding cassette (ABC) transporters. Both of these transporters are members of the MDR/TAP subfamily (as stated in Entrez gene database) whose members share a lot of

homology and are involved in resistance to certain toxic drugs, hence their name "multidrug resistant" like verapamil.

Identifying the SP phenotype depends on the use of the negative control (usually verapamil or a monoclonal antibody) in the fluorescence-activated cell sorting (FACS) experiment. However other ATP binding cassette (ABC) transporters are capable to transport verapamil out of the cells and hence give the SP phenotype. It has not been shown that the antibodies that have been used in SP phenotype specification in the cornea at least are blocking specifically only ABCG2. Additionally intra-assay variation of verapamil efflux is common Due to technique limitations.

FACS sorting for negative Hoechst 33342 dye staining in the corneal epithelium has identified the SP phenotype in 0.3-0.5% of the sorted cells from limbal but not central corneal epithelial cells. (Watanabe et al. 2004; Wolosin et al. 2004).

In another study, flow cytometry with ABCG2 monoclonal antibody showed that 2.5–3% of the total limbal cell population were ABCG2-positive (De Paiva et al., 2005) and that these ABCG2-positive cells were had higher colony-forming efficiency, in vitro, suggesting that ABCG2 is enriching for corneal limbal stem cells.

Immunolocalisation experiments consistently localised ABCG2 in the plasma membrane of positive cells in the basal (De Paiva et al., 2005) and also in the

suprabasal layers of the limbal epithelium (Chen et al., 2004; Watanabe et al., 2004; Wolosin et al., 2004), whereas no positive staining was observed in the corneal epithelium.

These studies suggest that ABCG2 definitely enriches for stem cells in the corneal epithelium.

1.2.3. Regulation of corneal stem and TA cells

1.2.3.1 Cytokines as regulators of corneal stem and TA cells

Consistently, before trying to understand possible regulators it needs to be underlined that one should discriminate between limbal basal cells and stem cells since the basal limbus contains early transient amplifying cells as well (Cotsarelis et a. 1989), adding to the problem, it is not know to what the stem cell- TA cell transition.is reversible *in vivo* and *in vitro*.

There are four patterns of interactions with respect to cytokines and their receptors in the human corneal-limbal epithelium to fibroblast communication (Kruse, Scheffer and Tseng 1992; Li and Tseng 1995; Li, Scheffer and Tseng 1995; Joyce and Zieske 1997; Li, Lee and Tseng 1999). These are:

- Type I cytokines: These are TGF-α, IL-1β, PDGF-BB, which are expressed only by epithelial cells, but their receptors are predominantly (EGFR and IL-1R) or exclusively (PDGFR-b) produced by fibroblasts.

- Type II cytokines: These are IGF-I, TGF-β1, TGF-β2, TGF-β3, LIF and bFGF, which are expressed in epithelial cells and fibroblasts while their receptors are expressed there too.

- Type III cytokines: Like KGF and HGF, expressed only by fibroblasts. Their receptors (KGFR and HGFR/c-met respectively) are expressed only by epithelial cells.

- Type IV cytokines: These are M-CSF and IL-8 which are expressed on epithelial cells and fibroblasts. Their receptors are expressed on immune and inflammatory cells.

Before looking at which growth factor influences what and how, the following should first be considered.

All the known signals fibroblasts will receive from epithelial cells in the cornea are TGF-α, IL-1b , PDGFBB, IGF1, TGF-β1, 2 and 3, LIF and bFGF. All the possible signals epithelial cells can receive from fibroblasts are IGFI, TGFβ 1, 2 and 3, LIF, bFGF, KGF and HGF (Li and Tseng

Under that context, Li and Tseng (1999) show that EGF upregulated LIF, HGF, downregulated KGF and M-CSF. TGFb upregulated EGFR, PDGFR-b, bFGF and TGFβ1, suggesting epithelium produced TGFb will activate fibroblasts more effectively than tear-derived EGF, which is logical considering the location and the short half-life of growth factors. PDGF-BB upregulated EGFR, PDGFR-b, bFGF and TGFb1, as well as IL-8. IL-1b upregulate KGF expression (in limbal fibroblasts more than in corneal fibroblasts), IL8 and M-CSF, while they downregulate PDGFR-b.

It seems that all these factors would have a devastating effect on undifferentiated stem cells or early progenitors. Nevertheless those cells manage to remain undifferentiated.

Limbal fibroblasts definitely send messages to the limbal basal area, but it is not clear which cells are influenced by them, the stem cells, or corneal epithelial early progenitor cells. There is evidence on cultured rabbit corneal epithelium that EGF, bFGF and NGF stimulate the proliferation of limbal and corneal epithelial cells. TGF-beta inhibits proliferation on these cells (Kruse, Scheffer & Tseng 1992; Li, Lee & Tseng 1999). This fact is in agreement with the later establishment of the idea of all TGF-beta and receptors for all three isoforms are present in the limbal epithelium. It appears therefore that a balance between proliferative and antiproliferative signals exists in the limbus but not in the periphery or centre. It is important to indicate once more that the assay used by Kruse, Scheffer and Tseng lacks specific activation of limbal

stem cells so it is not known what cells of the basal limbus receive which messages.

1.2.3.2 Retinoic acid

Retinoic acid is one of the factors in the serum that are thought to be responsible for the differentiation of limbal stem cells. It is an important modulator of epithelial

proliferation and differentiation (Fuchs 1981; Hashimoto 1985; Kruse 1994). High concentrations of retinoic acid (more than 10-6M) concentrations inhibits the formation of colonies both in peripheral corneal cultures and in limbal cultures, low concentrations (10-8 –10-7M) will increase the colony formation only in limbal stem cell cultures (Kruse and Tseng 1993). In the same study, it was observed that in low concentration retinoic acid treated cultures, one of the morphologically distinct colony types arising , was a special subpopulation of progenitor cells in the limbal epithelium which was very similar (it could even be) stem cells. However it is very unlikely that this was not achieved by synergistic action of other factors.

Other serum factors might influence limbal cells. Addition of FBS in corneal cell cultures results in drop of colony formation and proliferation as concentrations of FBS rose. This has the opposite effect in limbal epithelial cells though. Formation of limbal colonies and their proliferation are stimulated. It is not known if the specific subpopulations of cells that are stimulated are stem cells. (Kruse1994). It is more probable that TA cells were the ones stimulated.

1.2.3.3 Extracellular matrix as a regulator.

Extracellular matrix (ECM) cell interactions are a major regulating factor in corneal epithelium. The composition of the matrix influences half life of growth factors, projects attachment sites to the cells above the basal lamina. These interactions are not just for anchorage. There is a chain of events involving the differentiation and migration of these cells (direct paradigm is CAM's which are so well studied in cancer and developmental biology). There is much evidence that the control of these interactions sets the standard in penetrating wound healing (because small scale epithelial wound healing circumvents the ECM-cell communications since they are not needed). It is not known if the extracellular matrix is regulating the stem cells, but the same patterns of control exist for the corneal TAC and the early progenitors on the basal limbal epithelium. Since the niche formation is true for the limbus, we can characterise that as a contribution of ECM to stem cell control either due to structure composition or due to different diffusivity the limbal ECM will offer to GFs. But it is not known if the ECM contacting the stem cells will employ other regulatory mechanisms than that contacting the TACs.

Significant heterogeneity exists among the basement membranes of different body sites, but within tissues too (Potten CS, editor. Stem cells. London: Academic Press; 1996), in terms of laminin and type IV collagen. In AE27

antigen immunohistological studies by Kolega et al. (1989), the antigen appear in patches in the limbus when it is uniformly distributed in corneal tissue. Its presence appears to be related with K3 expression. The nature of this antigen is not known though so we cannot subtract biochemical information.

Laminin, entactin, heparin sulphate proteoglycan KF-1 (Kolega 1989) and bullous pemphigoid antigen (Ben-Zvi et al. 1986) are uniformly distributed throughout corneal conjunctival and limbal epithelia (as cited in Potten: Stem cells).

Cell to matrix interactions involve integrins. Integrins are considered cellular receptors of ECM. They do play an important role in migration maturation and differentiation in the TA cell population in the cornea in normal conditions and more importantly during wound healing, This study is sought to gain an insight into the mechanisms by which cell contacts could be controlling cell fate decisions of stem cells

1.2.4 Asymmetric cell division.

Since progeny of stem cells are not able to self maintain a tissue and do not have the capacity to avoid differentiation or to produce a large amount of their own progeny it is imperative that at some point stem cells undergo asymmetric cell division that results in two daughter cells of different qualitative traits; one that is a stem cell and one that is not. As far as logic is

concerned this is the only imperative ability of a stem cell is asymmetric division that leads to self renewal

A central question in developmental biology is how a single cell can divide to produce two progeny cells that adopt distinct fates (Ho 2004).

1.2.4.1 Asymmetric division in mammalian stem cells

In the developing nervous system of mouse models, proteins that segregate asymmetrically during mitosis have been identified. Asymmetric localization of Numb and Notch homologues has been observed in mammalian neural stem cells (Chenn et al. 1995; Wakamatsu et al.1999; Zhong et al 2000; Cayouette et al. 2002). Neural progenitor cells in the cortex divided asymmetrically to produce different lineages (Qian et al. 1998) as determined by video time-lapse microscopy.

Great insight into how a cell division becomes asymmetric comes from studies in the ventricular zone of the developing mammalian cortex as well as studies in *drosophila* neural system development (Chenn et al. 1995; Hirate et al. 1995). Using the ferret model, neural precursors were seen to divide and daughter cells either stayed in this zone and continue to undergo self-renewing divisions, or migrated distally to differentiate (Chenn et al. 1995). Furthermore those daughter cells showed unequal inheritance of Notch1 immunoreactivity. Intriguing results from the same study indicated that cleavage orientation during neural precursor cell division coincided with that

asymmetry (Chenn et al. 1995). Specifically, the asymmetry was observed to arise only by divisions with a vertical orientation to the ventricular surface of the neural tube. Similar asymmetry with respect to the distribution of the homeodomain protein Prospero after neural precursor cell division was observed during *drosophila* (Hirate et al 1995). Additionally, proteins implicated in cell fate determination such as Notch, Numb, and Minibrain were shown to be distributed asymmetrically during mitosis of neural precursors of the developing cortex (Zhong 1996, 2000)

Therefore it seems that at least in the developing neural system, asymmetric cell division leads to the formation of cells with unequal fates and coincides with asymmetric localisation of several proteins during cell division. This asymmetry is believed to be related with the orientation of cell division plane.

1.2.4.2 Asymmetric divisions in mouse epithelial cells.

.Asymmetric cell division is arising as the mechanism to explain stratification of epithelia. There are several examples in *drosophila* and *C. Elegans* studies of how asymmetric cell division and mitotic spindle orientation are interelated (Betschinger & Knoblich 2004; Cowan & Hyman 2004) A first line of evidence in mammals of such relation , comes from a recent study of epithelial stratification by Lechler and Fuchs (2005). Dividing, basal epithelial cells of the mouse tongue and epidermis, localize two crescents at their apical side, namely the LGN–mInsc–Par3 complex and the NuMA-dynactin complex in order to align their spindles perpendicularly to the basement membrane. This division generates a suprabasal cell committed to differentiation and a proliferative basal cell. The apical localization of the two crescents is directed

by atypical protein kinase C (PKCz in case of the epidermal epithelium in mouse). In the same study it was shown, by the use of knock out mice for integrin b1, catenin-a and p63, that the ability to localise those components to the apical side of the basal cell depends on functional integrin b1, catenin-a and p-63 molecules. If any of these components is absent basal epithelial cells of tongue and epidermis loose their ability to localize the crescents to their apical side and therefore to align their spindle perpendicularly to the basement membrane as well as divide asymmetrically. Thus it can be suggested that as far as our knowledge allows an epithelial cell is controlling its asymmetrical cell division at least in part by attaching to the basement membrane and to its neighbors.

What would be interesting is to determine if the asymmetry in terms of daughter cell fate in this case arises due to the fact that one cell remains attached to the basement membrane and one is displaced to the suprabasal layer, or if there is also a qualitative difference in the two daughter cells due to asymmetric localisation of components of the parental cell.

However, it is not known if this type of mechanism is true for the asymmetry of stem cell division with respect to self maintenance. It remains to be seen if this mechanism controls asymmetry of stem cell division *in vivo*. Also it will provide a new perspective into the results of in *vitro studies*

The implications of such a mechanism in the cornea could be important since p63 is expressed by both basal cells of the limbus and the periphery (Pellegrini et al) and as it will be discussed in the general discussion some

factors that affect components of that control system were found to be up-regulated in the basal limbus.

1.2.4.3 Asymmetric cell kinetics

The first demonstration that mammalian cells could divide with determined asymmetric cell kinetics in adult derived murine mammary epithelium cells in culture also identified p53 tumor suppressor as the first candidate for an intrinsic asymmetric cell kinetics control gene. (Sherley et al 1995 a&b). In the same studies it was observed that when p53 was upregulated by less than 50% above the endogenous wild type basal expression levels in these cells it induced a switch from symmetric cell kinetics, which produce two dividing daughters (underlying the exponential kinetics that typify established cell lines), to asymmetric cell kinetics. The asymmetric cell kinetics were characterized by divisions producing one continuously dividing daughter and one viable daughter arrested in G1/S of the cell cycle (Sherley et al 1995 b).

Given the fact that p63 is a p53 homologue (Yang et al. 1998, 2000) it becomes very interesting to investigate if p63 is modulating the levels of p53 activity in stem cells turning the kinetics to asymmetric.

1.2.4.4 Asymmetry and wound healing

With respect to asymmetry and wound healing in the cornea some older studies on PKC molecules could give some insight. When Hirakata and co-workers (1992) studied the effect of PKC (protein kinase C) inhibitors and

activators on corneal re-epithelialisation in the rat, they found that the inhibitors of PKC substantially downregulated the rate of re-epithelialisation after wound healing, whereas PKC activators did not affect that rate at all. What is interesting about this investigation is that they used the Gibson organotypic culture model to culture 3mm diameter epithelial abrasions taken from the central cornea areas. Therefore these cultures did not contain any stem cell population. Nevertheless the study implied a significance of this control in proliferative basal epithelial cells. Scheffer, Tseng & Li (1996) then made a comparison of PKC expression between normal and aniridic human ocular surfaces including the limbus and the cornea. They indicated that normal limbal basal epithelium is characterized by simultaneous expression of PKCa and PKCg from all the other ocular epithelia. In aniridic mice, limbal epithelia have different PKC distributions between basal, suprabasal and superficial limbal cells. These results seen through the light of the emerging role of aPCK in asymmetric cell division of proliferating cells (Lechler and Fuchs 2005) are creating questions about the existence of similar asymmetric cell divisions in the corneal epithelial basal cells. It also remains to be seen if such mechanisms are playing a role in asymmetric stem cell division in the corneal epithelium.

1.2.5 Chromatin remodelling and switching between Active and Inactive gene programs.

Different cells have different properties and those properties are regulated by proteins and therefore genes. One process that needs to be regulated in order to end up with cells that are different is to switch gene programs on or off. Mechanisms that regulate the switch between transcriptionally active or inactive genes are discussed in this section due to the indications that such mechanisms are in action in stem cell lineage determination both in development and in adults (Roloff and Nuber 2005)

Eukaryotic genomes are described as transcriptionally active (euchromatin) or transcriptionally silent (heterochromatin). Heterochromatin is defined as the fraction of the genome that remains visibly condensed during interphase.

More recently, heterochromatin has been defined as genomic regions that are gene poor, contain large blocks of repetitive DNA, are inaccessible to DNA-modifying reagents and replicate late in the cell cycle (Elgin 1996; Henning 1999). Heterochromatin is characterized by increased methylation of the cytosines in CpG islands of the DNA , decreased acetylation of histones and increased methylation of lysine-9 in histone H3, which now provides a binding site for heterochromatin protein 1 (HP1), which blocks access by the transcription factors needed for gene transcription (reviewed in Rice and Allis 2001).

In contrast the genes in euchromatin are active and thus show decreased methylation of the cytosines in CpG islands of the DNA increased acetylation of histones and decreased methylation of lysine-9 in histone H3. (Rice and Allis 2001)

An originally transcriptionally becomes and remains inactivated when displaced from its normal euchromatic position to the vicinity of heterochromatin (Reuter and Spierer 1992; Karpen 1994). It is extremely interesting that epigenetic inheritance of this inactivated state is propagated during mitosis and through the germ-line during meiosis (Grewal et al. 1996; Cavalli and Paro 1998). This epigenetic phenomenon, known as position effect variegation (PEV), provides an attractive model of molecular imprinting that specifies the transcriptional state of genes in stem cells. It is logical that a stem cell in order to remain one need to have the same areas shut down before and after mitosis. In fact maintenance of cellular memory through epigenetic chromatin modifications is characteristic of neural (Molofsky et al. 2003) and hematopoietic (Iwma et al. 2004) stem cells. Interchange between states of activation of genes would be the switch between stem cell identity and TA cell identity although it is not known whether this process is reversible.

Chromosomes undergo significant changes in structure twice during the cell cycle. First, at the G_2/M transition, the chromosomes condense to form individual compact structures. Second, at the M/G_1 transition, the chromosomes return to their de-compacted interphase state. These structural transformations are believed to be essential for complete segregation of genomes into daughter cells during mitosis and to provide differential access

for soluble factors to active genetic loci while keeping inactive ones in the silent compact state.

The high level of compactness is achieved by ordered folding of DNA through its interaction with chromosomal proteins. Interaction of DNA with histones gives rise to nucleosomes and a 30 nm chromatin fibre (Wigler and Axel 1976). The mode of DNA folding at higher levels of compaction and molecular mechanisms involved in formation and maintaining of higher order chromatin structures remain largely elusive.

Histones are subject to a wide range of post-translational modifications throughout the cell cycle including phosphorylation, acetylation, and methylation (Cheung et al. 2000)

Histone acetylation emerges as a central switch that allows interconversion between permissive and repressive chromatin structures and domains (Eberharter & Becker 2002) .These principles are not only at the heart of transcriptional regulation but are also likely to govern other processes involving chromatin substrates, including replication, site-specific recombination and DNA repair (Wolffe and Hayes, 1999; Roth et al., 2001).

Methylation of H3 at lys 9 has been shown to ectopically silence genes in cancer cells (Nguyen et al. 2002). Methylation and acetylation of H3 Lys 9 are antagonistic and it has also been shown that H3 Ser10 phosphorylation antagonises H3 Lys9 methylation (Cheng et al. 2000; Rea et al. 2000)

Phosphorylation of chromosomal proteins has been implicated in controlling the formation of mitotic chromosomes (Heck et al. 1989; Guo et al.1995; Ajiro et al. 1996; Kimura et al.1998; Wei et al. 1999). We do not yet know the full list of histone modifications that occur in mitosis, but it likely will include changes in ubiquitination and phosphorylation on other histones (Bradbury 1992; Hsu et al. 2000).

Histone H3 phosphorylation was first identified in mitotic cells and has since been recognized as a ubiquitous mitotic modification (Gurley et al, 1973; Gurley et al. 1978; Hendzel et al. 1997). However, phosphorylation of H3 Ser10 also occurs in more discrete chromatin regions during activation of transcription and coincides with histone H3 acetylation on the same nucleosomes (Mahadevan et al. 1991; Barratt et al.1994 Clayton et al.2000). This kind of specific combinatorial modification has been proposed to form a "histone code" that would form a marked chromatin surface that could recruit chromatin remodeling and modification activities or factors mediating higher order chromatin structures (Strahl et al. 2000).

Phosphatase 1 (PP1) can directly inhibit Aurora kinase b mediated phosphorylation of Histone 3 during interphase (Murnion et al. 2001). Histone H3 Ser10 and the linker histone B4 are phosphorylated in mitotic chromosomes, whereas histones H2A and H4 are phosphorylated in interphase chromatin (Murnion et al. 2001).

Eluates of isolated mitotic chromosomes contain the mitotic histone H3 kinase, and this activity is associated with the X aurora-B kinase. The X aurora-B-associated activity is inactivated by treatment with phosphatase, showing that it requires phosphorylation for its activity. Furthermore, the X aurora-B-associated activity exists in interphase chromatin but is inactive. This form is activated by inhibition of PP1 and incubation in ATP, showing that PP1 activity directly inhibits X aurora-B in interphase chromatin.

One complete component of the switch between active (euchromatin) and inactive (heterochromatin) genome as it can be derived from current studies that have been discussed involves:

Histone H3 de-acetylation of Lys9 possibly mediated by phosphorylation of Ser10 and subsequent methylation of Lys9 and tethering of a heterochromatin protein (HP) to this site which results in condensation and/or inability of transcription factors to reach the heterochromatin as well as neighboring regions. The mechanism is illustrated in figure 1.2.

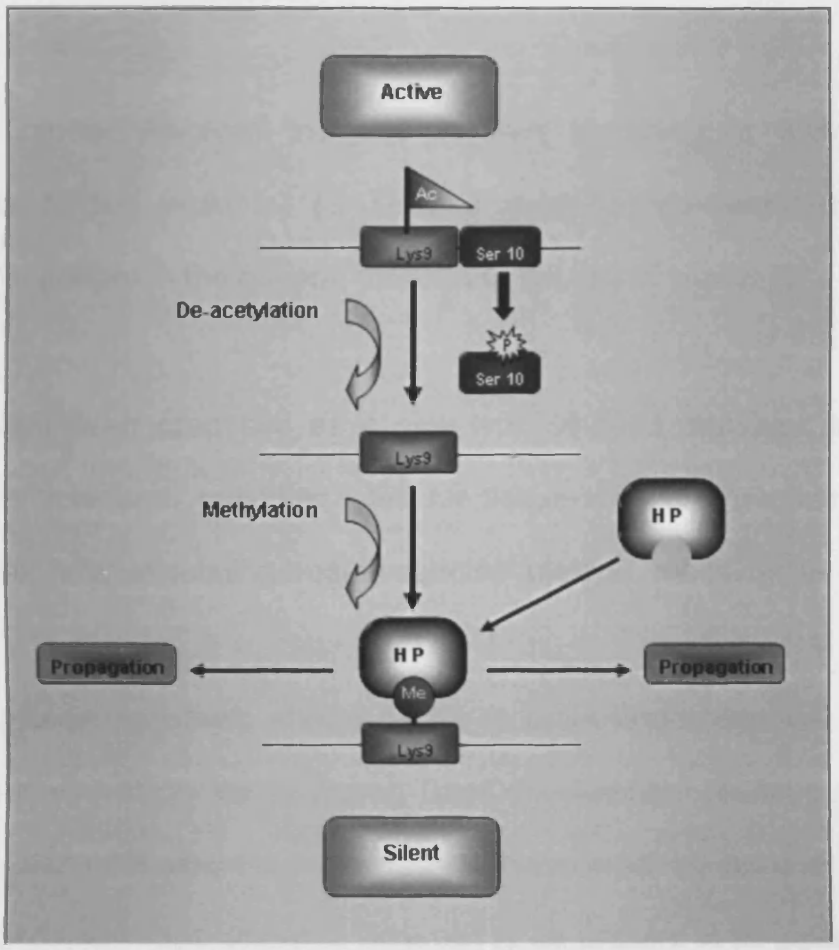

Figure 1. 3 Temporal pathway leading to the establishment of transcriptionally silent heterochromatic regions with regard to the covalent modifications in the histone H3 tail. The acetyl group on H3 Lys9, a modification often associated with transcriptionally active regions, is removed by an Histone deacetylase prior to methylation by a histone methylase after phosphorylation of Ser10. Then a HP (heterochromatin protein) selectively recognizes and binds to the H3 Lys9-methyl modification resulting in the self-assembly and propagation of heterochromatin and transcriptional silencing.

Another protein involved in gene-program switching is special AT-rich sequence binding protein 1 (SATB1). It is mentioned here because it will become important in the general discussion section (Chapter 7).

SATB1 had been proposed as a new type of gene regulator with a novel nuclear architecture, providing sites for tissue-specific organization of DNA sequences and regulating region-specific histone modification (Cai et al. 2003)

SATB1 protein has been shown so far to orchestrate temporal and spatial expression of multiple genes during T-cell development (Alvarez et al. 2000), although the phenomenon of transcriptional control by histone acetylation-deacetylation and methylation is believed to be present in all types of somatic and germ line cells.

SATB1 is a cell-type specific nuclear protein that recruits chromatin-remodelling factors and regulates numerous genes during thymocyte differentiation. It was found that in thymocyte nuclei, SATB1 is distributed in a cage-like 'network', circumscribing heterochromatin and selectively tethering specialized DNA sequences onto its network (Alvarez et al. 2000). Many gene loci are anchored by the SATB1 network at specific genomic sites, and this phenomenon is precisely correlated with proper regulation of distant genes.

In *Satb1*-wild type T-cells the binding site of SATB1 is marked by acetylation of histone H3 at Lys9 and Lys14 peaks and extends over a region of roughly 10 kb covering genes regulated by SATB1. By contrast, in *Satb1*-null thymocytes, this site is marked by methylation at H3 Lys9.

1.3. Principles and applications of gene arrays.

1.3.1 General Concept

Gene arrays are a continuously developing technology that has recently been established. Microarray technology can be useful for making estimates of the abundance of particular messages relative to a designated source of mRNA that serves as a reference library. In the last 4 years a plethora of microarray types has emerged. Expression studies today can adapt many strategies. The main three types of expression studies that can be performed with the use of array technology are high density oligonucleotide arrays, low density-custom made microarrays from specific BAC clones of cDNA and a third one that is being under development is the ChIp-Chip array which is using a genomic DNA array to hybridise fragments of DNA immunoprecipitated by an RNA poly II antibody and specific transcription factors of interest to locate the genes that are being inhibited or enhanced by specific growth factors.

There are three fundamental stages in a microarray experiment.

The first involves the microarray fabrication itself. This step requires a cDNA bacterial clone inventory. Collecting an inventory of cDNA bacterial clones that represent the genes whose message abundance we wish to survey is followed by deposition of them on the microarray chip (usually a glass chip, but this is going to be analysed further later). High density oligonucleotide arrays utilise fabrication techniques like photolithography and ink-jet printing make direct DNA synthesis on the chip of short sequence DNA.

In the second step RNA is extracted from the cell samples to be examined, purified, and used as the substrate for reverse transcription and often in-vitro translation in the presence of fluor-derivatized nucleotides, in order to label them and use them as probes in the microarray experiment. This procedure provides the tagged representations of the mRNA pools of the samples that will be hybridized to the gene-specific cDNA detectors immobilized on the microarray.

The third step the actual hybridization procedure takes place. Then the data are ready to be extracted. At this stage fluor-labeled cDNAs hybridize to their complements on the microarray, and the resulting localized concentrations of fluorescent molecules are detected and quantified.

1.3.2 Microarray Fabrication

This first step involves the extraction of cDNA fragments from a cDNA bacterial clone inventory. This is either achieved either by DNA purification and subsequent PCR amplification of the desired cDNA reference fragment, or by direct PCR to the vector clone by using vector specific primers. After the collection of an inventory of cDNA bacterial clones, that represent the genes whose message abundance is to be surveyed, the fragments will be deposited on the microarray chip (usually a glass chip, but this is going to be analysed further later). There are three main techniques for cDNA deposition on the chip photolithography, ink jetting (piezoelectric technology), mechanical microspotting and derivatives thereof.

1.3.2.1 Deposition Techniques

Photolithography

Photolithography uses semiconductor fabrication technology. Photomasks direct spatially defined, solid face DNA synthesis through the use of light which is allowed on the surface at a desired spot (the one non-masked). Light activates modified phosphoramidite versions of the four DNA bases for DNA synthesis (Fodor 1991). Each coupling step of the reaction, results in the addition of a single base to the growing single DNA chains at thousands of defined locations (Fodot 1991). In this way high density oligonucleotide arrays achieve an unparalleled homogeneity between arrays.

Ink-Jetting (piezoelectric technology)

The piezoelectric technology is identical to the ink-jet system used in desktop printers. Micro-delivery jets provide cDNA fragments at specific locations on the biochip in a non-contact fashion directing sub-nanolitre volumes of negatively charged DNA with the use of electric fields. The jets are navigated above the biochip surface by an X, Y, Z, motion control system.

Microspotting

Unlike ink-jet technology, microspotting utilizes a print head containing microspotting pins, capillaries or tweezers to deliver the pre-made cDNA or other molecules from reagent trays on the biochip surface. Microspotting again uses a similar X, Y, Z navigation system for accurate deposition.

All of these technologies have evolved to the stage that they print in such a density, that a considerable amount of genes can be represented on a single biochip. High density oligonucleotide arrays though have reached the capacity to include the entire human and mouse genome. The requirements of the experiment with respect to throughput, density, cost, quality and flexibility, determines which of the printing techniques will be used to fabricate the array.

1.3.3 Data extraction and analysis.

After the fluorescent samples have been left to hybridise to the microarray, any unbound DNA fragments are washed away and the remaining bound cDNA fragments are located on the spatially addressed spots of the microarray. Every spot is referenced to a corresponding already known DNA fragment coming from either the cDNA clones or synthesised fragments. In this way when the fluorescence of every spot is detected and filed, an estimate of the level of expression of the particular gene from can be drawn. How accurate this estimate will be is a question of many parameters.

For the detection of the bound fluorescent sample molecules throughout the surface of the biochip, confocal scanning devices and CCD cameras have been used.

Excitation, of the sample in order to emit light that will be detected. Excitation is provided by using lasers, arc or filament lamps, or LEDs. Any way the excitation light is produced, it must limit its wavelength in a way that it will not overlap the emission. Lamps and LEDs require filters to select the appropriate spectrum of excitation. Lasers are able to produce light at a single, well-known wavelength (except diode lasers).

Multiple excitation can result either by using lamps and LEDs with an adjustable wavelength tuner employing a series of filters, or by using multiple lasers. The excitation light whatever origin it might have is directed on the microarray. There are two ways. Flood illumination is one way and it is the

one applied to CCD camera scanners. The other way is used in the confocal scanners where the light is directed to a very small part of the sample each time.

What is absolutely essential to consider, in describing detection systems and microarrays in general, is that they are meant to detect the area concentration of fluorescent dye. Related factors, that determine if the area concentration is proportional to the actual expression level of a gene, are i) the quality of the RNA extraction and/or amplification protocols, ii) the quality of the deposition procedure of the microarray itself and iii) the quality of the detector.

In confocal scanning devices (scanners), a laser beam excites small regions (around 100mm) on the substrate sequentially by moving the substrate and/or the confocal lens, such that all of the substrate has been scanned in two dimensions, in a particular depth of focus. When the laser beam excites these small areas of the substrate, molecules on its light path will emit light. This emitted light will be a result of the fluorescent cDNA target dye molecules, background fluorescence, due to other molecules present and glass of the biochip, laser light refraction (which is a reflection of the image of the sample). In order to separate all of the unwanted light from the one coming from the labelled molecules, a series of mirrors, filters and lenses are used. These will be the first measure for correcting the light output. Other measures apply as well as will be discussed later.

Following the emitted light collection, the light is then converted to an electrical signal usually with a photomultiplier tube (PMT). Then digital signal processors of the machine will convert the electrical signal into a digital signal which is ready to be handled by algorithms of the software. The speed of data collection in microarrays is far greater than that of other hybridisation based assays used (1-5 minutes compared to 1-10 days respectively) and with far more genes questioned with each experiment.

Most DNA arrays will have samples that are labelled with multiple fluorescent probes, usually from two to four. If differential gene expression is to be considered in terms of microarrays, one probe can be used for each sample preparation. Complications may arise if more than two samples are to be tested in the same array, because the emitted wavelength of each probe needs to be considerably away (50nm) if cross-talk problems need to be solved. The sample will be scanned at the two or more wavelengths and the ratios of these fluorescence emissions will represent the differential gene expression. The fact that ratios are the ones that are important in differential gene expression analysis reduces the need for absolute calibration of the sample preparation process.

The efficiency of the detection of fluorescence and therefore of the data extraction is dictated by many things. What happens during data harvesting is that fluorescent intensity of each dot to be analysed is compared to the ones of the local background intensities.

Cross talk problems are eliminated in high density oligonucleotide arrays since each sample is hybridised to a single array.

1.3.3.4 Detectivity

Detectivity is defined as the minimum dot fluorescent brightness that can be distinguished from the background when the sensitivity is set so that the brightness element of the sample produces an intensity level at the full scale. Detectivity can be measured with special pre-made microarrays that incorporate dilution series. The detectivity is then addressed by the dimmest dot that can be detected. Detectivity is also dependent on the characteristics of a sample preparation.

1.3.3.5 Sensitivity

Is the conversion efficiency of light power to a digital value at a particular wavelength? Sensitivity influenced only by the hardware's capabilities and not the quality of the sample. Sensitivity can reduce detectivity when both the excitation and the detector are adjusted at their maximum values (if a very dim scan data are processed). Adjusting excitation to the maximum results in saturated data values should be questioned. A balance between those two must be decided.

1.3.3.6 Cross-talk

When multiple dyes are used in order to label our samples, interference of the excitation wavelengths of each dye can occur. In an analysis such as differential gene expression this would influence the expression ratio between the two compared channels. Cross talk can be greatly reduced with appropriate selection of dyes and excitation laser wavelengths. As a rule of thumb these wavelengths must be approximately 50nm apart, in order to allow proper filtering. In addition to that measure, narrow band emission filters on the dye peaks, with good attenuation of out-of-band wavelengths can be used. Cross-talk is not an issue when high density oligonucleotide arrays are used.

1.3.3.7 Resolution

The resolution of the scanner is the degree of spatial division capabilities during fluorescence reading. These equal fragments that the surface is divided to are called pixels. The size of the pixel can vary to 5, 10, and 20 mm depending on the device. The smaller the pixels are the better the resolution. The pixel dimensions need to be no larger than 1/8 to 1/10 of the diameter of the smallest dot in the microarray to be analysed. In this way, edge effects and other defects can be rejected at the quantification stage.

1.3.3.8 Field Size

The greater the glass chip (slide) is the more dots it can accommodate. The general considerations here are that the 1-1.5mm at the edges of the slide cannot be used because it may be chipped or not flat which would result in background fluorescence interference and unequal amount deposition and unrelated reading from the confocal variation of depth of reading surface. A 1.5 cm area at the one end of the chip is used as a handle. Thus many scanners use a 60mm field in longitude. That means the minimum field is around 22mmX60mm with a maximum of 22mmX73mm.

1.3.3.9 Uniformity

Uniformity can be referred to as the measure of fluorescence emission and detection consistency. The problem of non-consistent fluorescence emission and detection can arise by either scanning motion deviating from the focal plane (important if we consider the depth of focus usually adjusted to a few tens of microns) or by irregularities of the surface itself.

Non-uniformity can be dealt with increasing the depth of focus by enlarging the confocal pin-hole, thereby decreasing the standard deviations of the "flatness" parameter. This of course will be done in the expense of image artefacts being created. So a balance between those two must be decided especially in the case of rescuing a microarray experiment. Most users seek ± 10% scanner uniformity across the image field.

1.3.3.10 Image geometry

Because most quantification software after the data is retrieved applies a fixed grid to the image and expects to find dots in the centre of each box, the size of the image and pixel placement linearity matters. However, there are software programs that apply a dynamic grid model on the image produced by the microarray. This is a big consideration of the deposition procedure as well.

1.3.3.11 Throughput

After the resolution, the size and number of channels to be scanned on the microarray have been defined from the user, throughput specification can be addressed. The number of samples that can be scanned in a day depends on how accurate the result is desired to be. CCD cameras have high throughput but the detectivity falls dramatically (worse then first generation confocal scanners). When n many wavelengths (multichannel scanning) are scanned, data collection time increases. To increase the throughput in this case, colour separating beam-splitters are placed in the emission light path that will lead the light in multiple detectors, and subsequently to more signal processing modules, so that all the channels can be scanned at once. Generally a first generation scanner will spend 5-15 minutes for a 20mmX60mm field at 10m m pixel size resolution.

1.3.4 Affymetrix technology in more detail.

GeneChip probe arrays are manufactured using technology that combines photolithography and combinatorial chemistry.1.2 Up to 1.3 million different oligonucleotide probes are synthesized on each array. Each oligonucleotide is located in a specific area on the array called a probe cell. Each probe cell contains hundreds of thousands to millions of copies of a given oligonucleotide. Probe arrays are manufactured in a series of cycles. Initially, a glass substrate is coated with linkers containing photolabile protecting groups. Then, a mask is applied that exposes selected portions of the probe array to ultraviolet light. Illumination removes the photolabile protecting groups enabling selective nucleoside phosphoramidite addition only at the previously exposed sites. Next, a different mask is applied and the cycle of illumination and chemical coupling is performed again. By repeating this cycle, a specific set of oligonucleotide probes is synthesized with each probe type in a known location. The completed probe arrays are packaged into cartridges.

The system (Lockhart *et al.*, 1996) uses oligonucleotides with length of 25 base pairs that are used to probe genes. Typically, each gene will be represented by 16–20 pairs of oligonucleotides referred to as *probe sets*. The first component of these pairs is referred to as a perfect match (*PM*) probe. Each *PM* probe is paired with a mismatch (*MM*) probe that is created by changing the middle (13th) base with the intention of measuring non-specific binding. The *PM* and *MM* are referred to as a *probe pair* (Affymetrix Expression manual).

1.4. Laser capture micro-dissection.

Laser capture microdissection (LCM) has been identified as a quick and effective method of microdissecting complex tissue specimens for molecular analysis. Laser capture microdissection (LCM) was first described in 1996 (Emmert-Buck 1996). The system has been subsequently commercialised and used in many laboratories. A thermoplastic ethylene vinyl acetate transfer film containing a near-infrared absorbing dye, attached to a 6 mm diameter rigid, flat cap, is placed in contact with a routinely prepared tissue section. The film over the cells of interest is precisely activated by a near-infrared laser pulse and bonds strongly to the selected cells. Although the laser transiently raises the temperature of the transfer film to 90C, its energy is absorbed by the film and is poorly absorbed by biological tissue (Sirivatanauksorn 1999). Nucleic acids and proteins recovered from these cells are therefore not degraded by heat conduction (Goldstein 1998). Removal of the cap from the tissue section effectively procures the targeted cells. The identity of the transferred cells attached to the film can then be recorded by image capture. The cap is fitted in a microfuge tube containing lysis buffer and DNA, RNA, and proteins can then be extracted for molecular analysis. Since no coverslip is used in LCM, the reduction in refractive index means that most light passing through the tissue is scattered, which can obscure cellular detail at high magnifications. The isolation of cells from immunohistochemical or (molecule-specific) fluorescent labelled section improves sample imaging and can help in obtaining specific cell populations more precisely.(Fend 1999)

The Arcturus LCM system uses variable laser-transfer sizes from less than 7·5 to 30 μm, and a cylinder-based LCM instrument and novel convex geometry for the ethylene vinyl acetate transfer film and it was developed in the last years (Suarez-Quian 1999). Selection, capture, and dissection on a single-cell can be achieved by this method. The capture zones of the Arcturus system are 200 times narrower than the original LCM system. Using a smaller beam and briefer pulses (less than 1 ms) limits the melting of the polymer to spots of 6μm, thus allowing the capture of single cells from different types of tissue sections (see results).

The optics of all microdissection systems are very poor because no coverslip can be used and the light that is passing through the tissue gets scattered. Haematoxylin and eosin staining, as well as immunostaining of frozen tissues and subsequent dissection of the cells of interest (Fend 1999) are possible and have been documented. There are also reagents that stain the tissue while stabilising the RNA (Arcturus). These methods can improve the optics but the degree of mRNA degradation need to be addressed.

Aim of Study

Considering the vast amount of knowledge available regarding corneal epithelial cell homeostasis, regulatory mechanisms that control stem cell maintenance and differentiation are poorly understood. Nevertheless since the corneal epithelium exhibits a linear pattern of differentiation, the isolation and investigation of gene expression of the conjunctival epithelium, the basal limbus, basal periphery and basal central cornea is going to facilitate the understanding of the molecular mechanisms that are actively regulated at progressive stages of the corneal stem cell lineage and possibly identify specific corneal epithelial stem markers, thereby facilitate future basic science and clinical research on corneal epithelial stem cells.

The main hypothesis is that cells at different stages of the corneal stem cell lineage that reside in a linear basal limbo-corneal axis will indeed be differentially regulated at the transcriptional level. In other words, that the main component of variance in transcription arises from the type of cells being analysed. And that those differences can be realised at a global level by employing single cell laser capture techniques as well as mRNA amplification techniques to analyse their complete transcriptome by high density oligonucleotide arrays.

The overall objective of the research was to identify target genes that could serve as markers of corneal epithelial stem cells as well as genes involved the regulation of corneal stem cell homeostasis.

Therefore, aims of this study are to:

- **to develop a technique, by which, to isolate single/small numbers of cells from defined regions of the mouse cornea**

- **amplify RNA extracted from these cell populations in a linear fashion**

- **determine the differential gene expression profiles of epithelial cells isolated from central, peripheral, limbal corneal and conjunctival epithelium.**

- **test the experimental hypothesis.**

- **Identify target genes selectively expressed all along the progressive stages of the corneal epithelial cell lineage that are important in corneal epithelial stem cell homeostasis.**

Chapter 2

General Methods

2.1. Molecular Biology

2.1.1. RNA stabilisation in tissues or cells

RNA was stabilised in tissues and cells, destined for RNA isolation, by preservation in RNA*Later*® (Ambion, UK). When tissue were stabilized they were first cut in fragments whose thickness did not exceed 0.5cm at least in one side, to facilitate penetration of the stabilizer and tissues and cells were completely submerged in RNA*Later*®. Tissues were kept at 4°C in this solution for up to a month or at -20°C or lower for archiving.

2.1.2. Trizol RNA isolation from tissue.

50mg of fresh or RNALater treated tissue were homogenized using a mortar and pestle and/or a Dounce homogenizer to homogenize frozen tissue. The procedure was scaled up for larger quantities. If tissue was snap frozen, it was pulverized, using a bead in a snap frozen TEFAL vial and stainless steal bearings, using a dismembrator shaking at full speed for 1 minute.

To every 50mg fresh, RNALater treated, or frozen pulverized tissue, 1 ml Trizol was added and the mixture was further homogenised at room temperature for up to 5 minutes to allow for nuclear protein complexes to degrade. Genomic DNA was sheared by two passes through a 26 gauge needle. For larger corneal tissue e.g. adult mice corneas, a 5 minute centrifugation step at 12 000g, 4°C in a Boeco centrifuge was added to pellet any insoluble debris.

To the supernatants or cell lysates 0.2 ml chloroform per 1ml initial Trizol reagent treatment was added. Lysates were shaken vigorously by hand for 15 seconds and incubated further at room temperature for 2-15 minutes.

Samples were centrifuged at 12,000*g* for 15 minutes at 4°C. Following centrifugation, RNA was transferred to a new microcentrifuge tube by isolating the colorless upper aqueous phase. RNA was precipitated from the aqueous phase by mixing with 0.5ml isopropyl alcohol. Samples were incubated at room temperature for 10 minutes and then centrifuged at 12,000*g* for 10 minutes at 4°C. Supernatants were discarded and RNA pellets ware washed with at least 1ml of 75% ethanol. Samples were vortexed briefly and centrifuged at 7,500*g* for 5 minutes at 4°C.

Supernatants were discarded and RNA pellets were partially dried for 5 minutes.
RNA was either stored at -80°C or resuspended in nuclease free molecular biology grade water (Sigma).

2.1.3. RNA isolation and cleanup from laser microdissected cells or from tissue RNA preparations.

RNA was isolated and further cleaned up to remove DNA, salts or residual protein using RNeasy mini columns (Quiagen, UK) together with on-column DNAse treatment using the RNase-Free DNase Set (Quiagen, UK) according to manufacturers instructions.

Cells or RNA isolated by the Trizol method were treated with 350µl Lysis Buffer, supplemented with β-mercaptoethanol (β-ME) (10µl β-ME per 1ml lysis buffer). Laser microdissected cells were left to lyse in the buffer at 42°C for 15 min. Then 250µl ethanol (96–100%) was mixed into the samples (cell lysate or diluted RNA), before loading samples onto an RNeasy mini column inserted into a 2ml collection tube. Columns were centrifuged for 15 seconds at 8000*g*. Columns were washed with 350µl Buffer RW1 and centrifuged for 15 seconds at 8000*g*.

Columns were then loaded with 27 units of DNAse I in 80µl buffer RDD (supplied with the kit) and residual DNA was digested on the column at 30°C for 15 minutes. Columns were then washed with a further 350µl Buffer RW1, followed by another two washes with 500µl buffer RPE. The tube was closed gently and centrifuged for 15 seconds at 8000*g* to wash the column. The flow-through was discarded.

Pure total RNA was eluted with the desired volume of nuclease free molecular biology grade water (Sigma).

2.1.4. RNA agarose gel electrophoresis.

The same protocol was used for DNA as well. The integrity of 0.5-3µg total RNA was estimated by agarose gel electrophoresis. Total RNA was run on a 1.2% agarose gel (molecular biology grade agarose) prepared with RNAse free TE buffer (10 mM Tris/HCl pH 7.5 and. 1 mM EDTA). The gel was

prepared in a microwave oven and left to cool to 60°C. Ethidium bromide was added in a final concentration of 0.2µg/ml in the gel, as well as in the running buffer. Gels were cast and left to cool at room temperature. All chemicals were purchased from Sigma.

The gel was run on an RNAse free BioRAD gel electrophoresis apparatus at 5 V/cm in TE buffer. Results were visualised by photographing the gel on a UV transilluminator.

2.1.5. RNA quantitative and qualitative analysis by spectrophotometry.

RNA sample absorption at 260 and 280nm was read using a bench top spectrophotometer. The concentration of RNA was estimated by measuring the absorbance at 260 nm (*A*260) in a spectrophotometer. Readings that were greater than 0.15 were taken under consideration due to spectrophotometry limitations (*Maniatis et al.,* Molecular Cloning: A Laboratory Manual). All materials and reagents that were used were free of Rnases. For RNA analysis total RNA was dissolved in pure HPLC grade water (Fisher)

An absorbance of 1 unit at 260nm corresponds to 40µg of RNA per ml in pure water (*Maniatis et al.,* Molecular Cloning: A Laboratory Manual). The concentration and yield of total RNA in a sample was calculated by using the following formula:

Concentration of RNA sample = 40 x *A*260 x dilution factor (µg/ml)

Total yield = concentration x volume of sample (ml)

Purity of RNA was estimated by calculating the ratio of the absorbance readings of a sample at 260nm and 280nm (*A*260/*A*280). High purity is often indicated by ratios of 1.8 and above, when RNA is diluted in pure water (Wilfinger 1997)

2.1.6. RNA quality and quantity analysis by capillary electrophoresis.

For the purposes of qualitative and quantitative analysis of low amounts of total RNA, the RNA 6000 Nano Assay kit was performed using the Agilent 2100 Bioanalyzer. The limitations of quantitative range of the assay are 25-500ng/µl total RNA and 5-500ng/µl for qualitative range.

The reagents that were used for this assay were those in the RNA 6000 nano assay kit (Agilent) and the RNA 6000 ladder. (Ambion)

Gel-Dye Mix preparation

All gel-dye mix reagents were protected from light and stored at 4°C when not used. Firstly, 200µl gel matrix was filtered with a 0.2µm pore diameter filter column (provided with the kit) by centrifuging at 1500g for 10 minutes at room temperature.

Then 65µl filtered RNA gel matrix was mixed with 1µl RNA dye concentrate by vortexing into an RNAse free 1,5ml microcentrifuge tube. Tubes were then spun at 13000g for 10 minutes at room temperature.

Sample preparation:

The ladder was heated at 100°C for 5 minutes to eliminate secondary structure formation. RNA samples were denatured at 70°C for 2 minutes prior to loading.

Capillary electrophoresis chip preparation

To prepare the chip, 9µl of gel-dye mix were dispensed into the appropriate wells using the provided plunger according to manufacturers instructions

Loading the RNA 6000 Nano Marker and Ladder

5µl RNA 6000 Nano Marker was pipetted into the ladder and sample wells, prior to the addition of 1µl RNA 6000 ladder into the well ladder.

Loading the Sample

1µl sample was loaded in each of the 12 sample wells prior to vortexing the chip with an IKA vortexer for 1 minute. Chips were then loaded and run in an Agilent Bioanalyzer 2100 and results were acquired and analysed by the integrated Agilent software.

2.1.7. Amplification control spike preparation

Two hundred ng of total RNA of each sample was used as this starting amount was found to perform more linearly (see section **3.2.5**) In order to monitor the amplification and labelling process, four exogenous poly-adenylated prokaryotic controls were spiked directly into RNA samples just

prior to amplification and labelling to be used as positive controls to monitor the entire GeneChip eukaryotic target labelling process.

The same amount of *in vitro* synthesised, polyadenylated transcripts for *lys*, *phe*, *thr*, and *dap* genes of *B.subtilis* were spiked in each sample in the following concentrations below in Table 2.1

Poly-A RNA controls	Final concentration
lys	1:100000
phe	1:50000
thr	1:25000
dap	1:7500

Table 2.1 Concentrations of Poly aRNA control spikes in samples

Poly-A RNA Controls Final Concentration

All reagents were provided in the GeneChip® Eukaryotic Poly-A RNA Control Kit (Affymetrix).

2.1.8. First round RNA amplification

Materials for the first round of amplification were provided in the RiboAmp® OA 1 round RNA amplification kit (Arcturus).

First round first strand cDNA synthesis

Single strand cDNA was synthesised using an oligonucleotide that incorporated the T7 promoter at the 3' end of mRNA of 10µl total RNA-control spike mixture. 1ng (in 1µl volume) of the following primer was added:

[AAACGACGGCCAGTGAATTGTAATACGACTCACTATAGGCGC(T)24]

The mixture was heated at 65°C for 5 minutes to reduce secondary structure formation and the primer was left to anneal at 4°C for at least 1 minute.

Reverse transcriptase (buffer and reverse transcriptase premixes were included in the kit) reaction mixture was prepared and 9µl was added to the RNA template. RT-reaction at 42°C for 45 minutes was performed on a MJ Research thermal cycler. For amplification qualitative studies 2µl were removed. RNA was degraded by adding 2µl of provided RNAse mixture, incubating at 37°C for 20 minutes and terminating the reaction by 95°C treatment for 5 minutes.

First round Second strand synthesis

Second strand cDNA was synthesised by adding 1µl of random primers, incubating at 95°C for 2 minutes and chilling at 4°C for at least 2 minutes. Second strand reaction mixture provided, contained premixed Second-Strand Reaction Buffer, BSA (1mg/ml), DNA Polymerase I, RNase H, *E. coli* DNA ligase and ATP. 30µl were added to first stand cDNA reaction and incubated at 25°C for 5 minutes, 37°C for 10 minutes and 70°C for 5 minutes. Double stranded cDNA was then purified by cDNA affinity column purification methods using the mini columns provided. Double stranded cDNA was eluted in 11µl of pure nuclease-free water (Sigma).

In vitro transcription (IVT)

IVT reaction components (T7 RNA polymerase IVT buffer containing RNase inhibitor and DTT) were provided in the kit. All reaction components, apart

from T7 RNA polymerase, were brought to room temperature. T7 polymerase was added and 1.12µl reaction mixture were added to the double-stranded cDNA template and mixed. IVT was performed at 42°C for 3 hours in the MJ thermocycler, flicking and centrifuging tubes, once in the first half hour and then twice after one hour. Then reactions were brought to 4°C and left to react overnight. Remaining cDNA template was digested with 1µl DNAse I mix (provided in the kit) for 15 minutes at 37°C.

Amplified RNA (aRNA) generated from the IVT was purified using affinity column purification and eluted with 12µl nuclease free water (Sigma).

2.1.9. Second round amplification

For second round first strand cDNA synthesis the same method was used up to the purified double stranded cDNA stage (section 1.8) The modifications were that **a)** random primers primed the first strand synthesis and the T7-poly d (T) primer primed the second strand synthesis and that **b)** no nuclease digestion was performed at the end of the 1st strand synthesis. 2 µl pure double stranded cDNA were removed for semi quantitative RT-PCR studies for the purposes of validating array sensitivity.

IVT labeling reaction.

For second round amplification and labeling, the ENZO Bioarray™ High Yield™ RNA transcript Labelling kit was used. The following components

were mixed with the double-stranded cDNA of the second round second strand synthesis (containing the T7 promoter). All the product of the first strand synthesis after removal of 2µl i.e. 10µl was used for the IVT labeling reaction:

10ul purified cDNA

12ul DEPC H2O

4ul 10x Hy reaction Buffer

4ul 10x Biotin Labeled Ribonucleotides

4ul 10x DTT

4ul 10x RNase Inhibitor mix

2ul 20x T7 RNA polymerase

IVT labeling reaction was performed on a wet bench-top tube heating block at 37°C for 5 hours, flicking the tubes and briefly centrifuging, every half hour, to remix components.

cRNA generated from IVT labelling reaction was purified using RNeasy RNA Purification Mini kit (Qiagen) and using the RNA Cleanup Protocol according to manufacturer's instructions. 1µl of pure cRNA was assayed for purity and quantity by nanodrop machine using electric conduction to supply concentration and 260/280 ratios. 1µl was used for capillary electrophoresis to assay for cRNA integrity. All samples were diluted to a concentration of 1µg/µl with nuclease free water prior to fragmentation. 20µg of cRNA were used for fragmentation. The rest were kept in -80°C.

2.1.10. Fragmentation of cRNA.

Fragmentation was performed using the affymetrix fragmentation kit. The following components were mixed: 20μg in 20μl of pure water, 20μg biotin labelled cRNA (final concentration 0.5 μg/μl), 8μl 5x fragmentation buffer (200mM Tris-Acetate, pH 8.1, 500mM potassium acetate, 150mM magnesium acetate) and DEPC H2O to make the final volume to 40μl. The reaction mixture was incubated at 94°C for 35 minutes in an MJ bench top thermocycler. Reaction was terminated at 4°C.

2.1.11. GeneChip Hybridisation.

All components were provided by Affymetrix hybridisation kit. The following components were mixed to prepare the hybridisation cocktail, with DEPC H2O added to a final volume of 300μl.

Component	Volume	Final concentration
Fragmented cRNA 15μg,	30μl	0.05μg/μl
Control Biotin labelled oligo B2, 3nM,	5μl	50pM
20x Eukaryotic Hybridisation spike controls	15μl	
bioB		1.5pM
bioC		5pM
BioD		25pM
Cre (Affymetrix)		100pM
Herring Sperm DNA (10mg/ml blocking reagent)	3μl	0.1mg/ml
Acetylated BSA (50mg/ml blocking reagent)	3μl	0.5mg/ml
2x Hybridisation Buffer	150μl	

Final 1X concentration of hybridisation buffer was 100mM MES {12X stock: 70.4g MES free-acid monohydrate, 193.3g MES sodium Salt/L pH 6.6}, 1M [Na+], 20mM EDTA, 0.01% Tween 20.

The reaction mixture was denatured at 99°C for 5 minutes prior to applying to the GeneChip.

Hybridisation Conditions

Mouse 430_2 GeneChip (Affymetrix) was prehybridised using 200μl 1X hybridisation buffer (see above) at 45°C for 10 minutes at 60rpm. 200μl denatured Hybridisation cocktail was applied to the chip. The GeneChip was

hybridised for 16 hour at 45°C and 60rpm in a GeneChip Hybridisation Oven 640.

Washing and Staining of the GeneChip

The following wash and staining steps were carried out using an automated process using the GeneChip Fluidics Station 400:

- Post Hybridisation wash #1: 10 cycles of 2 mixes/ cycle with wash buffer A at 25°C - non-stringent (6xSSPE, 0.01% Tween 20)
- Post Hybridisation wash #2: 4 cycles of 15 mixes/ cycle with wash buffer B at 50°C -stringent (100mM MES, 0.1M [Na+], 0.01% Tween 20)
- 1st Stain: 10 minutes at 25°C (SAPE Stain: 300μl 2x MES stain buffer {41.7ml 12x MES, 92.5ml 5M NaCl, 2.5ml 10% Tween 20/ 250ml total volume in DEPC H2O}, 24μl 50mg/ml acetylated BSA, 6μl 1mg/ml Streptavidin-R-Phycoerythrin conjugate, 270μl DEPC H2O, 600μl total volume.
- Post Stain Wash: 10 cycles of 4 mixes/cycle with wash buffer A at 25°C
- 2nd Stain: 10 minutes at 25°C (Antibody Stain: 300μl 2x MES stain buffer {see above}, 24μl 50 mg/ml acetylated BSA, 6μl 10mg/ml normal goat IgG, 3.6μl 0.5mg/ml biotinylated anti-streptavidin antibody, 266.4μl DEPC H2O, 600μl total volume.
- 3rd Stain: 10 minutes at 25°C (SAPE stain: see above, 600μl total volume).

- Final Wash: 15 cycles of 4 mixes/cycle with wash buffer A at 30°C.

The GeneChip was filled with wash buffer A ready for the scanning procedure.

Scanning of GeneChips

GeneChips were scanned using an Affymetrix®. GeneChip®. Scanner 3000 system.

- 2x scans were conducted using the following settings: pixel value = 3µm, wavelength = 570nm
- Absolute and comparison analysis were conducted using the following settings for scaling: All Probe Sets: Target Signal = 500, Normalisation: Scale Factor = 1

2.1.12. Reverse transcription.

SuperScript™ III First-Strand Synthesis System (Invitrogen) was used with for reverse transcription of total RNA templates. All reaction components are included in the SuperScript™ III First-Strand Synthesis System kit (Invitrogen). DNA thermal Cycler 9600 was used for all reactions.

First-Strand cDNA Synthesis

1pg-5µg total RNA was converted into first-strand cDNA. All reaction components were mixed and briefly centrifuged before use. The following components were combined in a 0.2 or 0.5-ml RNAse free tube: total RNA of

up to 5 µg total RNA in a desired volume, 2.5 µM of oligo(dT)20, 1 µl of 10mM dNTP mix and made up to a final volume of 10µl with DEPC-treated water. The mixture was incubated at 65°C for 5 minutes, and then placed on ice for at least 1 minute.

The following cDNA Synthesis Mix was prepared, adding each component per reaction in the indicated order: 2µl 10XRT buffer, 4µl 25mM $MgCl_2$, 2µl 0.1M DTT, 1µl RNaseOUT. (40U/µl) and 1µl SuperScript. III RT (200U/µl). Then 10 µl cDNA Synthesis mix was added to each RNA/primer mixture

Reverse transcription reaction was incubated for 50 minutes at 50°C and terminated at 85°C for 5 minutes. Reaction tubes were then chilled on ice.

RNA was digested by adding 1µl RNase H (premixed) to each tube and incubating for 20 minutes at 37°C. First strand cDNA was stored at -20°C or used for PCR immediately.

2.1.13. Semiquantitative real time PCR.

Semiquantitative PCR (Q-PCR) reactions were carried out in 96 well optical reaction plates using cDNA that was generated from the same amount of total RNA, with the same RT protocol. 2µl of second round second strand double stranded cDNA (which at this stage has the T7 promoter incorporated) was used. The three repetitions of each SQ-RT PCR reaction came from the 3 independent repetitions of the array, i.e. from 3 different 12week old C57BL6

male mice. Each of the 2µl was diluted 10, 100, 1000 and 10.000 times to create 5 respective samples.

For Q-PCR reactions, the SYBR Green JumpStart Taq ReadyMix was used. Reaction mixtures contained: 20mM Tris-HCl (pH 8.3), 100mM KCl, 7mM $MgCl_2$, 0.4mM each dNTP (dATP, dCTP, dGTP, TTP), 0.05unit/µl Taq DNAPolymerase, JumpStart Taq antibody, and SYBR Green I. All reactions were performed in 50µl reaction volumes that contained 1XSYBR Green JumpStart Taq ReadyMix, 1X internal reference dye, 400nM each of plasmid-specific primers, and various concentrations of template DNA.

Amplification of GAPDH mRNA was performed as the internal control gene. Target and control GAPDH gene forward and reverse primers were designed to amplify a 365bp gene fragment and spanned introns. These are listed in appendix A.

The PCR was initiated with a 1-minute denaturation step at 95°C. Initial denaturation was followed by 40 cycles at 95°C for 15 seconds, 1-minute annealing at 60°C, and 1-minute extension at 72°C. Cycling was followed by a 4°C hold. The PCR assay was performed using the ABI Prism 7700 Sequence detector (Applied Biosystems) and ABI Prism 7700 software. The threshold cycles (Ct) were calculated using ABI Prism 7700 Software (Applied Biosystems). Normalisation was performed against *GAPDH* using the using the Comparative cycle threshold (C_t) Method, using the following equation:

Relative Expression = $2^{Ct\,(GAPDH) - Ct\,(Target)}$, where Ct is the cycle threshold.

While this method includes a correction for non-ideal amplification efficiencies (i.e., not 1; Reference 21), the amplification kinetics of the target gene and reference gene assays must be approximately the same. To validate that the amplification efficiencies were similar the slope of the plot of log cDNA dilution versus ΔCT was calculated and the reaction efficiencies were considered similar if the slope was less than 0.1 (Livak & Schmittgen, 2001).

Five µl of reaction end products were run on a 2% agarose gel to ensure reaction specificity.

2.2. Immunohistocytochemistry methods

2.2.1. Wax-embedding of corneal tissue.

Corneal excision

For all mammals, apart from *rattus* and *mus musculus* species, the corneas were excised by scoring the sclera 2mm away from the cornea with a clean scalpel, two to three hours after the sacrificing. Eyes were transported on ice. For the *rattus* and *mus* species, the front half of the eye was dissected by scalpel under a dissection microscope, after it had been enucleated and directly transferred on chilled PBS pH 7.4 (phosphate buffered formalin). All corneas used were examined to ensure the absence of scars or wounds.

Fixation

Mouse, rat, porcine, bovine and rabbit eyes corneas were dissected, human corneas were donated from the National Eye Bank (Bristol) and also were

fixed in 10%NBF (neutral buffered saline) and embedded in paraffin wax. The corneas were dehydrated by immersion in 50% v/v ethanol/H_2O for 30 minutes, 70% ethanol for 60 minutes, 90% overnight and finally in 100% for 60 minutes.

Paraffin Embedding

Samples were fixed in 50/50 alcohol-chloroform solution for 30 minutes, 100% chloroform for 30 minutes and 100% fresh warm chloroform 30 minutes. The samples were transferred to a bottle of molten paraffin wax (60°C) and placed in a 60°C incubator for one hour. Wax was refreshed and samples were incubated for a further 30 minutes. Then, by using a clean pair of forceps, the corneas were taken out of the wax bottles and placed in moulds half-filled with wax, topped up with more paraffin wax, and then left to start solidifying on a cold plate. After approximately 30 minutes, the blocks were placed in a refrigerator at 4°C.

Wax sectioning

Sections of 7μm were taken from all the wax embedded corneas and stored in paper trays. Adjacent sections were floated on cold water, then transferred to a 40-45°C water bath containing 1/50 v/v Mayers albumin. The straightened sections were laid side by side on Histobond® RA positively charged glass slides (LAMB, UK). The slides were than placed on a hot plate at 60°C for 30 minutes before they were transferred to a 60°C oven overnight, in order to allow the tissue to dry and adhere on the glass slide.

2.2.2. Preparation of Frozen Sections

One human, two pig and two bovine fresh corneas and three albino rat eyes were cryo-fixed in a container of isopentane that was submerged in liquid nitrogen. Then the frozen corneas were placed in moulds that were filled with OCT embedding medium and the blocks were frozen in liquid nitrogen, and subsequently stored at - 20°C.

Sectioning of frozen corneas.

Eight μm thick sections were obtained by using a cryostat at –18°C. Sections were transferred to Superfrost Plus® glass slides (Mayer-Clase) and left to air dry for six hours. Then the slides were used for staining according to the following protocol. Sections were transferred to acetone (Sigma) for 10 minutes. Sections were air-dried and, at room temperature, washed in 1xPBS for 5 minutes and placed in a humidified chamber.

2.2.3. Immunostaining Procedure

Antibodies that were used are listed in appendix D. Bis-benzimide (Hoechst) was used as a counter-stain. Negative controls were used for each antibody.

Wax sections were fixed in xylene (BDH) for 5minutes, transferred to fresh xylene for a further 5minutes, then transferred to two changes of 100% ethanol (BDH) for 1 minute, 1 minute in 90% ethanol (v/v), 1 minute in 70%

ethanol (v/v) and 1 minute in 50% ethanol (v/v) before rinsing in running water for 10 minute. Finally sections were immersed in 1x PBS for 10 minutes. At this point the previously air-dried frozen sections were subjected to the same procedures as the wax sections.

Proteinase K (20μg/ml) digestion followed for 20 minutes. For intracellular protein immunoreactions sections were treated with 0.2% Triton-X 100 (Sigma) for ten minutes followed by 3 washes of 1xPBS (3 minutes each) only in cases that no blocking was used. For blocking and background reduction, a solution of 5% normal serum (from secondary antibody host species) 5% BSA (bovine serum albumin) in PBS was applied for 30 minutes. Sections were then circled using a paraffin pen. Primary antibodies, diluted in PBS, were deposited on separate sections. Appendix B lists the antibodies and their concentrations that were used for this study. For control sections either 1xPBS or the appropriate control IgG type was used. The antibodies were left to probe the tissue overnight in the hermetically closed humidity chamber. Then the sections were washed three times in 1xPBS for 3 minutes. The secondary FITC conjugated anti-mouse-Fc-fragment antibody or donkey anti-goat AlexaFluor 488 (Molecular Probes) was applied (after making sure that no droplets were left on the tissue from the previous PBS wash) on the sections at a 1/320 or 1 in 1000 dilution. Sections were incubated for 2 hours. The slides were washed three times in 1x PBS for 3 minutes in order to remove any unbound secondary antibody.

Counter-staining and mounting

Bis-benzimide (Hoechst 33345) was diluted in water-soluble Hydromount (BDH) at 2μg/ml concentration. Sections were mounted in the Hydromount and wrapped in foil to prevent bleaching.

Imaging

Images of immunostained sections were acquired using a Leica DM RAZ microscope integrated with a Leica DC500 digital camera using Leica QFluoro software. For all the sections images using a FITC (excitation wavelength 590nm, emission wavelength 520nm) filter and a DAPI filter (excitation 372nm, emission 456nm) were captured.

2.3 Tissue source of microarray and Semiquantitative RT-PCR studies.

Three male, C57BL6 mice that were kept in different cages under the same diet plan and the same light conditions for 3 weeks in the animal house were sacrificed at 12 weeks of age in order to obtain their corneas for Microarray analysis and subsequent semiquantitative RT-PCR studies.

Chapter 3

Method Development:

Optimisation of laser-assisted cell microdissection and RNA linear amplification techniques.

3.1 In vivo Gene Expression analysis methods.

Defining genes differentially regulated in cell populations enriched either for stem, transient-amplifying or differentiated epithelial cells initially required a reliable method which permits accurate isolation of cells from histological sections whilst preserving RNA integrity. Additionally, selection of specific cells imposed limitations on the number of cells that were to be isolated. To overcome such limitations and acquire enough labelled cRNA for high density oligo-array analysis, a robust linear RNA amplification protocol was developed.

The development of methods related to the isolation of specific cells as well as the identification of linear amplification is presented in the "laser assisted microdissection methods" and "linear amplification" parts of this chapter.

3.1.2 Laser Assisted Microdissection Methods

3.1.2.1 Aims

The aim was to identify the most appropriate method of isolating single cells from histological sections with high RNA recovery and minimal impact on RNA integrity.

3.1.2.2. Introduction

There are several methods of isolating cells from a histological section. The criteria for the suitability of the method of selection were that:

a) It would not require preparatory sample treatments that are deleterious to RNA integrity and quantity or may contaminate RNA with chemicals affecting PCR and reverse transcription reactions,
b) The method itself would not inflict damage on the RNA molecules to the extent that would prevent RNA amplification,
c) The technique should isolate single cells or a small number of cells in order to distinguish between epithelial layers with minimal to no contamination by unwanted cells
d) Since the method is intended for single cell isolation, the RNA damage needs to be assessed for single cell resolution

There are two microdissection methods that are suitable for functional microgenomic applications, both are laser-assisted: laser capture microdissection (LCM) and laser microdissection and pressure catapulting (LMPC). This study compared the two methods with respect to the damage each technique inflicted on mRNA. As an indication of damage, a 3'-5' RT-PCR assay was developed in which the ratio of 3' to 5' end of a selected gene was determined by semi-quantitative RT- PCR.

The first demonstration of laser microdissection of cells for expression analysis came from studies of Eberwine on single microdissected neurons (Eberwine et al. 1992). Both methods have been used successfully in recent years (for LCM: Kobayashi et al. 2004; Glanzer and Eberwine 2004; Fukui et al. 2005 Barrier et al. 2005, for LMPC: Miyoshi et al 2005) bringing forward for the first time the possibility to focus gene expression profiling to the specific cell types of interest, opening the way for functional microgenomic analysis of cells. They allow researchers to shed light to the specific function of a cell type in a particular tissue and the signalling pathways used by cells to a single cell resolution. This gave a new and deeper understanding of how cells function and are organised into tissues as well as to the strategies of tissue homeostasis and repair (Luo et al. 1990) and gave a better understanding of cancer development (Leethankul et al. 2000; Alevizos et al. 2001; Luzzi et al. 2001).

Both microdissection techniques utilise lasers. In order to use cells, that have been previously microdissected by laser, for gene expression analysis it is important to select a method that will impose minimal damage to the RNA inflicted by the lasers. Such a method should deliver minimal heat transfer to the RNA molecules either by utilising lasers at wavelengths that are not the absorbtion maxima of RNA or in some other way. There is a plethora of studies analysing the effect of lasers on cells. Figure 3.1 reviews and condenses all of the known effects of UV wavelengths on cells and macromolecules according to absorption maxima (a) or relative response per photon (b). The UV spans a large region of the spectrum. It is arbitrarily

divided into three regions, which are UV-C (200-290 nm), UV-B (290-320 nm) and UV-A (320-400 nm). Of these, only UV-C is known to cause mutations, as nucleic acids and proteins are maximally excited at the UV-C as we can see in Fig. 3.1a.

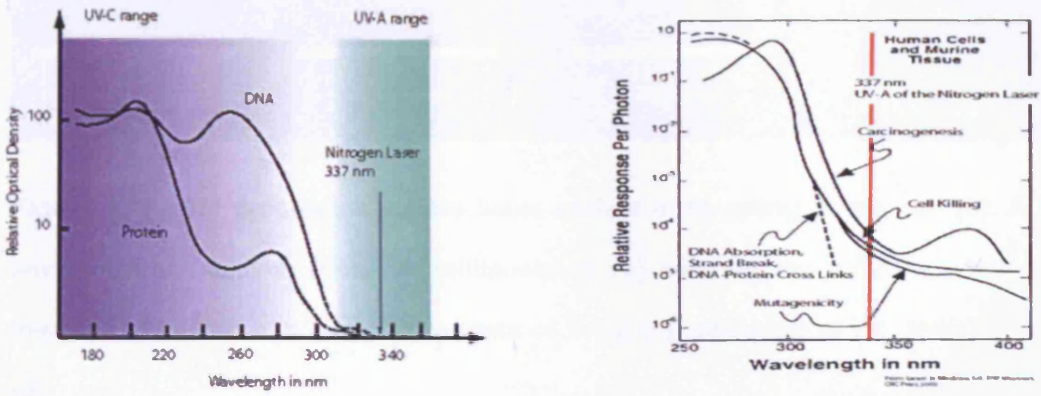

Figure 3. 1a) Absorption maxima of nucleic acids and proteins within the 200-290 nm (UV-C) and b) the effects of wavelength on cells presented as relative response per photon (proportional to thermal energy absorbed by molecular bonds) note that at around 337nm the relative response per photon count is minimal levels 3, adapted **from Lasers in Medicine, Ed.: R. W. Waynant, CRC Press, 2002**

3.1.2.3. Laser Capture Microdissection

This method makes use of an inverted microscope, fitted with a near-infrared laser. Histological tissue sections are mounted on standard glass slides. A cap, fitted with a transparent, 100-µm-thick, ethylene–vinyl acetate film, is then placed over the section (see Figure 3.2). A very low energy guide beam

is used to select a location on the tissue section. Then a laser is fired which provides enough energy to transiently melt the thermoplastic film in the selected location, binding it to the targeted cells.

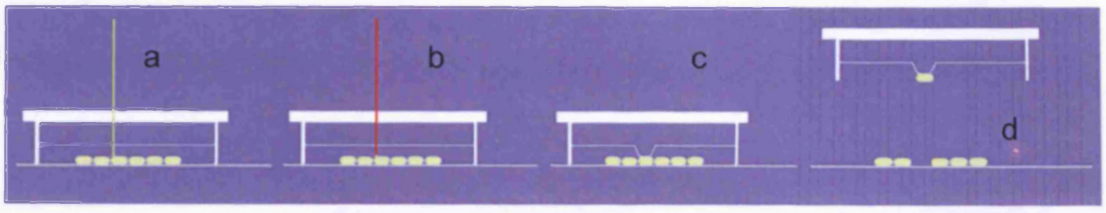

Figure 3. 2 LCM process: a visible laser assists in targeting of the cell (a). A higher energy laser beam is fired for milliseconds (b) causing the ethylene vinyl acetate membrane to melt and curve at the site of firing (c), attaching to the cell(s) of interest (d).

The laser diameter can be adjusted from 7.5 to 30μm so that individual cells or a cluster of cells can be selected. Although the plastic film absorbs most of the thermal energy and the pulse lasts for a fraction of a second, hence some damage to biological macromolecules is expected to occur.

3.1.2.4. Laser Microdissection Pressure Catapulting.

This technique utilises an inverted microscope equipped with a guided 337nm nitrogen laser. A laser micro-beam precisely circumcises a selected area from $1/100^{th}$ to 100 μm diameter, spanning from chromosomes to large tissue areas with a clearly cut gap between selected and non-selected areas (Fig. 3.3a and b. In addition, unwanted cells can be selectively destroyed with a few laser shots to achieve entirely homogeneous samples. The driving force of the catapulting of cells is the expansion of microplasma induced by the laser. The

process is performed with a pulsed nitrogen laser and not an infrared laser, therefore heat formation during the ablation process is minimised and there is no heating of the selected sample or of the adjacent material. Hence, the biological information of the selected specimen and the neighbouring material remains unimpaired.

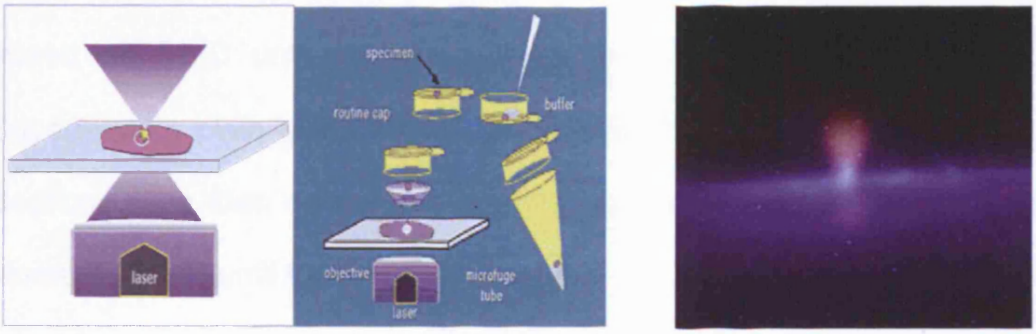

Figure 3. 3 a) The inverted microscope laser platformb) specimens are catapulted in microcentrifuge caps c) example of microplasma at the focal point of the LCM pulse picture taken by Dr. A. Vogel, Medical Laser Laboratory Lóbeck, Germany.

3.1.2.5. Determination of the least destructive cell isolation technique

The two methods were evaluated with respect to the damage that each inflicted on mRNA. As an indication of the damage, a 3'-5' RT-PCR assay was developed in which the ratio of 3' to 5' end of a selected gene was determined by semi-quantitative RT- PCR. The method is described in detail in section 3.1.3.3.

3.1.3. Materials and methods.

3.1.3.1. Tissue source and processing

Three mouse corneas were dissected from eyes of different 6-9 week old male C57BLC mice. Each cornea was treated with RNALater (Ambion) at $4^{O}C$, overnight then snap-frozen and embedded in OCT (Lamb) and then stored at $^{-}80^{O}C$ until sectioned. 7μm sections were collected on either Superfrost or plain glass slides (LAMB) at $-20^{o}C$, using a Leica cryotome. Sections were then dehydrated in 70% ice cold ethanol for one minute and stored at $-80^{O}C$ until further use.

On the day of cell isolation, sections were transferred on dry ice or in liquid nitrogen and were only removed from the coolant when they were to be processed. On every occasion, sections were processed one at a time. To process, the tissues were removed from liquid nitrogen, placed in 70% ice-cold ethanol for 10 seconds then stained with 0.1% cresyl violet acetate (in 50% ethanol) for another 30 seconds. Next sections were briefly dipped in nuclease free molecular biology grade water and dehydrated again in 50%, then 70% ethanol for 30 seconds each, followed by two one-minute washes in 100% ethanol. They were left for one minute to dry before microdissection.

For LCM, an additional protocol was used in which an end step was added, which involved two more washes with 100% xylene, each lasting one minute, to make the tissue more brittle.

3.1.3.2. Laser Assisted Microdissection.

To address the effectiveness of both microdissection methods, a thousand cells were isolated as single cells or as 20 cell tissue fragments by LCM and LMPC. For LCM, the Arcturus PixCell IIe LCM Instrument was used and "Laser Microdissection and Pressure Catapulting" was performed on a PALM microlaser platform. In both systems, there is a high resolution digital camera coupled and integrated with a software interface for capturing images.

3.1.3.2.i. Laser Capture Microdissection (LCM)

For this procedure only Superfrost slides were used to avoid undesirable tissue detachment. After the tissue was prepared, it was flattened gently using Arcturus strips so that there are no anomalies before the thermoplastic cap was placed on top. Histological slides were placed under the Arcturus microscope and the desired area was focussed. Then, the desired laser diameter, power (mW) and duration of the pulse were selected from the system interface. Under direct visualisation, a few test shots in an area of the

plastic that is not above the tissue section were fired in order to confirm that the desired surface area of the thermoplastic cover was activated with the minimal laser power and duration. This varied between sections depending on the shape of the section. The power and time of the laser beam pulse were usually set on 40mW and 30msec achieving a 15μm diameter indentation.

3.1.3.2.ii. Laser Pressure Catapulting (LMPC)

For this procedure only plain glass slides were used to facilitate cell catapulting with the minor laser power. Following tissue preparation, the slides were placed under the microscope of the PALM platform. First an area of no interest was located in the tissue. Using the setting called "close-cut" in the user interphase, the laser was programmed to cut a 0.1μm path at an indicated position. The laser focus and power were tested for cutting. Then, for the catapulting pulse, the laser focus and power was also tested and adjusted. Following testing, areas of interest were located and focussed. Using the user interface the areas of interest were highlighted and assigned a number. Then a standard 0.5ml PCR tube cap, which contained a 10μl droplet of PCR grade mineral oil (sigma) in the centre, was placed directly above the section by an automated arm. After laser activation, the desired area was isolated and the user was prompted to change the cap for the next area of interest, having to reactivate the laser. The laser settings for focus and power were given from the interface in a 1-100 scale bar. The focus varied between sections due to variations in slide thickness (even a 0.1μm deviation needed to be adjusted for). The power of the laser never exceeded 65% of the total laser power.

Directly after each laser session, isolation caps were placed on their corresponding tubes. Tubes were labeled and placed in liquid nitrogen and subsequently stored at -80^{O}C for no more than a week, until they were subjected to RNA isolation.

3.1.3.2.iii. Image Capture

Pictures of the areas of the tissue before and after the cells were isolated were taken with a high resolution digital camera coupled with the inverted microscopes to document each cell sample. Successful and unsuccessful isolations were counted on the basis of acquired cells in the cap, in order to assess the success rate of each type and method of isolation.

3.1.3.3. RNA isolation and 3'/5' PCR amplification assay.

Control RNA from three fresh whole mouse corneas and total RNA from microdissected cells was isolated using the Rneasy mini kit (Qiagen). Total RNA samples from the three fresh corneas, as well as from three independent cell pools isolated by LCM and LPC, were reverse transcribed using recombinant reverse transcriptase Superscript III (Invitrogen) as described in section **2.1.3**. and **2.1.12**. The total volume of reaction was 50µl.

Then 1µl of each cDNA from each of the three control and each experimental samples was subjected to PCR amplification of the 3' and the 5' end of

GAPDH. In order to amplify a 150bp fragment of the 3' and the 5' end, the following respective primers sets were used:

	3'end region	5'end region
Forward	**TCTCCATTGGTGGTGAAGACA**	**GCCTCTCTTGCTCAGTGTCC**
Reverse	**ACTCCACTCACGGCAAATTC**	**TGCGACTTCAACAGCAACTC**

Table 1. GAPDH primers used for the 3'-5' assay.

Control cDNA samples were diluted 10^4 times, prior to PCR, to prevent subsequent saturation of the gel bands after PCR. PCR products were run on a 1.2% agarose gel stained with 0.01 ethidium bromide and photographed under UV using a gel-doc system, as described in section **2.1.4**. Gel band intensities were calculated by Image J software available from the NIH website, www.nih.gov. The relative degradation (%) of mRNA was calculated using the following equation:

$$\left.\begin{array}{l} \dfrac{\text{3prime intensity of Positive Control}}{\text{5prime intensity of Positive Control}} = C \\ \dfrac{\text{3prime intensity of Experimental}}{\text{5prime intensity of Experimental}} = E \end{array}\right\} \Rightarrow \text{\% Degradation} = \frac{C-E}{C} \times 100$$

3.1.4. Results

3.1.4.1. Minimum amount of cells that could be isolated by LCM were 5-10, whilst by LMPC single cells were reproducibly isolated.

Pictures of the areas that cells were isolated from are presented in the following figure (**Fig. 3.4**) depicting a typical result of a cell isolation by each method.

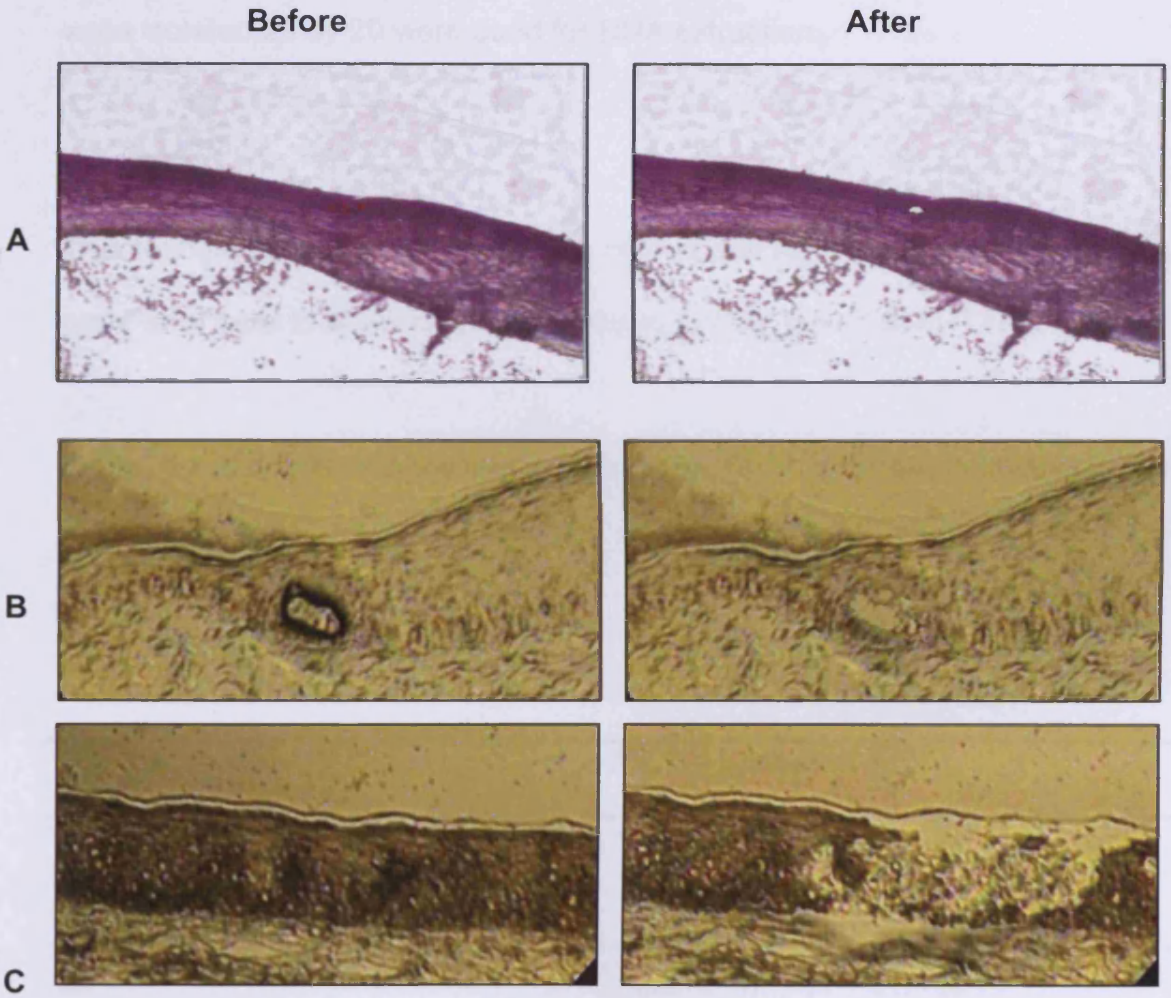

Figure 3. 4 Corneal epithelial tissue sections before and after microdissection. Single cells isolated by LMPC (A). Tissue isolated by LCM: 5-10 cells (B) and 100 cells (C).

LCM

It was observed that LCM success rate improved dramatically by the addition of the end step involving the xylene wash (Table **3.1**). For sections that were not treated with xylene, usually the whole tissue section would detach when the LCM cap was removed. Even when xylene was used, single cells could not be isolated. The least amount of cells that could be isolated by LCM was 5-10. As the success rate for LCM was very low, only samples of cells that were isolated 20 by 20 were used for RNA extraction.

LMPC

This technique had a 100% success rate in cell isolation independent of the number of cells to be isolated with a single laser pulse. (**Table 3.1**)

Table 3.2 summarises the success rate of each type and method of cell isolation

Number of cells	*% Success Rates for 100 isolations.*		
	LCM no xylene	*LCM xylene*	*LMPC*
1	0	0	100
20	10	32	100

Table 3.2 Success rates of different cell isolation methods. Successful were counted as the isolations where only the desired cells were clearly isolated in the cap.

3.1.4.2. LMPC microdissection imposes significantly less degradation than LCM as confirmed by 3'-5' ratio analysis of GAPDH.

The percent (%) relative degradation of GAPDH mRNA transcripts, measured for each isolation was used in order to assess the order of damage to RNA by each technique. Using this measure, it can be observed that LCM imposed more than six times degradation on GAPDH mRNA transcripts than LMPC as seen in Fig. 3.5A (see red and yellow columns). When cells were isolated in tissue fragments containing 20 cells each (20 at a time) by both techniques only 2.2% more mRNA transcripts were not full length for cells isolated by LMPC in comparison with fresh cells. In the case of LCM % relative degradation was 13.8% (see Fig. 3.5A).

This means that in LCM degradation of RNA is higher than that inflicted by LMPC when a comparable surface area is isolated.

As can be seen in **Fig. 3.5a**, even when single cells were isolated, approximately 3% of the mRNA is not full length transcript. That is not to say that from this 3% no information would be detectable by microarrays, since Affymetrix arrays calculate the signal from probe sets that correspond usually to 3' end areas of transcripts.

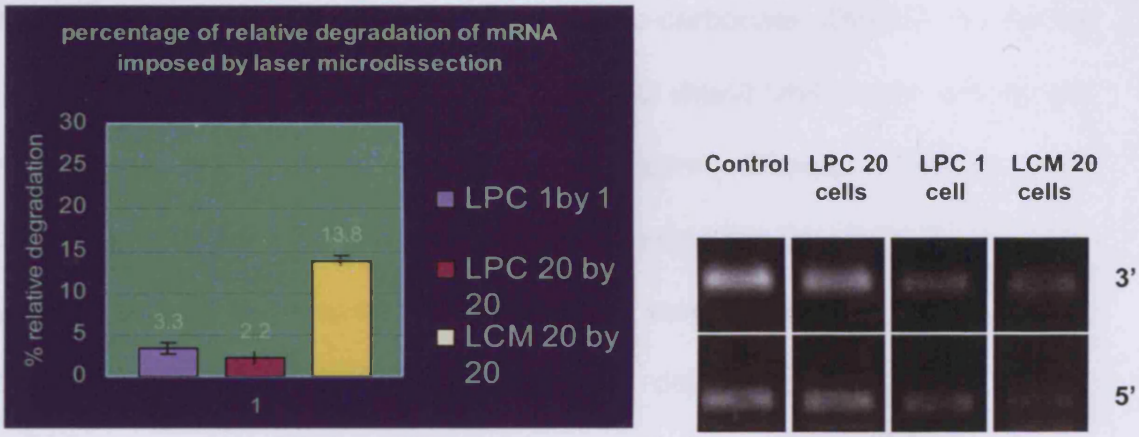

Figure 3. 5 a) Percentage of relative 5' degradation compared to control total RNA. LPC allowed for isolation of cells with intact total RNA showing a 3.3% (± 0.4) relative degradation for single cells. This degradation was less then LCM, which demonstrated 13.8% (± 0.9) for cells isolated 20 by 20, as confirmed by 3'/5' amplification. a) Gel electrophoresis of 3'-5' GAPDH PCR following isolation of cells using different techniques.

3.1.5. Discussion

3.1.5.1. The method prevented RNA degradation due to Rnases as well as chemical modification of RNA.

RNA degradation may occur due to Rnase digestion or by extreme local free energy that could arise with radiation or heat. External RNases were avoided by using solutions and apparatae that were Rnase free or that RNases have been blocked by treatment with di-ethyl pyro-carbonate (DEPC). As far as internal Rnases are concerned, the factors that would limit Rnase activity are temperature, presence of inhibitors and water. Internal RNases were controlled by using a Zn^{++}- based fixative, reducing the time that the tissue is hydrated as well as keeping the temperature very low ideally throughout the complete processing time. When tissue is dehydrated Rnase activity is significantly limited. Also by reducing the free energy of the environment, the enzymatic reaction rates are reduced. RNases have extremely low activity at -80°C, although they do possess activity at temperatures above -50°C. Nevertheless reaction rates are so low that weeks are needed until RNA degradation is detectable. There are several Rnase inhibitors. In most of the cases they are not recommended when RNA is to be used in PCR-RT-PCR reactions because carryover amounts can be deleterious to such reactions. The best solution for blocking internal RNases is a Zn^{++} solution. The commercial name of such a solution is *RNALater*® (Arcturus, UK) which protects RNA in the tissue for a week at room temperature and indefinitely at -20°C. When tissue is removed from the solution it is protected for a further 10 minutes.

To avoid any degradation of RNA due to internal RNases, the staining and tissue preparation protocols were designed to keep the tissue dehydrated as much as possible. Some chemicals used as fixatives or dyes in traditional histology protocols have a devastating effect on the RNA due to chemical modification of RNA species. RT-PCR reactions can be impaired as a result of carryover formalin (Masuda 1999). It has been observed that RNA becomes resistant to extraction (Finke 1993) probably due to cross-linking with proteins (Park 1996). Thus traditional protocols were not recommended for use in microdissection with regards of gene expression profiling (*in situ* hybridisation can be performed with success using formalin fixed tissue). That does not come as a surprise, since during *in situ* hybridisation, the only reaction that takes place involving the tissue is the hybridisation itself. Degradation of mRNA in that case can also be beneficial since it can reduce mRNA secondary structure formation. In the protocol that was developed and used tissues were immersed in RNA later, then cryo-fixed, embedded and stored at -80°C to minimise RNA degradation.

Determining a suitable histological stain in order to easily isolate cells was also of concern. One could argue that haematoxylin/eosin staining does not interfere with DNA or RNA preparation and it is one of the most routinely used histological procedures. However for staining and distaining the tissue effectively from haematoxylin itself, more than one minute should be given in water or blueing solution, increasing the time that the tissue remains hydrated.

On the other hand, cresyl violet acetate can be dissolved in ethanol and it is a basic dye that stains nucleic acids. The name is 9-Amino-5-imino-5H-benzo(a)phenoxazine acetate salt the molecular formula is:

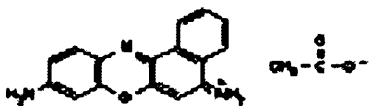

Figure 3. 6 9-Amino-5-imino-5H-benzo(a)phenoxazine acetate salt (Cresyl violet acetate).

It is soluble in ethanol as well as water and therefore allows for tissue staining and distaining to be performed in 50%ethanol instead of pure water, thus maintaining tissue in dehydrated state. Staining and distaining takes less than 30 seconds and therefore cresyl violet acetate was the preferred stain prior to microdissection of cells that were to be analysed for gene expression profiling.

3.1.5.2. LMPC proved ideal for expression profiling and had less an effect on RNA integrity than LCM

RNA degradation due to UV light was reduced greatly by using a Laser pressure catapult microdissection system.

A microplasma is a state of matter consisting of free electrons, ions and other species created when molecular bonds are broken because the sum of photon energy is equal to or greater than the energy of molecular bonds. This becomes more probable in the focus of the laser beam because multiple photons interact with the molecular bonds of biomolecules providing energy to bonds exceeding 3.6 eV. Therefore the microplasma is created only in the focus of the laser beam which is far less then micrometers in diameter.

The plasma has a tremendously high expanding velocity and it is created, expanded and collapsed in nanoseconds. The plasma expansion is the driving force for the catapulting process. The time for heat transformation to the boundaries of the cutting path is much too short which eliminates any chances of heat transfer outside the area of the microplasma so any unwanted degradation of biomolecules is prevented. This was reflected in the results of 3'/5' ratios identified following cell isolation by the two methods.

LMPC imposed far less degradation on RNA then LCM. It was also observed that the size of the isolated region in LMPC had a very limited effect on the overall quality of the resulting RNA. Even when single cells were isolated, the effect of the laser had no significant catastrophic effect on RNA integrity. Moreover it facilitated a more accurate selection of cells because of the small thickness of the target beam.

The results suggest that mRNA from cells isolated by LMPC and LCM is highly suitable for Affymetrix array analysis, since the manufacturer

recommends that a 3'/5' ratio of 1.5-2 (25-50%) is adequate. Nevertheless, because more downstream reaction steps such as amplification and labelling are going to impose their own effect on the final cRNA transcripts prior to fragmentation and loading, the less degraded the RNA is in the beginning, the better the quality and reliability of the array results will be. The results therefore indicated that LMPC is the "safest" choice when it comes to gene expression profiling

LMPC also eliminated the need for non-transfer controls which were essential for the LCM since the membrane is in direct contact with the tissue and can result in isolation of unwanted cells. As it is stated in the results section usually during LCM complete tissue section or large areas would be lifted with the LCM cap necessitates such controls.

3.1.5.3. Conclusion

LMPC has proved to be the most reliable method for laser microdissection of cells from histological sections, regarding the use of cells for gene expression analysis. It reproducibly and accurately selected for the desired cell without imposing RNA damage that would disable gene expression analysis by high density oligonucleotide arrays. There was no previous literature on the comparative effect of the two techniques on the RNA as well as their comparative advantages and disadvantages as far as microdissection for gene expression analysis is concerned.

3.2. LINEAR RNA AMPLIFICATION

3.2.1. Aims

The aim of the experiment was to identify a method for amplifying small amounts of mRNA linearly in order to acquire adequate quantity for microarray analysis.

3.2.2. Introduction

The amount of labelled mRNA needed in order to perform gene expression analysis with Affymetrix arrays is about 25μg. The labelling process is an *in vitro* transcription (IVT) reaction using cDNA as a template to transcribe it to RNA called cRNA or aRNA and incorporates biotinylated nucleotides into the newly synthesised RNA. The amount of total RNA that is obtained from cells that were laser micro-dissected is several orders of magnitude lower to that required. Therefore to perform mRNA analysis with microarrays an RNA amplification process must be performed on the mRNA of the samples obtained from the laser microdissected cells.

The important prerequisite when performing RNA amplification for use in gene expression studies is that the process should not change the relative abundance of gene transcripts of the initial sample. In more detail, mRNA is a complex mixture of several copies of each gene transcript. Genes can be transcribed from one to tens of thousands of copies per cell. It is apparent that

in a comparative gene expression analysis, it is essential that genes transcribed to any abundance should be amplified to the same degree.

PCR based amplification efficiency greatly depends on the sequence to be amplified. Additionally, several regions of one gene transcript could then serve as primers to other transcripts and the result would be a greatly distorted. It would be unfeasible to amplify RNA with a PCR based protocol linearly. Therefore the protocol selected to amplify the mRNA linearly was transcription based. In IVT, a T7, T3 or SP6 RNA polymerases are commonly used. The most commonly used mechanism for RNA amplification is a T7 based linear amplification method first developed by Van Gelder, Eberwine and coworkers (Van Gelder et al. 1990, Eberwine et al. 1992). This method utilises a synthetic oligo(dT) primer containing the phage T7 RNA polymerase promoter to prime the synthesis of first strand cDNA by reverse transcription of the poly(A)+ RNA component of total RNA. Second strand cDNA is synthesised by degrading the poly(A)+ RNA strand with Rnase H, followed by second strand synthesis with *E. coli* DNA polymerase I. Amplified antisense RNA (aRNA) is obtained from *in vitro* transcription of the double-stranded cDNA (ds cDNA) template using T7 RNA polymerase.

Several IVT and in particular T7 RNA polymerase based methods have been presented for the amplification and labeling of small quantities of total RNA, which is then suitable for high density oligonucleotide microarray analysis.5–7, as well as cDNA microarray analysis.8–10. However, the overall sensitivity and reproducibility of linear transcript amplification is still under-documented.

In order to assess the linearity of RNA amplification, understand the limitations of the technique and also evaluate the amount of RNA to be used as the starting amount for linear amplification, an initial, small scale gene expression experiment was conducted using total RNA from human corneal epithelial cells from the 2.040 pRSV-T cell line as a gold standard. From that, 2μg, 500ng, 50ng and 10ng were amplified, labeled and hybridised on high density oligo-arrays. In this way, any changes that RNA amplification imposed on gene transcripts would become evident and then quantified by comparative gene expression analysis of non-amplified vs. amplified samples.

3.2.3. Materials and methods

3.2.3.1. RNA isolation, quantitation & electrophoresis.

RNA was isolated using Trizol from 1.8 $x10^5$ cells of the human corneal epithelial 2.040 pRSV-T cell line as described in section **2.1.2**. Cells were counted with a haemocytometer. RNA quantity and purity was estimated by spectrophotometry at 260, 280 nm using a Boeco bench-top spectrophotometer. Twenty μg of total RNA was digested with 10 units of DNase I (Stratagene) in premixed DNAse I buffer provided, for 15 minutes, at 37°C, then cleaned-up of any solvents and DNase with RNeasy columns as described in section 2.1.3. RNA integrity was assessed by gel electrophoresis. For gel electrophoresis 1.2μg was run on a 1.2% agarose gel in TE buffer, staining for nucleic acids with ethidium bromide as described in section 2.1.4. The RNA was processed immediately after cleanup.

3.2.3.2. Amplification

Four samples of different amounts of the cleaned total RNA were amplified. The four samples represented the corresponding amount of RNA derived from $2.4x10^5$, $6x10^4$, 6000 and 1200 human corneal epithelial cells from the 2.040 pRSV-T cell line as spectrophotometric quantitation indicated. The RiboAmp™ OA RNA Amplification (Arcturus) kit was used according to the manufacturer's instructions. Briefly, the RNA was reverse transcribed to cDNA and T7 polymerase promoter was incorporated by using a poly d(T) T7promoter. Second strand synthesis followed using exogenous primers. The RNA strand was digested with Rnase H pre-diluted in appropriate buffer according to the kits manufacturer's instructions. Then cDNA was cleaned with column purification. 2µl from each sample was removed and stored at -20°C.

I*n vitro* transcription utilising T7 RNA polymerase yielded antisense RNA. The aRNA was then reverse transcribed to cDNA and double-stranded (ds) cDNA synthesis followed to generate ds cDNA which is compatible with the ENZO labelling kit for Affymetrix arrays. The IVT products as well as the initial RNA were analysed by the Agilent Bioanalyzer RNA pico chip. Then cRNA was fragmented and hybridised on Test3 Affymetrix arrays to reveal linearity of amplification.

3.2.3.3. Analysis

Probe sets were analysed with Affymetrix Microarray suit software. The software performed background subtraction. The three chips were normalised

so that the trimmed mean of intensity values, excluding the top and bottom 2% of intensities. A scatter plot of the $\log_2$ signal intensity was generated between non-amplified and each of the amplified samples.

]

3.2.4. Results.

3.2.4.1 Total RNA starting amount, as little as 50ng, produced enough template for RNA labelling

Amplification by this protocol resulted in aRNA quantities of at least 1µg which is enough to use in labelling IVT reactions. The amplification (Amplifn) factor is an estimated value based on the fact that mammalian mRNA content of total RNA is about 1%. This is estimated firstly to acquire an idea of reaction performance (see Table 3.3).

		$2.4x10^5$	$6x10^4$	$6x10^3$	NonAmplif.
Ampl^n	Total RNA input	2µg	500ng	50ng	NA
	aRNA output	23µg	6.07µg	1.012µg	NA
	Amplifn factor	1100	1214	1012	NA
Labelling	Input	1µg	1µg	1µg	12µg

Figure 3. 7 Amplification reaction performances in output of aRNA and labelling reaction inputs (estimated 1% of total RNA weight to be mRNA)

The amplification factor can also be used to depict that the resulting values of weight of aRNA output. Although every transcript has the added T7 promoter and usually some 5' sequences are not included in the final aRNA transcripts, the amplification factor can be used as an estimate how many µg of total RNA would theoretically correspond to the given amount of aRNA. Since generally about 20µg total RNA is needed as an input for a labelling IVT reaction, according to Affymetrix recommendations, then 50ng (corresponding almost

to 50μg of theoretical total RNA) of starting total RNA in the amplification reaction would be enough for a complete array experiment.

3.2.4.2 Amplification IVT transcript lengths.

Reaction end product quality was assessed by means of end product transcript length. As we can see, reactions which started with 2 and 0.5μg gave end products the majority of which were between 200-2000. The reaction starting with 50ng of total RNA produced end products of larger molecular weight which is depicted at the smear in lane 3 of Fig. 3.8B and curve in Fig. 3.8C. This means that for that reaction the overall IVT procedure was more successful since it amplified more full-length transcripts than the other reactions.

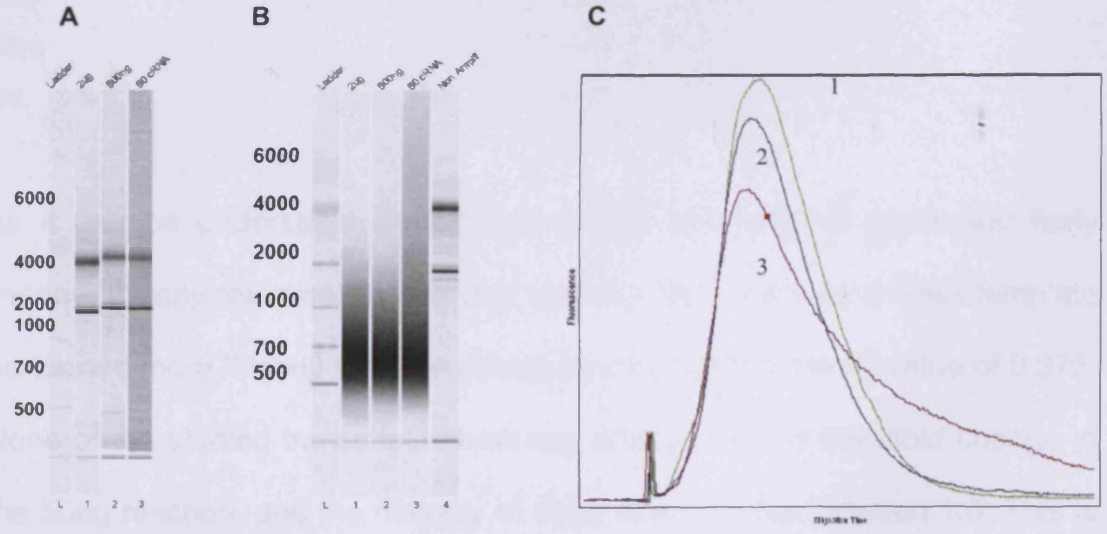

Figure 3. 8 Electropherogram of total RNA before amplification (A). Lanes B2, B3, B4 and curves 1, 2 and 3 in panel C correspond to the product aRNA of the reactions starting with 2μg, 500ng and 50ng respectively. Lane B4 illustrates the electropherogram of non-amplified RNA (lane 2, 3, 4).

3.2.4.3. Effect of total RNA starting amount on IVT amplification linearity.

Data analysis produced a signal intensity value for each probe set in non-amplified and each of the amplified samples (Fig. 3.9). In order to compare the linearity of the amplification reactions the scatter plot of the log_{10}(normalised intensity values) between the non-amplified and each of the amplified samples was created. To test how good the non-amplified sample correlates with each of the amplified samples the R^2 value for this correlation was calculated. This provides a measure to test which amplification reaction correlates best with the non-amplified sample and therefore understand which starting amount affects the linearity of amplification less.

Amplification Reaction	R^2 value
50ng	0.976
500ng	0.919
2µg	0.827

As it can be understood from those values all reactions performed fairly linearly. Clearly the amplification that started with a 50ng total RNA template performed more linearly than the others as indicated by the R^2 value of 0.976. None of the studied transcripts show any scatter beyond the 2fold change in the 50ng reaction, and the majority of them seems to be between 1.5. This is true for low as well as high abundance gene transcripts. In contrast starting amounts of 500ng and 2µg had a higher impact on the relative transcript abundances after the amplification, we can observe in figure 3.9B and C some genes are either crossing or surpass the 2-fold change line

The amplification reaction that started with 50ng of total RNA does no influence high abundance genes more than low abundance ones. All genes are linearly amplified, however for fold changes less than 1.5 we cannot be sure that the variation the amplification reaction is contributing is less than the biological variation. (Figure 3.9 is in the next page)

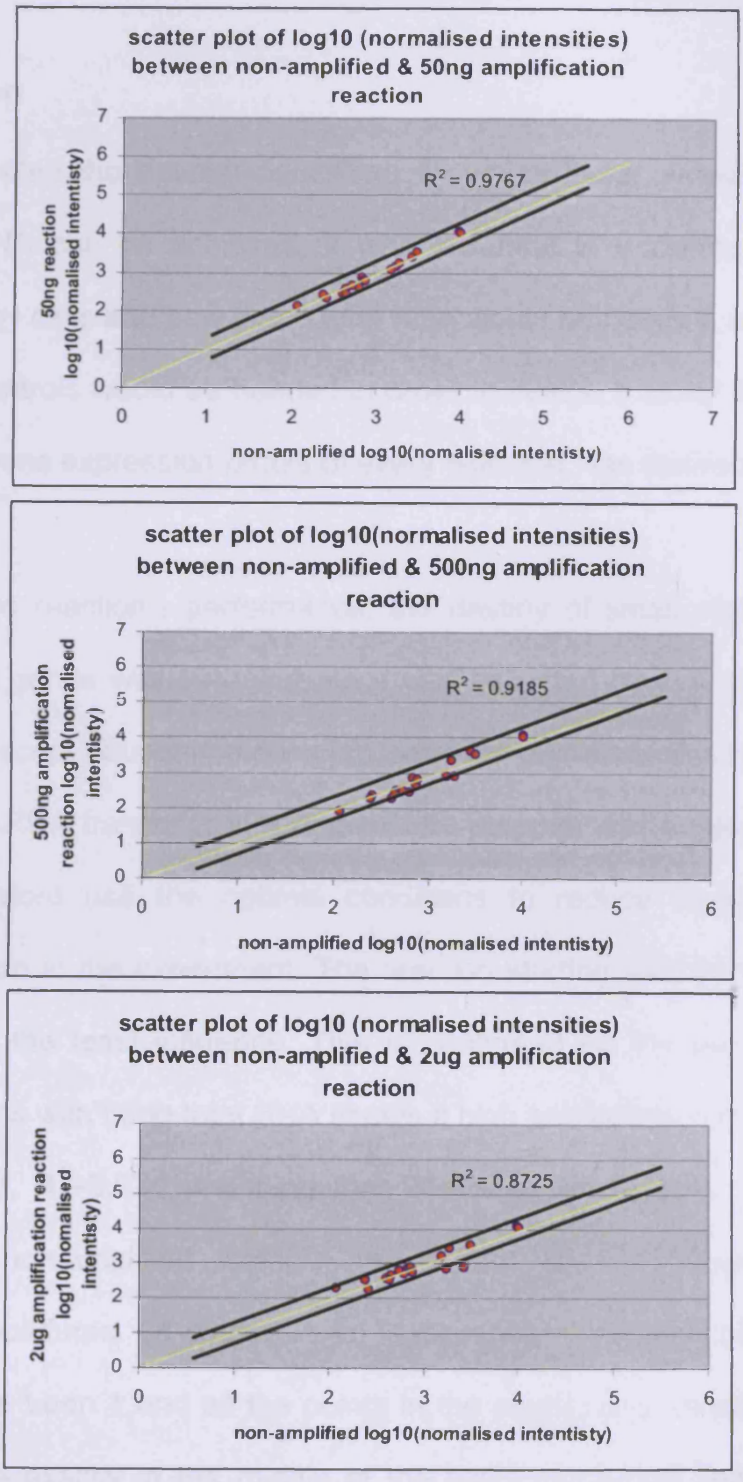

Figure 3. 9 Scatter plot of the $\log_{10}$ normalised intensity measurements between amplified and non-amplified samples of the normalised detection signals for the probe sets called present in all samples.

3.2.5 Discussion

This study revealed the optimal conditions by which linear amplification of mRNA into aRNA can be achieved. It was essential to understand in the cornea how many cells and how much total RNA would be needed, as well as, what kinds of controls would be needed in order to design a study that would reveal the true gene expression profile of every type that was desired.

By assessing the reaction's performance, the destiny of small medium and high abundance genes was revealed. As it was indicated by this preliminary experiment, transcript abundance does influence the efficiency of amplification of a particular mRNA transcript to a degree, the purpose was to identify how much and therefore use the optimal conditions to reduce input of non-biological variation in the experiment. The reaction starting with 50ng of total RNA presenting the least influence. This is confirmed by the fact that the reaction that starts with 50ng total RNA shows a high correlation with the non-amplified sample, R^2=0.976, meaning that 97.6% of the variation between amplified and non-amplified sample is related and not induced by experimental procedures. Of course in an ideal reaction, theoretically the R^2 value would have been 1 and all the points in the scatter plot should appear as a straight line exactly in the middle of the two fold change lines (1 fold change=no change). This shows the limitations of the technique and it indicates that internal controls are needed in order to be able to visualise the linearity of amplification in the actual gene expression experiment. In optimal

conditions, for fold changes less than two we cannot be sure that the variation the amplification reaction is contributing is less than the biological variation. However the 2 fold change difference alone cannot be used a selection criterion since it is likely that there will are some genes with less than two fold difference that are significantly differentially modulated.

As it was observed, the less total RNA that was being used the more linear the amplification reaction tended to be. The optimal total mRNA input in the reaction was found to be between 100 and 50ng. The availability of reaction components has to be optimal for a reaction to work. The amount of reactants will influence any biological reaction. This is because although 500ng of total RNA might seem a low amount to start a microarray experiment, in the end of the amplification reaction nearly 6µg of aRNA which corresponds to mRNA is produced. One could estimate that this resembles an experiment starting with 500µg of total RNA when the recommended is from 10-50. It is therefore likely that the large amount of RNA that is being applied to the labelling reaction is depleting the reaction components very fast. This in turn would mean that the transcripts that have a better chance to utilise the reaction components and therefore be labelled would be the high abundance ones. Indeed the low abundance transcripts present a much larger scatter than the high ones in reactions that started with 500ng of total RNA and more. This effect is being limited by using less total RNA.

To be able to detect the true changes to any transcript abundance, in any reaction in any case and also be able to normalise for potential changes, the

use of controls would be desirable. As a consideration for following experiments it was indicated by these experiments that internal reaction controls would be valuable. Bacterial mRNA transcripts at different abundances each were later used in every amplification reaction which confirmed linearity in subsequent experiments. These experiments also added another point of view that has to be considered. As is shown, different starting amounts of total RNA amplified with slightly different efficiency. The amplification factor, although at the same levels, was not identical. Considering the problems that could arise from this, since the only RNA species that participates in the IVT is the mRNA, if we start with the same total RNA of two different cell types, it is likely that those cell types would have the same percentage of mRNA in the total RNA pool. Although the reaction will amplify all transcripts to the same degree, this degree will be different between different cell types. Potentially this could interfere with our ability to detect changes in gene expression. Normalisation of results, according to a set of 100 house keeping genes proposed by Affymetrix or global normalisation of results correcting for the global amplification, would control for that change.

3.2.6 Conclusions

The experiments indicated that total RNA amounts of above 500ng do not amplify as linearly as lower amounts such as 50ng. It was also understood that even when low amounts of total RNA are amplified, amplification reaction controls are needed in order to be able to test for the linearity of amplification.

Chapter 4

Validation of techniques

4.1 Aims

- To normalize intensity values for each probe set on the high density oligonucleotide array of each region for the three repetitive experiments and prepare the data for comparative analysis

- To validate the quality of the starting total RNA, the yield and quality of the resulting amplified aRNA and validate the quality of the cRNA before and after fragmentation.

- To test weather the hypothesis that those cells are differentially regulated at the transcriptional level.

- To validate the reproducibility of the hybridization experiments.

- To validate linearity of the amplification procedure

4.2 Introduction

There was a need to use a method to analyse the vast amounts of data generated by high density oligonucleotide gene expression. To combine the 16–20 probe pair intensities for a probe set and then all the probe sets interrogating a given gene transcript, that exist on Affymetrix microarray chips in order to define a measure of expression that represents the amount of the corresponding mRNA of each gene transcript, the robust multiarray average method was used.

One of the most widely accepted methods was model based analysis that was introduced in 2001, which can detect and exclude outliers in the data (Li et al .2001). A new method that is even more efficient than Li and Wong model based method is robust multiarray average method. RMA handles background-adjusted, normalized, and log-transformed *PM* values in order to produce an expression value that is exhibiting reduced bias and non experimental variance, and increases the sensitivity and specificity of the final measure of expression as determined by comparison to real-time quantitative gene expression analysis. (Bolstad 2002, Irizarry et al 2003).

The RMA analysis provided a measure of expression level for each of the gene transcripts present on the array (around 78% of the genome). In order to identify genes that are differentially regulated in each area, the limbus, peripheral central cornea and conjunctiva), pair wise comparisons were

performed first for each of the areas against the other. The *p*-value of a Welch's t-test was calculated for each comparison.

Identifying differentially expressed genes between the different experimental areas simply by selecting for a cut-off fold change does not necessarily mean that those differences reflect on true biological meaning. It needs to be identified whether the variance in gene expression can be attributed to the actual difference of the transcriptome of the cells that are being compared, or due to other external factors that increase variance. Additionally if the actual variance is little then it becomes a challenge to identify meaningful differences between gene expression profiles.

To test therefore the hypothesis that limbal, peripheral, central and conjunctival areas have distinctive expression profiles principal component analysis was employed. In this analysis the three principal components of gene expression variance were used to cluster the twelve individual experiments in a three dimensional graph. Additionally PCA plots of control probe sets were prepared to confirm luck of clustering as a negative control.

4.3. Results

4.3.1 Total RNA integrity

Total RNA integrity was examined by capillary electrophoresis. All total RNA samples were found to have their RNA uncompromised as indicated in the gel electrophoresis figure reconstruction (figure 4.1). All total RNA samples exhibited the distinct double intensity of the 28S in relation to the 18S ribosomal RNA band, indicative of high quality, non-degraded RNA.

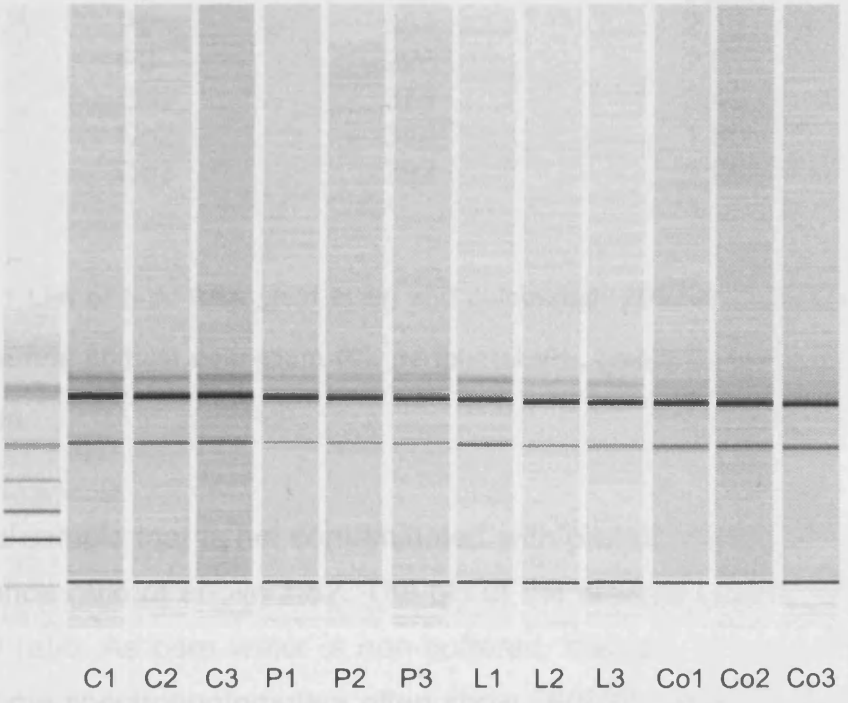

Figure 4. 1Electropherogram of total RNA isolated by laser catapult from mouse central corneal epithelium (C), peripheral (P), limbal (L) and conjunctival (Co) epithelium.

4.3.2 Total RNA purity and yield

Yield and purity measurements for all mRNA samples are listed in the following table. Samples were of high purity typically had a 260/280 ratio of 2 and above.

Sample	RNA yield (ng)	260/280
C1	504	1.86
C2	527	2.34
C3	486	2.56
L1	531	2.07
L2	562	2.31
L3	502	1.94
P1	935	2.22
P2	954	2.18
P3	925	2.03
Co1	378	3.40
Co2	344	1.80
Co3	392	1.99

Table 4. 1 List of total RNA yield in ng and calculated 260/280 absorbance ratios for mouse central corneal epithelium (C), peripheral (P) , limbal (L) and conjunctival (Co) epithelium.

Ideally a sample that is not contaminated with protein should have a 260/260 absorbance ratio of above 1.82. The pH of the solution greatly influences the 260/280 ratio. As pure water is non-buffered, this can influence the 260/280 ratio. Some spectrophotometers often show 260/280 ratios of pure RNA to be above 2.3. In order to ensure the purity of RNA preparations the full absorption spectra of each sample were analysed for absorption at wavelengths spanning from 220 to 350 nm (fig. 4.2). In this was any additional peaks appearing apart from the expected at 260 would indicate some sort of contamination.

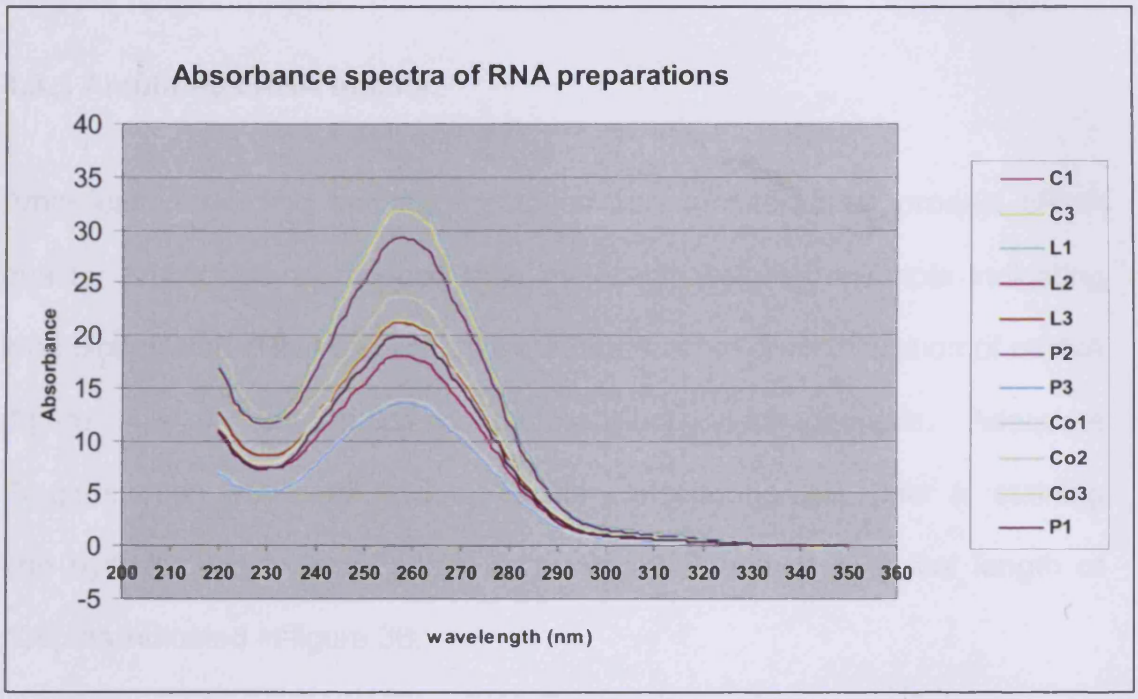

Figure 4. 2 Graph illustrating the curves of the absorbance of each RNA preparation at wavelengths spanning from 220-350nm. Note that there are no other peaks apart from the one expected at 260nm since the absorbance maximum for nucleic acids is at 260nm. There is no peak at 280nm where the absorbance maximum of proteins is, indicating the absence of protein and high purity of the RNA preparation.

The actual reason for the high 260/280 ratios is due to the software of the nanodrop spectrophotometer. The software algorithm calculates the 260/280 ratio by using the slope of the curve that the squared values of absorption spectrum present between 260 and 280nm. This line is not fitted optimally by the software resulting in slightly distorted 260/280 ratios. To ensure that there is no degradation the RNA integrity was analysed with capillary electrophoresis, the results of which are presented in the next section.

4.3.3 Amplified cRNA quality.

Amplification reaction and fragmentation was monitored for product cRNA quality. Amplification produced high molecular weight transcripts indicating long biotinylated cRNA transcripts were produced after amplification of mRNA (figure 4.3 A) as indicated by capillary electrophoresis. Adequate Fragmentation was confirmed by capillary electrophoresis, prior to staining and hybridisation to array chips. Fragmented RNA had a typical length of 50bp as indicated in figure 3B.

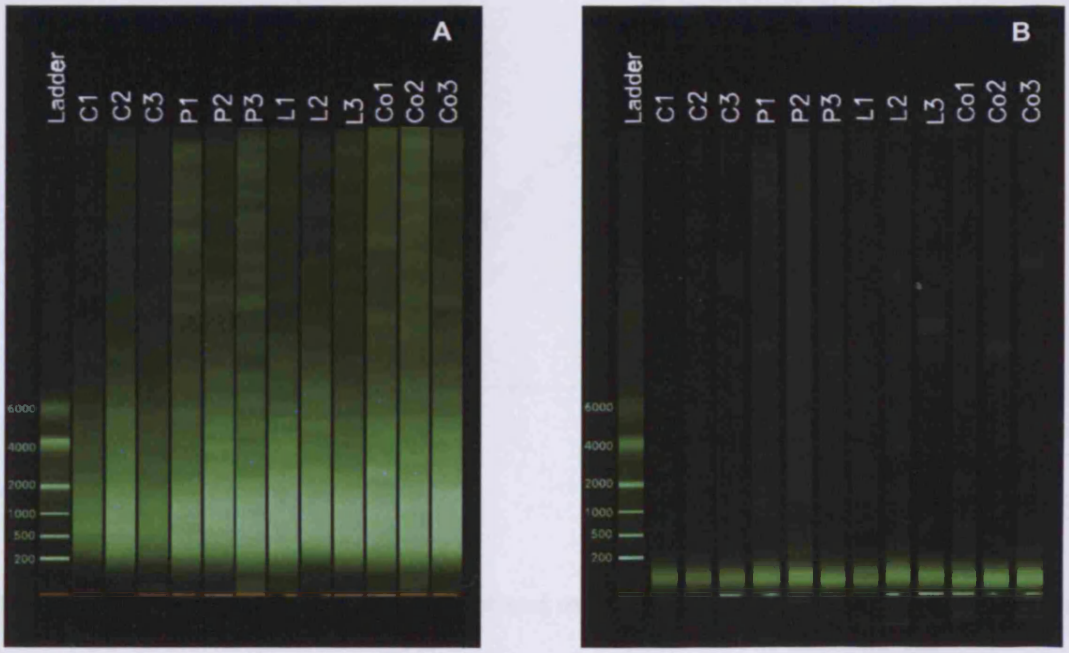

Figure 4. 3 Electropherogram of capillary electrophoresis of amplified cRNA (A) and fragmented cRNA from all experimental samples. C, P, L and Co corresponds to cRNA derived from mRNA of central, peripheral, limbal and conjunctival basal cells respectively.

Additionally, after the chips were analysed, the Affymetrix MAS5 software permits to monitor the actual 3'/5' ratio of each gene in each array as a quality control measure. The recommended ratios (x_n) in order to meet the manufacturer's specifications are $x \leq 3$. As it can be seen in figure 4.4 the slopes of the lines of the plotted intensities of probes spanning from 5' to 3' is the 3'/5' ratio for each of the experiments around and were found to be no more than 1.6, indicating high cRNA integrity.

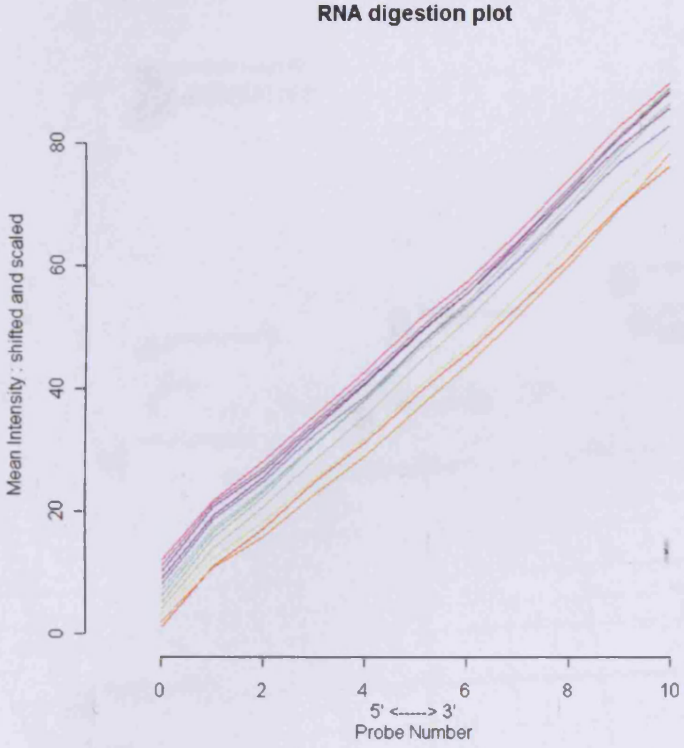

Figure 4. 4 This is a graph of the normalised mean intensity values of each probe of all gene transcripts in the array for 10 probes that span the entire length of the gene transcript.

4.3.4 Principal Component analysis confirms the experimental hypothesis.

PCA analysis confirmed that the variance of gene expression between different experimental cell types can be attributed to the area the mRNA was extracted from. Experimental sets from the same tissue are clustered together in distinct separate clusters (figure4.5).

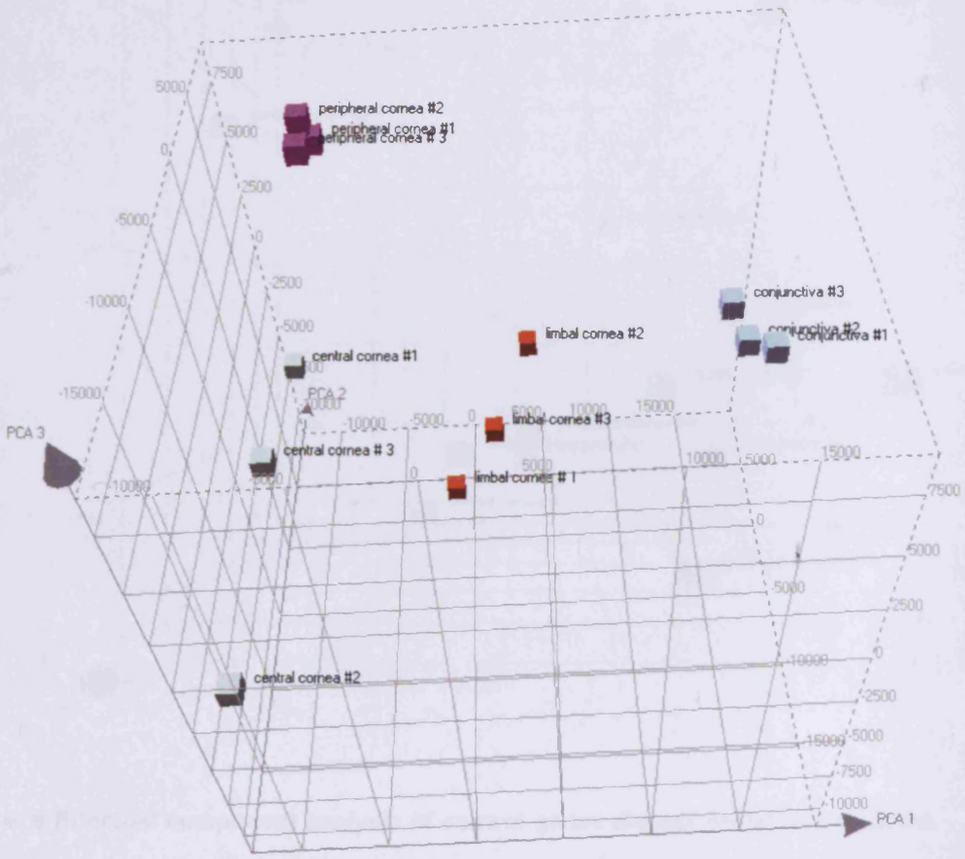

Figure 4. 5 PCA analysis clusters each experimental area differentially. Conjunctival, limbal, peripheral and central mRNA profiles constitute distinctive clusters in a PCA plot, revealing that the major variation of gene expression arises from the differential location the mRNA profiles belonged to.

Control probe sets belonging to transcripts of genes that are expressed at the same level in all cells, such as housekeeping genes, as well as microarray quality control spiked probes did not cluster individually, as expected, confirming the luck of variation between control probe sets (figure 4.6).

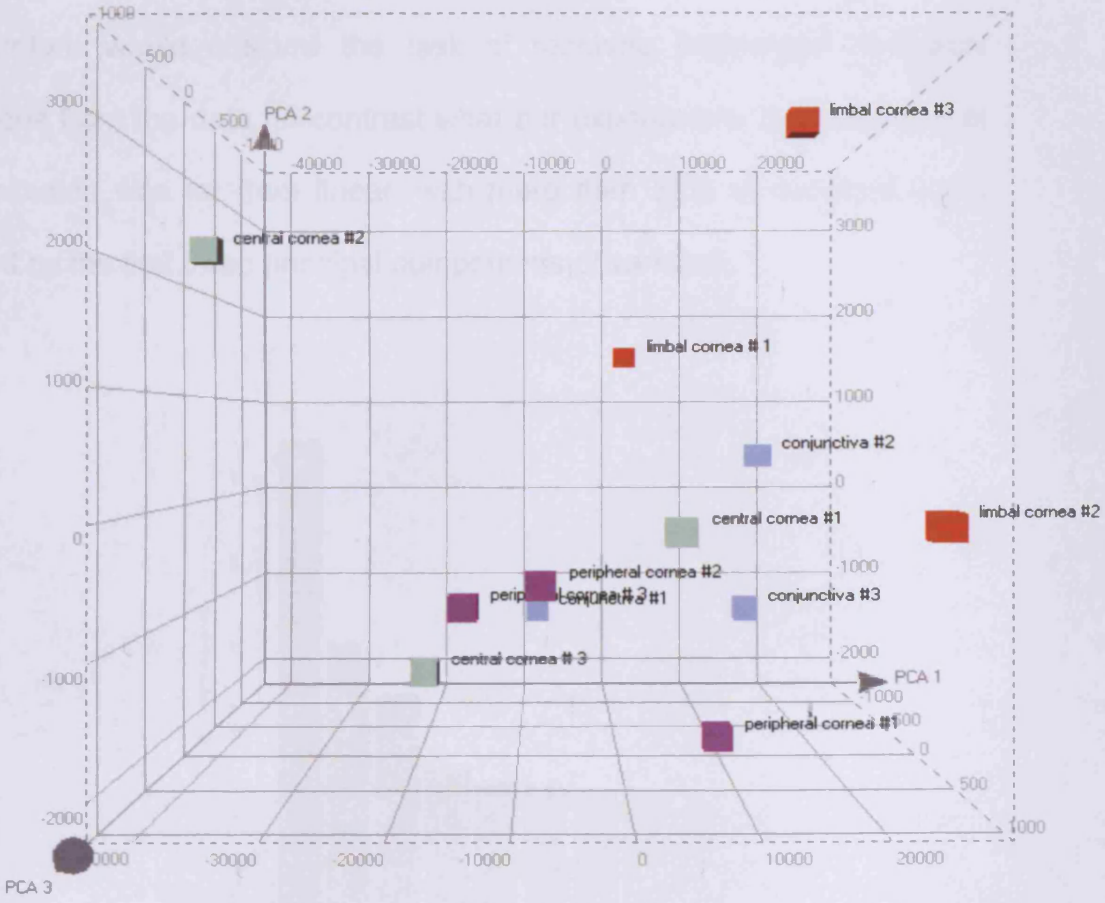

Figure 4. 6 Principal component analysis of control genes did not reveal any clusters. The lack of clustering confirms the lack of variation of the expression of non-differentially expressed control probe sets between regions.

In order to show that the experimentally induced variation was limited, al the principal components of variation were plotted in relation to the percentage of variation they are able to explain. If the % variation explained by succeeding principal components of variation tends to be linear it could serve as an indication that the variation that was induced due to experimental procedures exceeds the actual biological variation ,which is the subject of the experiment and therefore would obscure the task of reaching meaningful biological conclusions from the data. In contrast what our experiments indicated is that this distribution was far from linear, with more than 55% of variation being explained by the first three principal components of variation.

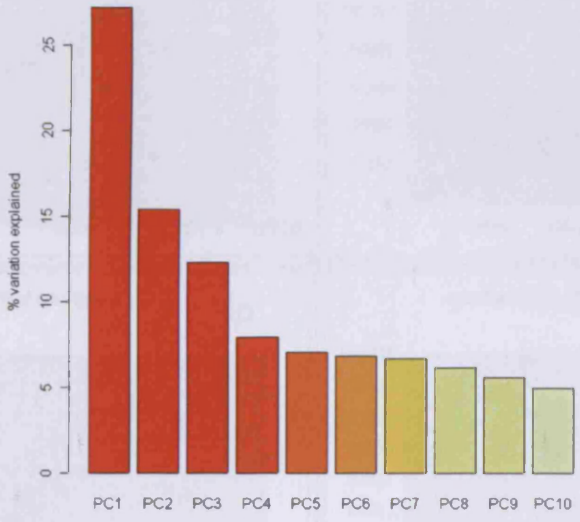

Figure 4. 7 The figure illustrates the non-linear distribution of the % of variation that is being explained by the principal components (PC) contributing to the total of variation. 57% of the variation is being explained by the first three components, indicating that the experimentally-induced variation was limited.

4.3.5 Result reproducibility.

The reproducibility of the results is underlined by the high correlation coefficients (r) of the replicate samples. These have a mean value of 0.96 and a range of 0.92 to 0.99. Figure 4.8 illustrates the correlation coefficients and the scatter plots of the experimental repetitions. It has to be noted that in order to have a clear view of the experimental reproducibility the raw intensity values were plotted instead of the RMA corrected ones, and both the ones that were called significant and non-significant by the analysis of variance are illustrated.

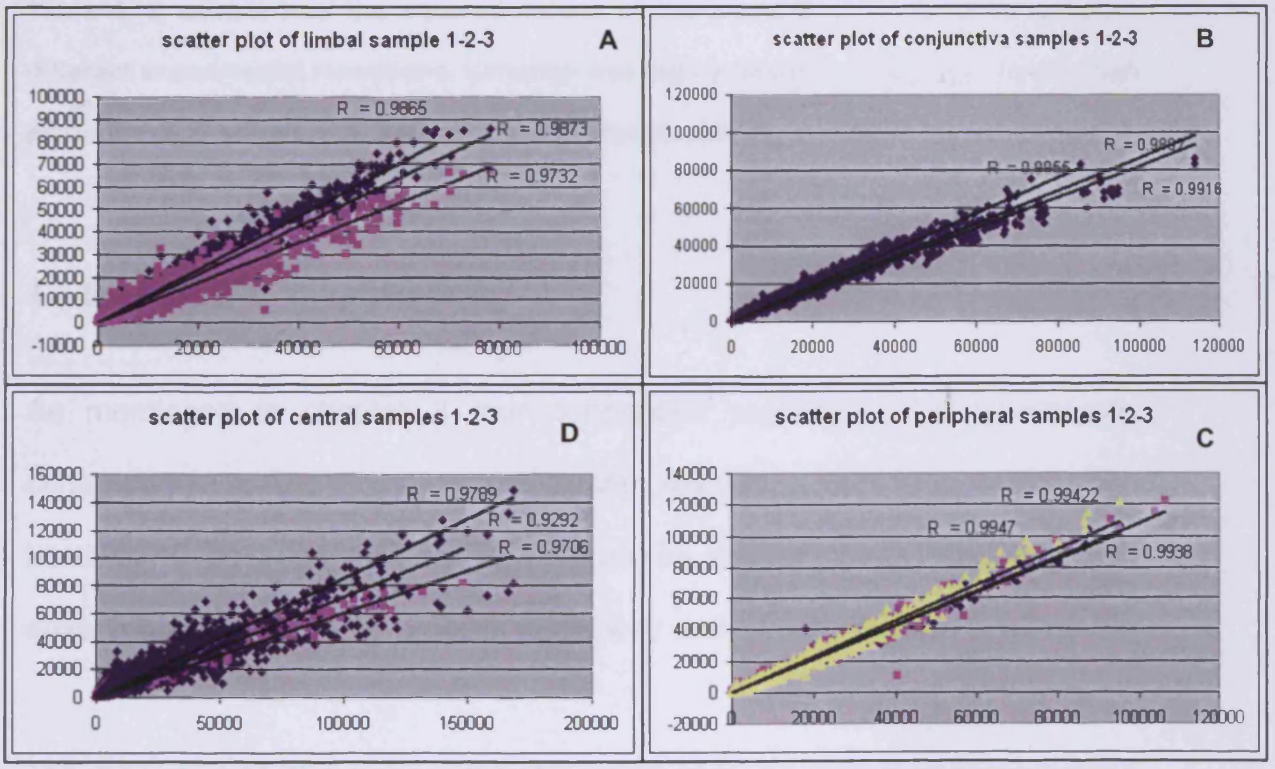

Figure 4. 8 Graphs A, B, C, D, represent the scatter plots of repetitions 1-2, 1-3 and 2-3 of the conjunctival, limbal, peripheral and central corneal microarray experiments respectively. The Correlation coefficients (R) for each comparison is given for each set of data.

The R^2 values of each comparison are summarized in the next table. As the R^2 values indicate, even the lowest correlation (R^2 value of 0.86) shows that there is an 86% of the variance between these two experiments is related. This explains therefore that the results exhibit a high degree of reproducibility.

	Experiments 1-2 R^2	Experiments 1-3 R^2	Experiments 2-3 R^2
Conjunctival samples	0.983374	0.978619	0.991202
Limbal samples	0.947252	0.974774	0.973267
Peripheral samples	0.989433	0.984626	0.987815
Central samples	0.958352	0.863475	0.942191

Table 4. 2 summarises the squared values of the correlation coefficients between different experimental repetitions. Variation was highly related as explained by the high proximity of R^2 values to 1, indicating result reproducibility.

4.3.6 Linearity of Amplification

As mentioned in chapter 3 four exogenous poly-adenylated prokaryotic controls were spiked directly into RNA samples just prior to amplification and labelling to be used as positive controls to monitor the entire GeneChip eukaryotic target labelling process in the way described in section 2.1.7

The mean values of the raw signal intensities of these control transcripts were plotted in a scatter plot in order to see how good they correlate with their predetermined relative abundance ratios. The R^2 value for this correlation was 0.9897, indicating that 98.97% of the variance in those ratios of those transcripts before and after amplification is related, confirming lack of

experimentally induced variance, i.e. confirming that the reaction did not change those ratios. The graph is represented in figure 4.9

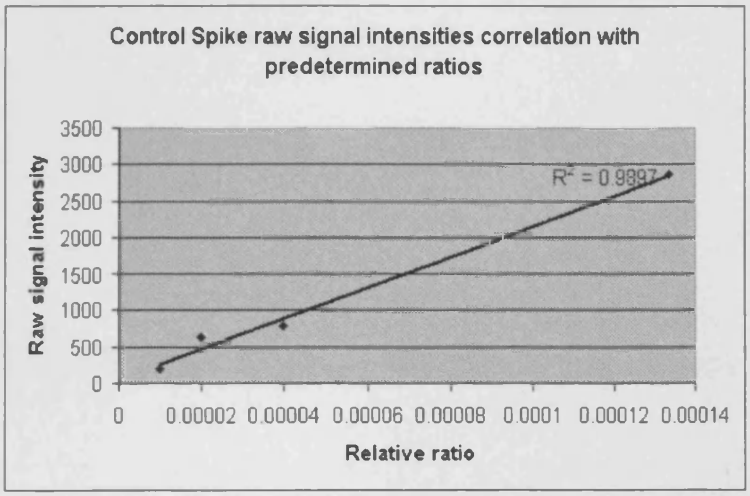

Figure 4. 9 The linear outcome of the amplification reaction is illustrated since the raw intensity values of control spikes correlate with predetermined abundance ratios (R^2= 0.9897)

4.3.7 Distribution of P-values for pair wise comparisons between regions.

The distribution of p-values that were generated from a two way, t-test for two samples of unequal variance is presented in the figure below (Figures 4.10 A, B and C) and demonstrates the occurrence of each *p*-value in the complete set of genes for each pair wise comparison between the regions that were studied. The occurrence of *p*-values gives an image of the specificity that can be expected in the comparison of each area against another. Due to the fact that multiple hypotheses (45101 hypotheses, one for each probe set) that are being tested in this experiment, a 0.05 p-value limit of the t-test will result in type I error, i.e. in the increase of false positives. To correct for that a false

discovery rate correction on the p-values can be performed using the Benjamini and Hochberg (1995) method. The following figures, 4.10-4.12, use the distribution of raw *p*-values (next page).

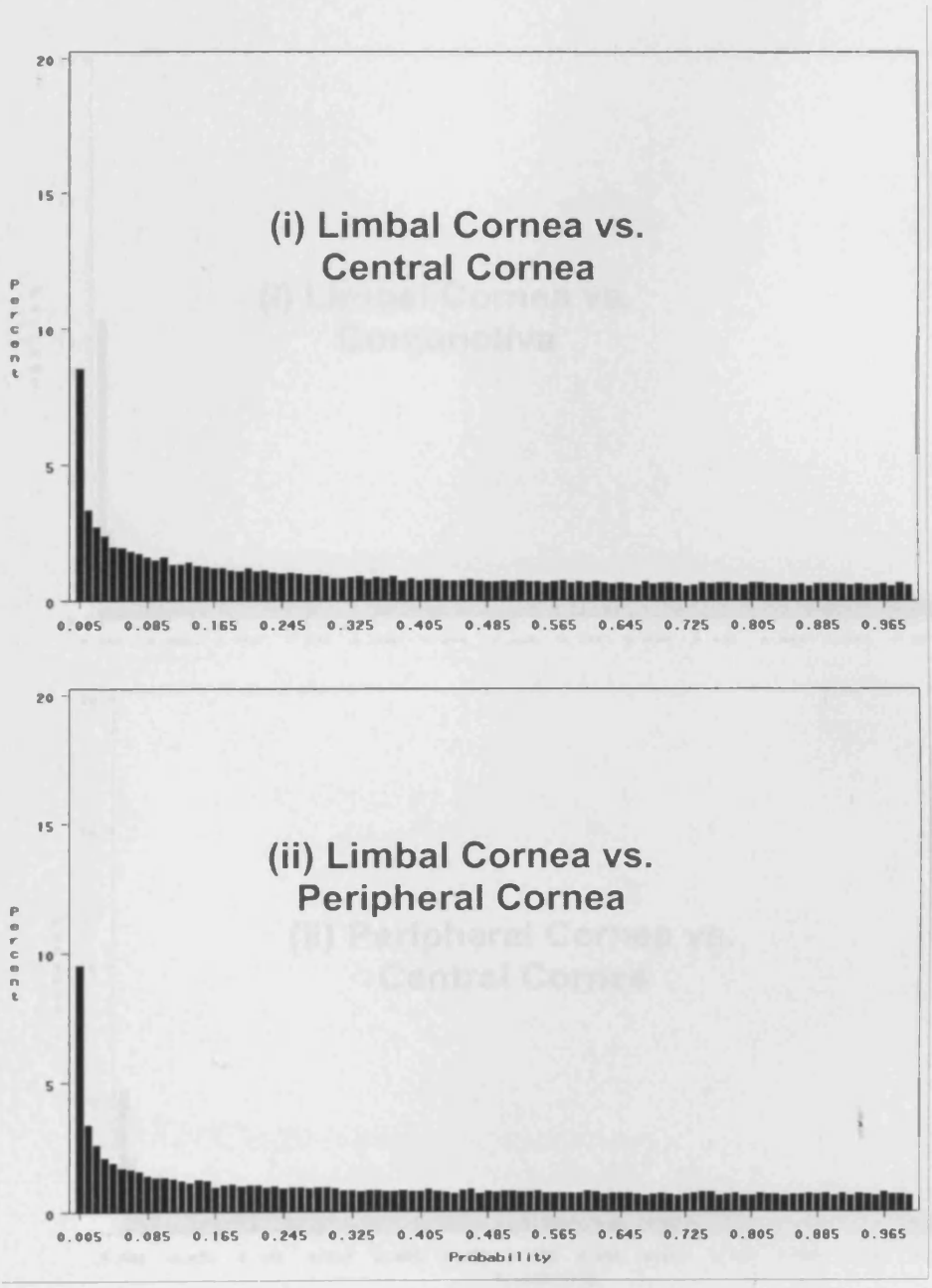

Figure 4. 10 illustrates the distribution of *p*-values that resulted from a two way t-test for two samples of unequal variance, comparing the expression of each gene between two areas. (i) Corresponds to limbus versus central cornea, (ii) limbus versus peripheral cornea.

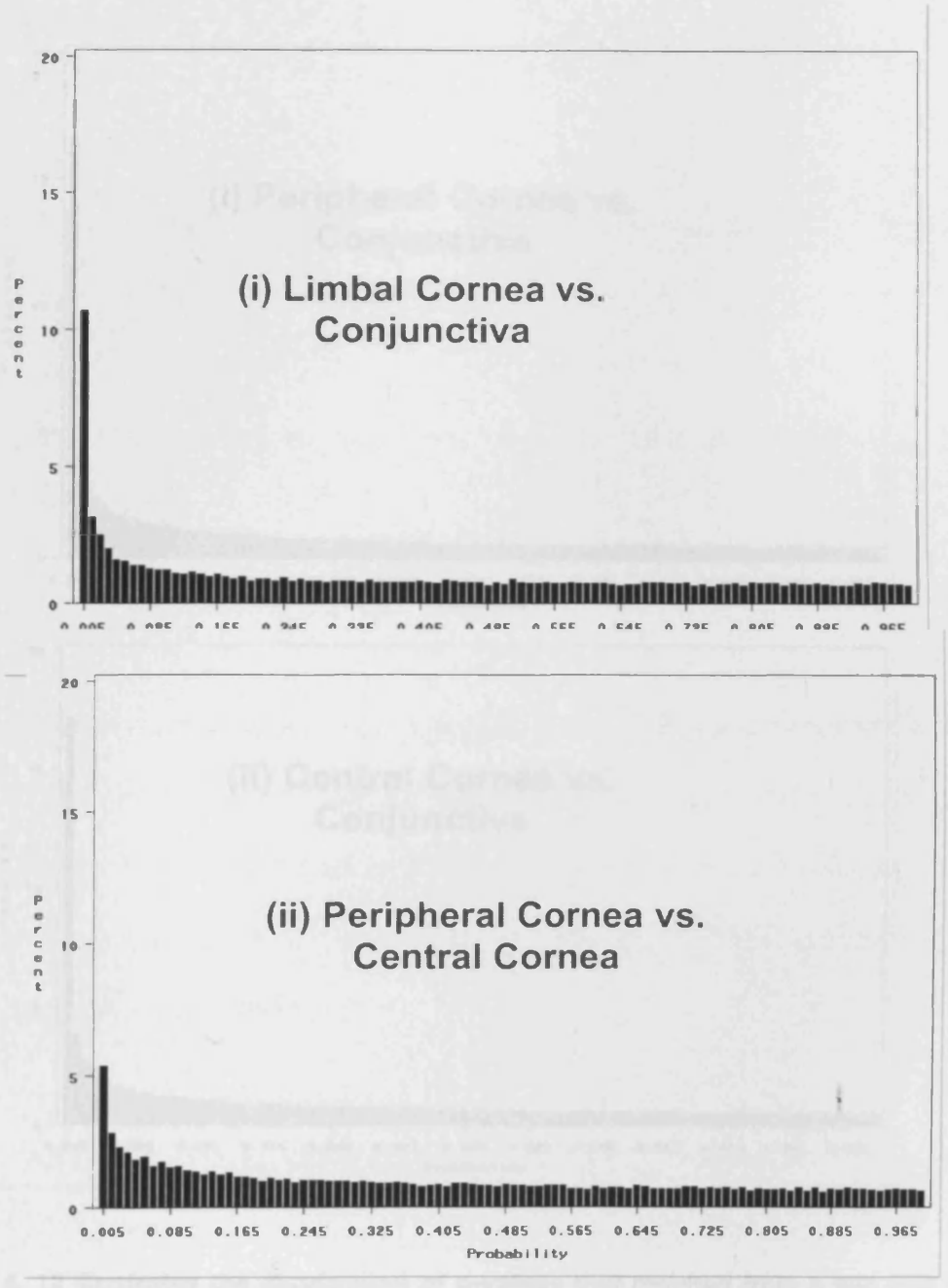

Figure 4. 11 illustrates the distribution of *p*-values that resulted from a two way t-test for two samples of unequal variance, comparing the expression of each gene between two areas. (i) Corresponds to limbus versus conjunctiva, (ii) peripheral versus central cornea.

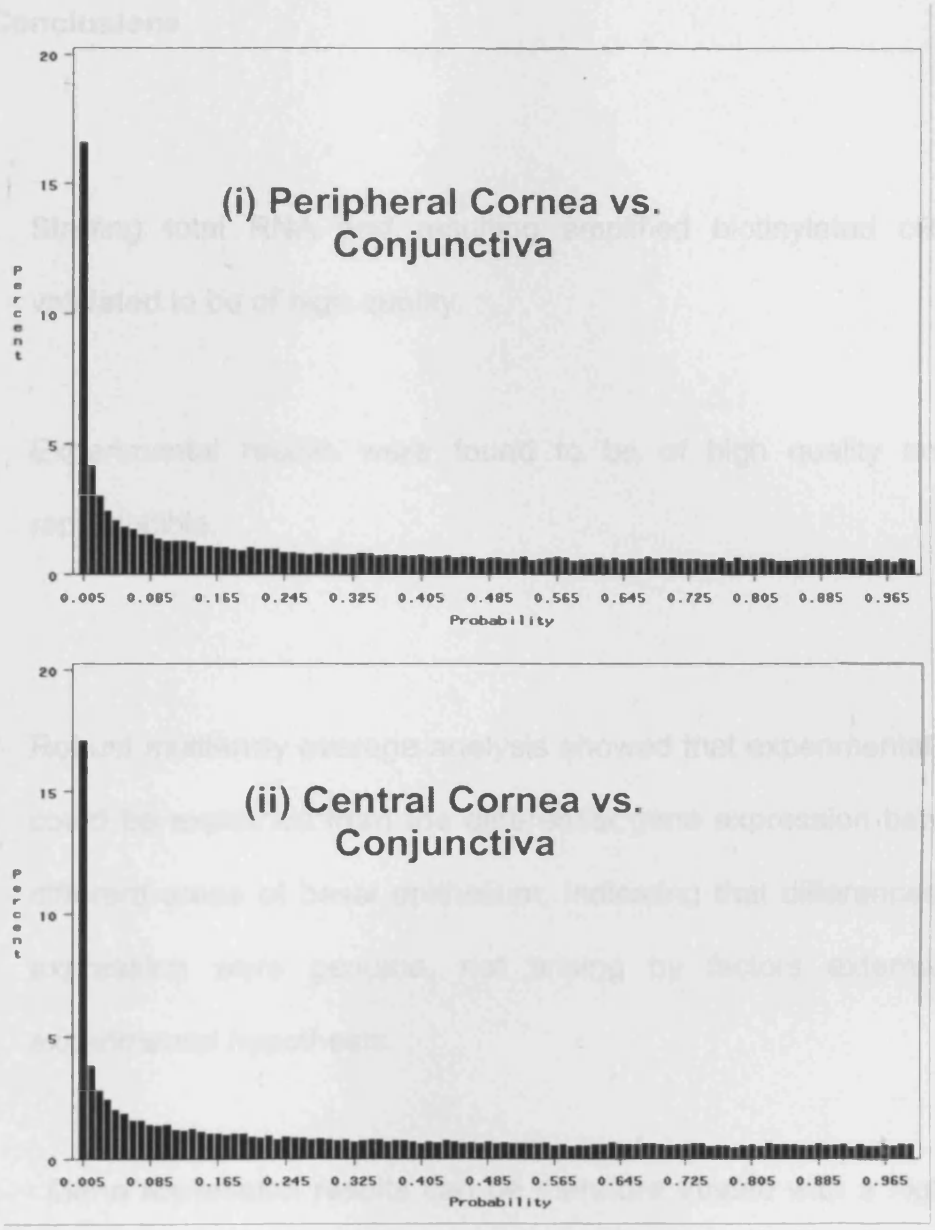

Figure 4. 12 illustrates the distribution of *p*-values that resulted from a two way t-test for two samples of unequal variance, comparing the expression of each gene between two areas. (i) Corresponds to peripheral cornea versus conjunctiva, (ii) central cornea versus conjunctiva.

4.4 Conclusions

- Starting total RNA and resulting amplified biotinylated cRNA was validated to be of high quality.

- Experimental results were found to be of high quality and highly reproducible.

- Robust multiarray average analysis showed that experimental variance could be explained from the differential gene expression between the different areas of basal epithelium, indicating that differences in gene expression were genuine, not arising by factors external to the experimental hypothesis.

- Gene expression results can be therefore trusted with a high degree of confidence.

CHAPTER 5

Gene expression profiles of corneal epithelial cells of successive hierarchical positions in the corneal lineage.

5.1 Aims.

- To reveal the gene expression profile of basal cells of the limbus, peripheral and central corneal epithelium.

- To use these profiles in order to identify strong candidates for stem cell markers from the genes which are specifically up-regulated in the corneal stem cell compartment, the limbus.

- To identify the main biological functions, and the genes that control them, that are selectively up or down modulated in the corneal epithelial stem cell niche (limbus), as well as in the periphery (enriched in transient-amplifying cells) and the central cornea (enriched in differentiating cells).

5.2 Introduction

In order to make sense of stem, TA and differentiated cell biology and the genes that possibly dictate cell phenotype from microarray data, genes that are selectively upregulated or downregulated in each region were filtered out from calculating the mean robust multiarray average values (RMA values) of expression value difference of each gene for each region in relation to the other regions. The RMA expression measure was used because it was proven that it is better than the measure that MAS 5 provides as well as performs better than the Li and Wong model-based expression index (Irizarry et al. 2003). It was observed that expression is better measured using log-

transformed perfect-mach (PM) values (given as an output of the Affymetrix system) that are then adjusted for global background and across array normalisation,. The researchers, after evaluating all available expression summary measures using spike-in and dilution study data, assessing their behavior in terms of bias, variance, the ability to detect known differential expression levels, proven that RMA offers the greatest sensitivity and specificity in detection of differential expression using high density oligonucleotide array platforms (Irizarry et al.2003

High density oligonucleotide arrays produce a vast amount of data. In order to reduce complexity of data, most researchers use clustering mathematics techniques. At the moment the field is trying to identify several methods to reduce need for the involvement of a researcher to make sense of the data due to their large number.

Clustering in mathematics is a way of reducing complexity of a sum of values. Usually clustering mathematical methods are employed when trying to reduce the level of complexity by gradually segregating a large sum of values to progressively smaller clusters according to a desired criterion.

There are several ways to achieve this and several methods of clustering, such as hierarchical clustering, k-means clustering, and functional clustering. All of these clustering methods are very powerful tools in analyzing gene expression data because they can be used (amongst other things) to find cluster of genes that are co-regulated between two different data sets by

clustering according to some criterion of co-variance. The value of these kinds of clustering though is great when a set of experimental conditions that can be defined by the researchers can be selectively changed. For example cell cultured cells or tissues that are treated can be compared with non-treated and then observe the clusters of genes that are co-regulated by a selective definable input. In studies comparing different tissues though the regulation of genes is multifactorial, hence there are high chances that clusters of co-regulated genes that result from such methods of clustering can be circumstantial, due to the many factors which govern that co-variance. Therefore, for the purpose of this study the data were clustered according to gene ontology.

Correlation between genetic co-regulation and affiliation to a common biological process is not necessarily the case when numerical cluster algorithms are applied to gene expression data. Clustering the data according to gene ontology uses the tree of the Gene Ontology database as a framework for numerical clustering, and thus allowing a comprehensible and robust visualisation of gene expression data at various levels of the ontology tree (Adryan and Schuh 2004). Gene Ontology (GO) is the most widely accepted unified and structured vocabulary for the description of genes and their products in any organism, performed in most of the current genome projects (Henning et al. 2003).

In gene ontology clustering, as the ontological tree progresses from general to very specialised description of gene ontology the clusters fit progressively better. Branches of that tree can cross when the gene or genes have

ontologies that belong to both branches. Therefore the ontologies that would have the maximum probability value are the most indicative of the specific processes that are being actively regulated amongst genes.

5.3 Materials and methods

The specific methods are described in detail in Chapter 2. In this section methods are briefly described mentioning any additional information.

5.3.1 Isolated areas, RNA isolation and pre-data acquisition procedures

Three independently isolated replicates were used for each area from three respective adult 12 week old male C57BL6 mice. The regions of interest, namely the basal layer of the limbal, peripheral corneal and central corneal epithelium as well as basal and suprabasal conjunctival layers, depicted in Fig. 5.1, were isolated by Laser Microdissection and Pressure Catapulting (LMPC) method described in detail in section 3.1.3.2.ii. Briefly, cells were isolated from tissues pre-treated with *RNAlater*® (Ambion, UK) that were frozen and embedded in OCT (Lamb) and sectioned with a cryotome on plain glass slides. LMPC was performed using a PALM Microlaser platform (PALM, Germany)

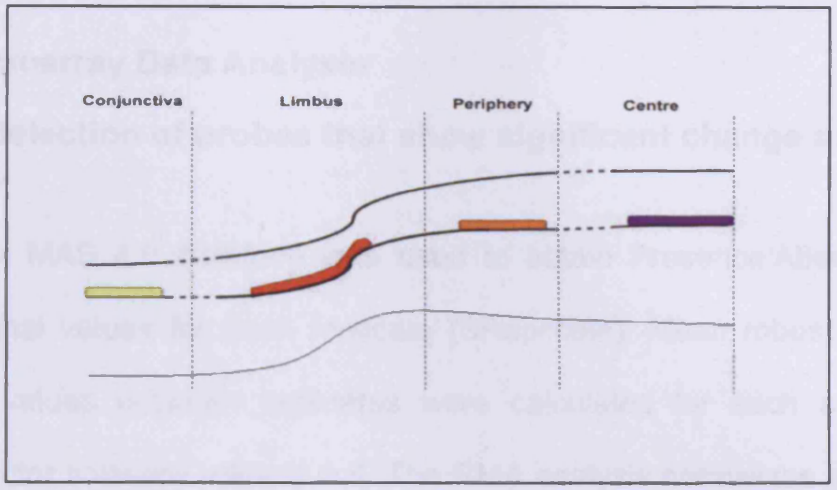

Figure 5. 1A schematic representation of the areas that were isolated by Laser Microdissection and Pressure catapulting method

RNA was extracted using Rneasy mini columns (QUIAGEN) as described in section 2.1.3. RNA was linearly amplified and labeled by *in-vitro* transcription as in sections 2.1.8 and 2.1.9. The procedure was optimised as in section 3.2.3.2

Then labeled cRNA was fragmented and hybridised on GeneChip® Mouse Genome 430 2.0 arrays as described in sections 2.1.10 – 2.1.12. Using these arrays the expression level of over 39,000 transcripts and variants from over 34,000 well characterized mouse genes as well as 6000 EST (expressed sequence tag) sequences was analyzed.

5.3.2Microarray Data Analysis

5.3.2.1 Selection of probes that show significant change across the data set.

Affymetrix MAS 4.0 Software was used to obtain Presence/Absence (P/A) calls, Signal values for each replicate (SReplicate). Mean robust multiarray average values between replicates were calculated for each array using Bioconductor software release 1.6. The RMA analysis normalizes all samples so that the median of intensity of all the perfect mach probes is the same among all experiments. The end value of expression is a $\log_2$ transformed value.

To define a set of genes that is differentially expressed in each area of the ocular tissue the expression of that gene was compared pair wise between all possible combinations of pair wise comparisons. A multiple comparison approach was avoided because for the purposes of this study it was important to be able to see which genes are differentially modulated in a step wise fashion going from the stem cell enriched area (limbus) to the first generation TA enriched area (periphery) or to the later generation enriched area (centre).

For each comparison a two-tailed, type 3 test was used, also called a Welch's t – test. A two tail test was used because in the pair wise comparison a gene in one area (e.g. limbus) can have an expression that is lower or higher than the other (e.g. periphery). The test assumed that the two samples have unequal variance, because it is safer to assume that the variance of expression between the two tissues that are being compared is the same,

although some potentially differentially expressed genes are lost this way to the expense of rejecting false positives.

Since the comparisons were pair wise for the purpose of this study, in each analysis there is only one null hypothesis that states: Gene A is not differentially expressed between area one and area two. Selecting for genes that have a *p*-value equal or lower than 0.05, we selected the genes that would have less than 95% chance of one gene appearing differentially expressed by chance between two regions. If we needed to compare gene A with all the other regions at once that the argument of the null hypothesis would be different. Multiple hypothesis testing methods would have been needed because we would have as many null hypotheses as the tissues we compare against.

However in each sample there are 45101 probe sets, all of which generate a *p*- value for the null hypothesis, and there are 45101 null hypotheses generated. When there are multiple hypotheses being tested the use of a 0.05 p-value limit is going to result in cumulative type I error, meaning that there is a much greater chance for false positives to appear in the data. To control for this type of error, a false discovery rate approach was used for each of the pair wise comparisons. For false discovery rate correction of the p-value the Benjamini and Hochberg method can be used, but it is not included in the selection criteria because although it reduces the false discovery rate it increases the False Negative rate. In this study it was preferred to minimise false positives at the expense of identifying false negative results.

Fold changes C were calculated individually for each data set against the other. Fold changes of 1.5 or more were specifically and sensitively detected by analysing results based on RMA values (Irizarry et al. 2003). Individual replicates of each sample were averaged, and mean SSample, logFCSample, Reference and standard deviation (SDSample) of S and FC were calculated for each probe. The following equation was used:

$$FCsample = 2^{(\log_2 Sample - \log_2 Reference)}$$

All logarithmic transformations were done to base 2. The average P/A call for the sample was calculated as follows:

P/A value = (P*2 +M) / Number of replicates,

where:

P = number of replicates called "Present"

M = number of replicates called "Marginal"

The probe was called "Present" in a given sample, if P/A value >1.0, it was called "A" otherwise.

5.3.2.2 Gene ontology clustering.

Gene ontology clustering was performed using the Netaffx analysis centre (Affymetrix) which uses the GO-Cluster software algorithm developed by Boris Adryan and Reinhard Schuh at Max-Planck-Institute, Göttingen, Germany (Adryan and Schuh 2004) This software is integrated in the Affymetrix NetAffix Analysis centre. The probability that a gene or an EST belonged to a given cluster, better than any other gene or EST in the data set, was calculated

automatically and the results were visualised as single vectorial graphs using the Affymetrix gene ontology mining tool and customising for node color selection. Red indicated maximum probability and blue, minimum probability. The end points of those ontological trees that exhibited the highest probability were the clusters that were selected as an indication of the specialised processes up or down regulated in the cells of interest.

Files of the probe set identities were uploaded in the Netaffx analysis centre and the gene ontology reference numbers of each probe-set was returned in CSV (comma separated value) format. After clusters were visualised the gene ontology reference number depicted at each point on the ontological tree in the vectorial graphs was searched in the CSV database to find the Affymetrix Probe set ID's that belonged to each cluster. The gene name and symbol was then searched in the annotated gene list in Microsoft Excel format using the probe set ID's.

NOTE: Throughout the Chapter figures of these vectorial graphs depicting the gene ontology trees are illustrated. Some-times those graphs are too large to fit in a printable format in the thesis. Whenever it is not feasible to fit them the Gene list with the probe number is given under the gene ontology reference name that constitutes the cluster. 5.4 Results

5.4.1 Corneal limbal basal cell gene expression profile

5.4.1.1 Genes enriched in limbal basal cells.

One hundred and fifty genes and forty ESTs were found to be specifically upregulated in the corneal limbal basal cells, in relation to expression values of those genes in cells isolated from the conjunctiva, peripheral or central regions of the cornea. The reason the conjunctival dataset was also subtracted was to end up with corneal lineage specific genes. The selection criteria stated that probes should have an Absent-Present (A-P, see section **5.3.1.1**) value of at least 1.00 in the corneal limbal basal cell arrays and that their fold change should be equal or greater than 1.5. Moreover the probe sets should exhibit an ANOVA two-tail t-test value of equal or less than 0.05.

The list of all the genes is presented at tables C.1 a-e in Appendix C. The tables contain the gene symbols and names, chromosomal location, as well as UNIGENE database reference numbers and fold changes. Genes and EST's found to be specifically up or down regulated in each region belonging to this list were used to identify clusters of biological and molecular function specifically upregulated in the corneal limbal basal epithelium by gene ontology clustering.

5.4.1.2 Gene ontology clusters of genes specifically up-regulated in limbal basal epithelial cells.

The gene ontology clusters that display the highest probability of existence amongst all other possible gene ontologies as well as the genes that constitute the ontological cluster are presented in the form of tables in the following sections. Additionally the cluster tree-view diagrams are presented whenever the size allows it. To facilitate the presentation each general ontological category that displayed clusters is presented separately.

5.4.1.2.1 Cell cycle-related gene clusters.

Fifteen probe sets that have cell cycle related gene ontology were found to be upregulated in the basal limbus. These corresponded to 7 genes and an EST and clustered in a) meiosis recombination (Fig. 5.2), DNA repair (Fig. 5.2), b) mitotic spindle orientation and sister chromatid segregation (Fig. 5.2) or c) traversing start control point of G1 (Fig. 5.2), d) Chromosome segregation.(Fig. 5.3)

The genes and names of the ontological cluster they belonged are listed in Table 5.1. The ontological tree view of the cell cycle related gene clusters created by the Netaffix Analysis centre integrated software is illustrated in Figures. 5.2 and 5.3

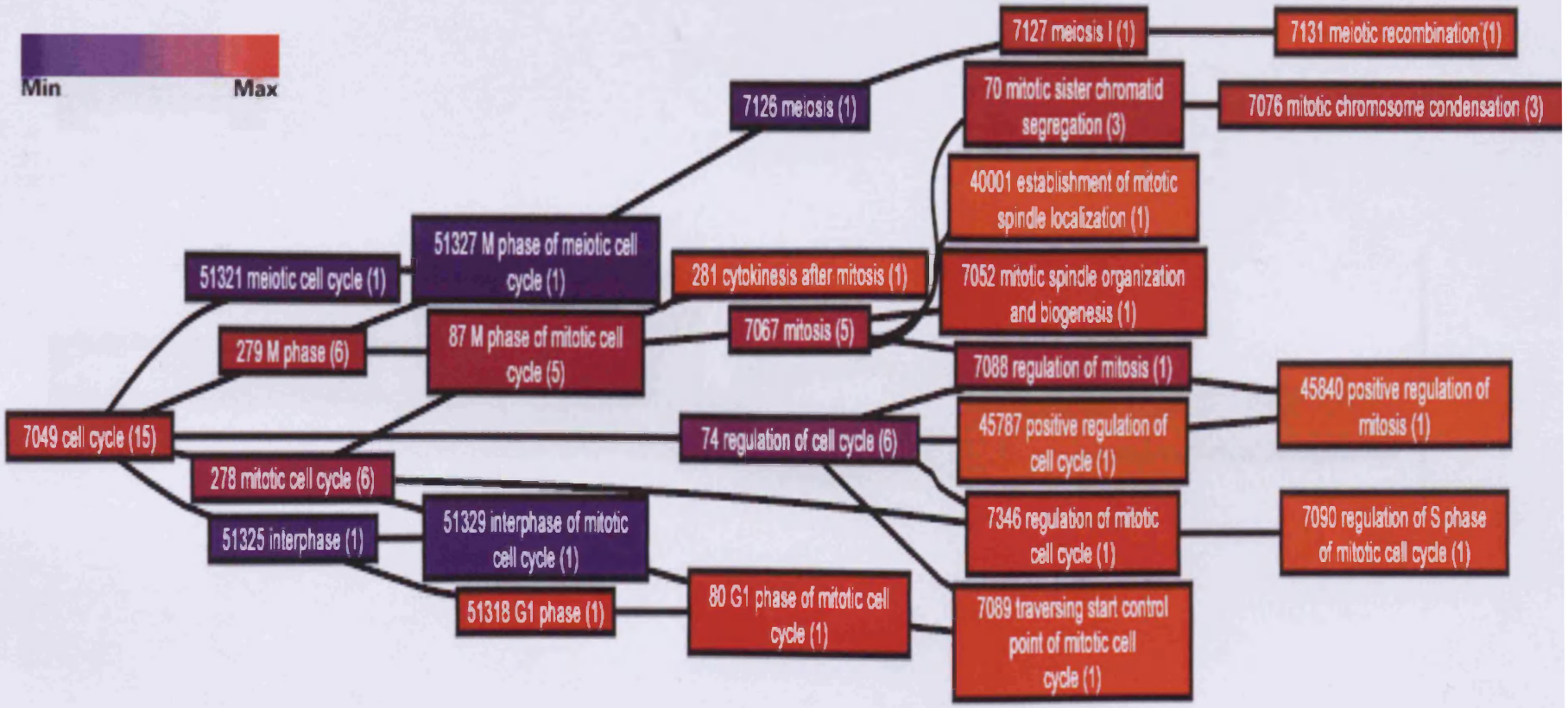

Figure 5.2: Tree view of Cell cycle gene ontology related clusters of genes found up-regulated in corneal limbal basal cells with specific gene ontology term public database reference number. Min-Max node colour specification refers to the probability of the genes with the given ontology to form an individual cluster.

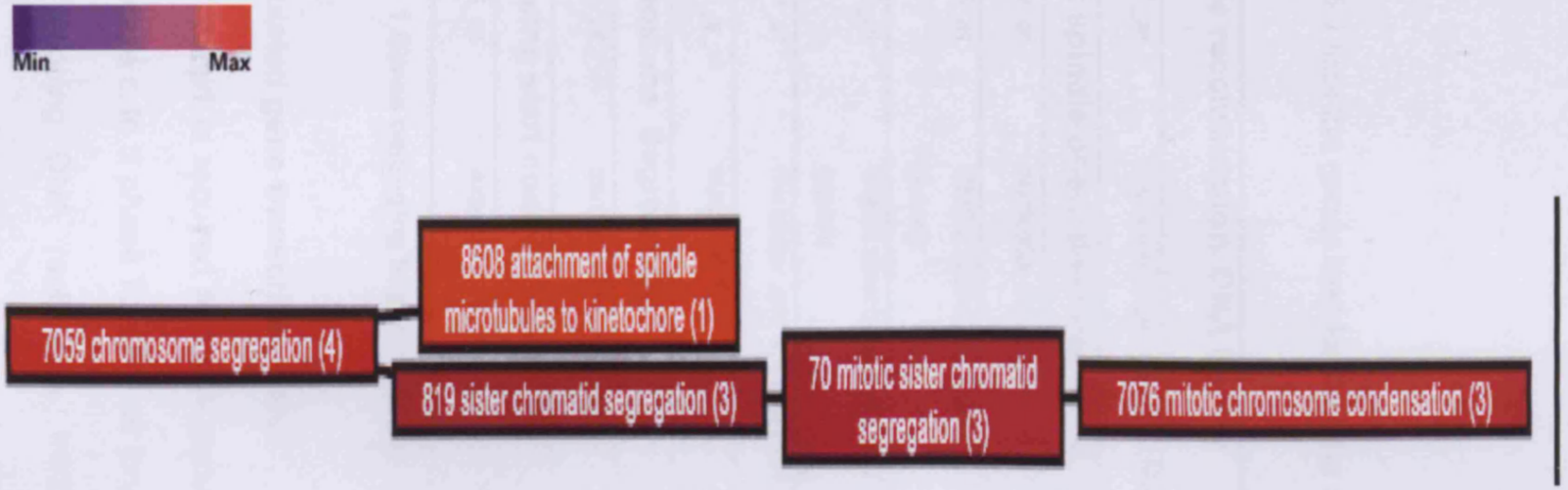

Figure 5.3: Tree view of chromosome condensation gene ontology related clusters of genes found upregulated in corneal limbal basal cells. The specific gene ontology database reference number is designated. Min-Max node colour specification refers to the probability of the genes with the given ontology to form an individual cluster.

Table 5.1 lists the genes that formed the above clusters.

Meiosis recombination, DNA Repair		
1452241_at	topoisomerase (DNA) II beta binding protein	**Topbp1**
Mitotic spindle orientation and sister chromatid segregation		
1416309_at	nucleolar and spindle associated protein 1	**Nusap1**
1448635_at	SMC2 structural maintenance of chromosomes 2-like 1 (yeast)	**Smc2l1**
1427275_at	SMC4 structural maintenance of chromosomes 4-like 1 (yeast)	**Smc4l1**
1416309_at	nucleolar and spindle associated protein 1	**Nusap1**
1415849_s_at	stathmin 1	**Stmn1**
Chromosome Segregation		
1435005_at	centromere protein E	**Cenpe**
Traversing start control point of G1		
1418334_at	expressed sequence AA545217	**AA545217**

Table 5. 1 Genes belonging to gene ontology clusters related to cell cycle

Upregulated gene transcripts were:

- Topbp1 is required for DNA replication and that it interacts with DNA polymerase ε. In S phase TopBP1 co localizes with Brca1 at focal points there is no ongoing DNA replication. Inhibition of DNA synthesis leads to delocalisation of TopBP1 together with Brca1 to replication forks, suggesting a role in rescue of stalled forks (Mäkiniemi et al. 2001)

- Smc 2 and 4 are proteins involved in transport, cell cycle, chromosome segregation , mitotic chromosome condensation and organisation (Uzbekov et al 2002; Freeman, Aragon-Alcaide and Strunnikov 2005)

- Nusap1 is a recently discovered protein involved in establishment of mitotic spindle localisation and positive regulation of mitosis by mitotic sister chromatid segregation after the end of mitosis (Raemaekers et. al 2003).

- Stathmin 1 has been shown to be involved in spindle organisation and inhibition of microtubule polymerisation during mitosis. Moreover it is involved in axonogenesis (Liu et al. 2005)

- Cenpe, centromere protein E, was identified as a separate cluster of chromosome segregation related ontology by itself. Centrosome-associated protein E is a kinesin-like motor protein that accumulates in the G2 phase of the cell cycle. (Yen et al. 1991; Yen et al. 1992). Unlike other centrosome-associated proteins, it is not present during interphase and first appears at the centromere region of chromosomes during prometaphase (Tanudji et al. 2004). CENPE is proposed to be one of the motors responsible for mammalian chromosome movement and/or spindle elongation (Liu et al. 2003).

- The expressed sequence AA545217 that has an ontology related to traversing the start control point of G1 is of great interest since Bickenbach (2004) very recently shown that while the majority of epithelial SCs reside in the G1 phase of the cell cycle, they are not held out of the cell cycle. It would

be interesting to further investigate if this EST belongs to a gene and maybe clone the gene to further investigate its function in epithelial stem cells.

5.4.1.2.2 Transcription-related gene clusters.

The genes that constituted these clusters are listed in the Table 5.4 below. The relevant clusters are illustrated in Figure 5.4. Seven genes were found to be upregulated in the corneal limbal basal cells in transcription-related clusters. These were grouped into those that regulate transcription, six of them had a Dna dependent and one a polymerase II promoter dependent transcription gene ontology, as shown in Table 5.2 and Fig. 5.4.

Table 5. 2 Genes that belong to the gene ontology clusters related to regulation of transcription

Regulation of transcription DNA dependent		
1450008_a_at	catenin (cadherin associated protein), beta 1	**Ctnnb1**
1437313_x_at	high mobility group box 2	**Hmgb2**
1433742_at	ankyrin repeat domain 15	**Ankrd15**
1433575_at	SRY-box containing gene 4	**Sox4**
1428890_at	fem-1 homolog c (C.elegans)	**Fem1c**
1419555_at	E74-like factor 5	**Elf5**
Regulation of transcription from polymerase II promoter		
1417719_at	sin3 associated polypeptide	**Sap30**

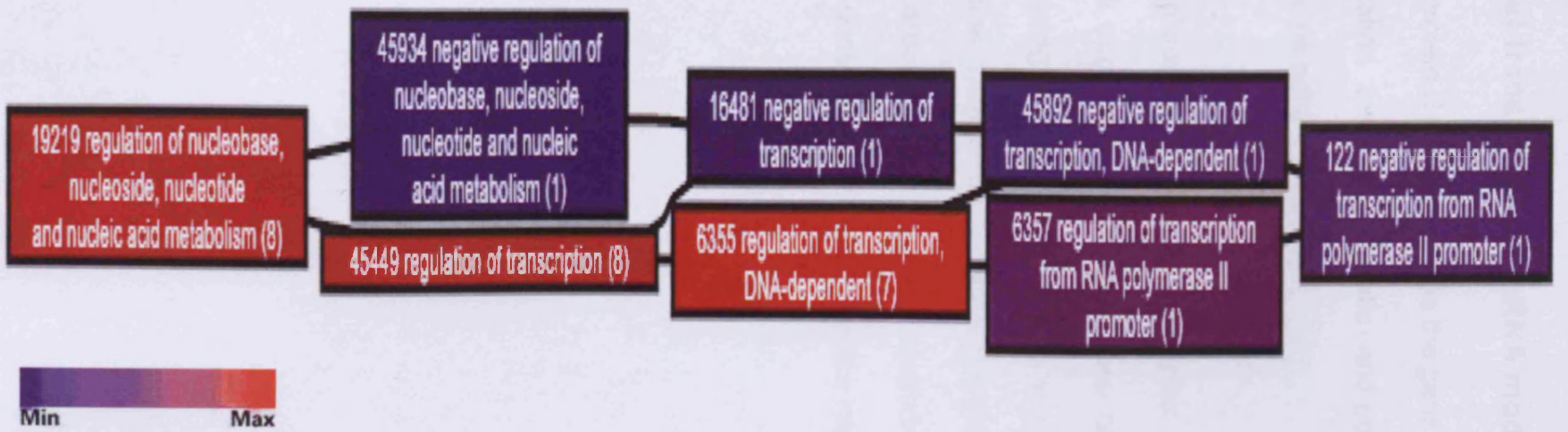

Figure 5.4: Tree view transcription related gene ontology related clusters of genes found upregulated in corneal limbal basal cells with designated specific gene ontology database reference numbers. Min-Max node colour specification refers to the probability of the genes with the given ontology to form an individual cluster.

5.4.1.2.3 Post-transcriptional mRNA modification cluster.

Only Apolipoprotein B (apobec1) was the gene forming five sub clusters of the RNA modification ontology. Specific end-point sub-cluster of these was cytidine to uridine editing (**Fig 5.5**).

Apobec1, apolipoprotein B editing complex 1, was identified as a single cluster with a nucleotide metabolism gene ontology. Apobec is involved in mRNA processing (Chester et al. 2003), specifically in cytidine to uridine, it exhibits cytidine deaminase activity (Mukhopadhyay et al. 2002). It is hydrolysing carbon-nitrogen (but not peptide) bonds, in cyclic amidines. Additionally it contains a nuclear localisation domain (Blanc 2003).

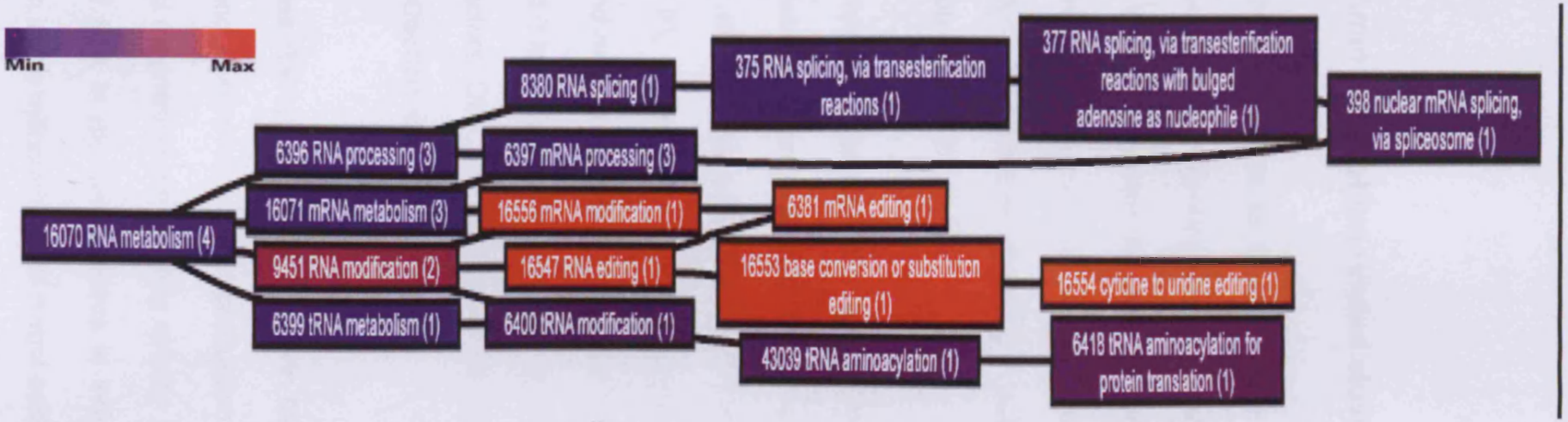

Figure 5.5: Tree view of mRNA processing related gene ontology related clusters of genes found upregulated in corneal limbal basal cells with designated specific gene ontology database reference numbers. Min-Max node colour specification refers to the probability of the genes with the given ontology to form an individual cluster.

5.4.1.2.4. Vitamin metabolism related cluster of genes upregulated

Two probe-sets were found to have a water soluble vitamin metabolism ontology. These were representing two genes namely Pyridoxal kinase (Pdxk) and Riboflavin kinase (Rfk) were found to be upregulated in the corneal limbal basal cells that formed the vitamin metabolism related gene clusters. Pdxk was found to form a pyridoxine metabolism sub cluster and Rfk a riboflavin biosynthesis sub cluster (**Fig. 5.6**)

Pyridoxal (pyridoxine, vitamin B6) kinase Pdxk, is a major protein of pyridoxine metabolism (Hanna et al.1997), It exhibits nucleotide binding, ATP binding, metal ion binding activity and converts vitamin B6 to pyridoxal-5-phosphate (PLP), an essential cofactor in the intermediate metabolism of amino acids and neurotransmitters. The expression of PDXK shows circadian oscillations and it is regulated in the mouse liver and brain by the 3 PAR bZIP transcription factors, Dbp, Hlf, and Tef, which also show circadian oscillations in expression (Gachon et al. 2004).

Riboflavin kinase Rfk is involved in riboflavin biosynthesis. It localises to the mitochondria and is involved in FAD production. It exhibits riboflavin kinase, transferase and magnesium ion binding activity. (Karthikeyan et al 2003). The upregulation of RFk in the basal limbus is indicative of increased levels of FAD production in the mitochondria of limbal epithelial cells.

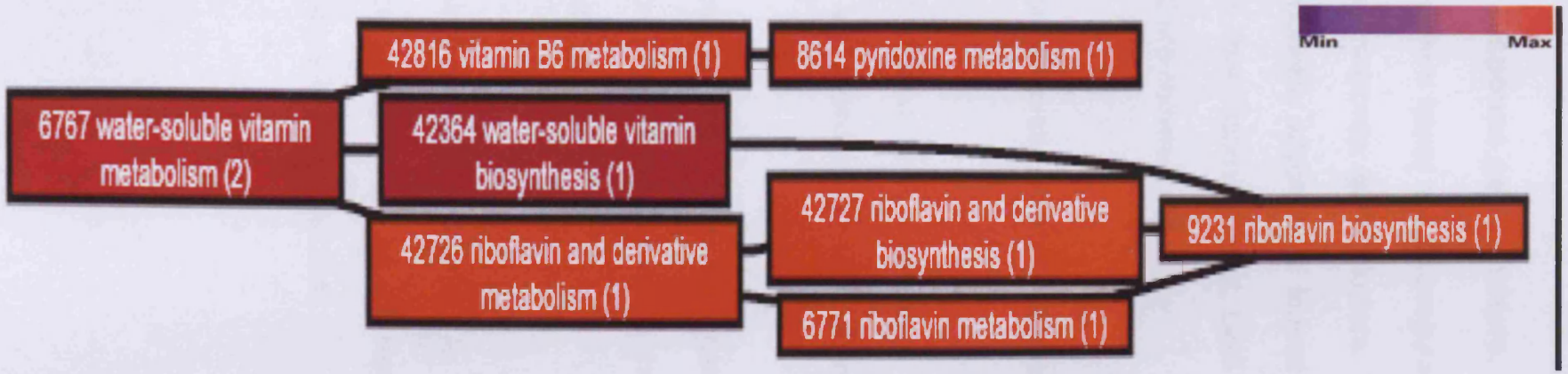

Figure 5.6: Tree view of vitamin metabolism related gene ontology related clusters of genes found upregulated in corneal limbal basal cells with specific gene ontology t database reference numbers. Min-Max node colour specification refers to the probability of the genes with the given ontology to form an individual cluster.

5.4.1.2.5 Stress response gene clusters.

Twelve probe-sets were found to be upregulated in the corneal limbal basal cells in the stress response gene clusters. There were four sub clusters exhibiting high probability which were formed by three genes. The clusters were of wounding, fear response, heat, DNA damage, and oxidative stress gene ontology and are shown in Fig. 5.7.

All genes that belonged to stress response related clusters were:

- Caspase 1, (Casp1) is a mediator of the response to hypoxia proteolysis and peptidolysis and induction of apoptosis.

- Peroxiredoxin 1, (Prdx1) exhibits peroxidase activity, and it is involved in regulation of NF-kappaB-nucleus import in response to oxidative stress activity.

- DnaJ (Hsp40) homolog, subfamily A, member 1. Dnaja1 is a heat shock protein and acts as in protein repair, possibly folding proteins in a metal ion dependent mechanism.

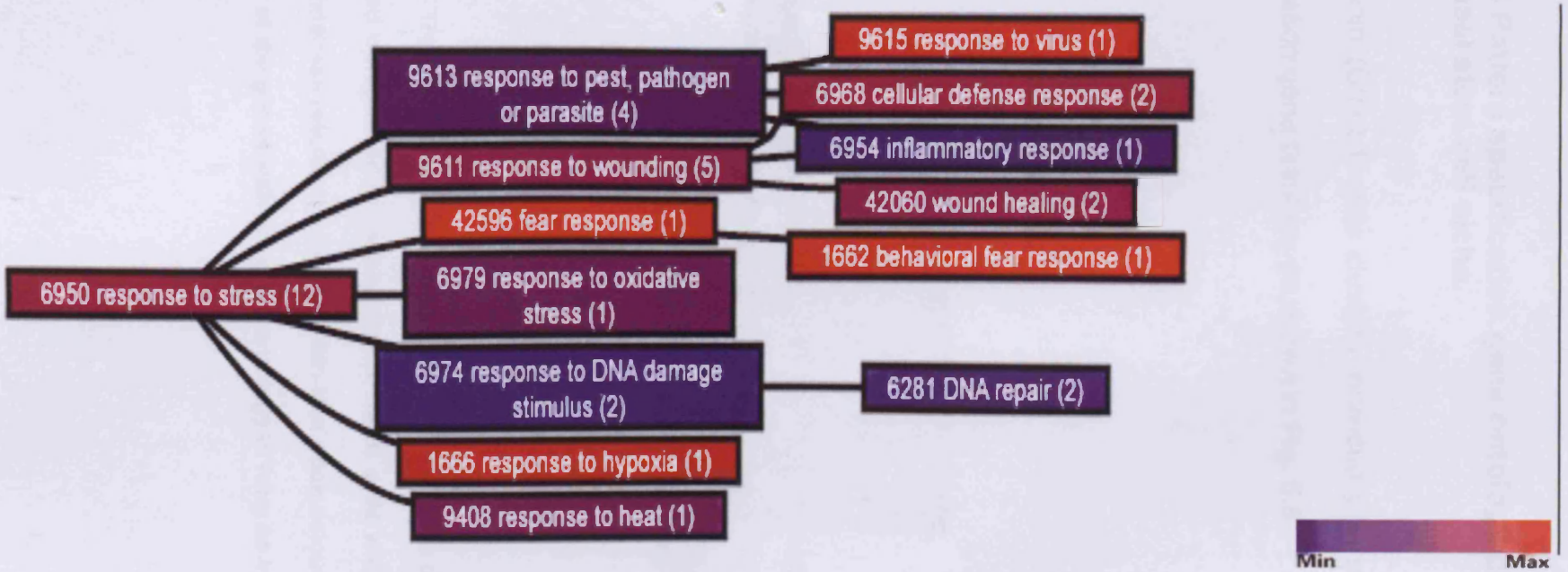

Figure 5.7: Tree view of stress response related gene ontology related clusters of genes found up-regulated in corneal limbal basal cells with designated specific gene ontology database reference numbers. Min-Max node colour specification refers to the probability of the genes with the given ontology to form an individual cluster.

5.4.1.2.6 Pattern specification gene ontology cluster upregulated in the corneal stem cell niche.

Beta-catenin (Ctnnb1) also clusters individually in pattern specification and axis formation gene ontology as shown in **Fig. 5.8**.

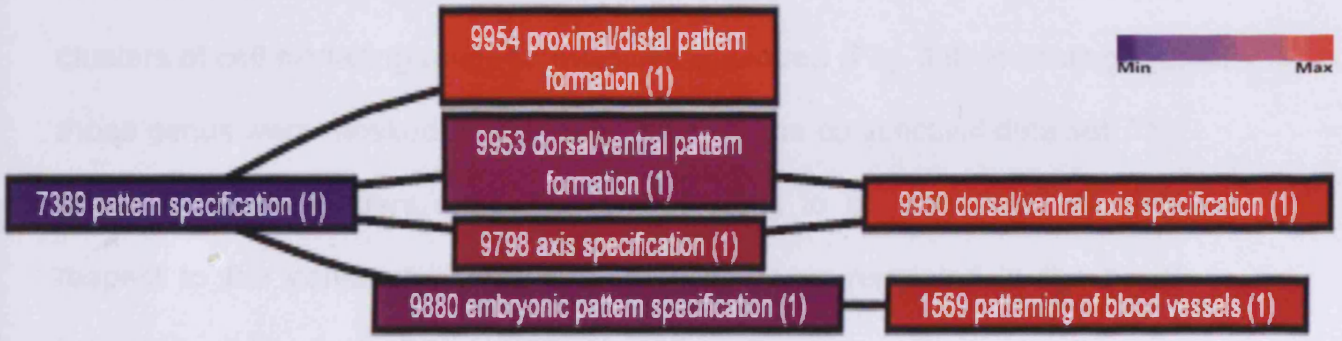

Figure 5. 8 Tree view of pattern specification related gene ontology related clusters of genes found upregulated in corneal limbal basal cells with designated specific gene ontology database reference numbers. Min-Max node colour specification refers to the probability of the genes with the given ontology to form an individual cluster.

5.4.1.2.7 Cell signalling clusters

As mentioned earlier, the limbal basal data set was compared to those of all other regions in order to identify limbal specific genes and EST's and these genes and EST's were clustered with respect to gene ontology. In that case genes did not cluster at all in clusters of cell signalling related ontology. In order to overcome this problem the limbal basal set was compared with only the ones of corneal origin and not conjunctiva. When this dataset was used, clusters of cell signalling related ontologies appeared (**Fig. 5.9**) indicating that those genes were masked by the comparison to the conjunctival data set. The genes of those clusters although are not going to be limbal specific with respect to the conjunctiva they are likely to be up-regulated in the basal limbus in relation to the basal periphery and centre.

Forty probe sets that correspond to 27 genes were found to be forming the clusters of a cell signalling related ontology. All probe sets together with their respective gene name and sub-cluster they belonged are listed in **Table 5.3a-b.** Figure 5.8 is included solely to depict the clusters that were formed. The treeview was too large in order to fit even in an appendix.

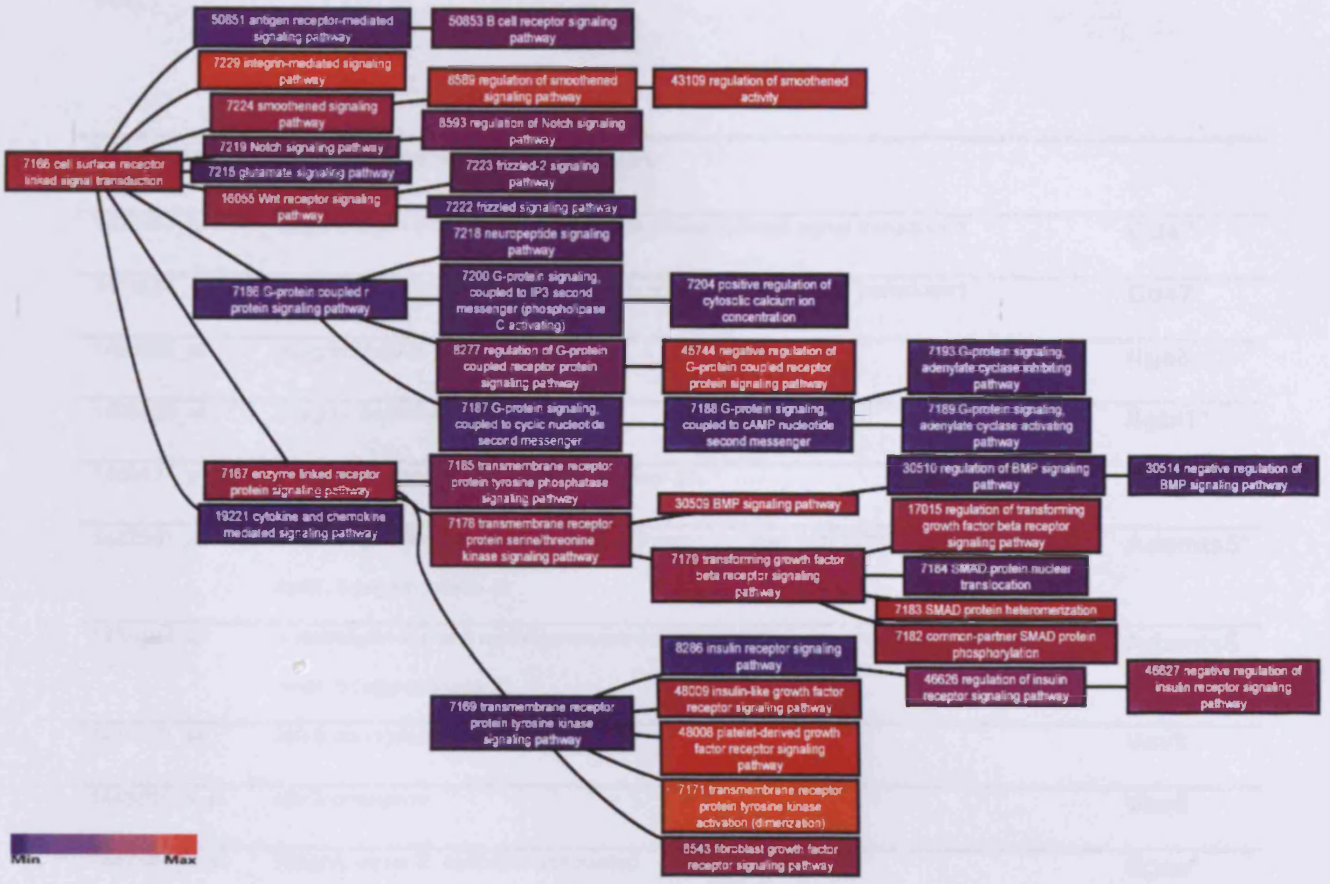

Figure 5.9 Tree view of cell signalling related gene ontology related clusters of genes found up-regulated in corneal basal cells with specific gene ontology term public database reference number. Min-Max node colour specification refers to the probability of the genes with the given ontology to form an individual cluster.

Table 5.3 a: Genes, with designated Affymetrix probe identities, belonging to cell signalling clusters of genes up-regulated in the limbus.* (indicates genes that were only identified after the comparison of gene expression excluded the conjunctival data set).

Integrin mediated signalling pathway		
1428187_at	CD47 antigen (Rh-related antigen, integrin-associated signal transducer)	**Cd47**
1419554_at	CD47 antigen (Rh-related antigen, integrin-associated signal transducer)	**Cd47**
1454966_at	integrin alpha 8	**Itga8**
1425039_at	integrin, beta-like 1	**Itgbl1***
1460427_a_at	a disintegrin and metalloprotease domain 28	**Adam28***
1422561_at	a disintegrin-like and metalloprotease (reprolysin type) with thrombospondin type 1 motif, 5 (aggrecanase-2)	**Adamts5***
1456404_at	a disintegrin-like and metalloprotease (reprolysin type) with thrombospondin type 1 motif, 5 (aggrecanase-2)	**Adamts5**
1417122_at	vav 3 oncogene	**Vav3**
1448600_s_at	vav 3 oncogene	**Vav3**
1447541_s_at	integrin, alpha E, epithelial-associated	**Itgae***
1416953_at	connective tissue growth factor	**Ctgf***
Smoothened signalling pathway		
1427049_s_at	smoothened homolog (Drosophila)	**Smo***
1428853_at	patched homolog 1	**Ptch1***
Noch Signalling pathway		
1437303_at	interleukin 6 signal transducer	**Il6st***

Table 5.3b: Genes, with designated Affymetrix probe identities, belonging to cell signalling clusters.* (indicates genes that were only identified after the comparison of gene expression excluded the conjunctival data set).

Wnt receptor signalling pathway		
1422751_at	transducin-like enhancer of split 1, homolog of Drosophila E(spl)	**Tle1***
1450008_a_at	catenin (cadherin associated protein), beta 1, 88kDa	**Ctnnb1**
1448593_at	WNT1 inducible signaling pathway protein 1	**Wisp1***
1448594_at	WNT1 inducible signaling pathway protein 1	**Wisp1**
1449340_at	sclerostin domain containing 1	**Sostdc1***
1455214_at	microphthalmia-associated transcription factor	**Mitf***
1418534_at	frizzled homolog 2 (Drosophila)	**Fzd2***
1437284_at	frizzled homolog 1 (Drosophila)	**Fzd1***
1450044_at	frizzled homolog 7 (Drosophila)	**Fzd7***
1422602_a_at	wingless-related MMTV integration site 5B	**Wnt5b***
1439373_x_at	wingless-related MMTV integration site 5B	**Wnt5b**
1448201_at	secreted frizzled-related sequence protein 2	**Sfrp2***

Table 5.3c: Genes, with designated Affymetrix probe identities, belonging to cell signalling clusters.* (indicates genes that were only identified after the comparison of gene expression excluded the conjunctival data set).

Serine threonine kinase signalling		
BMP signalling		
1423635_at	bone morphogenetic protein 2	**Bmp2***
1448208_at	MAD homolog 1 (Drosophila)	**SMAD1***
1459843_s_at	MAD homolog 1 (Drosophila)	**SMAD1***
TGF-BETA signalling		
1423635_at	bone morphogenetic protein 2	**Bmp2***
SMAD heterodimerisation		
1448208_at	MAD homolog 1 (Drosophila)	**SMAD1***
1459843_s_at	MAD homolog 1 (Drosophila)	**SMAD1***
Common partner of SMAD phosphorylation		
1419256_at	spectrin beta 2	
Negative regulation of G-protein coupled receptor signalling		
1444409_at	Rabphilin 3A-like (without C2 domains)	**Rph3al***
Negative regulation of insulin receptor signalling pathway		
1455899_x_at	suppressor of cytokine signalling 3	**Socs3***
Insulin like growth factor receptor signalling		
1425458_a_at	growth factor receptor bound protein 10	**Grb10***
PDGF receptor signalling pathway		
1419123_a_at	platelet-derived growth factor, C polypeptide	**Pdgfc***
1449351_s_at	platelet-derived growth factor, C polypeptide	**Pdgfc***

5.4.1.3 Genes downregulated in corneal limbal basal epithelial cells.

Genes specifically downregulated in the corneal limbal basal epithelium were identified by RMA analysis. Criteria were that the probes should have an A-P value of at least 1.00 in central and limbal basal epithelium and that their fold change should be equal or less than 1.5. Additionally the probe sets should exhibit an ANOVA 2 tail t test value of equal or less than 0.05.

The gene list together with gene symbols and names, chromosomal location, as well as UNIGENE database reference numbers and fold changes is presented at **Table C.2** in **appendix C**. Clusters of biological and molecular functions specifically downregulated in the corneal limbal basal epithelium were identified by gene ontology clustering.

5.4.1.3.1 Ontological clusters of genes downregulated in limbal basal epithelial cells.

There were three genes on that cluster category. The ontological cluster and sub-clusters that were formed are illustrated in figures **5.10** and **5.11**

Necdin (Ndn) was the gene that constituted to the calcium homeostasis gene ontology cluster (see **fig. 5.10 A**) as well as the Regulation of cell growth gene ontology cluster (see figure **5.10 B**). Ectopic expression of necdin induces differentiation of mouse neuroblastoma (Kobayashi, Taniura, and Kazuaki Yoshikawa 2002). The protein binds to and represses the activity of cell-cycle-promoting proteins such as SV40 large T, adenovirus E1A, and the transcription factor E2F. Necdin also interacts with p53 and works in an additive manner to inhibit cell growth (reviewed by Forslund and Nordqvist 2001). This result agrees with the results from the specifically up-regulated genes in the basal limbus which show that those cells might not be held out of the cell cycle. Additionally E2F5 was found to be specifically up-regulated in basal limbal cells but it did not fulfil the Presence-Absence criteria.

Special AT-rich sequence binding protein 1 (Satb1) was the gene that constituted the cluster of histone methylation gene ontology (see **fig. 5.11 A, B** and **C**). SATB1 is a cell-type specific nuclear protein that recruits chromatin-remodelling factors and orchestrates temporal and spatial expression of multiple genes during thymocyte differentiation (Alvarez et al. 2000). This is could be indicative of a suppressive mechanism of a gene program switch

towards differentiation, active in corneal epithelial stem cells or early-lineage cell of the basal limbus.

ST8 alpha-N-acetyl-neuraminide alpha-2, 8-sialyltransferase 4 (St8sia4) was the gene in the protein glycosylation gene ontology cluster (See figure 5.10 A). This agrees with the findings of Wolosin and Wang (1995) in the rabbit cornea which show that alpha-2,3 sialylation differentiate the limbal and corneal epithelial cell phenotypes (Wolosin and Wang 1995). The results indicate that a similar mechanism exists in mice and suggests that the transcriptional repression of sialyltransferases might be the actual mechanism.

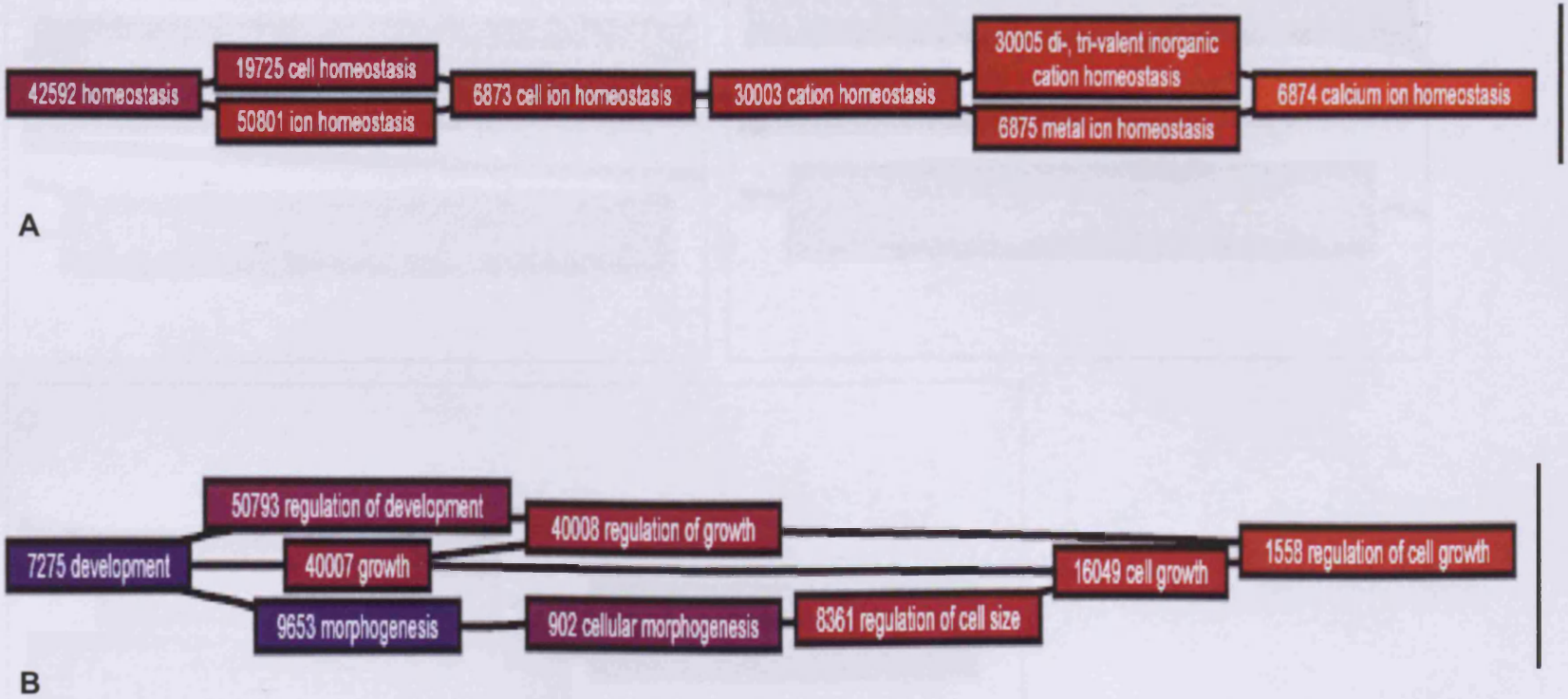

Figure 5.10: Tree view of homeostasis (A), development (B) related gene ontology clusters of genes found down-regulated in corneal basal cells with designated specific gene ontology database reference numbers. Min-Max node color specification refers to the probability of the genes with the given ontology to form an individual cluster.

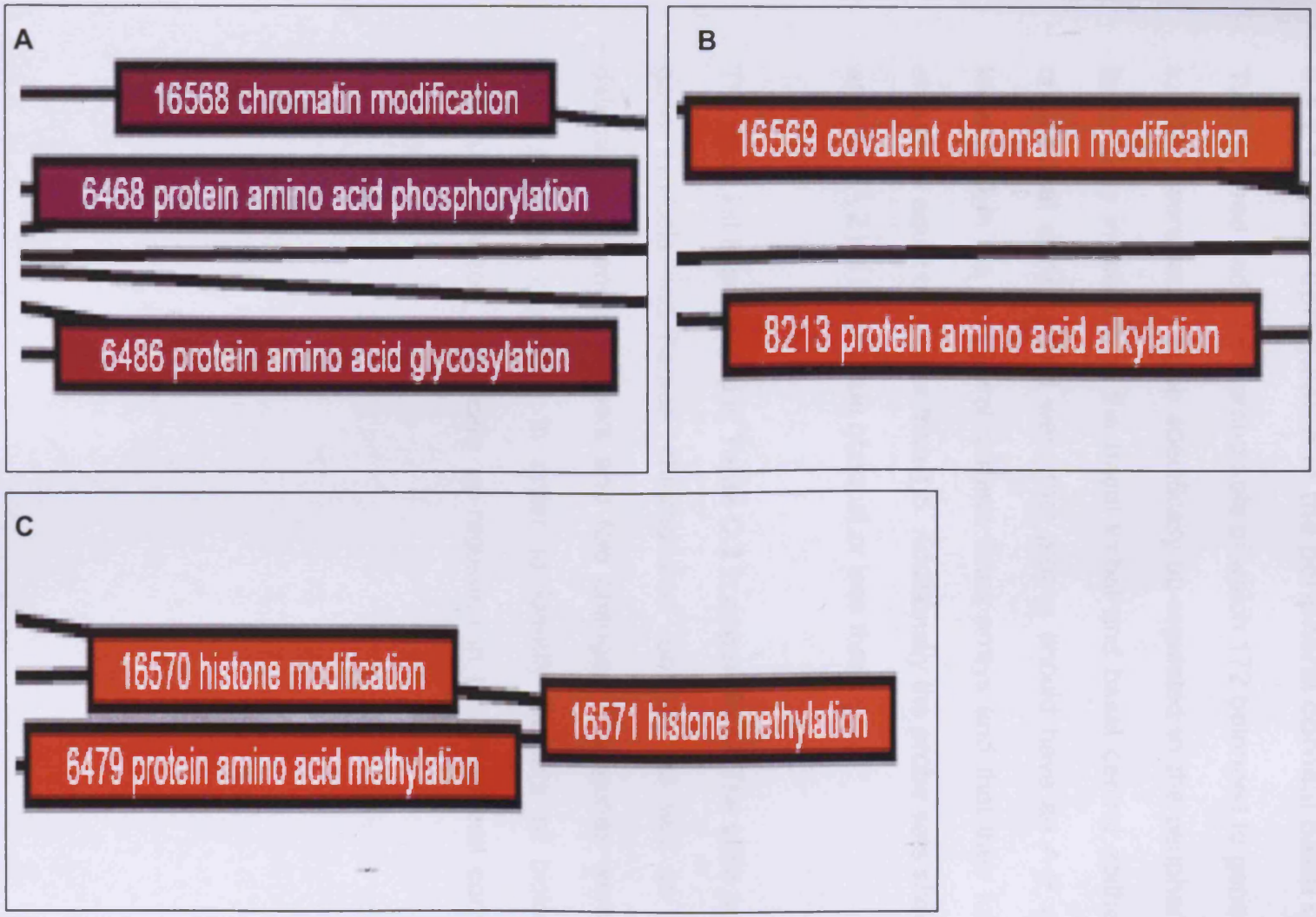

Figure 5.11: Tree view of metabolism-related gene ontology clusters of genes found downregulated in corneal basal cells with designated specific gene ontology database reference number. Min-Max node colour specification refers to the probability of the genes with the given ontology to form an individual cluster. A, B and C are consecutive fragments of the picture that illustrated the tree.

5.4.2 Peripheral basal cell gene expression profile.

5.4.2.1 Genes upregulated in the peripheral corneal basal cells.

Two hundred and eighty probe sets of which 172 belonged to genes and 108 to ESTs were found to be specifically up-regulated in the peripheral corneal basal cells in relation to the basal limbal and basal central epithelium. The criteria that were applied were that probes should have an A-P value of at least 1.00 in the peripheral corneal basal arrays and that their fold change should be equal or greater than 1.5. Additionally the probe sets should exhibit an ANOVA 2 tail t test value of equal or less than 0.05.

The gene list is presented at **Table C.3** in **appendix C**. The table contains the gene symbols and names, chromosomal location, as well as UNIGENE database reference numbers and fold changes. The genes were used for gene ontology clustering in order to identify clusters of biological and molecular function specifically up-regulated in the peripheral corneal basal epithelium.

5.4.2.1.1 Gene ontology clusters of genes upregulated in the peripheral corneal basal cells.

The following table (**Table 5.4 a-c**) lists the gene ontology clusters with their respective genes that were identified as up-regulated in peripheral corneal basal cells.

Table 5.4 a: The table lists the genes that belong to the gene ontology clusters identified as up-regulated in peripheral basal cells

Circadian rhythm		
1421087_at	period homolog 3 (Drosophila)	**Per3**
1425099_a_at	aryl hydrocarbon receptor nuclear translocator-like	**Arntl**
Nitrix oxide biosynthesis		
1454995_at	dimethylarginine dimethylaminohydrolase 1	**Ddah1**
Nuclear mRNA splicing via spliceosome		
1447447_s_at	serine/arginine repetitive matrix 1	**Srrm1**
Xenobiotic metabolism		
1422438_at	epoxide hydrolase 1, microsomal	**Ephx1**

Table 5.4b: The table lists the genes that belong to the gene ontology clusters identified as up-regulated in peripheral basal cells

Aromatic compound catabolism		
1422438_at	neurotrophic tyrosine kinase, receptor, type 2	**Ntrk2**
Peptidyl threonine phosphorylation		
1451478_at	cDNA clone MGC:32448 IMAGE:5043159	
Transcription		
1455154_at	GLI-Kruppel family member GLI3	**Gli3**
1450093_s_at	zinc finger and BTB domain containing 7	**Zbtb7**
Actin cortical patch assembly		
1449660_s_at	coronin, actin binding protein 1C	**Coro1c**
Regulation of G-protein coupled receptor		
1418189_s_at	receptor (calcitonin) activity modifying protein 2	**Ramp2**
1418188_a_at	receptor (calcitonin) activity modifying protein 2	**Ramp2**
G-protein signalling coupled to IP3 second messenger (PLC activating)		
1417500_a_at	transglutaminase 2, C polypeptide	**Tgm2**
JNK cascade		
1436791_at	wingless-related MMTV integration site 5A	**Wnt5a**

Table 5.4c: The table lists the genes that belong to the gene ontology clusters identified as up-regulated in peripheral basal cells

Wnt signalling cascade		
1436791_at	wingless-related MMTV integration site 5A	**Wnt5a**
1450772_at	wingless-related MMTV integration site 11	**Wnt11**
Rho protein signal transduction		
1416511_a_at	CDC42 effector protein (Rho GTPase binding) 4	**Cdc42ep4**
Cellular morphogenesis/ photoreceptor cell development		
1417904_at	DNA cross-link repair 1A, PSO2 homolog (S. cerevisiae)	**Dclre1a**
Mechanoreceptor		
1420838_at	neurotrophic tyrosine kinase, receptor, type 2	**Ntrk2**

5.4.2.2 Genes downregulated in the periphery

Thirty seven genes and four EST's were specifically down-regulated in the periphery were as identified by RMA analysis. The criteria that were used were that probes should have an A-P value of at least one in all the regions apart from the periphery and that their fold change should be equal or less than 1.5. Additionally the probe sets should exhibit an ANOVA 2 tail t test value of equal or less than 0.05.

The gene list is presented at **Table C.4 in appendix C**. The table contains the gene symbols and names, chromosomal location, as well as UNIGENE database reference numbers and fold changes. The genes were used for gene ontology clustering in order to identify clusters of biological and molecular function specifically down-regulated in the peripheral corneal basal epithelium.

5.4.2.2.1 Gene ontology clusters of genes down-regulated in basal peripheral epithelial cells.

The only clusters that were seen were formed by caveolin 1 (Cav1). Caveolin, caveolae protein 1 (Cav1), forms a "negative regulation of Mapk activity" as well as a "negative regulation of nitric oxide biosynthesis" ontological cluster within down-regulated genes in peripheral corneal basal epithelial cells. (**Fig 5.12**).

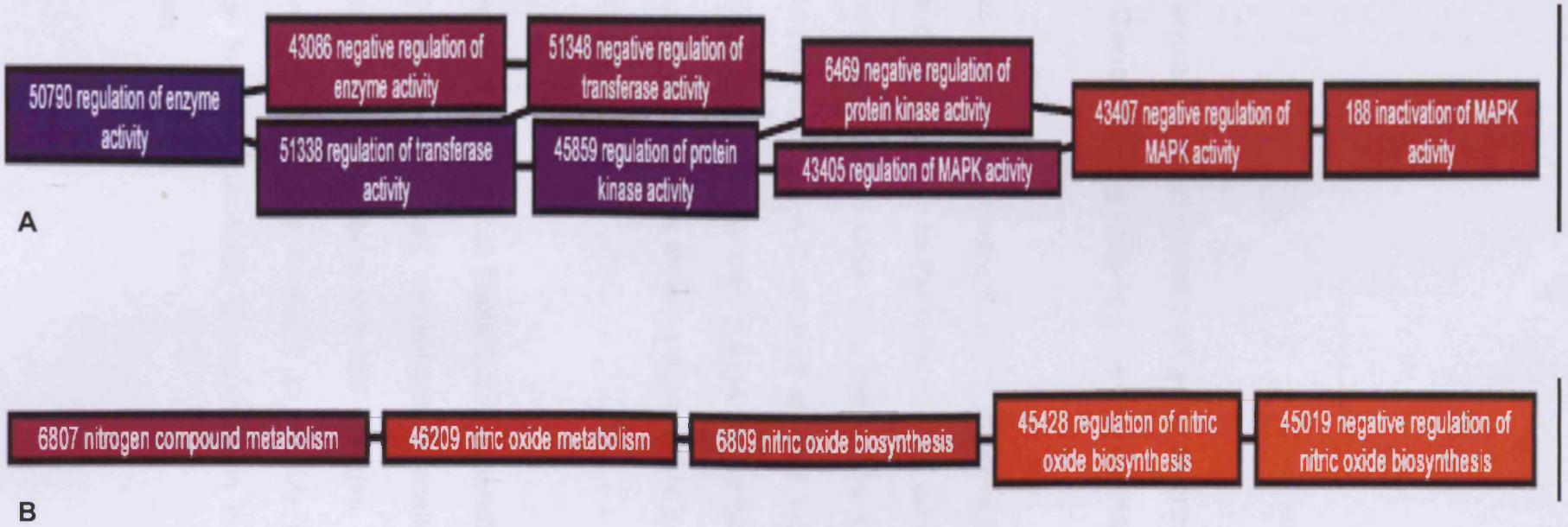

Figure 5.12. Tree view of negative regulation of MAPK activity (A) and negative regulation of nitric oxide synthesis (B) gene ontology related gene ontology related clusters of genes found down-regulated in corneal basal cells with designated specific gene ontology database reference numbers. Min-Max node color specification refers to the probability of the genes with the given ontology to form an individual cluster.

5.4.3 Central Corneal Basal Cell gene expression profile.

5.4.3.1 Genes Up-regulated in Central corneal epithelial basal cells.

78 genes and 18 ESTs were found to be up-regulated in the corneal basal epithelial cells in relation to the ones in basal peripheral and the limbal cells. The genes are listed in table 5.9. The criteria that were applied were that probes should have an A-P value of at least 1.00 in the peripheral corneal basal arrays and that their fold change should be equal or greater than 1.5. Additionally the probe sets should exhibit an ANOVA 2 tail t test value of equal or less than 0.05.

The gene list is presented at **Table C.5** in **appendix C**. The table contains the gene symbols and names, chromosomal location, as well as UNIGENE database reference numbers and fold changes. The genes were used for gene ontology clustering in order to identify clusters of biological and molecular function specifically up-regulated in the peripheral corneal basal epithelium.

5.4.3.1.1 Gene ontology clusters of gene upregulated in central basal epithelium.

Seven genes of the ones found in upregulated specifically in the central corneal basal cells in relation to those in basal peripheral and limbal cells were involved in eight gene ontology clusters with a high probability. The genes are listed in **Tables 5.5 a & b**.

Table 5.5 a: Lists the gene ontology clusters and their respective genes, found to be up-regulated in central corneal epithelial basal cells.

nitric oxide mediated signal transduction		
1422557_s_at	metallothionein 1	**Mt1**
G-protein signaling, adenylate cyclase inhibiting pathway		
1419449_a_at	guanine nucleotide binding protein, alpha inhibiting 2	**Gnai2**
apoptotic mitochondrial changes release of cytochrome c from mitochondria		
1455456_a_at	translocase of inner mitochondrial membrane 50 homolog (yeast)	**Timm50**
zinc ion homeostasis		
1422557_s_at	metallothionein 1	**Mt1**
negative regulation of translational initiatiation		
1434976_x_at	eukaryotic translation initiation factor 4E binding protein 1	**Eif4ebp1**
pyrimidine deoxyribonucleotide diphosphate biosynthesis		
1450484_a_at	thymidylate kinase family LPS-inducible member	**Tyki**

Table 5.5b lists the gene ontology clusters and their respective genes, found to be up-regulated in central corneal epithelial basal cells.

S-adenosylmethionine biosynthesis		
1438386_x_at	methionine adenosyltransferase II, alpha	**Mat2a**
1438630_x_at	methionine adenosyltransferase II, alpha	**Mat2a**
1438976_x_at	methionine adenosyltransferase II, alpha	**Mat2a**
1456702_x_at	methionine adenosyltransferase II, alpha	**Mat2a**
anterior-posterior compartment specification		
1447640_s_at	pre B-cell leukemia transcription factor 3	**Pbx3**

The study confirms earlier data that exclude metallothioneins as limbal stem cell markers. These cysteine-rich metal-binding intracellular proteins have been linked to cell proliferation and have been shown to be strongly expressed by basal limbal cells of human corneas (Lauweryns et al. 1993b). It also was immunolocalised in the same study to suprabasal epithelial cells at the limbus in a mosaic-like pattern, to clusters of TC in the superior cornea, and to basal cells in the corneal epithelium. Studies from Schlotzer-Schrehardt and. Kruse described weak immunoreactivity in basal cells of the limbal epithelium, but stronger in superficial cells of all ocular surface epithelia.

5.4.3.2 Genes downregulated in the central cornea.

Twelve genes and four ESTs were found to be specifically downregulated in central corneal basal cells in relation to the basal peripheral and limbal cells The criteria that were used were that probes should have an A-P value of at least one in all the regions apart from the periphery and that their fold change should be equal or less than 1.5. Additionally the probe sets should exhibit an ANOVA 2 tail t test value of equal or less than 0.05.

The gene list is presented at **Table C.6** in **appendix C**. The table contains the gene symbols and names, chromosomal location, as well as UNIGENE database reference numbers and fold changes. The genes were used for gene ontology clustering in order to identify clusters of biological and molecular function specifically down-regulated in the peripheral corneal basal epithelium

5.4.3.2.1 Gene ontology clusters of genes downregulated specifically in basal cells of the central corneal epithelium.

The ontological clusters of genes down regulated in basal cells of the central corneal epithelium are listed in **Table 5.6**

Regulation of cell growth	
Igfbp4	insulin-like growth factor binding protein 4
Transcription	
Atf2	activating transcription factor 2
Ubiquitin dependent catabolism	
Ube2h	ubiquitin-conjugating enzyme E2H
Proteolysis	
Pcolce	procollagen C-proteinase enhancer protein
Dephoshorylation, Transmembrane receptor tyrosine phosphatase signalling	
Ptprk	protein tyrosine phosphatase, receptor type, K
Transport	
Slc13a2	solute carrier family 13 (sodium-dependent dicarboxylate transporter), member 2
Nsf	N-ethylmaleimide sensitive fusion protein

Table 5.6: Ontological clusters of genes down regulated in basal cells of the central corneal epithelium

5.5 Discussion

The gene expression profile of basal cells of the limbus, peripheral, and central cornea was revealed in this study. These expression profiles can be used as an atlas of gene expression for a variety of further studies. For the purposes of this thesis, emphasis was given on the mechanisms that are relevant to the cells of the corneal stem cell niche.

As it was discussed in the introduction, the basal limbus consists of stem cells and transient amplifying cells, whereas the peripheral basal epithelium is enriched in transient amplifying cells of several generations and does not contain stem cells. The basal epithelium of the central cornea is enriched with more differentiated cells and does not contain stem cells. Therefore by selecting genes that were exclusively upregulated in each region would possibly identify some genes that are controlling basic biological functions that prevail in each region. Although it is thought that the percentage of stem cells among the limbal basal cells in mice is between 10-20% this number is below 1% in the periphery. Therefore stem cells are 10 to 20 times enriched in the basal limbus in relation to the periphery and even more in relation to the centre. Some of the genes that are up-regulated in the basal limbus in relation to all other regions are likely to be involved in processes and pathways that are uniquely ongoing in the basal limbus. Knowing that the defining property that differentiates stem cells from transient amplifying cells is asymmetric division leading to stem cell self-renewal, one would expect that genes that would be controlling these unique properties to be indicated as up-regulated

in the basal limbus when compared with basal epithelia that are barren o stem cells.

One can expect that many of the genes that appear upregulated in the corneal stem cell niche (i.e. the basal limbus) will be controlling mechanisms and processes that are unique or up-regulated in early transient amplifying cells, as compared to later transient amplifying cells.

Thus, the genes indicated to be up and down regulated in the basal limbus are expected to provide a valuable starting point for studying the differential molecular machinery and properties of stem cells and transient amplifying cells and allow us to focus and gain a further insight into stem cell biology

5.5.1 Selection of several targets for further analysis

In order to confirm protein expression and test array sensitivity, selected targets were carefully chosen for further RT-PCR analysis and immunohistochemistry. It would be virtually impossible to confirm all the targets that the array indicated, since this would maybe require many new time consuming studies that would be far greater then the time given for that of a Ph.D. study. Instead, several targets were chosen that were identified from RMA analysis, as well as transcripts that were identified as upregulated according to RMA analysis but did not fulfil the presence/absence criteria in order to confirm at least the results of the array to a satisfactory degree.

In order to do that, the targets that were chosen spanned from very low to very high raw intensity values (the ones given as an output from the GeneChip Scanner). Additionally, targets that were included, spanned a variety of roles such as receptors, nuclear factors, enzymes and structural proteins, which at the same time, have the potential to participate in important mechanisms in stem cells. These targets are listed in **Table 5.7** together with their raw mean intensity values.

Table 5.7 List of selected targets with their respective selection criteria for the purposes of confirmation of array sensitivity

Raw intensity value	Target gene	Presence-Absence Fulfilled
150	**Col4abp3**	N
150	**PTGER4**	N
200	**E2F5**	N (marginal)
220	**TLR3**	Y
550	**Areg**	Y
550	**SMC2**	Y
1000	**Rbp1**	Y
1200	**SMC4**	Y
1200	**NEK2**	1st prb Y2nd prb N
5000	**K14**	Y
10000	**Nmp1**	Y
15000	**Aldh6a**	Y
>20000	Catnb1	Y

Alcohol dehydrogenase 6 a (Adh6a) and cellular retinol binding protein 1(Rbp1) were found exclusively upregulated in the corneal epithelial stem cell compartment. Alcohol dehydrogenases and Rbp1 have been shown to be involved in the control of intracellular levels of retinoic acid (Molotkov et al. 2004). Retinoic acid has been shown to affect the proliferation of corneal epithelial stem cells both *in vitro* and *in vivo* (Tseng et al. 1988; Kruse et al. 1994)

In addition, nuclear receptors for retinoic acid and thyroid hormone regulate transcription of keratin genes (Tomic et al. 1990), including Keratin 14, which was found to be enriched in the corneal stem cell compartment of the mouse in this study. The regulation of keratin gene expression by RAR and T3R occurs through direct binding of these receptors to the receptor response elements of the keratin gene promoters (Tomic et al. 1996). Thus confirmation of K14 target by RT-PCR and immunohistochemistry could prove beneficial for further studies as a determinant of differential cell type (stem or TA). Further supporting the need for the confirmation of K14 is the availability of transgenic mice with K14 promoter targeted expression cassettes using the K14 promoter (Vaezi et al. 2002) that are publicly available by the Jackson Lab.

There is only one study so far that identified a protein of the Toll like receptor family in corneal epithelial cells (Song et al. 2001). TLR4 was found to be expressed in the corneal epithelium and it is thought that it might play the role of bacterial pathogen lipopolysaccharide receptor (Song et al. 2001). It was therefore decided that it would be interesting to investigate the expression of

toll like receptor 3 since these mediators of innate immunity may be of importance in an immunologically privileged organ as the eye.

Nuclear β-catenin/TCF signalling pathway is essential for the maintenance of epithelial stem cells in the small intestine as well as the hair follicle. The proliferative compartment of the gut was depleted of stem cells in TCF4 double knock-outs, which die shortly after birth (Korinek 1998). There was a 75% reduction in stem cells in the hair follicle in mice with targeted mutations of downstream targets of nuclear β-catenin/TCF complex. (Waikel et al 2001).

Nucleophosmin, also known as NPM, B23, NO38, is a nucleolar protein directly implicated in cancer pathogenesis. The *NPM1* gene is found mutated and rearranged in a number of haematological disorders (Morris et al. 1994; Redner et al. 1996; Yoneda et al. 1996; Falini et al. 2005; Grisendi et al. 2005). The region of chromosome 5 to which *NPM1* maps is deleted in a proportion of *de novo* human myelodysplastic syndromes (MDS) (Van den Berghe et al. 1997; Westbrook et al. 2000; Giagounidis et al. 2004; List et al. 2004) and loss of chromosome 5 is extremely frequent in therapy-related MDS (Olney et al. 2002; List et al. 2004). NPM's role in oncogenesis is controversial as it has been attributed with both oncogenic and tumour suppressive functions (Kondo et al. 1997; Colombo et al. 2002; Bertwistle et al. 2004; Kurki et al. 2004).

This line of evidence suggests a possible role of nucleophosmin in lineage decisions for the hematopoietic system.

Since corneal neoplasias are an extremely rare event and they only have been associated with limbal epithelium (Kruse et al. 2000) and nucleophosmin has not been identified before in the corneal epithelium, this was an interesting target to further investigate, firstly to confirm its presence, and also in expression studies.

5.5.2 Conclusions

- The gene expression profile of basal cells of the limbal, peripheral and central cornea was realised.
- Mechanisms that potentially may regulate important biological functions of cells in the stem, TA and mature cell compartment were identified in order to direct further experiments assigning the genes in stem, early and late transient amplifying cells.
- Gene targets of interest were selected for further experiments to validate the microarray data and also confirm protein expression in the corneal epithelium

Chapter 6

Confirmation and molecular characterization of Microarray targets.

6.1 Aims

- To test for array sensitivity and confirm the levels of selected mRNA transcripts indicated as upregulated in the corneal stem cell niche from the microarray data.
- To confirm protein expression of selected targets from the microarray data in corneal epithelial cells.

6.2 Introduction

To test for the sensitivity of the microarray experiments and confirm the levels of mRNA transcripts, several targets that were found to be up-regulated in the corneal stem cell compartment were chosen according to the following criteria:

To include targets that will not fulfil Presence/Absence criteria but will be designated as up-regulated by RMA analysis.

To include target genes that their raw intensity values as given by MAS5 output software would scan from the lowest (150) to highest values (20000) and thus confirm array sensitivity.

To test target genes that would be partners on potential fundamental control mechanisms of stem cells and/or could serve as stem cell markers.

The targets as well as details on their raw expression intensity value their P/A status and the test applied are designated in the following table:

Raw intensity value.	Target gene	Presence-Absence Fulfilled	Tested for: RNA (R) or Protein Expression (P)
150	**Col4abp3**	N	R
150	**PTGER4**	N	R & P
200	**E2F5**	N (marginal)	R
220	**TLR3**	Y	R & P
550	**Areg**	Y	P
550	**SMC2**	Y	R &P
1000	**Rbp1**	Y	R & P
1200	**SMC4**	Y	R
1200	**NEK2**	1st prb Y2nd prb N	R
5000	**K14**	Y	P
10000	**Nmp1**	Y	R&P
15000	**Aldh6a**	Y	R
>20000	**Catnb1**	Y	P

Table 6.1 Lists the target genes selected for confirmation of array sensitivity purposes, their raw detection values, Presence-Absence criterion fulfilment and the tests that were applied to confirm expression.

6.3 Materials and methods

The methods used were Semiquantitative real time RT-PCR and Immunohistocytochemistry and are explained in detail in sections 2.1.12 and 2.1.13.

The primers were designed by acquiring the mRNA sequence for the specific transcripts from NCBI's public nucleotide sequence database available online at www.ncbi.nlm.nih.gov/entrez. Primer 3 software was used to design the primers publicly available online at http://frodo.wi.mit.edu/cgi-bin/primer3/primer3_www.cgi. The primer sequences together with detailed information and specifications are listed in Table A.1 in appendix A.

For immunohistochemistry experiments the antibodies and specific details are included in Table B.1 in appendix B. Eyes from three 12-week-old C57BL6 male mice, which were different from the ones used for microarray analysis and RT-PCR studies. Nevertheless mice were kept on the same diet and diet plan as well as light conditions as the ones used for microarray and RT-PCR studies.

6.4 Results.

6.4.1 Semiquantitative RT-PCR confirms up-regulated target expression in the corneal stem cell compartment.

6.4.1.1 Alcohol dehydrogenase 6 a mRNA is up regulated in the basal limbus

Semiquantitative analysis shown that the alcohol dehydrogenase 6 a transcript (Aldh6a) is up regulated in limbal epithelial basal cells in relation to peripheral and central corneal epithelial cells and basal and suprabasal cells of the conjunctiva. The fold change differences between the basal limbus and the rest of the areas as estimated by RT-PCR as well as by microarray analysis are listed in **Table 6.2** . Figure **6.1** illustrates the relative expression of Aldh6a between regions as determined by semiquantitative RT-PCR using GAPDH as an internal control.

	Fold Difference as determined by:	
Areas	**SQ-RT-PCR**	**Microarray**
Limbus-Periphery	3.29	2.77 (present)
Limbus-Centre	4.98	4.76 (present)
Limbus-Conjunctiva	4.84	3.97 (present)

Table 6.2 Lists the fold difference in abundance of Aldh6a transcripts between the basal limbus (Limbus) and the basal periphery (Periphery) and both basal and suprabasal conjunctiva (Conjunctiva). Present indicates the presence of the gene in the limbal arrays according to selection criteria.

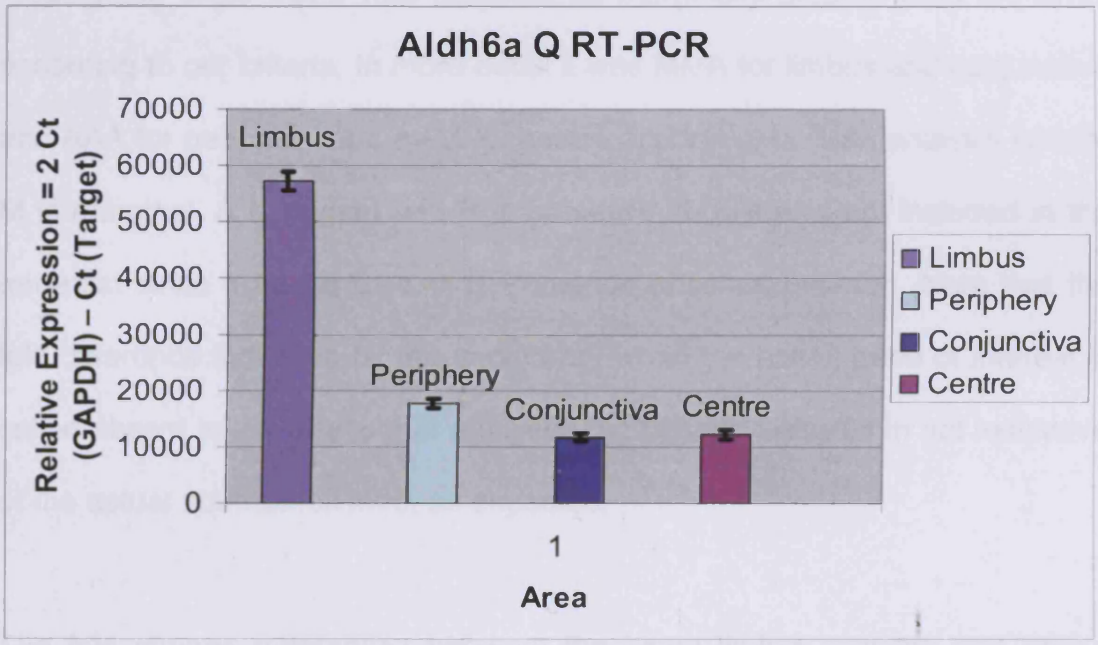

Figure 6.1. Semiquantitative real time RT-PCR of Aldh6a gene transcript expression confirms up-regulation in the limbus.Ct refers to the cycle threshold (Ct) number. SEM Limbus ±1598, Periphery ± 810, Conjunctiva ± 654, Centre ±829.

6.4.1.2 E2F transcription factor 5 (E2F5), p130-binding mRNA is up regulated in the basal limbus

Semiquantitative analysis shown that the E2F transcription factor 5 (E2F5), p130-binding transcript (E2F5) is only expressed to a detectable level in limbal epithelial basal cells and undetectable in peripheral and central corneal epithelial cells and basal and suprabasal cells of the conjunctiva. This is showing that the specific probe set printed on the array might need redesigning since E2F5 was detected as marginally present from the array according to our criteria. In more detail it was MMA for limbus and conjunctiva and AAA for periphery and AAM for centre according to RMA analysis (where M is marginal, A is absent and P is present). Thus it was not included in the gene list since it had a 0.66 (<1) Presence absence criterion. Note that the fold difference indicated by the microarray when the actual gene of interest is called absent in the arrays that analyses the desired samples in not indicative of the actual abundance ratio, as expected.

The fold change differences between the basal limbus and the rest of the areas as estimated by RT-PCR as well as by microarray analysis is listed in **Table 6.3**

Figure **6.2** illustrates the relative expression of E2F5 between regions as determined by semiquantitative RT-PCR using GAPDH as an internal control.

	Fold Difference as determined by:	
Areas	**SQ-RT-PCR**	**Microarray**
Limbus-Periphery	323.67	2.56 (m.absent)
Limbus-Centre	1922.42	3.79 (m.absent)
Limbus-Conjunctiva	1448.40	3.02 (m.absent)

Table 6.3 Lists the fold difference in abundance of E2F5 transcripts between the basal limbus (Limbus) and the basal periphery (Periphery) and both basal and suprabasal conjunctiva (Conjunctiva). M.absent indicates the marginal absence (0.66) of the gene in the limbal arrays according to selection criteria.

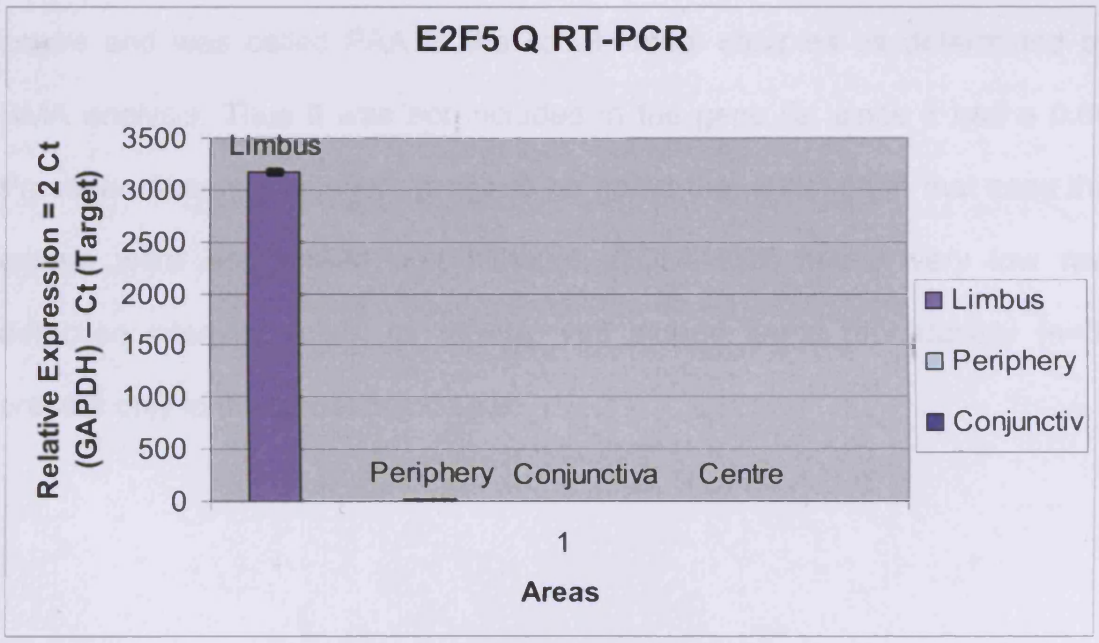

Figure 6. 1. Semiquantitative real time RT-PCR of E2F5 gene expression confirms up-regulation in the limbus.Ct refers to the cycle threshold (Ct) number. SEM Limbus ±21.9 Periphery ± 0.05, Conjunctiva ± 0.07, Centre ±0.05.

6.4.1.3 Collagen, Type IV, alpha-3 binding protein (COL4A3BP) mRNA is up regulated in the basal limbus

Semiquantitative analysis shown that the Collagen, Type IV, alpha-3 binding protein (COL4A3BP) transcript is only expressed to a detectable level in limbal epithelial basal cells and undetectable in peripheral and central corneal epithelial cells and basal and suprabasal cells of the conjunctiva.

The fold change differences between the basal limbus and the rest of the areas as estimated by RT-PCR as well as by microarray analysis is listed in **Table 6.4**

COL4A3BP was AAA (A indicates absent) in conjunctiva, basal periphery and centre and was called PAA in the basal limbal samples as determined by RMA analysis. Thus it was not included in the gene list since it had a 0.66 Presence-Absence criterion. It has to be noted that although in that case the criteria were not fulfilled and although COL4A3BP has a very low raw detection intensity value, its mRNA was indeed found reproducibly (n=3) present only in the limbal basal cells.

	Fold Difference as determined by:	
Areas	**SQ-RT-PCR**	Microarray
Limbus-Periphery	3491.71	5.81 (m.absent)
Limbus-Centre	12040	1.92 (m.absent)
Limbus-Conjunctiva	**70.5×10^3**	23.15 (m.absent)

Table 6.4 Lists the fold difference in abundance of COL4A3BP transcripts between the basal limbus (Limbus) and the basal periphery (Periphery) and both basal and suprabasal conjunctiva (Conjunctiva). M.absent indicates the marginal absence (0.66) of the gene in the limbal arrays according to selection criteria.

Figure **6.3** illustrates the relative expression of COL4A3BP between regions as determined by semiquantitative RT-PCR using GAPDH as an internal control.

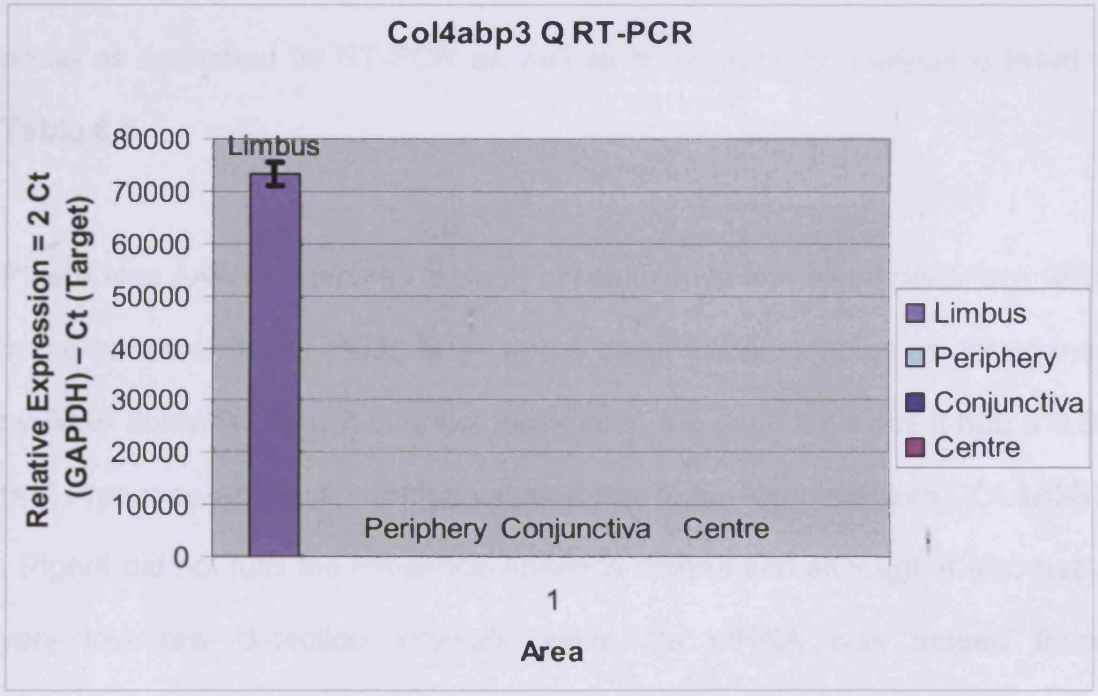

Figure 6. 2 Semiquantitative real time RT-PCR of Col4abp3 gene expression confirms up-regulation in the limbus.Ct refers to the cycle threshold (Ct) number. SEM Limbus ± 2340.36, Periphery ± 0.68, Conjunctiva ± 0.02, Centre ±0.17.

6.4.1.4 Prostaglandin E receptor 4 mRNA is up regulated in the basal limbus

Semiquantitative analysis shown that the Prostaglandin E receptor 4 (Ptger4) transcript is only expressed to a detectable level in limbal epithelial basal cells and undetectable in peripheral and central corneal epithelial cells and basal and suprabasal cells of the conjunctiva.

The fold change differences between the basal limbus and the rest of the areas as estimated by RT-PCR as well as by microarray analysis is listed in **Table 6.5**

Ptger4 was AAA (A indicates absent) in conjunctiva and basal periphery, MAA in the centre and was called MMA in the basal limbal samples as determined by RMA analysis. Thus it was not included in the gene list since it had a 0.66 (<1) Presence-Absence criterion value. It has to be noted that like COL4A3BP , Ptger4 did not fulfil the Presence-Absence criteria and although it also has a very low raw detection intensity value, its mRNA was indeed found reproducibly (n=3) present only in the limbal basal cells.

	Fold Difference as determined by:	
Areas	**SQ-RT-PCR**	Microarray
Limbus-Periphery	3491.71	5.81 (m.absent)
Limbus-Centre	12040	1.92 (m.absent)
Limbus-conj	**70.5×10^3**	23.15 (m.absent)

Table 6.5 Lists the fold difference in abundance of Ptger4 transcripts between the basal limbus (Limbus) and the basal periphery (Periphery) and both basal and suprabasal conjunctiva (Conjunctiva). M absent indicates that the probe was called marginally absent by RMA analysis.

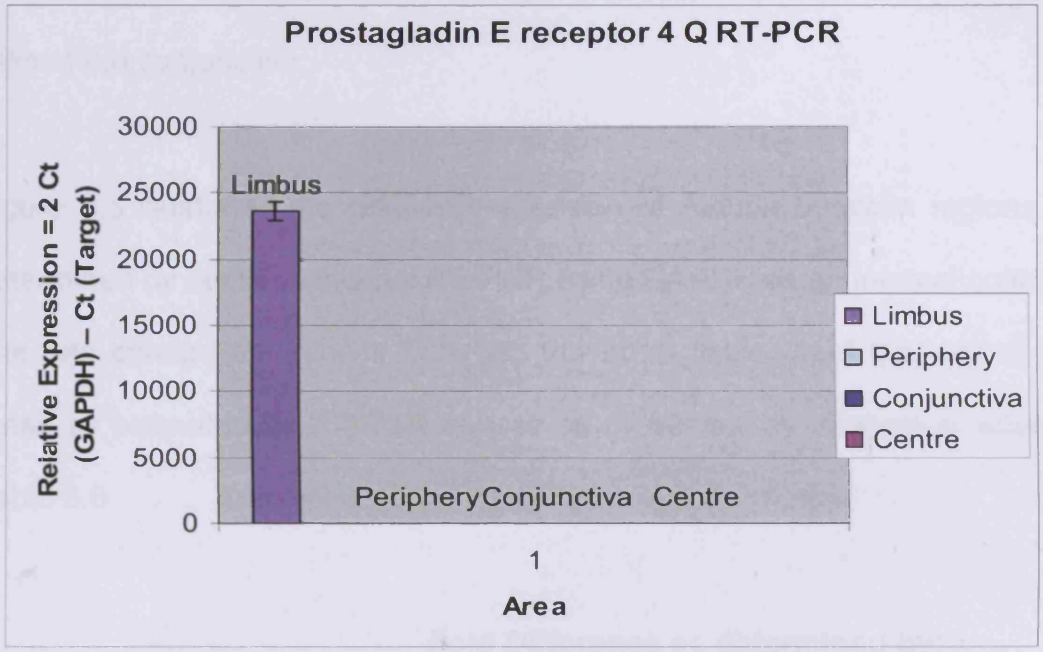

Figure 6. 3. Semiquantitative real time RT-PCR of PTGER4 gene expression confirms up-regulation in the limbus.Ct refers to the cycle threshold (Ct) number. M Limbus ± 737

6.4.1.5 Retinol-binding protein I, cellular (RBP1) mRNA is up regulated in the basal limbus

Semiquantitative analysis shown that the retinol-binding protein I, cellular (RBP1) transcript is upregulated in limbal epithelial basal cells in relation to peripheral and central corneal basal epithelial cells and basal and suprabasal cells of the conjunctiva.

Figure 6.5 illustrates the relative expression of Aldh6a between regions as determined by semiquantitative RT-PCR using GAPDH as an internal control. The fold change differences between the basal limbus and the rest of the areas as estimated by RT-PCR as well as by microarray analysis is listed in Table 6.6

	Fold Difference as determined by:	
Areas	**SQ-RT-PCR**	Microarray
Limbus-Periphery	2.88	3.27 (Present)
Limbus-Centre	1.50	3.23(Present)
Limbus-Conjunctiva	**1.92**	2.43(Present)

Table 6.6 Lists the fold difference in abundance of Rbp1 transcripts between the basal limbus (Limbus) and the basal periphery (Periphery) and both basal and suprabasal conjunctiva (Conjunctiva).

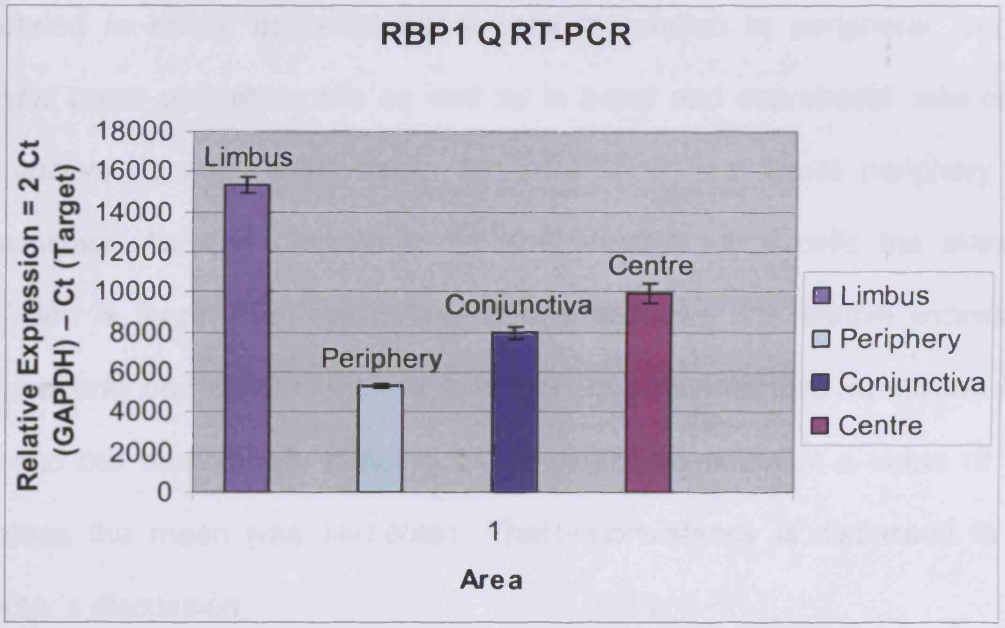

Figure 6. 5 Semiquantitative real time RT-PCR of Rbp1 gene expression confirms up-regulation in the limbus.Ct refers to the cycle threshold (Ct) number. SEM Limbus ± 374, Periphery ± 113, Conjunctiva ± 334, Centre ±490.

6.4.1.6 SMC2 structural maintenance of chromosomes 2-like 1 (yeast) mRNA is up regulated in the basal limbus

SMC2 structural maintenance of chromosomes 2-like 1 (yeast) is also called SMC2 (SMC2). The official name indicates that this gene is the homologue of the yeast SMC2, also called SMC2 in humans and mice.

Semiquantitative analysis shown that the SMC2 gene transcript is up-regulated in limbal epithelial basal cells in relation to peripheral, central, corneal basal epithelial cells as well as in basal and suprabasal cells of the conjunctiva. It was undetectable by RT-PCR in the basal periphery and conjunctiva. As it is obvious in fig. 6.6, central basal cells the standard deviation is larger than the mean. This is because the relative expression value of only one experiment was 3217.15241 but the other two repetitions were 564 and 560 respectively bringing the standard deviation at a value of 1532 whereas the mean was 1447.60981. That inconsistency is discussed in this chapter's discussion.

Figure 6.6 illustrates the relative expression of SMC2 between regions as determined by semiquantitative RT-PCR using GAPDH as an internal control. The fold change differences between the basal limbus and the rest of the areas as estimated by RT-PCR as well as by microarray analysis is listed in Table 6.6

	Fold Difference as determined by:	
Areas	**SQ-RT-PCR**	Microarray
Limbus-Periphery	646.11	2.11 (Absent)
Limbus-Centre	718.82	1.67 (Absent)
Limbus-Conjunctiva	**4.82**	2.89 (Present)

Table 6.7 Lists the fold difference in the abundance of SMC2 transcripts between the basal limbus (Limbus) and the basal periphery (Periphery) and both basal and suprabasal conjunctiva (Conjunctiva). Absent ad Present refer to the presence absence call of the array.

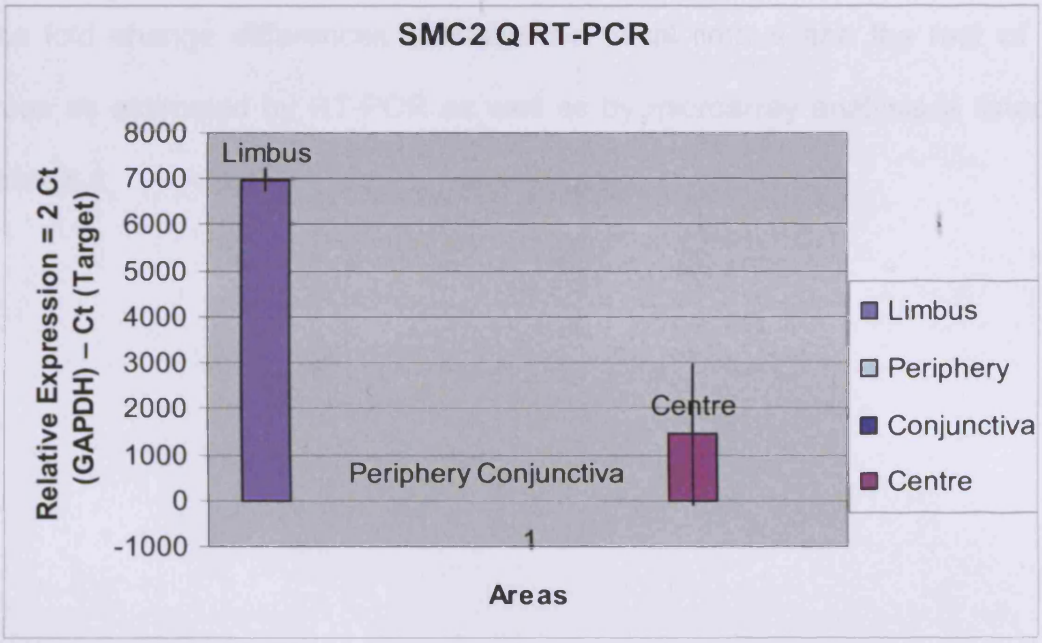

Figure 6. 4. Semiquantitative real time RT-PCR of SMC2 gene expression confirms up-regulation in the limbus.Ct refers to the cycle threshold (Ct) number. SD Limbus 230, centre 1532

6.4.1.7 SMC4 structural maintenance of chromosomes 4-like 1 (yeast) mRNA is up regulated in the basal limbus

SMC4 structural maintenance of chromosomes 2-like 1 (yeast) is also called SMC4 (SMC4). The official name indicates that this gene is the homologue of the yeast SMC4, also called SMC4 in humans and mice.

Semiquantitative analysis shown that the SMC4 transcript is upregulated in limbal epithelial basal cells in relation to peripheral and central corneal basal epithelial cells and basal and suprabasal cells of the conjunctiva.

Figure 6.7 illustrates the relative expression of SMC4 between regions as determined by semiquantitative RT-PCR using GAPDH as an internal control. The fold change differences between the basal limbus and the rest of the areas as estimated by RT-PCR as well as by microarray analysis is listed in Table 6.8

	Fold Difference as determined by:	
Areas	**SQ-RT-PCR**	Microarray
Limbus-Periphery	1.74	1.73 (Present)
Limbus-Centre	4.13	1.80 (Present)
Limbus-Conjunc.	**2.61**	2.17 (Present)

Table 6.8 Lists the fold difference in abundance of SMC4 transcripts between the basal limbus (Limbus) and the basal periphery (Periphery) and both basal and suprabasal conjunctiva (Conjunctiva).

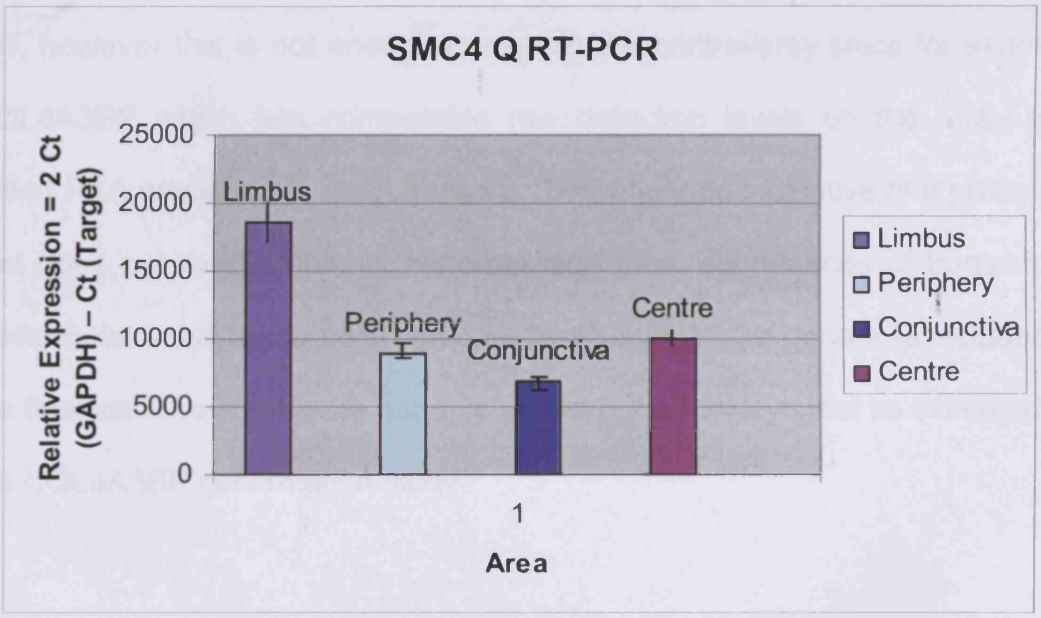

Figure 6. 5 Semiquantitative real time RT-PCR of SMC4 gene expression confirms up-regulation in the limbus.Ct refers to the cycle threshold (Ct) number. SEM Limbus ± 1365, Periphery ± 784, Conjunctiva ± 330, Centre ±522.

6.4.1.8 Toll-like Receptor 3 mRNA is up regulated in the basal limbus

Semiquantitative analysis shown that the Toll-like Receptor 3 transcript (Tlr3) is only expressed, to a detectable level, in limbal epithelial basal cells and is undetectable in peripheral and central corneal epithelial cells and basal as well as in suprabasal cells of the conjunctiva. The transcript was found to be PMM in the basal limbal, PPM in the conjunctiva and MMA and AAA in peripheral and central basal corneal samples respectively. It did fulfill the Presence-Absence criteria and therefore was included in the gene list. As it can be seen in figure 6.8 it was absent in all other samples apart from the limbal one. It is surprising that there was consistently (n=3) no detection in the conjunctiva sample in SQ RT-PCR experiment. The raw detection level was low, however this is not enough to explain the controversy since for example COL4A3BP which has comparable raw detection levels on the array was called PAA according to RMA analysis. This might be indicative of a probe set that does not exhibit optimal performance in low abundances of transcripts. Nevertheless due to our selection criteria robustness the gene was included in the final list. The criteria are not only robust but also very strict as indicated by the COL4A3BP confirmation study.

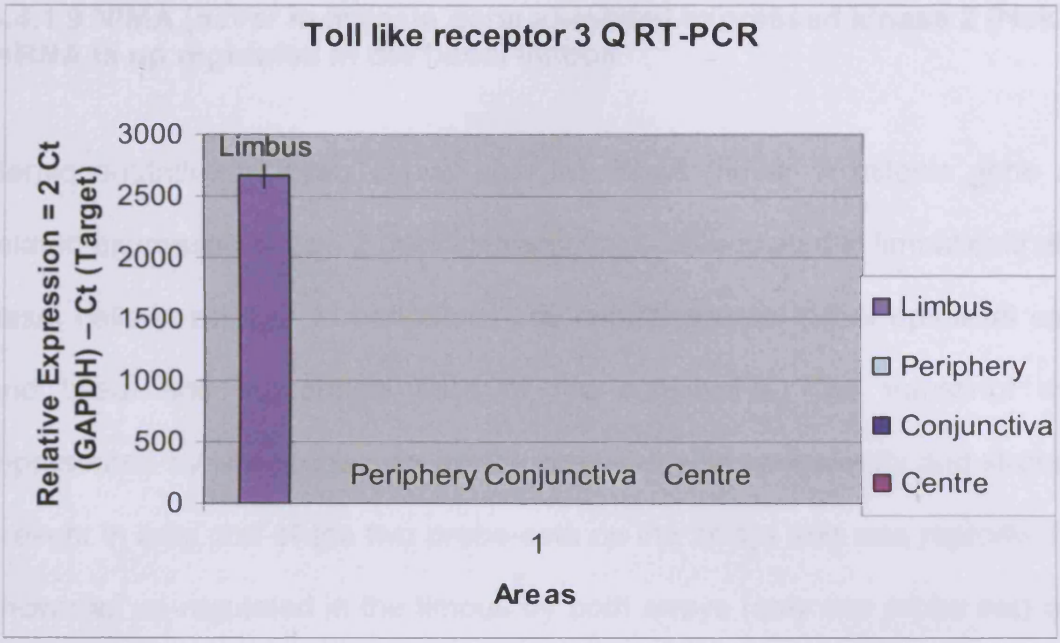

Figure 6. 6. Semiquantitative real time RT-PCR of TLR3 gene expression confirms up-regulation in the limbus.Ct refers to the cycle threshold (Ct) number. SEM Limbus ±162, Periphery ± 0.3, Conjunctiva ±0.2, Centre ±0.8.

	Fold Difference as determined by:	
Areas	**SQ-RT-PCR**	**Microarray**
Limbus-Periphery	1673.75	3.16 (Present)
Limbus-Centre	1835.86	2.58 (Present)
Limbus-Conjunctiva	1193.72	1.93 (Present)

Table 6.9 Lists the fold difference in abundance of Tlr3 transcripts between the basal limbus (Limbus) and the basal periphery (Periphery) and both basal and suprabasal conjunctiva (Conjunctiva). Present indicated the fulfilment of Presence-Absence criterion for the basal limbal samples as determined by RMA analysis.

6.4.1.9 NIMA (never in mitosis gene a)-related expressed kinase 2 (Nek2) mRNA is up regulated in the basal limbus

Semiquantitative analysis shown that the NIMA (never in mitosis gene a)-related expressed kinase 2 (Nek2) transcript is upregulated in limbal epithelial basal cells in relation to peripheral and central corneal basal epithelial cells and basal and suprabasal cells of the conjunctiva. The transcript was represented by two probe-sets on the arrays. It was consistently and strongly present in only one of the two probe-sets on the arrays and was reproducibly shown as up-regulated in the limbus by both arrays (only one probe set) and SQ RT-PCR (n=3). This inconsistency between the two probe sets was the reason it was not included in the gene list. It is a rather large transcript (3121 nucleotides long). It was impossible unfortunately to obtain probe design information in order to be able to explain why the specific probe set was called absent in all samples.

Figure 6.9 illustrates the relative expression of Nek2 between regions as determined by semiquantitative RT-PCR using GAPDH as an internal control. The fold change differences between the basal limbus and the rest of the areas as estimated by RT-PCR as well as by microarray analysis are listed in Table 6.10. Note that for these calculations only value from the present probe set were used.

	Fold Difference as determined by:	
Areas	**SQ-RT-PCR**	Microarray
Limbus-Periphery	2.88	3.23 (Present)
Limbus-Centre	1.50	3.27(Present)
Limbus-Conjunctiva	**1.92**	2.43(Present)

Table 6.10 Lists the fold difference in abundance of Nek2 transcripts between the basal limbus (Limbus) and the basal periphery (Periphery) and both basal and suprabasal conjunctiva (Conjunctiva). Present indicated the fulfilment of Presence-Absence criterion for the basal limbal samples as determined by RMA analysis.

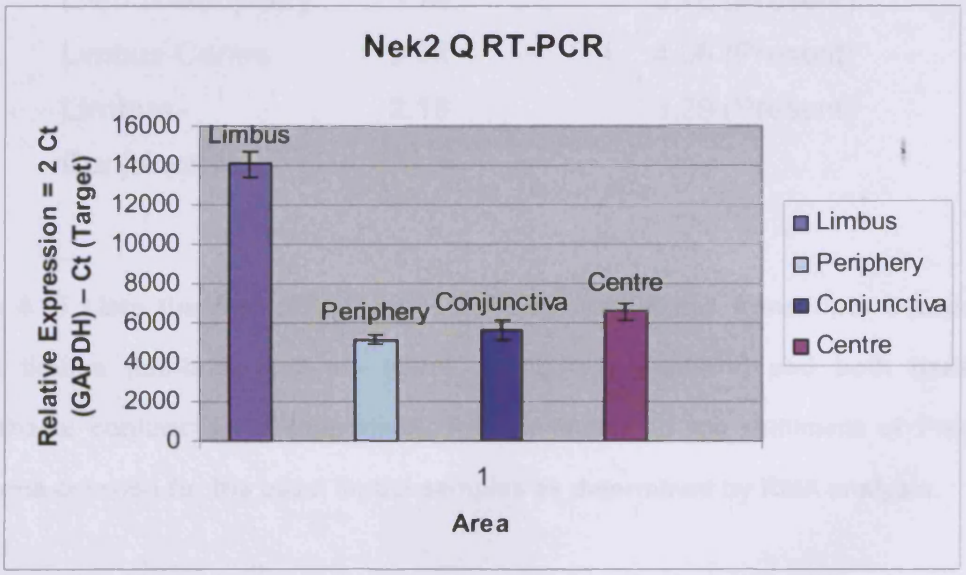

Figure 6. 7 Semiquantitative real time RT-PCR of Nek2 gene expression confirms up-regulation in the limbus.Ct refers to the cycle threshold (Ct) number. SEM Limbus ±640, Periphery ±239, Conjunctiva ±521, Centre ±423.

6.4.1.10 Nucleophosmin 1 (Nmp1) mRNA is up regulated in the basal limbus

Semiquantitative analysis shown that Nucleophosmin 1 (Nmp1) transcript is upregulated in limbal epithelial basal cells in relation to peripheral and central corneal basal epithelial cells and basal and suprabasal cells of the conjunctiva. It was shown to be strongly present in all samples and repetitions.

	Fold Difference as determined by:	
Areas	**SQ-RT-PCR**	Microarray
Limbus-Periphery	3.78	3.76 (Present)
Limbus-Centre	2.36	4.06 (Present)
Limbus-Conjunctiva	**2.16**	3.29 (Present)

Table 6.11 Lists the fold difference in abundance of Nmp1 transcripts between the basal limbus (Limbus) and the basal periphery (Periphery) and both basal and suprabasal conjunctiva (Conjunctiva). Present indicated the fulfilment of Presence-Absence criterion for the basal limbal samples as determined by RMA analysis.

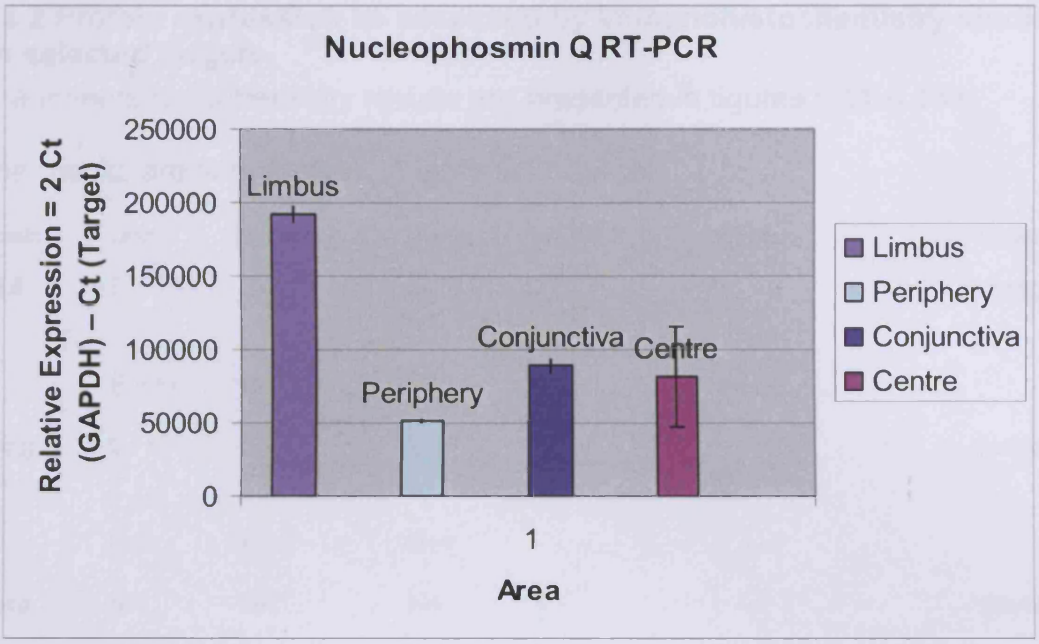

Figure 6.8. Semiquantitative real time RT-PCR of Nucleophosmin 1 gene expression confirms up-regulation in the limbus.Ct refers to the cycle threshold (Ct) number. SEM Limbus ±4778, Periphery ±1407, Conjunctiva ±3998, Centre ±34300.

6.4.2 Protein expression as assessed by immunohistochemistry studies on selected targets.

The immunohistochemistry results are presented in figures 6.11-6.13in

The results are summarized in table 6.12 bellow

Protein	Limbus	Periphery	Centre	reactive?	Specificity	Localisation
K14	S -	S-	S-	Y	++	cytoplasm
	B +++	B-	B++			
Areg	S++	S++	S++	Y	++	nuclear
	B++	B++	B++			
Beta	NA	NA	NA	Y	-	membrane
Catenin						
Rbp1	NA	NA	NA	Y	-	
SMC2	-	-	-	Y	-	NR
TLR3	+	+	NA	Y	-	NR
Nmp1	++	+	+	Y	-	membrane
PTGER4	++	++	+	Y	+	Apical memb

Table 6.12 Summary of immunohistochemisrty results. S and B refers to suprabasal and basal respectively, NR refers to not relevant (since unspecific). + refers to weakly positive immunoreactivity or weak specificity. ++ and +++ means strong and stronger respective immunoreactivity or specificity. Y indicates that the antibody was reactive for the experimental and negative for the control samples.

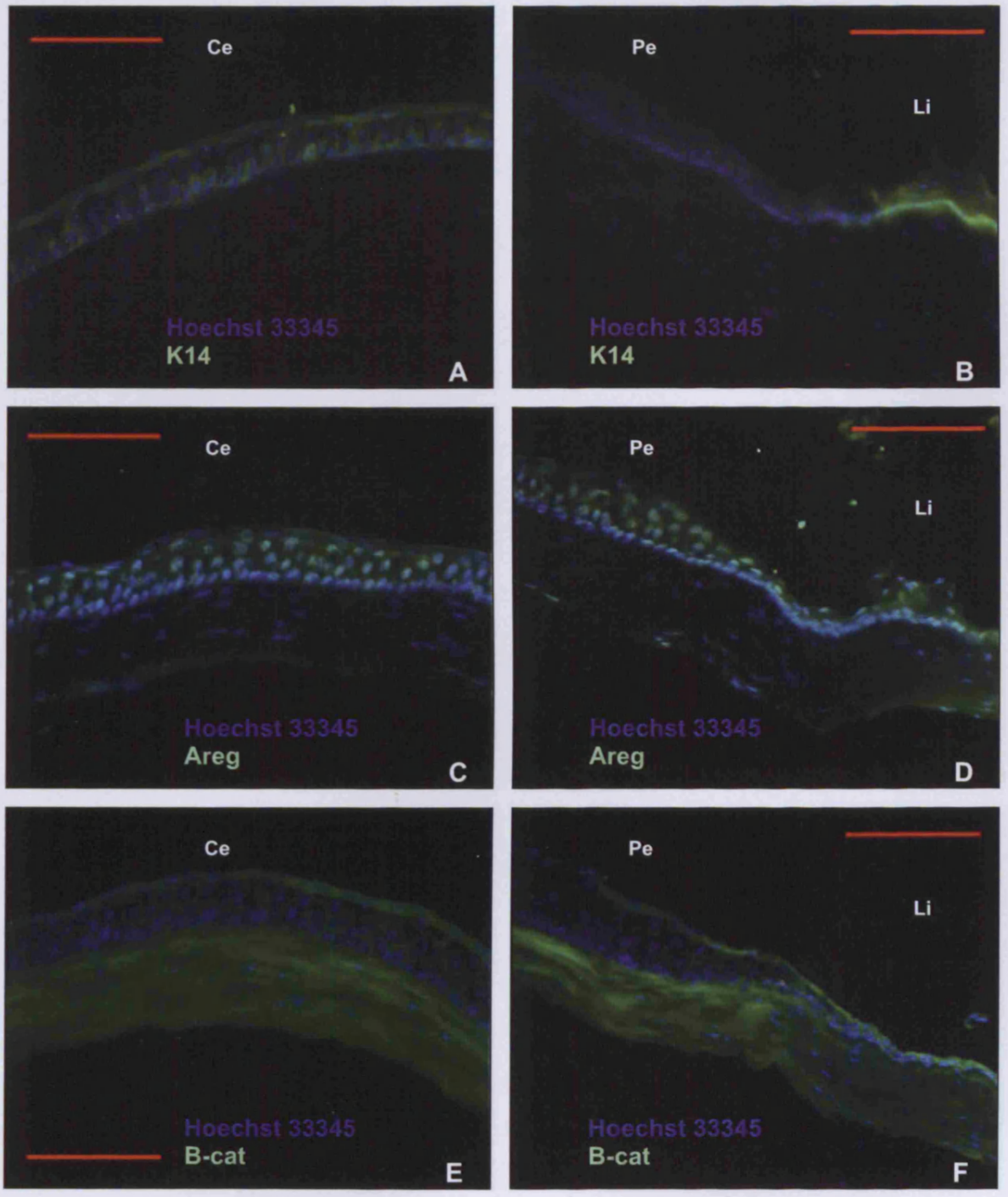

Figure 6.9. Immunohistochemical localisation of Keratin 14 (A&B), Amphiregulin (C&D), β-catenin (E&F) in the central cornea, designated as 'Ce' (A,C,E) peripheral cornea designated an 'Pe' (B,D,F) and limbus, designated as 'Li' (B,D,F). Calibration bar (A-F) = 100μm

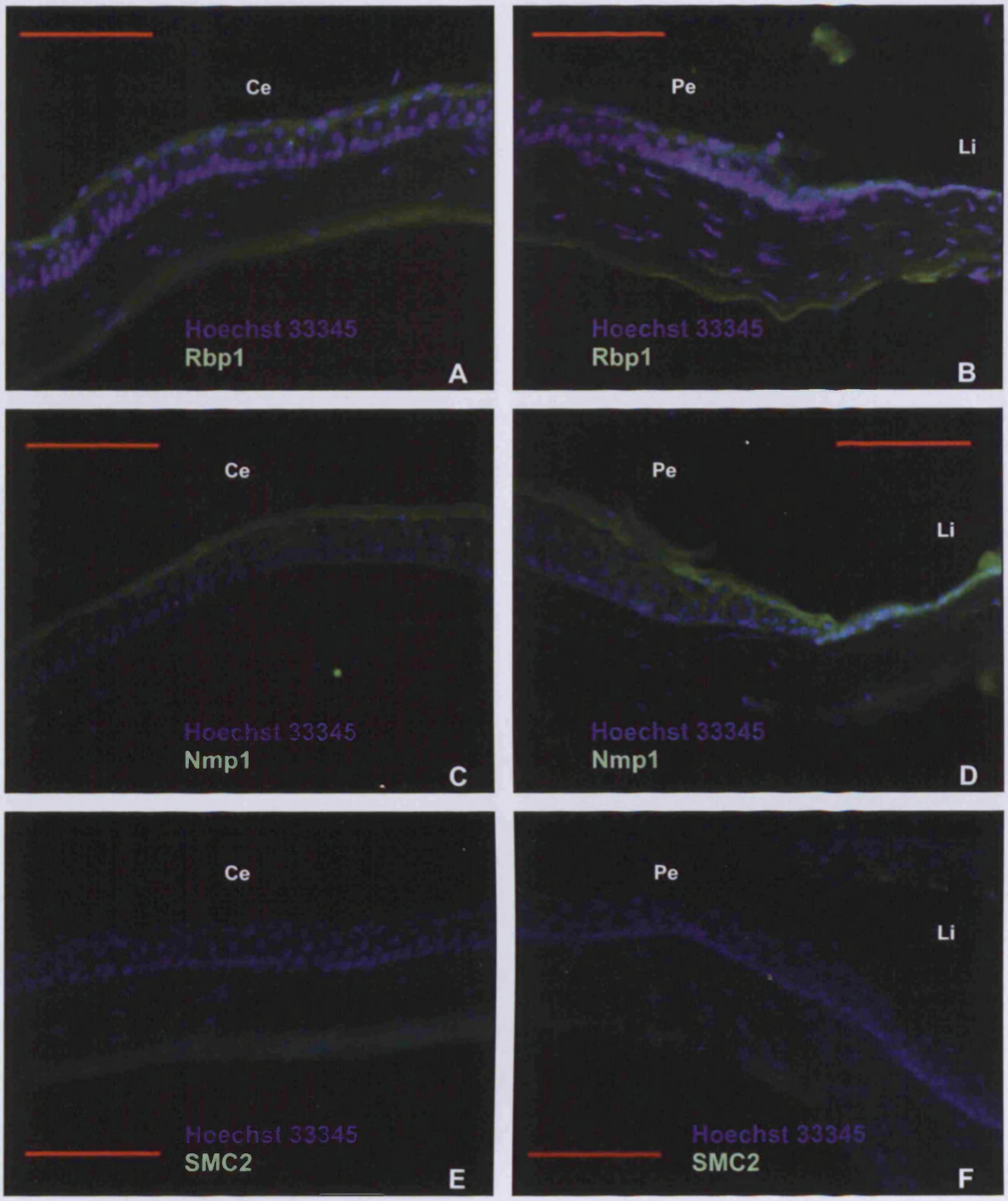

Figure 6. 10. Immunohistochemical localisation of Retinol binding protein 1 (A&B), nucleophosmin 1 (C&D), and SMC2 (E&F) in the central cornea, designated as 'Ce' (A,C,E) peripheral cornea designated an 'Pe' (B,D,F) and limbus, designated as 'Li' (B,D,F). Calibration bar (A-F) = 100μm

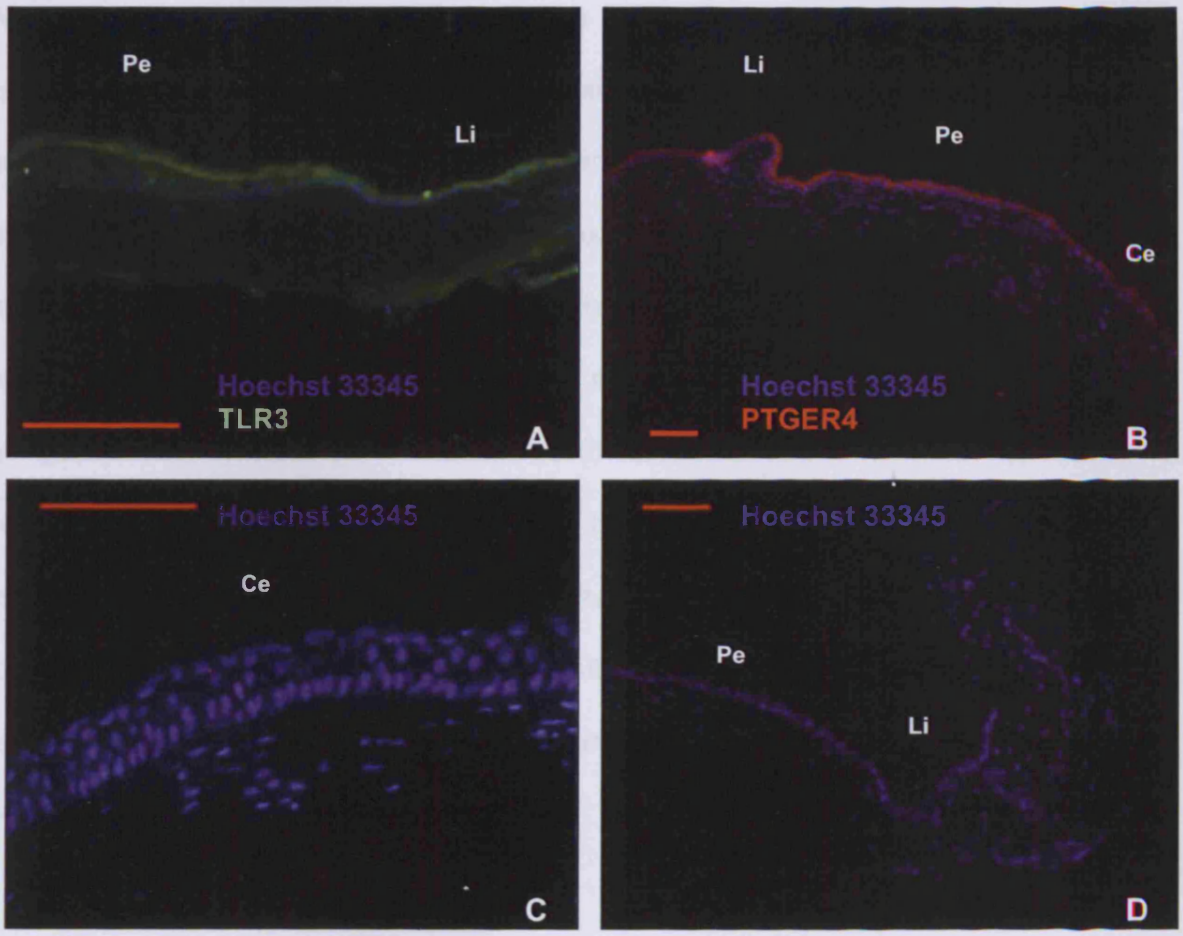

Figure 6. 11. Immunohistochemical localisation of Toll like receptor 3 (A), Prostaglandin E receptor 4 (B), β-catenin (E&F) in the central cornea, designated as 'Ce' (A,C,E) peripheral cornea designated an 'Pe' (B,D,F) and limbus, designated as 'Li' (B,D,F). Calibration bar (A-F) = 100μm

Although the results were positive, since the antibody immunoreacted only with experimental samples and not the negative control, the lack of positive control is evidently inhibiting the declaration of a positive statement that the proteins are indeed expressed, with the exception perhaps of Keratin 14 and amphiregulin. As mentioned earlier, due to the enormity of the data that was acquired with high density oligonucleotide array analysis of the basal epithelia of essentially the complete cornea and the restriction of time for the completion of this Ph.D. research much of the protein expression studies were impossible to finish thoroughly. For this reason the study was more focussed towards the confirmation of the array sensitivity which was indeed found to be reproducibly sensitive for nearly all the target genes that were cross-studied by semiquantitative RT-PCR.

Further studies on these and other targets will involve a thorough immunohistochemical investigation of protein localisation in the cornea and will be coupled with western-blot analysis. Localisation of mRNA transcripts will be facilitated in future studies with RNA *in-situ* hybridization studies.

Conclusions:

The quantitation of expression using high density oligonucleotide arrays and performing RMA analysis and filtering by this study's selection criteria was able to deliver target genes that reflected true differences in mRNA levels between basal cells of the epithelia that were studied.

Chapter 7

General Discussion

7.0 General Discussion

7.1 Summary of results

This study's main hypothesis was that cells at different levels of the corneal stem cell hierarchy, which exist in different regions of the cornea, were differentially regulated at the transcriptional level, and that those differences can be revealed by employing single cell laser capture as well as mRNA amplification to analyse their complete transcriptome by high density oligonucleotide arrays.

By isolating single cells from the basal layers of the limbus, peripheral and central cornea, and conjunctiva, the global gene expression profile of cells at consecutive stages of the corneal stem cell hierarchy were revealed.

Firstly, techniques that allowed the isolation of single cells from histological sections in a manner that would not compromise the quality of RNA were developed. Laser catapult microdissection was found to be the optimal method, since it could yield total RNA of high purity and integrity.

Then a method for RNA amplification which ensured that all genes represented in the same proportions, as before amplification, was developed so that the data of differential gene expression obtained from microarrays was accurate. Thus a linear amplification method, which amplified all the mRNA transcripts of a given sample, derived from pools of single cells, to a degree that could be analysed by high density oligonucleotide arrays, was optimised.

This included the use of control exogenous mRNA transcripts to monitor and ensure linear amplification of experimental transcripts.

The performance of microarrays to analyse differential gene expression in basal cells of the corneal limbus, periphery and centre and conjunctiva generated a huge amount of data. In order to analyse such overwhelming amount of data, appropriate mathematical methods were identified and employed. These included the use of Robust Multiarray Average method. The list of genes that were specifically and reproducibly up-regulated in each of the stages of the corneal stem cell hierarchy was obtained as a result.
Clustering probabilistic methods that assign gene clusters according to gene ontology were used to reduce data complexity and be able to visualise complete clusters of biological activity, cellular components or that are up or down regulated in each cell population. Array sensitivity was confirmed by semiquantitative RT-PCR.

The specificity of gene expression is subject to further investigation however. This is because although the study compared a stem cell enriched population of cells with populations containing no stem cells, it is more likely that not all biological variation between populations is due to this difference in population identity (i.e. stem cell or TA cell) but could for example be arising due to the microenvironment each population was isolated from. Therefore in order to specify further, the target genes can be studied using loss of function and over expression methods in clonal assays.

These genes require further investigation in order to understand what really governs stem cell regulation, as well as the regulation of transient amplifying cells of different stages of the lineage and mature cells in the cornea. Thus the results of this study will facilitate future research into understanding such mechanisms and may be exploited for therapeutic purposes, either by identifying pathological mechanisms and/or by culturing corneal limbal stem cells for transplantation.

Probing into putative mechanisms, the following discussion attempts to offer initial observations as to the importance of some of the differentially expressed genes, identified in this thesis, in the regulation of corneal epithelial cell homeostasis.

7.2. Putative regulatory mechanisms of corneal stem cells, as well as cells in early and late stages of the corneal stem cell hierarchy.

7.2.1 Chromatin remodeling and histone modification mechanisms in the corneal stem cell compartment

It was observed in this study that genes that are responsible for histone modifications and chromatin remodeling were differentially regulated between the corneal epithelial stem cell compartment and the rest of the corneal epithelium. Namely, genes coding for structural maintenance of chromosomes proteins 2 and 4 as well as for, protein phosphatase 1, catalytic subunit, beta isoform (Ppp1cb), were up-regulated in the basal limbus. In contrast, special

AT-rich sequence binding protein 1 (SATB1) was downregulated. The possible significance of those findings is discussed below.

As was detailed in the introduction, the main way to switch complete gene programs on and off is provided by histone modifications. Histone H3 de-acetylation of Lys9 is possibly mediated by phosphorylation of Ser10 (by mitotic kinases e.g. aurora kinase b) and subsequent methylation of Lys9 and tethering of a heterochromatin protein (HP) to this site which results in condensation and/or inability of transcription factors to reach the heterochromatin as well as neighbouring regions.

There are indications arising from this study that histone H3 Ser10 phosphorylation might be inhibited and methylation of lys9 might be induced in cells of the cornel stem cell niche, since they over-express both SATB1 and Ppp1cb and express Aurora kinase b at basal levels.

Phosphatase 1 (PP1) is known to directly inhibit Aurora kinase b mediated phosphorylation of Histone 3 during interphase (Murnion et al. 2001). Since limbal basal epithelial cells over express protein phosphatase 1, catalytic subunit, beta isoform (Ppp1cb) and are also expressing aurora kinase b, although at basal levels as revealed by this microarray study, this kind of inhibition could be active in cells of the corneal stem cell compartment. Note that the low levels of Aurora kinase B are perhaps not surprising since this is a mitotic kinase and only 10% of cells in the basal limbus of mice were shown to

be dividing at any given time as determined by label retaining studies (Cotsarelis et al. 1989)

A gene program switching system can be proposed in which Aurora kinase B activity, which would normally phosphorylated Ser 10 of H3 coinciding with acetylation of Lys 9 and therefore formation of euchromatin and transcriptional activation of specific genes, is hindered by Ppp1cd activity (see figure 8.1 b). This would indicate that gene programs are being switched off and others are switched on as the cell progresses down the differentiation pathway.

The hypothesis is further supported by the fact that the gene that constituted the downregulated cluster of histone methylation ontology was SATB1. The down regulation of SATB1, specifically in the corneal basal limbus, implies that stem cells of the corneal limbus silence some of their genes which are being

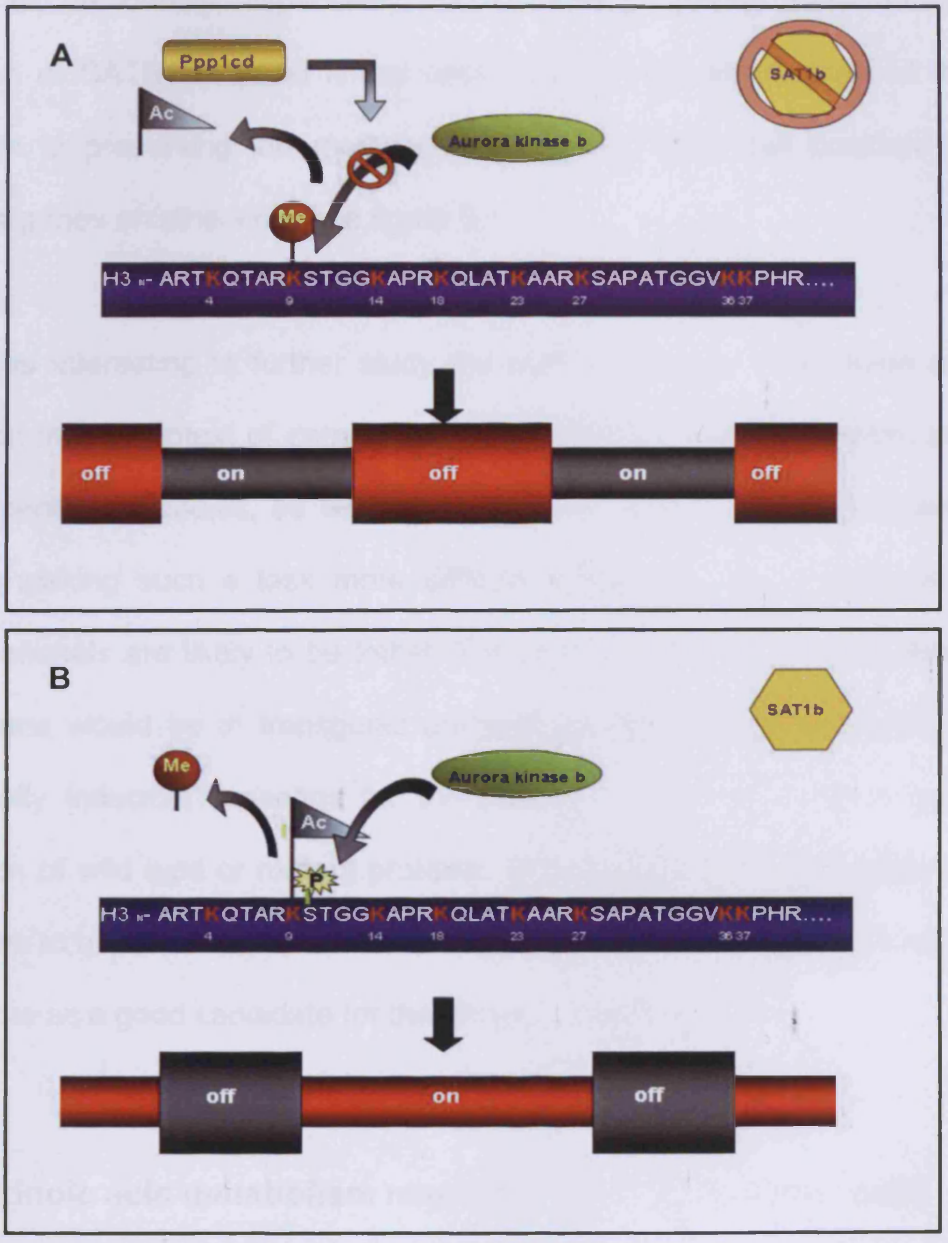

Figure 7.1 Putative model of gene switching upon consecutive early lineage steps in the corneal stem cell compartment. Sets of active genes in the earlier cell (grey) are switching to later lineage gene programs (red). Thin regions of chromosomes indicate euchromatin and thick heterochromatin. Ppp1cd could hinder acetylation of Lys9 and therefore activation of chromosomal regions mediated by phosphorylation of Ser10 by Aurora kinase b and keeps the TA genes off. Then acetylation of Lys9 and activation of those regions could be enhanced in TA cells which would not have Pppc1b there to safeguard the methylation of Lys9 further enhanced by the presence of SATB1.

histone methylation-acetylation to switch gene programs off or on depending on stem or TA identity respectively. Recapitulating, specific transcriptional repression of SATB1 in basal limbal cells indicates the significance of this repression in preserving the memory-switch to the stem cell position i.e. stemness genes on others off (see figure 8.1).

It would be interesting to further study the state of histone methylation and acetylation in the context of corneal stem and TA cells. However, there is a lack in specific antibodies, as well as mutants for methylated or acetylated histones, making such a task more difficult. Additionally, such mutants in higher mammals are likely to be lethal. The best way maybe to study these mechanisms would be in transgenic animals with targeted (tissue-specific) conditionally inducible cassettes for the genes of interest for either over-expression of wild type or mutant proteins. Of importance, is that Keratin 14 was shown to be over expressed in the basal limbus. The K14 gene promoter might serve as a good candidate for the generation of such mice.

7.2.2 Retinoic acid metabolism mechanism in corneal stem cells

Both alcohol dehydrogenase 6 and cellular retinol binding protein 1 gene transcripts were found exclusively upregulated in the corneal epithelial stem cell compartment. The cellular transport and biological activity of retinoids may be mediated by their specific cytoplasmic binding proteins namely cellular retinol binding protein (CRBP) and the cellular retinoic acid binding protein (CRABP) which may function as shuttles, targeting retinoic acid (RA) to nucleosol fraction and/or as a regulator of the cellular concentration of RA

(Cornic et al. 1992). All-trans retinoic acid is known to induce cellular retinol-binding protein in human skin in vivo (Fisher et al. 1995).

Hard evidence of a mechanism that controls intracellular levels of retinoic acid came from a study that has shown that the opposing actions of cellular retinol-binding protein and alcohol dehydrogenase control the balance between retinol storage and degradation (Molotkov et al. 2004).

For cells that express CRBP1, most intracellular retinol is bound non-covalently to CRBP1, leaving very little free retinol (Ross et al. 1993, Napoli et al. 1999). The small fraction of free retinol always remains and is oxidised by alcohol dehydrogenases, forming retinaldehyde which is then converted to retinoic acid by oxidation (Molotkov et al. 2004)

In corneal epithelial cells, in vivo studies indicate that a retinoic acid mediated control plays an important role on corneal stem cell proliferation. All-trans retinoic acid reverses conjunctivalisation of the cornea after epithelial denudation, four months post injury. This could imply that retinoic acid induces proliferation of corneal epithelial stem cells. Long term reconstitution cannot be assumed since corneas were followed for 32 days (Tseng et al. 1988).

In vitro studies on corneal epithelial cells show a dose-dependent manner of retinoic acid control of stem cell proliferation and differentiation (Kruse et al. 1994). Low concentrations of retinoic acid (10^{-9} to 10^{-7} M) stimulated the colony forming efficiency of limbal cultures but did not change that of

peripheral corneal cultures. In the latter, a concentration of 10^{-8} M induced the emergence of two new types of colonies, one of which exhibited clues of self renewal. Retinoic acid concentrations above 10^{-8} M stimulated normal differentiation of both limbal and peripheral corneal epithelial cells (Kruse et al. 1994).

The conclusion that arises from the above studies is that it seems that corneal epithelial stem cells have a specific up-take threshold of retinoic acid. If that threshold is saturated than several differentiation mechanisms start taking place.

As this study indicates, corneal epithelial stem cells possibly control their intracellular level of retinoic acid by CRBP1 and Adh6a. A possible mechanism could involve both of these proteins, in controlling the levels of available retinoic acid inside the cell. In such mechanism, CRBP1 would work as a buffer of retinoic acid by storing retinol which is needed for retinoic acid production. In turn ADH6, being also expressed, could be converting the remaining retinol to retinaldehyde, making it available for oxidation and retinoic acid production. The balance of these two factors therefore could serve a mechanism of retinoic acid availability, which in turn has been recognised as a major mechanism controlling stem cell proliferation and/or differentiation. To verify that, further experiments that will include clonal analysis of cells under the influence of different concentrations of retinol, conducted on wild type cells and cells in which the target genes are altered using loss of function and overexpression methods can be used

7.2.3 Insight into asymmetric cell division of basal cells of the corneal stem cell compartment.

7.2.3.1 Possible roles of β-catenin related mechanisms in the corneal stem cell niche.

It was obvious that β-catenin was upregulated at the transcriptional level in the corneal stem cell niche. Although confirmation of protein expression and intracellular localisation of the β-catenin protein was not possible, because b-catenin activation and subsequent translocation to the nucleus is transient, the role of β-catenin in corneal stem cells can be possibly explained by carefully observing the literature on β-catenin and related molecules in other stem cells.

Transient activation of β-catenin signaling by nuclear localisation in adult mouse epidermis is sufficient to induce new hair follicles and continuous activation induces hyperproliferation of those cells (Lo Celso et al. 2004). This is indicative that catenin acts, in part, in a concentration dependent manner

pinpointing that the level and localisation of expression of β-catenin is a very important determinant of cell fate for adult mouse epidermis stem cells.

Further evidence of dose dependent inhibition of embryonic stem differentiation has been previously reported in experiments where increased doses of nuclear β-catenin by specific *APC* mutations abolished the ability and sensitivity of ES cells to differentiate into the three germ layers (Kielman et al. 2003)

The significance of β-catenin related mechanisms in epithelial stem cells

The nuclear β-catenin/TCF signalling pathway is essential for the maintenance of epithelial stem cells in the small intestine. The proliferative compartment was depleted of stem cells in TCF4 double knock-outs, which die shortly after birth. (Korinek 1998).

Follicular epithelial stem cells show a 75% reduction in number as determined by label retaining experiments, when targeted expression of c-Myc oncogene which is a downstream target of the of β-catenin/TCF complex, is directed to basal cells of the follicular epithelial stem cell compartment using the K14 promoter (Waikel et al 2001).

How could β-catenin participate in asymmetric or symmetric cell division in stem cells? Are there any other possible factors that are likely to be acting together with β-catenin in such decisions?

Other factors which are likely to be involved in such mechanisms

The position of the mitotic spindle plays a key role in the spatial control of cell division. Polarity cues in combination with the control of spindle orientation ensure the correct segregation of cell-fate determinants during development (Gonczy et al. 2002). The correct spindle position is achieved through interactions between spindle, astral MT and cortical actin. Interestingly, in the Drosophila embryo, the β-catenin homolog Armadillo is required to tether the spindle to cortical actin (McCartney et al. 2001). This complex contains α-catenin, β-catenin and a protein related to APC, and it is likely to interact with a protein of the EB1 family which localises to the plus end of growing MT (Su et al 1995). The same type of complex might allow cadherin/catenin to regulate MT dynamics in interphasic cells.

Asymmetrically distributed DE-cadherin is essential to determine the mitotic spindle orientation (Borgne et al. 2002). The small GTPase Cdc42, acting through a Par6 - atypical protein kinase C (aPKC) complex, is also required to establish asymmetric cell division. Whether Cdc42 regulates glycogen synthase kinase-3β and APC in the context of asymmetric cell division remains to be determined (Etienne-Manneville et. al.2003) CDC42, a small Rho GTPase, regulates the formation of F-actin-containing structures through its interaction with the downstream effecter proteins.

Possible involvement of Cdc42ep3 in the regulation of asymmetric division of corneal stem cells.

This thesis demonstrated that corneal limbal basal cells have upregulated Cdc42ep3 transcripts (Cdc42 effecter protein, Rho GTPase binding, 3). Cdc42ep3 is a member of the Borg family and contains a CRIB (Cdc42/Rac interactive-binding) domain. CRIB domain containing proteins bind to, and negatively regulate the function of, CDC42. Cdc42ep3 can interact with CDC42, as well as with the ras homolog gene family, member Q (ARHQ/TC10). Keeping that fact under consideration the discussion is continued in order to show why that would be of importance.

It has been previously reported that disruption of F-actin causes a loss of cortical association of LGN31. Thus basal limbal cells which over express cdc42ep3 are likely to have disrupted F-actin. Cortical association of LGN protein is essential for the formation of a LGN–mInsc–Par3 complex at the apical side of the dividing basal epithelial cells in the epidermis (Lechler et al. 2005).

The apical LGN–mInsc–Par3 crescent, as well as, the apical localisation of NuMA-dynactin complex is dictated by the apical localisation of atypical protein kinase C (PKCz in epidermal cells).

Those two crescents are composed of proteins whose drosophila, yeast or c-elegance homologues are involved in the polarisation of differentiation determinants such as Ash1 as well as in specification of maternal type

switching in yeast by the HO endonuclease dependent definition of attenuation of maternal cell.

So far PKCz has been shown to always localise at the apical side of a basal cell in an integrin β1 or catenin-α manner. It can therefore be proposed that apical localisation of atypical protein kinase C and therefore of the LGN–mInsc–Par3 and NuMA-dynactin crescents is dependent both on adhesion to the basal membrane through integrins and adherens junction dependent adhesion of a stable F-actin-cadherin link through a stable b-catenin/a-catenin complex in epithelial cells of the epidermis in mice. Therefore the apical localisation of those two crescents could serve as a molecular centre for the association of key cell commitment or differentiation factors, just as the basally oriented integrins are known to form a localisation site for growth-promoting factors. Thus an epithelial cell, by attaching to the basement membrane and to its neighbors, can form a vertical axis of cell division by asymmetric distribution of key components.

Basal epithelial of tongue and epidermal epithelial cells of p63 knockouts mice have been shown that loose their ability to asymmetrically localise those components and divide symmetrically in a perpendicular axis.

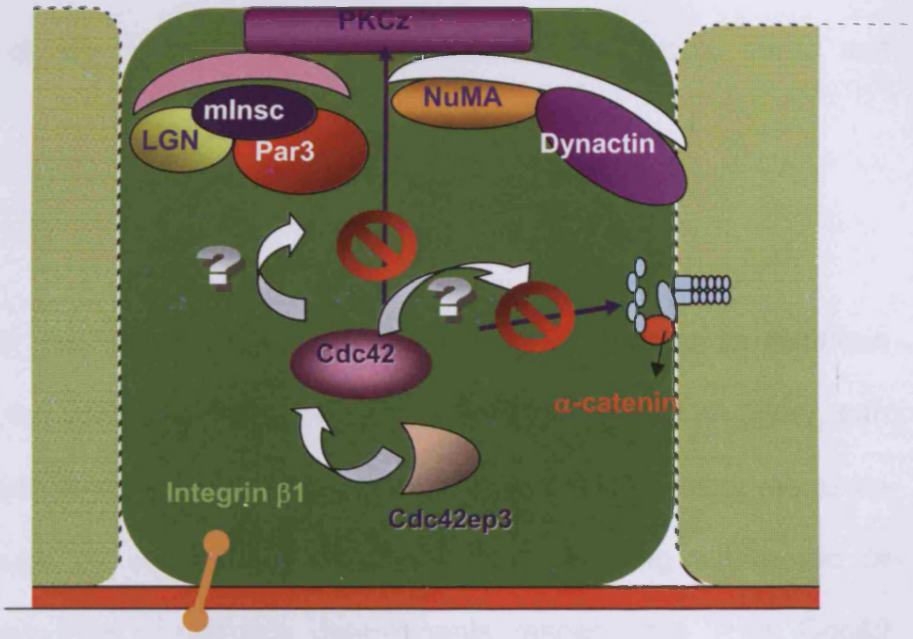

Figure 7.1. The apical localisation of the LGN- mInsc-Par3 and Numa-Dynactin crescents in a PKCZ dependent manner is illustrated. This localisation has been shown to be controlled at least in part by Cdc42 protein. Cdc42ep3 negatively regulates Cdc42 through its CRIB domain. The possible role(s) of cdc42ep3 in this mechanism is illustrated.

Since Cdc42efector protein is indeed expressed by corneal stem cells, it would be valuable to determine whether it acts on disrupting F-actin association with the β-catenin/α-catenin complex and if that disruption leads to symmetric cell division which in the case of a stem cell would mean self renewal.

As discussed in the introduction, corneal stem cells in order to maintain homeostasis of the corneal epithelium, especially in the case of an injury, can modulate their self renewal frequency. They therefore could possibly modulate their perpendicular or vertical cell division with a resulting symmetric or asymmetric distribution of cell fate determinants respectively. Thus Cdc42 effector protein, as well as p63, although likely to be in the core of a stem cell fate control mechanism for corneal stem cells, further investigation is needed into what kind of other interactions would govern the dynamics of such decisions in stem cells.

Also, apical localisation of those crescents is not enough to explain how cells can control in what direction to divide. Additionally it needs to be specified which specific cells in the hierarchy and more specifically in the stem cell compartment express the proteins so that we can understand if we are likely to have successive asymmetries resulting in a TA cell or self renewal through just one asymmetrical cell division at the stem cell level.

Nevertheless, the study sets a promising frame for further studies into such dynamics. A good candidate strategy of controlling the directionality of such decisions could be changes in membrane potential that pass from cell to cell through gap junctions. Taking under consideration the fact that corneal basal limbal cells lack connexins 43 and 50, together with the fact that corneal stem cells self renew to a higher rate, even immediately after a central corneal wound, pinpoints towards a role for gap junctions in altering tissue dynamics. Messages of altered tissue dynamics may travel through gap junctions to the basal limbal transient amplifying (TA) cells, changing the local dynamics of the basal limbus and thus, changing the self renewal frequency of stem cells. When the message reaches TA cells, they start dividing thereby loosing their adherence junction connection to stem cells. This could in turn be the key message for stem cell fate decision mechanisms. A possible mechanism that could alter the dynamics up to the transitional zone between the limbus and the periphery is discussed in the next section.

7.2.4 Putative role of a Calcium-Nitric oxide dependent mechanism in corneal epithelial homeostasis

The role of regulation of the levels of nitric oxide in corneal epithelium homeostasis remains unknown. However there are reports of upregulated nitric oxide synthase (NOS) under inflammation (Sennlaub et. al. 1999; Kim et al. 2002). It has to be noted that the cornea is a tissue under constant contact with oxygen.

NOS catalyses the formation of nitric oxide from arginine and O_2. Once formed, nitric oxide diffuses only locally through tissues and is highly labile since it is a free radical allowing for quick interactions. It plays an important role in mediating many local cellular interactions. For example, release of acetylcholine from adjacent tissues promotes influx of Ca^{2+} into endothelial cells lining blood vessels. After Ca^{2+} binds to calmodulin, the resulting complex stimulates the activity of NO synthase (Sato and Murota 1995). The nitric oxide that is formed diffuses from the endothelial cell and into neighbouring smooth muscle cells where it binds to and activates soluble guanylate cyclase resulting in increased cGMP levels (Sato and Murota 1995).

Potential factors involved in NO related mechanisms of homeostatic control of the corneal epithelium

Both calcium/calmodulin-dependent protein kinase Camk1d and dimethylarginine dimethylaminohydrolase 1 Ddah1 were upregulated at the transcriptional level in the basal periphery. DDAH1 is an enzyme that

metabolises methylated arginine to citrulline and methylamine, thus working to produce nitric oxide (NO) (Mishima 2004). Camk1d has recently been identified as a Ca (++)/calmodulin-dependent kinase (Verploegen et al. 2000). Additionally caveolin, caveolae protein 1 (Cav1), a negative regulator of nitric oxide synthesis (Sato et al. 2004) is depleted in the peripheral cornea.

These findings suggest that the nitric oxide regulatory mechanism involving calcium is active in the peripheral corneal epithelium. This could serve as a regulatory mechanism of homeostasis. If the calcium balance changes an NO signal could quickly diffuse in neighbouring epithelial or stromal cells and signal for the change in local tissue dynamics in less then 30 seconds.

It could be that NO levels and intracellular calcium mobilisation are co-regulated in peripheral corneal epithelial cells. Transglutaminase 2 activity can be inhibited by nitrosylation of up to 15 of the 18 of its cysteine residues in a Ca^{+2} dependent manner (Lai et al. 2001). This is intriguing since Transglutaminase 2 (TG2) is a protein involved in a variety of mechanisms. Membrane bound TG2 can act as a signalling mechanism from seven transmembrane helix receptors to phospholipase C (Iismaa et al. 2000). Phospholipase C is activated when relieved of its inhibition by GDP–TG2 upon TG2 binding to GTP (Murthy et al 1999).

TG2 activated by Ca^{2+} interacts with and modifies major components of the cytoskeleton. It has been shown that upon retinoic acid treatment, transamidation of RhoA in a TG2-dependent manner induces the binding of RhoA GTPase to ROCK-2 protein kinase, subsequent autophosphorylation of

ROCK-2 and phosphorylation of vimentin which can lead to the formation of stress fibres and increased cell adhesion (Singh et al. 2001). These events are prevented by TG2 inhibition. Therefore inhibiting the activity of transglutanminase 2 by nitrosylation of the cysteine residues could serve as a constant "proliferate and migrate" signal on TA cells of the periphery.

It was observed in previous studies that clusters of 5-10 basally located cells termed "transitional cells" situated in the peripheral corneal epithelium in areas near the transitional zone of the periphery to the limbus exits in vimentin positive foci (Lauweryns et al. 1993). The nitric oxide-calcium mechanisms could potentially act through transglutaminase 2 in transitional cells; signal them to proliferate upon damage in the centre or the periphery, therefore contributing to homeostasis of the corneal epithelium. If this mechanism is indeed active, its influence on decisions in the limbal epithelium need to determined. It would be interesting to further investigate this control, although if so, it would be essential to address those mechanisms both under physiological conditions and upon wounding.

7.2.5 COL4A3BP and ceramide metabolism in limbal basal epithelial cells might give an indication of G-protein coupled receptor inhibition

Raya et al. (1999) identified a HeLa cell cDNA encoding a deduced 624-amino acid protein, designated COL4A3BP. Raya et al. (1999) termed the protein GPBP (Goodpasture antigen-binding protein). GPBP was initially identified as a protein that could bind a carboxy-terminal non-collagenous

region of human collagen alpha3 (IV) chain in a cell-free system (Raya et al. 1999). Immunohistochemistry showed diffuse, predominantly cytosolic staining of specific cell types in numerous tissues.

COL4A3BP was found to have a phosphatidylinositol-4-monophosphate (PIP4) -binding activity in experiments on ceramide intracellular transport studies. Ceramide is synthesised at the endoplasmic reticulum and translocated to the Golgi compartment for conversion to sphingomyelin. The main pathway of ceramide transport to the Golgi is genetically impaired in a mammalian mutant cell line, LY-A, expressing a splicing variant of the GPBP (GPBP-delta26) that was 26 amino acids shorter than COL4A3BP (Hanada et al. 2003). This was due to impaired PIP4 binding activity.

These results suggest that some cells in the basal limbus have an upregulation of ceramide conversion to sphingomyelin. It cannot be certain which cells of the early lineage are likely to express the protein but it is likely that calcium homeostasis is going to be interplexed with ceramide metabolism in a mechanism involving COL4A3BP.

PIP3-G-protein coupled receptor activity is inhibited in the basal limbus.

When the limbal data set was not compared to the conjunctival one, then rabphilin 3A-like (without C2 domains) (Rph3al) was seen to form a cluster of negative regulation of G protein coupled receptor activity. In contrast, basal peripheral cells were shown to have upregulation of transglutaminase 2

mRNA transcription which as discussed earlier has a G-protein signalling coupled to IP3 second messenger (PLC activating) ontology. This could suggest that in some cells of the basal limbus there might be an inhibition of PIP3-G-protein coupled receptor activity. This inhibition might be relieved in TA cells of the basal periphery since if they over express transglutaminase 2 protein and do not over express Rph3al.

It would be very interesting to further study this system in the context of which cells in the lineage express the said proteins and then further study the biochemistry of such a mechanism.

7.1.6 ST8 alpha-N-acetyl-neuraminide alpha-2,8-sialyltransferase transcriptional repression might be the reason limbal and corneal epithelial cell phenotype are distinguished by sialylation of cell surface molecules in mice

As described in section 5.4.1.3.1, ST8 alpha-N-acetyl-neuraminide alpha-2,8-sialyltransferase 4 (St8sia4) was specifically downregulated at the transcriptional level in the basal limbus. Wolosin and Wang (1995) demonstrated that rabbit limbal epithelial cells expressed unsialylated galactose residues that are recognized by peanut lectin (PNA) and that lack any sialic acid bound through □ -2,3 bonds on their cell surface molecules. Cells in the periphery and centre had a-2,3 sialic acid residues appearing on their cell surface instead, leading the researchers to propose that

differentiation correlated with sialylation of surface molecules by the expression or activation of a-2,3-sialyltransferase (Wolosin and Wang, 1995). These results underline the undifferentiated state of the limbal basal cells that were analysed in this study and agree with these previous findings, indicating that a similar phenomenon is true in the mouse. Additionally, they indicate that the selective transcriptional repression of St8sia4 might be the mechanism which explains this phenomenon.

7.2 Conclusion and future directions.

The cornea presents a linear spatial pattern of differentiation and that cells of different stages of the stem cell lineage hierarchy reside in distinct anatomical locations of the cornea. This allowed for the development of methods for the analysis of the complete transcriptome of these cells, so that the relative abundances of each gene transcript in successive stages of hierarchy in-vivo could be determined. Additionally, the protein expression of several target genes from the vast array of targets that were revealed was also investigated.

This study has produced a very substantial amount of data that requires further exploration to ascertain exact roles and functions of differentially expressed genes and/or their proteins in corneal epithelial cell homeostasis. Such realisations are likely to greatly augment our understanding of epithelial stem cell biology.

Future Work

Future work on selective genes and regulatory mechanisms will involve:

- Cellular localisation of gene transcripts of interest by RNA *in situ* hybridisation

- The confirmation of protein expression of genes and post translational modifications on the proteins of interest by western blotting, additional immunohistochemistry experiments on tissues both in steady state homeostasis and during wound healing, as well as pathological tissues.

- The study of those mechanisms in-vitro

- The targeted inducible knock-out of genes of interest using the cre-lox system, under the control of promoters of genes that are found to be reproducibly expressed in the cells of interest.

APPENDIX A. Primers

Table A. 1a Oligonucleotide Primer sequences used throughout this study

Gene transcript	Primer sequence (5'-3')	nucleotides	Tm
GAPDH	gtgttcctacccccaatgtg	20	60.09
	gggatagggcctctctcttg	20	60.17
Aldh6a F	atcattcaggaaaagccatcc	21	55.9
Aldh6a R	acctcgtttcaggagaacagc	21	59.8
Col4abp3 F	agacgagtggaggaagcgta	20	59.4
Col4abp3 R	ctccagatggcaatgatgtg	20	57.3
Nek2 F	ggtctgcaaatggatgtgtg	20	57.3
Nek2 R	tctctgagccctccaggtta	20	59.4
Rbp1 F	cgctttctgtccagtgcata	20	57.3
Rbp1 R	caggtttgctagcgtcatca	20	57.3
SMC4l1 F	tgagattgatgcagctctgg	20	57.3
SMC4l1 R	ttgttttgggttcactgcaa	20	53.2
Nmp1 F	agatctctggcagtggagga	20	59.4
Nmp1 R	ggtggagttccatccttgaa	20	57.3

Table A.1 b Oligonucleotide Primer sequences used in this study

Gene transcript	Primer sequence (5'-3')	nucleotides	Tm
E2F5 F	atgacctcacacagccttcc	20	59.4
E2F5 R	catctgctggggtaggagaa	20	59.4
Ptger4 F	gaagggctgtcttcatctgg	20	59.4
Ptger4 R	cgtagcttctgccatcttcc	20	59.4
SMC2l1 F	cgtgctgacagaagctgaag	20	59.4
SMC2l1 R	caccaggcaaaagggtagaa	20	57.3
Tlr3 F	atatgcgcttcaatcgcttc	20	55.3
Tlr3 R	caggagcatactggtgctga	20	59.4

Appendix B. Antibodies

Antibodies for Cytokeratin 14, TLR3, SMC2, RBP1, Areg (amphiregulin), and Npm1 were all purchased from Santa Cruz Biotechnology, Inc (USA). The antibody for β-catenin was purchased from BD Biosciences (UK). PtgER4 antibody was purchased from Abcam (UK). For all other target immunoreactions apart from β-catenin and Ptger4, Alexa Fluor 488 donkey antigoat secondary was used. For the last two, Alexa Alexa Fluor 594 goat antirabbit and Alexa Fluor 488 donkey antimouse were used for Ptger 4 and β-catenin targets respectively.

Table B.2 The following table list the antibodies, information about the antibodies that were used, as well as the specific details of each experiment. C or N –ter refers to C or N terminus. m,r,h,d,s refer to mouse, rat, human, dog and sheep respectively. Mono or poly refer to monoclonal or polyclonal nature of the primary antibody.

Target	CK14	TLR3	SMC2	RBP1	Areg	Npm1	Catnb1	PtgER4
Clone/Ref. name	Poly/C-14	Poly/T-17	Poly/A-16	Poly/N-17	Poly/C-13	Poly/C-19	Mono/14	Poly/-
Isotype	IgG	IgG	IgG	IgG	IgG	IgG	IgG1	IgG
Raised in	goat	goat	goat	goat	goat	goat	mouse	Rabit
Reacts with	m,r,h	m,r,h	m,h,r	m,h,r	m,h,r	m,h,r	M,h,r,d,s	M,h,r
Epitope	C-t,h	Extrc. dom	N-t,h	C-t,h	C-t,h	C-t,h	C-t m(200r)	Unkn/n
Concentration	1:50	1:50	1:50	1:50	1:50	1:50	1:50	1:100
Time	4h	4h	4h	4h	4h	4h	4h	o/n
Catalogue No	sc-17104 Santa Cruz	sc-23323 Santa Cruz	sc-10709 Santa Cruz		sc-5796 Santa Cruz	sc-6013 Santa Cruz		
Temperature °C	23	23	23	23	23	23	23	4

APPENDIX C. Gene lists

Table C.1 a-e: Genes upregulated in the corneal limbal basal cells. Official gene names and symbols as well as Unigene reference numbers and chromosomal location (ChroLocn) of each gene is designated.

Gene Symbol	Gene name	Fold change to		Unigene ID	ChroLocn	Welch's p-value	
		Periphery	Centre			L-P	L-C
Acsl3	acyl-CoA synthetase long-chain family member 3	2.5	2.66	---	1 C4|1 24.1 cM	0.0073	0.0677
Acta2	actin, alpha 2	8.88	7.06	213025	19 C3	0.0091	0.0036
Adh6a	alcohol dehydrogenase 6A (class V)	2.77	4.76	46265	3 G3	0.0504	0.0418
AI265725	Expressed sequence AI265725	2.73	1.68	355195	10	0.0041	0.0110
Apobec1	apolipoprotein B editing complex 1	5.82	5.74	3333	6 F2|6 54.5 cM	0.0231	0.0287
Areg	amphiregulin	3.29	3.16	8039	5 E2|5 51.0 cM	0.0050	0.0191
Arhgap18	Rho GTPase activating protein 18	1.69	2.04	356496	10 A4	0.0462	0.0295
Arhgdib	Rho, GDP dissociation inhibitor (GDI) beta	3.43	5.13	2241	6 G1	0.0117	0.0028
Atp5f1	ATP synthase, H+ transporting, mitochondrial F0 complex, subunit b, isoform 1	2.2	1.85	251152	3 F2.2|3 57.0 cM	0.0228	0.0808
B2m	beta-2 microglobulin	7.01	4.41	163	2 F1-F3|2 69.0 cM	0.0428	0.0414
Calm2	calmodulin 2	2.45	1.95	329243	17 E4	0.0089	0.0063
Calmbp1	calmodulin binding protein 1	1.88	1.82	168523	1 F	0.0311	0.0249
Car13	carbonic anhydrase 13	7.84	8.17	158776	3 A2	0.0044	0.0060
Casp1	caspase 1	7.67	6.5	1051	9 A1|9 1.0 cM	0.0205	0.0229
Cast	calpastatin	1.8	2.08	29163	13 C1	0.0111	0.0133
Catnb	catenin beta	1.65	2.06	291928	9 F4|9 72.0 cM	0.0710	0.0209

Table C.1b: Genes upregulated in the corneal limbal basal cells

Gene Symbol	Gene name	Fold change to		Unigene ID	ChroLocn	Welch's p-value	
		Periphery	Centre			L-P	L-C
Ccrn4l	CCR4 carbon catabolite repression 4-like (S. cerevisiae)	1.96	2.28	86541	3 B-D	0.0005	0.0029
Cd47	CD47 antigen (Rh-related antigen, integrin-associated signal transducer)	3.32	1.92	31752	16 B5	0.0003	0.0006
Cdc42ep3	CDC42 effector protein (Rho GTPase binding) 3	3.61	3.05	140601	17 E3	0.0089	0.0196
Ceacam1	CEA-related cell adhesion molecule 1	4	3.58	322502	7 A2|7 5.5 cM	0.0004	0.1144
Cept1	choline/ethanolaminephosphotransferase 1	2.53	2.04	14816	3 F2.3	0.0002	0.0572
Chst9	carbohydrate (N-acetylgalactosamine 4-0) sulfotransferase 9	3.25	2.16	329304	18 A1	0.00982	0.03970
Clcn3	chloride channel 3	1.68	1.75	259751	8 B3.1|8 32.2 cM	0.00178	0.00348
Cldn1	claudin 1	4.44	4.47	289441	16 B1	0.00153	0.00029
Cldn23	claudin 23	1.93	1.78	37817	8 B1.1	0.01471	0.00645
Cmah	cytidine monophospho-N-acetylneuraminic acid hydroxylase	3.05	8.75	8396	13 A3.2	0.00096	0.00012
Defb1	defensin beta 1	2.68	2.93	5341	8 A4|8 9.0 cM	0.00177	0.00079
Dsg2	desmoglein 2	2.04	2.51	345891	18 A2|18 7.05 cM	0.00002	0.01073

Table C.1c: Genes upregulated in the corneal limbal basal cells

Ect2	ect2 oncogene	2.41	2.27	261453	3 B	0.02395	0.05717
Elf5	E74-like factor 5	3.07	1.78	20888	2 E3	0.00165	0.00523
Elovl5	ELOVL family member 5, elongation of long chain fatty acids (yeast)	3.07	2.33	19130	9 E1	0.02162	0.05513
Enpp3	ectonucleotide pyrophosphatase/phosph odiesterase 3	2.51	6.73	194888	10 A4	0.00363	0.00315
Ereg	epiregulin	2.33	2.3	4791	5 E2	0.07863	0.12172
Expi	extracellular proteinase inhibitor	12.47	10.48	1650	11 C	0.06946	0.06827
F5	Coagulation factor V	3.07	3.14	12900	---	0.00268	0.00592
Flrt2	Fibronectin leucine rich transmembrane protein 2	3.51	3.39	341948	12 D3	0.00000	0.00002
Gbp2	guanylate nucleotide binding protein 2	2.2	1.84	24038	3 H1|3 67.4 cM	0.03750	0.10331
Ggh	gamma-glutamyl hydrolase	3.97	5.9	20461	4 A3-A5	0.00050	0.00031
Grp58	glucose regulated protein	2.04	2.28	263177	2 E5|2 69.0 cM	0.00113	0.07734
H2-Q7	Histocompatibility 2, Q region locus 6	7.67	7.84	34421	---	0.05171	0.04555
Hnrpa1	heterogeneous nuclear ribonucleoprotein A1	1.64	1.8	299367	15 F3|15 61.7 cM	0.01089	0.02327
Il1r2	interleukin 1 receptor, type II	4.23	3.94	1349	1 B|1 19.5 cM	0.00807	0.00170

Table C.1d: Genes upregulated in the corneal limbal basal cells

Gene Symbol	Gene name	Fold change to		Unigene ID	ChroLocn	Welch's p-value	
		Periphery	Centre			L-P	L-C
Il1rn	interleukin 1 receptor antagonist	3.71	2.87	882	2 A3|2 10.0 cM	0.00966	0.00574
Impa1	inositol (myo)-1(or 4)-monophosphatase 1	1.82	1.65	183042	3 A1	0.00140	0.05611
Itga8	integrin alpha 8	3.84	5.9	329997	2	0.00282	0.00004
Krt1-13	keratin complex 1, acidic, gene 13	1.78	38.32	4646	11 D|11 58.49 cM	0.00337	0.00002
Krt1-14	keratin complex 1, acidic, gene 14	3.01	2.13	6974	11	0.00009	0.00069
Krt1-17	keratin complex 1, acidic, gene 17	11.88	11.16	14046	11 D|11 58.7 cM	0.01048	0.01194
Krt1-23	keratin complex 1, acidic, gene 23	4.29	3.14	290657	11 D	0.02538	0.02048
Lamp2	lysosomal membrane glycoprotein 2	2.41	1.78	486	X A3.1|X 13.0 cM	0.00027	0.05380
LOC434341	similar to nucleotide-binding oligomerization domains 27	2.28	1.97	---	8 C5		
Ltf	lactotransferrin	16.22	8.28	282359	9 F|9 70.2 cM	0.04708	0.05363
Manea	mannosidase, endo-alpha	2	2.04	245602	4		
Mat2b	methionine adenosyltransferase II, beta	1.68	1.89	293771	11 A5	0.00182	0.21747
Melk	maternal embryonic leucine zipper kinase	2.1	2.04	268668	4 B1|4 26.7 cM	0.03755	0.03005
MGI:2143217	X transporter protein 3 similar 1 gene	3.89	3.12	27208	9 F|9 71.0 cM		

Table C.1e: Genes upregulated in the corneal limbal basal cells

Moxd1	monooxygenase, DBH-like 1	8.63	10.34	285934	10 A3	0.00313	0.00296
Mylk	myosin, light polypeptide kinase	2.38	1.92	33360	16 B3	0.00062	0.00173
Nap1l1	nucleosome assembly protein 1-like 1	2.23	2.95	290407	10 D1|10 60.0 cM	0.01692	0.01266
Npm1	nucleophosmin 1	3.76	4.06	6343	11 A4	0.00026	0.03009
Nt5e	5' nucleotidase, ecto	9.58	49.18	244235	9 E3.2	0.00121	0.00211
Nusap1	nucleolar and spindle associated protein 1	2.2	2	290015	2 E5	0.02325	0.02958
Oit1	oncoprotein induced transcript 1	3.05	4.32	25351	14 A1	0.00683	0.00271
Palmd	palmdelphin	3.29	3.56	253736	3 G1|3 52.0 cM	0.03238	0.03300
Pdcd10	programmed cell death 10	1.8	1.68	316473	3 E3	0.03044	0.03814
Pdxk	pyridoxal (pyridoxine, vitamin B6) kinase	1.68	2.23	206159	10 C1|10 42.1 cM	0.02492	0.00056
Penk1	preproenkephalin 1	6.82	9.92	2899	4 A1|4 0.8 cM	0.03881	0.03549
Pik3cb	phosphatidylinositol 3-kinase, catalytic, beta polypeptide	1.78	2.01	213128	7 A3 9 E4	0.00032	0.00016
Plac8	placenta-specific 8	2.38	1.96	34609	5 E3|5 54.0 cM	0.06210	0.14124
Pon3	paraoxonase 3	3.2	3.68	9122	6 A1|6 0.5 cM	0.01133	0.00016
Popdc3	popeye domain containing 3	2.01	2.75	24748	10 B2|10 29.0 cM	0.03896	0.02658

Table C.1f: Genes upregulated in the corneal limbal basal cells

Gene Symbol	Gene name	Fold change to		Unigene ID	ChroLocn	Welch's p-value	
		Periphery	Centre			L-P	L-C
Ppp1cb	protein phosphatase 1, catalytic subunit, beta isoform	2.06	1.69	241931	5 B1	0.01618	0.02740
Prdx1	peroxiredoxin 1	2.45	1.64	30929	4 D1|4 47.0 cM	0.00318	0.04486
Prei3	preimplantation protein 3	1.73	1.61	291037	1 C1	0.00810	0.31862
Ptn	pleiotrophin	3.14	5.13	279690	6 B1|6 13.5 cM	0.03428	0.02006
Rap1b	RAS related protein 1b	2.53	1.69	233009	10 D2	0.01467	0.06129
Rasa2	RAS p21 protein activator 2	1.6	1.65	124502	9	0.02500	0.05961
Rbp1	retinol binding protein 1, cellular	3.27	3.23	279741	9 E3.3|9 52.0 cM	0.01575	0.02244
Reln	reelin	4.92	4.35	3057	5 A3-B1|5 8.0 cM	0.04263	0.05514
Rfk	riboflavin kinase	2.04	1.79	7013	19 B	0.01561	0.02612
S100a3	S100 calcium binding protein A3	2.85	3.43	703	3 F1-F2|3 43.6 cM	0.04072	0.03991
Samhd1	SAM domain and HD domain, 1	2.35	2.16	248478	2 H2	0.00003	0.00692
Sap30	sin3 associated polypeptide	5.86	6.41	118	8 B2|8 31.0 cM	0.00022	0.00119
Sat1	spermidine/spermine N1-acetyl transferase 1	2.01	2.04	2734	X F3-F4|X 65.2 cM	0.00440	0.13115
Serpinb1a	serine (or cysteine) proteinase inhibitor, clade B, member 1a	2.31	4.66	20144	13 A4|13 12.0 cM	0.00953	0.00056

Table C.1g: Genes upregulated in the corneal limbal basal cells

Gene Symbol	Gene name	Fold change to		Unigene ID	ChroLocn	Welch's p-value	
Serpinb2	serine (or cysteine) proteinase inhibitor, clade B, member 2	7.46	7.31	271870	1 E2.1|1 61.1 cM	0.00919	0.00879
Serpinb3a	serine (or cysteine) proteinase inhibitor, clade B (ovalbumin), member 3A	11.31	8.57	283677	1 E2.1	0.00645	0.06521
Serpinb3b	serine (or cysteine) proteinase inhibitor, clade B (ovalbumin), member 3B	4.47	4.17	337362	1 E2.1	0.00301	0.00642
Sfrs7	splicing factor, arginine/serine-rich 7	2.07	1.83	292016	17 E3	0.03928	0.04042
Slc35a1	solute carrier family 35 (CMP-sialic acid transporter), member 1	2.36	2.48	281885	4 A5	0.00038	0.02181
Slc5a8	solute carrier family 5 (iodide transporter), member 8	2.46	3.39	77381	10 C1	0.01098	0.01646

Table C.1h: Genes upregulated in the corneal limbal basal cells

Gene Symbol	Gene name	Fold change to		Unigene ID	ChroLocn	Welch's p-value	
Slc5a9	solute carrier family 5 (sodium/glucose cotransporter), member 9	3.53	3.81	26630	4 D1	0.00038	0.02181
Slc6a14	solute carrier family 6 (neurotransmitter transporter), member 14	2.75	3.03	253984	X A2	0.04159	0.05000
Smc2l1	SMC2 structural maintenance of chromosomes 2-like 1 (yeast)	2.11	1.67	2999	4 B3|4 18.5 cM	0.00297	0.06686
Smc4l1	SMC4 structural maintenance of chromosomes 4-like 1 (yeast)	1.73	1.8	206841	3 E2	0.02410	0.09437
Sox4	SRY-box containing gene 4	5.78	5.58	240627	---	0.00107	0.00217
Sprr2f	small proline-rich protein 2F	3.39	2.2	10692	3 F1|3 45.2 cM	0.00104	0.02019
Ssr4	signal sequence receptor, delta	1.79	1.97	831	X A7.2|X 29.5 cM	0.04156	0.00251
Stk17b	serine/threonine kinase 17b (apoptosis-inducing)	1.71	3.23	25559	1 C1.1	0.05331	0.02654
Stmn1	stathmin 1	1.67	1.8	271947	4 D3|4 65.7 cM	0.00556	0.00747
Syt14l	synaptotagmin 14-like	2.16	3.63	311393	12 C3	0.02656	0.02039
Tcfcp2l3	transcription factor CP2-like 3	1.82	1.93	244612	15 C	0.02807	0.01286

Table C.1i: Genes upregulated in the corneal limbal basal cells

Gene Symbol	Gene name	Fold change to		Unigene ID	ChroLocn	Welch's p-value	
		Periphery	Centre			L-P	L-C
Tgtp	T-cell specific GTPase	9.71	7.84	15793	11 B1.2	0.00364	0.03741
Tlr3	toll-like receptor 3	3.16	2.58	33874	8 B2	0.00188	0.00997
Tnfsf10	tumor necrosis factor (ligand) superfamily, member 10	3.07	2.93	1062	3 A3	0.03006	0.02401
Topbp1	topoisomerase (DNA) II beta binding protein	1.73	1.74	259893	9 F1	0.01893	0.00973
Upp1	uridine phosphorylase 1	5.06	5.86	4610		0.01322	0.00684
Utx	ubiquitously transcribed tetratricopeptide repeat gene, X chromosome	2.55	1.62	257498	X A1.2|X 5.5 cM	0.01164	0.09342
Vav3	vav 3 oncogene	2.57	3.2	282257	3 G1	0.00278	0.00253
Zic1	zinc finger protein of the cerebellum 1	2.28	2.11	335350	9 E3.2|9 61.0 cM	0.03657	0.04911

Table C.2a&b Genes specifically downregulated in corneal limbal basal epithelial cells. Gene names and symbols as well as fold change ratios and Welch's t-test *p*-values are listed for each gene. Additionally Unigene database reference ID and chromosomal location (ChroLocn) is given for every gene.

Table C.2a Genes specifically downregulated in corneal limbal basal epithelial cells.

Gene Symbol	Gene name	Fold change to		Unigene ID	ChroLocn	Welch's p-value	
		Periphery	Centre			L-P	L-C
Satb1	special AT-rich sequence binding protein 1	1.77	1.98	311655	17 C	0.00190	0.03862
Rps6ka2	ribosomal protein S6 kinase, polypeptide 2	3.92	2.2	259901	17 F4|17	0.01223	0.01431
EST	RIKEN cDNA 1300013J15 gene	2.22	1.63	100741	11 B2	0.01513	0.00608
St8sia4	ST8 alpha-N-acetyl-neuraminide alpha-2,8-sialyltransferase 4	2.2	2.69	306228	1 D	0.01679	0.00501
Procr	protein C receptor, endothelial	3.76	2.08	3243	2 H1-3	0.02997	0.05638
Map4k4	mitogen-activated protein kinase kinase kinase kinase 4	2.28	2.5	---	---	0.00103	0.05167
Ankrd24	ankyrin repeat domain 24	1.88	1.72	304382	10 C1|10	0.04100	0.04410
EST	similar to ENSANGP00000013261	2.13	2.01	29659	11 D	0.05042	0.05770
EST	RIKEN cDNA B230208H17 gene	1.54	1.62	29600	2 A3	0.00500	0.06447
EST	expressed sequence AI842788	2.87	2.48	329657	19 A		
Prss25	protease, serine, 25	1.85	1.67	21880	6 C3|6 34.75 cM	0.02344	0.32120

---	CDNA clone IMAGE:1328649	2.65	2.27	178550	---		
Nav1	neuron navigator 1	2.26	1.62	34977	1 E4	0.03717	0.24231

Table C.2b Genes specifically downregulated in corneal limbal basal epithelial cells.

Gene Symbol	Gene name	Fold change to Periphery	Unigene ID Centre	ChroLocn	Welch's p-value	L-P	L-C
Ndn	necdin	1.73	2.2	250919	7 C|7 28.0 cM	0.05970	0.05437
Dbp	D site albumin promoter binding protein	1.83	3.01	3459	7 B2|7	0.00125	0.08296
Lrrc20	ATPase, H+ transporting, lysosomal accessory protein 2	1.93	4	25148	23.0 cM X A1.1	0.00077	0.00733
EST	RIKEN cDNA 1500016O10 gene	24.79	5.19	207814	7 F3	0.03907	0.11275
---	Transcribed locus	2.75	2.52	22950	---	0.04311	0.05141
Car7	carbonic anhydrase 7	2.09	2.77	129265	8 D1	0.00310	0.02291
---	Transcribed locus	2.65	3.28	156172	---	0.00561	0.04281
Mapre2	microtubule-associated protein, RP/EB family, member 2	1.71	1.8	132237	18 A2	0.00185	0.00743
EST	RIKEN cDNA 1810057P16 gene	2.27	4.15	64962	11 E2	0.00040	0.00168
EST	expressed sequence AU044698	2.62	1.92	---	---	0.00125	0.05415
---	---	2.68	1.69	---	---		
EST	RIKEN cDNA 1700110N18 gene	1.63	1.65	25670	16 C1.3	0.01250	0.00349
Sdf4	stromal cell derived factor 4	2.14	1.45	293517	4 E2	0.04831	0.03818

Table C.3 a-m: Genes upregulated in the peripheral corneal epithelial basal cells. Official gene names and symbols, fold change ratios and Welch's t-test *p*-values as well as Unigene reference numbers and chromosomal location (ChroLocn) of each gene is designated.

Table C.3 a: Genes upregulated in the peripheral corneal epithelial basal cells

Gene Symbol	Gene name	Fold change to		Unigene ID	Chromosomal location	Welch's p-value	
		Limbus	Centre			P-L	P-C
A2m	alpha-2-macroglobulin	3.14	2	30151	6 F1|6 61.7 cM	0.00164	0.00162
A430031N04	hypothetical protein A430031N04	3.73	1.99	259328	16 B2	0.00586	0.04524
Abca8a	ATP-binding cassette, sub-family A (ABC1), member 8a	1.82	2.73	344148	11 E1	0.05807	0.01096
Abtb1	ankyrin repeat and BTB (POZ) domain containing 1	1.71	1.88	166858	6 D1	0.01260	0.01518
Agpat4	1-acylglycerol-3-phosphate O-acyltransferase 1 (lysophosphatidic acid acyltransferase, delta)	1.8	2.08	258300	17 A2	0.04920	0.00020
Ak2	adenylate kinase 2	2.1	1.72	29460	4 D2.2|4 61.0 cM	0.00015	0.03044
Ap3b1	adaptor-related protein complex 3, beta 1 subunit	1.67	1.84	21185	13 D1|13 47.0 cM	0.11103	0.03337
Aqp1	aquaporin 1	2.99	2.85	18625	6 B3|6 27.0 cM	0.06674	0.84868
Arhgap24	Rho GTPase activating protein 24	1.71	2.17	233880	5 E4	0.00300	0.00155
Arntl	aryl hydrocarbon receptor nuclear translocator-like	2.14	1.78	12177	7 F2-F3|7 52.0 cM	0.01370	0.04193

Table C.3 b: Genes upregulated in the peripheral corneal epithelial basal cells

Gene Symbol	Gene name	Fold change to		Unigene ID	Chromosomal location	Welch's p-value	
Bckdhb	branched chain ketoacid dehydrogenase E1, beta polypeptide	2.23	1.92	12819	9 E2-E3.1	0.00606	0.04463
Bcl2	B-cell leukemia/lymphoma 2	2.17	1.77	257460	1 E2.1|1 59.8 cM	0.01012	0.07843
Bsg	Basigin	1.82	1.85	726	10 C1|10 42.4 cM	0.00477	0.04259
Cct7	chaperonin subunit 7 (eta)	1.71	2.22	289900	6 D1	0.05086	0.00067
Cd9	CD9 antigen	1.93	1.83	210676	6 F3|6 58.0 cM	0.05080	0.15770
Cdc2l2	cell division cycle 2 homolog (S. pombe)-like 2	1.79	2.22	267410	4 E2|4 79.4 cM	0.02011	0.00051
Cdc42ep4	CDC42 effector protein (Rho GTPase binding) 4	2.23	1.65	293378	11 E2	0.00006	0.03061
Cdyl	chromodomain protein, Y chromosome-like	2.16	2.41	29002	13 A3.3|13 17.0 cM	0.00050	0.01046
Cdyl	chromodomain protein, Y chromosome-like	1.83	1.88	29002	13 A3.3|13 17.0 cM	0.00071	0.03214
Centg3	centaurin, gamma 3	1.93	2.58	250703	5 A3	0.04924	0.01228
Ces3	carboxylesterase 3	2.64	2.93	292803	8 C5	0.00218	0.01038
Cgn	Cingulin	1.89	1.75	87634	3 F2.1|3 43.3 cM	0.01372	0.00848
Chst5	carbohydrate (N-acetylglucosamine 6-O) sulfotransferase 5	3.48	2.66	25646	---	0.00332	0.00879
Clk2	CDC-like kinase 2	1.69	1.84	288098	3 F1	0.01343	0.01077

Table C.3 c: Genes upregulated in the peripheral corneal epithelial basal cells

Gene Symbl.	Gene name	Fold change to		Unigene ID	Chromosomal location	Welch's p-value	
		Limbus	Centre			P-L	P-C
Col5a1	procollagen, type V, alpha 1	2.93	5.74	7281	2 A2-B|2 18.0 cM	0.02066	0.02882
Col5a2	procollagen, type V, alpha 2	1.91	2.97	10299	1 C1	0.05804	0.00164
Col6a1	procollagen, type VI, alpha 1	2.22	5.5	2509	10 41.1 cM	0.02773	0.00002
Col6a2	procollagen, type VI, alpha 2	2.6	5.58	1949	10 41.1 cM	0.03435	0.00630
Col6a3	procollagen, type VI, alpha 3	2.66	3.05	7562	1 D|1 53.9 cM	0.02364	0.02863
Coro1c	coronin, actin binding protein 1C	1.83	1.78	260158	---	0.00870	0.03559
Coro1c	coronin, actin binding protein 1C	2.01	2.2	260158	---	0.00301	0.00589
Csk	c-src tyrosine kinase	1.64	1.61	21974	9 B|9 32.0 cM	0.14598	0.06129
Cyp3a13	cytochrome P450, family 3, subfamily a, polypeptide 13	2.77	1.99	289886	5 G2|5 78.0 cM	0.00053	0.00357
Cyr61	cysteine rich protein 61	2.13	1.61	1231	3 H2|3 72.9 cM	0.03325	0.04278
D10Wsu52e	DNA segment, Chr 10, Wayne State University 52, expressed	1.61	2.04	9257	10 C1|10 46.0 cM	0.01603	0.00642
D630048P19Rik	RIKEN cDNA D630048P19 gene	1.82	1.72	239583	7 A1	0.01917	0.01274

Table C.3 d: Genes upregulated in the peripheral corneal epithelial basal cells

Gene Symbl.	Gene name	Fold change to		Unigene ID	Chromosomal location	Welch's p-value			
		Limbus	Centre					P-L	P-C
Dclre1a	DNA cross-link repair 1A, PSO2 homolog (S. cerevisiae)	1.97	1.88	2805	19 D2			0.01970	0.04729
Ddah1	dimethylarginine dimethylaminohydrolase 1	2.01	1.6	234247	3 H3			0.00531	0.04917
Ddx27	DEAD (Asp-Glu-Ala-Asp) box polypeptide 27	1.72	2.48	295031	2 H3			0.03024	0.00211
Ddx47	DEAD (Asp-Glu-Ala-Asp) box polypeptide 47	1.93	2.38	166524	6 G1			0.05468	0.01079
Def6	differentially expressed in FDCP 6	1.8	1.96	204731	17 A3.3			0.00853	0.00992
Dkk2	dickkopf homolog 2 (Xenopus laevis)	2.08	3.18	103593	3 H2			0.04138	0.00319
Dpt	dermatopontin	2.06	3.34	28935	1 H2			0.06293	0.00038
Dyt1	dystonia 1	1.68	1.67	154994	2 B			0.04437	0.04230
E4f1	E4F transcription factor 1	1.97	1.8	163132	17 A3.3|17 12.0 cM			0.03028	0.01463
Egln3	EGL nine homolog 3 (C. elegans)	3.56	1.64	133037	12 C1			0.00288	0.03798
						6 G3|6 74.0 cM		0.02023	0.02423

Entpd8	ectonucleoside triphosphate diphosphohydrolase 6	1.78	2.11	177551	11 E2|11 75.0 cM	0.01098	0.00331

Table C.3 e: Genes upregulated in the peripheral corneal epithelial basal cells

Gene Symbl.	Gene name	Fold change to		Unigene ID		Chromosome	Welch's p-value	
		Limbus	Centre	Conj			P-L	P-C
Erdr1	erythroid differentiation regulator 1	2.1	2.04		288693	---	0.06120	0.02499
Erp29	endoplasmic reticulum protein 29	1.84	2.06		154570	5 F	0.04056	0.05950
Fads2	fatty acid desaturase 2	2.31	2		38901	19 B	0.01888	0.01642
Fgf1	fibroblast growth factor 1	2.01	1.8		241282	18 B3|18 19.0 cM	0.00099	0.02666
Galk1	galactokinase 1	1.61	2.36		2820	11 E2|11 78.0 cM	0.02575	0.02644
Galnt2	UDP-N-acetyl-alpha-D-galactosamine:polypeptide N-acetylgalactosaminyl transferase 2	2.06	1.72		33808	8 E2	0.01404	0.16190
Gdi1	guanosine diphosphate (GDP) dissociation inhibitor 1	1.62	2.11		205830	X B-C1|X 29.83 cM	0.01766	0.01274
Gga2	golgi associated, gamma adaptin ear containing, ARF binding protein 2	1.8	1.61		29619	7 F3	0.07037	0.00533
Glb1	galactosidase, beta 1	1.65	2.97		290516	---	0.02490	0.00715
Gli3	GLI-Kruppel family member GLI3	1.6	1.83		5098	13 A2|13 14.0 cM	0.01413	0.02509
Gmppa	GDP-mannose pyrophosphorylase A	1.92	1.83		23951	1 C3	0.00723	0.09048

Gtl2	GTL2, imprinted maternally expressed untranslated mRNA	1.75	4.96		289645	12 F1|12 54.0 cM	0.05404	0.00272

Table C.3 f: Genes upregulated in the peripheral corneal epithelial basal cells

Gene Symbl.	Gene name	Fold change to			Unigene ID	Chromosome	Welch's p-value	
		Limbus	Centre	Conj			P-L	P-C
Hcph	hemopoietic cell phosphatase	1.62	1.89		271799	6 F2|6 60.22 cM	0.00884	0.01125
Hlf	hepatic leukemia factor	2.23	1.87		158903	11 C-D|11 52.0 cM	0.00185	0.07293
Ifld2	induced in fatty liver dystrophy 2	2.71	2.62		276018	2 G3	0.00472	0.00382
Igfbp2	insulin-like growth factor binding protein 2	1.72	3.01		141936	1 C3|1 36.1 cM	0.00684	0.00247
Irx3	Iroquois related homeobox 3 (Drosophila)	2.58	2.87		238044	8 C5|8 42.1 cM	0.00259	0.00017
Itgb5	integrin beta 5	1.6	1.75		6424	16 B3	0.02990	0.02649
Jag2	jagged 2	2.36	2.58		186146	12 F1|12 57.9 cM	0.00092	0.00212
Kctd15	potassium channel tetramerisation domain containing 15	2.41	1.91		214380	7 B1	0.00181	0.00753
Kif13a	kinesin family member 13A	2.16	1.72		342703	13 B1	0.00291	0.01526
Krt2-6a	keratin complex 2, basic, gene 6a	1.93	2.2		302399	15 F2|15 58.77 cM	0.01375	0.00133

Limk2	LIM motif-containing protein kinase 2	2.03	2.16		124176	11 D	0.02778	0.01682
Lmnb1	lamin B1	2.07	1.82		4105	---		

Table C.3 g: Genes upregulated in the peripheral corneal epithelial basal cells

Gene Symbl.	Gene name	Fold change to			Unigene ID	Chromosome	Welch's p-value	
		Limbus	Centre	Conj			P-L	P-C
Lrig1	leucine-rich repeats and immunoglobulin-like domains 1	2.33	2.6		245210	6 D2|6 39.0 cM	0.06881	0.01146
Lrp1	low density lipoprotein receptor-related protein 1	3.51	2.35		271854	10 B2-D1	0.00718	0.05642
Lrp4	low density lipoprotein receptor-related protein 4	2.48	2.79		275149	2 E1	0.04177	0.04051
Lrpap1	low density lipoprotein receptor-related protein associated protein 1	1.79	2.11		277661	5 B2|5 20.0 cM	0.04747	0.00534
Lrpap1	low density lipoprotein receptor-related protein associated protein 1	1.92	2.35		277661	5 B2|5 20.0 cM	0.00722	0.00009
Ltb4dh	leukotriene B4 12-hydroxydehydrogenase	2.07	1.69		34497	4 C1	0.00085	0.05947
Lynx1	Ly6/neurotoxin 1	5.03	2.11		257067	15 D3	0.00000	0.01593
Madd	MAP-kinase activating death domain	1.77	1.82		36410	2 E1	0.04257	0.01844
Mamdc2	MAM domain containing 2	5.1	3.07		50841	19 B	0.01180	0.03064
Matn4	matrilin 4	1.72	3.1		29428	2 H3|2 94.0 cM	0.56677	0.06096
Mgea5	meningioma expressed antigen 5 (hyaluronidase)	1.77	1.6		122725	19 D1	0.00190	0.03292

Table C.3 h: Genes upregulated in the peripheral corneal epithelial basal cells

Gene Symbl.	Gene name	Fold change to		Unigene ID	Chrom. Loc.	Welch's p-value	
		Limbus	Centre			P-L	P-C
Mkrn1	makorin, ring finger protein, 1	1.73	1.71	270484	6 B1	0.00227	0.09438
Mrc2	mannose receptor, C type 2	1.95	2.53	235616	11 E1	0.05943	0.00050
Mta3	metastasis associated 3	1.83	2.07	277668	17 E4	0.05079	0.06846
Mthfd1	methylenetetrahydrofolate dehydrogenase (NADP+ dependent), methenyltetrahydrofolate cyclohydrolase, formyltetrahydrofolate synthase	2.03	2.25	29584	---	0.00404	0.01077
Nap1l4	nucleosome assembly protein 1-like 4	1.89	2.27	294625	7 F5|7 69.55 cM	0.01328	0.00942
	natural killer tumor recognition sequence	1.64	1.73	32842	9 F4|9 71.0 cM		
Nktr						0.44447	0.00600
Npnt	nephronectin	2.66	1.97	279310	3 G3	0.00031	0.07437
Nr1d1	nuclear receptor subfamily 1, group D, member 1	2.62	3.41	289490	11 D	0.00944	0.00892
Ntrk2	neurotrophic tyrosine kinase, receptor, type 2	2.62	3.27	130054	13 B2|13 36.0 cM	0.02012	0.00717
Olfml3	olfactomedin-like 3	2.11	2.04	211535	3 F2.2	0.02569	0.05041
Oplah	5-oxoprolinase (ATP-hydrolysing)	1.74	1.75	322738	15 D3	0.01914	0.00135
Pabpc1	poly A binding protein, cytoplasmic 1	1.6	2.07	371570	15 C	0.00571	0.10380
Pank3	pantothenate kinase 3	1.88	1.62	255044	11 A4		
Pdcd11	programmed cell death protein 11	1.77	1.88	41166	19 D2	0.01844	0.01389

Table C.3 i: Genes upregulated in the peripheral corneal epithelial basal cells

Gene Symbl.	Gene name	Fold change to		Unigene ID	Chromosomal location		Welch's p-value	
		Limbus	Centre				P-L	P-C
Per3	period homolog 3 (Drosophila)	3.23	2.51	7952	---		0.02086	0.03804
Phf15	PHD finger protein 15	1.64	1.85	121361	4 E2		0.04754	0.00856
Pias3	protein inhibitor of activated STAT 3	1.74	1.74	259996	11 B1.3		0.01688	0.03466
Pja1	praja1, RING-H2 motif containing	2.6	1.8	1635	3 F2.1		0.02473	0.03488
Pkm2	pyruvate kinase, muscle	1.99	1.6	8211	X C3|X 36.6 cM		0.00827	0.06524
Ppp2r5e	protein phosphatase 2, regulatory subunit B (B56), epsilon isoform	1.8	1.6	28399	5 G2		0.00223	0.05075
Prpf8	pre-mRNA processing factor 8	1.74	1.97	259626	---		0.02528	0.01168
Prss22	protease, serine, 22	1.83	2.13	3757	11 B5|11 45.0 cM		0.02142	0.07068
Psmd4	proteasome (prosome, macropain) 26S subunit, non-ATPase, 4	1.71	1.88	157351	17 A3.3|17 10.7 cM		0.00485	0.00886
Pvrl4	poliovirus receptor-related 4	1.91	2.14	263414	---		0.00107	0.00020

Table C.3 j: Genes upregulated in the peripheral corneal epithelial basal cells

Gene Symbl.	Gene name	Fold change to		Unigene ID	Chromosomal location	Welch's p-value	
		Limbus	Centre			P-L	P-C
Qscn6l1	quiescin Q6-like 1	1.99	1.68	116769	2 A3	0.03340	0.00576
Rab2l	RAB2, member RAS oncogene family-like	1.72	1.6	43777	17 B2	0.01710	0.00779
Ramp2	receptor (calcitonin) activity modifying protein 2	2.04	2.23	298256	11 D|11 61.5 cM	0.00522	0.02424
Rapgef3	Rap guanine nucleotide exchange factor (GEF) 3	1.92	1.65	24028	15 F1	0.00259	0.10837
Rin1	Ras and Rab interactor 1	2.1	1.71	271922	19 A	0.01809	0.05580
Rpl22	ribosomal protein L22	1.71	1.66	307846	4 E2	0.01637	0.04438
Rps6kb1	ribosomal protein S6 kinase, polypeptide 1	2.04	1.77	374825	11 C	0.03281	0.05138
Sdbcag84	serologically defined breast cancer antigen 84	1.6	1.61	141276	2 H2|2 92.0 cM	0.02418	0.01426
Sdc1	syndecan 1	1.74	1.64	2580	12 A1.1|12 1.0 cM	0.00587	0.01266
Secisbp2	SECIS binding protein 2	1.89	2.19	275981	13 B1	0.00717	0.02904
Sema4c	sema domain, immunoglobulin domain (Ig), transmembrane domain (TM) and short cytoplasmic domain, (semaphorin) 4C	1.71	2.3	29558	1 B	0.01619	0.00529
Sf3a3	splicing factor 3a, subunit 3	1.68	2.23	25779	4 D1	0.04660	0.05862
Sfrs8	splicing factor, arginine/serine-rich 8	1.88	1.6	288714	5 G1.3	0.00609	0.00979

Table C.3 k: Genes upregulated in the peripheral corneal epithelial basal cells

Gene Symbl.	Gene name	Fold change to Limbus	Centre	Unigene ID	Chromosomal location	Welch's p-value P-L	P-C
Siat9	sialyltransferase 9 (CMP-NeuAc:lactosylceramide alpha-2,3-sialyltransferase)	2.08	1.88	121485	6 35.59 cM	0.01320	0.00587
Slc26a7	solute carrier family 26, member 7	2.1	2.62	245210	6 D2|6 39.0 cM	0.04876	0.01290
Slc30a6	solute carrier family 30 (zinc transporter), member 6	2.1	2.2	296006	4 A1	0.01362	0.00483
Slc4a4	solute carrier family 4 (anion exchanger), member 4	2.43	2.41	243943	17 E2	0.03089	0.03519
Sphk2	sphingosine kinase 2	1.68	1.72	149776	14 C3|14 30.5 cM	0.03715	0.04194
Spon2	spondin 2, extracellular matrix protein	2.89	1.92	24222	7 B3	0.00670	0.01617
Srrm1	serine/arginine repetitive matrix 1	1.73	1.64	45044	17 B3	0.03620	0.00757

Table C.3 I: Genes upregulated in the peripheral corneal epithelial basal cells

Gene Symbl.	Gene name	Fold change to		Unigene ID	Chromosomal location	Welch's p-value	
		Limbus	Centre			P-L	P-C
Stk24	serine/threonine kinase 24 (STE20 homolog, yeast)	1.73	1.64	369092	14 E5|14 62.0 cM	0.00025	0.00101
Tcfap2b	transcription factor AP-2 beta	1.8	2.43	137021	1 A2-A4	0.01030	0.00175
Tcfe2a	transcription factor E2a	1.71	2.04	3406	10 C1|10 43.0 cM	0.04405	0.02985
Tef	thyrotroph embryonic factor	2.13	1.85	270278	15 E1|15 46.7 cM	0.00254	0.01025
Tgm2	transglutaminase 2, C polypeptide	2.5	1.85	330731	2 H1|2 89.0 cM		
Thoc3	THO complex 3	1.6	1.67	292487	13 B2	0.00254	0.02098
Tmpo	thymopoietin	1.85	1.85	159684	10 C2|10 49.0 cM	0.02130	0.03576
Ttll1	tubulin tyrosine ligase-like 1	2.17	2	235007	15 E1-E2	0.05531	0.08755
Ube2g2	ubiquitin-conjugating enzyme E2G 2	1.78	2.43	307906	10 C1|10 41.6 cM	0.00486	0.00264
Usp7	ubiquitin specific protease 7	2.13	1.65	295330	16 A1	0.00056	0.00250

Table C.3 m: Genes upregulated in the peripheral corneal epithelial basal cells

Gene Symbl.	Gene name	Fold change to		Unigene ID	Chromosomal location	Welch's p-value	
		Limbus	Centre			P-L	P-C
Vamp3	vesicle-associated membrane protein 3	1.75	1.6	273930	4 E1	0.00222	0.01319
Wnt11	wingless-related MMTV integration site 11	2.04	2.01	22182	7 E1|7 48.0 cM	0.04936	0.04640
Wnt5a	wingless-related MMTV integration site 5A	2.53	2.87	287544	14 A3|14 7.8 cM	0.02035	0.00574
Yy1	YY1 transcription factor	1.62	1.87	3868	12 F1|12 53.0 cM	0.04906	0.01953
Zbtb7	zinc finger and BTB domain containing 7	2.41	1.87	20920	10 B5.3	0.00289	0.14181
Zdhhc14	zinc finger, DHHC domain containing 14	2.41	1.77	328751	17 A1	0.01608	0.00731
Zdhhc14	zinc finger, DHHC domain containing 14	2.41	1.77	328751	17 A1	0.01608	0.00731

Table C.4 a&b : Genes specifically downregulated in corneal peripheral basal epithelial cells. The table includes gene symbols, names, fold changes, unigene ID and chromosomal location of each gene.

Table C.4a : Genes specifically downregulated in corneal peripheral basal epithelial cells.

Gene Symbol	Gene name	Fold change to		Unigen ID	Chrom. location	Welch's p-value	
		Limbus	Centre			P-L	P-C
Atf3	activating transcription factor 3	2.51	1.83	2706	1 H6	0.00571	0.07722
Bnip3	BCL2/adenovirus E1B 19kDa-interacting protein 1, NIP3	1.89	4.5	2159	7 F5	0.04952	0.00948
C1galt1	core 1 UDP-galactose:N-acetylgalactosamine-alpha-R beta 1,3-galactosyltransferase	2.6	1.73	102752	6 A1	0.01725	0.00828
Cd47	CD47 antigen (Rh-related antigen, integrin-associated signal transducer)	3.32	1.73	31752	16 B5	0.0003	0.01089
Cfl2	Cofilin 2, muscle	1.92	1.69	276826	12 C1	0.00002	0.04226
Chi3l1	chitinase 3-like 1	41.07	4.89	38274	1 E4|1 72.3 cM	0.00279	0.04776
Cxcl16	chemokine (C-X-C motif) ligand 16	2.46	1.78	358690	11 B4	0.00438	0.25464
Ddit4	DNA-damage-inducible transcript 4	1.87	1.84	21697	10 B3	0.04056	0.04238
Ecm1	extracellular matrix protein 1	2.5	2.16	3433	3 F2.1|3 45.4 cM	0.04750	0.52472
Ednrb	endothelin receptor type B	2.36	2.1	229532	14 E2.3|14 51.0 cM	0.00347	0.07704
Fhl1	four and a half LIM domains 1	3.12	1.78	3126	X A6-A7.1	0.02616	0.05545
Hist2h2bb	histone 2, H2bb	5.7	2.1	5220	---	0.02600	0.05152
Ifi203	interferon activated gene 203	2.77	1.88	261270	1 H3|1 95.31 cM	0.01996	0.02959
Lcn2	lipocalin 2	2.57	2.38	9537	2 A3|2 27.0 cM	0.00105	0.01223
Lgals1	lectin, galactose binding, soluble 1	2.6	2.04	43831	15 E|15 44.9 cM	0.02677	0.19873

Table C.4a : Genes specifically downregulated in corneal peripheral basal epithelial cells.

Gene Symbol	Gene name	Fold change to		Unigen ID	Chrom. location	Welch's p-value	
		Limbus	Centre			P-L	P-C
Ltf	lactotransferrin	16.22	1.96	282359	9 F|9 70.2 cM	0.04708	0.04007
Lzp-s	P lysozyme structural	11.96	1.85	177539	10 D2	0.04707	0.05603
Man1a	mannosidase 1, alpha	4.63	2	117294	10 B3	0.03084	0.00699
Mmp3	matrix metalloproteinase 3	40.5	1.99	4993	9 A1|9 1.0 cM	0.00059	0.05746
Pfkp	phosphofructokinase, platelet	2.13	1.75	273874	13 A1	0.07378	0.02425
Pglyrp1	peptidoglycan recognition protein 1	9.25	4.03	21855	7 A3	0.00036	0.02711
Soat1	sterol O-acyltransferase 1	3.12	1.84	28099	1 G3|1 81.6 cM	0.01627	0.04024
Sulf2	sulfatase 2	3.97	1.8	280459	2 H3	0.00116	0.04912
Sytl2	synaptotagmin-like 2	4.2	1.8	26751	7 D3	0.02904	0.10955
Trp53inp1	transformation related protein 53 inducible nuclear protein 1	2.33	2.1	28708	4 A1-A2	0.05777	0.11913
Ttr	transthyretin	11.24	2.6	2108	18 A2|18 7.0 cM	0.02253	0.05035
Tubb6	tubulin, beta 6	4.08	1.75	181860	18 E1	0.03445	0.05252

Table C.5 a-e: Genes upregulated in the central corneal epithelial basal cells. Official gene names and symbols, fold change rations, Welch's t-test *p*-values as well as Unigene reference numbers and chromosomal location (ChroLocn) of each gene is designated.

Table C.5 a Genes upregulated in the central corneal epithelial basal cells

Gene Symbol	Gene name	Fold change to		Unigene ID	Chro. Lctn.	Welch's p-value	
		Limbus	Periph			C-L	C-P
Acpp	acid phosphatase, prostate	2.85	2.5	19941	9 F1	0.04749	0.06168
Angptl4	angiopoietin-like 4	3.97	1.64	196189	17 B1	0.05307	0.12021
Ankrd29	ankyrin repeat domain 29	2.08	2.07	53865	18 A1	0.04145	0.05105
Asns	asparagine synthetase	5.06	4.41	2942	6 A1	0.00152	0.00570
BC040823	cDNA sequence BC040823	1.91	2.13	21577	2 H4	0.05555	0.04912
Bnip3	BCL2/adenovirus E1B 19kDa-interacting protein 1, NIP3	2.38	4.5	2159	7 F5	0.00765	0.00948
Bnip3l	BCL2/adenovirus E1B 19kDa-interacting protein 3-like	2.16	1.65	29820	14 D1|14 28.0 cM	0.00383	0.02178
Cxcl1	chemokine (C-X-C motif) ligand 1	3.43	2.99	21013	5 E-F|5 51.0 cM	0.03216	0.03590
D10Ertd438e	DNA segment, Chr 10, ERATO Doi 438, expressed	1.71	1.83	199964	10 B3|10 29.0 cM	0.04866	0.06201
Dnajd1	DnaJ (Hsp40) homolog, subfamily D, member 1	1.69	2.03	248046	14 D3		
Eif4ebp1	eukaryotic translation initiation factor 4E binding protein 1	3.32	1.99	6700	8 A4-B1|8 8.0 cM	0.04856	0.10675

Table C.5 b Genes upregulated in the central corneal epithelial basal cells

Gene Symbol	Gene name	Fold change to		Unigene ID	Chro. Lctn.	Welch's p-value	
		Limbus	Periph			C-L	C-P
Fgfbp1	fibroblast growth factor binding protein 1	1.73	1.68	46053	5 B3	0.06210	0.06513
Fos	FBJ osteosarcoma oncogene	1.72	1.68	246513	12 D2|12 40.0 cM	0.04344	0.00238
Fscn1	fascin homolog 1, actin bundling protein (Strongylocentrotus) purpuratus)	7.01	4.5	289707	5 G2|5 86.0 cM	0.02690	0.03140
Galm	galactose mutarotase	2.06	1.83	29098	17 E3	0.02571	0.06628
Gas5	growth arrest specific 5	2.41	1.93	270065	1 H2.1	0.06324	0.17022
Gatad2a	GATA zinc finger domain containing 2A	1.84	1.69	270044	8 B3.3	0.07058	0.23185
Ghr	growth hormone receptor	2.93	1.61	3986	15 A1|15 4.6 cM	0.00193	0.01875
Gnai2	guanine nucleotide binding protein, alpha inhibiting 2	1.74	1.88	196464	9 F1|9 59.0 cM	0.05495	0.03023
Ifit3	interferon-induced protein with tetratricopeptide repeats 3	1.87	2.06	271850	19 C3	0.00517	0.00137
Kalrn	kalirin, RhoGEF kinase	2.48	2.55	101990	16 B3		
Lmnb1	lamin B1	1.8	1.64	4105	18 D3|18 29.0 cM	0.54110	0.01146

Table C.5 c Genes upregulated in the central corneal epithelial basal cells.

Gene Symbol	Gene name	Fold change to		Unigene ID	Chro. Lctn.	Welch's p-value	
		Limbus	Periph			C-L	C-P
Lss	lanosterol synthase	2.43	2.03	55075	10 C1|10 41.1 cM	0.01810	0.02695
Lxn	Latexin	3.05	1.6	2632	3 E1|3 31.6 cM	0.03850	0.09999
Mat2a	methionine adenosyltransferase II, alpha	2.1	2.08	29815	6 C1	0.03713	0.25324
Mt1	metallothionein 1	2.46	1.71	192991	8 C5|8 45.0 cM	0.00854	0.02543
Narg1	NMDA receptor-regulated gene 1	1.65	1.64	275281	3 D	0.04707	0.03790
Ndrl	N-myc downstream regulated-like	2.19	2.1	---	15 D2	0.00644	0.00910
Odz4	odd Oz/ten-m homolog 4 (Drosophila)	2.46	1.89	254610	7 E1|7 47.7 cM	0.04254	0.04757
Pigf	phosphatidylinositol glycan, class F	2.22	1.68	219685	17 E4-E5|17 54.3 cM	0.00096	0.00240
Prkcb1	protein kinase C, beta 1	4.44	5.13	207496	7 F2|7 60.0 cM		
Psmc3ip	proteasome (prosome, macropain) 26S subunit, ATPase 3, interacting protein	1.75	1.64	18344	11 D	0.05377	0.00426
Pvrl2	poliovirus receptor-related 2	1.95	1.68	4341	7 A2|7 9.0 cM	0.00612	0.01282
Rai14	retinoic acid induced 14	1.78	1.89	212395	15 A2	0.00026	0.00170

Table C.5 d Genes upregulated in the central corneal epithelial basal cells.

Gene Symbol	Gene name	Fold change to		Unigene ID	Chro. Lctn.	Welch's p-value	
		Limbus	Periph			C-L	C-P
Ralb	v-ral simian leukemia viral oncogene homolog B (ras related)	2.11	1.68	27832	1 E2		
Rapgef5	Rap guanine nucleotide exchange factor (GEF) 5	3.05	1.73	227642	12 F2	0.00566	0.02173
Rgs2	regulator of G-protein signaling 2	1.66	1.77	28262	1 F|1 78.0 cM	0.00312	0.00130
Scd1	stearoyl-Coenzyme A desaturase 1	1.69	1.95	267377	19 C3|19 43.0 cM	0.00892	0.00017
Serpinb5	serine (or cysteine) proteinase inhibitor, clade B, member 5	2.11	1.71	268618	1 E2.1	0.00509	0.00691
Slc19a2	solute carrier family 19 (thiamine transporter), member 2	4.32	1.67	35444	1 H2.2|1 87.0 cM	0.02422	0.05690
Slc35e4	solute carrier family 35, member E4	1.72	1.64	171514	11 A1	0.00039	0.00026
St8sia4	ST8 alpha-N-acetyl-neuraminide alpha-2,8-sialyltransferase 4	7.67	3.76	306228	1 D	0.00192	0.01005
Thumpd1	THUMP domain containing 1	2.28	3.01	26392	7 F1	0.03671	0.02700

Table C.5 e Genes upregulated in the central corneal epithelial basal cells.

Gene Symbol	Gene name	Fold change to		Unigene ID	Chro. Lctn.	Welch's p-value	
		Limbus	Periph			C-L	C-P
Timm50	translocase of inner mitochondrial membrane 50 homolog (yeast)	2.43	1.72	167913	7 A3	0.01505	0.00348
Tor3a	torsin family 3, member A	2.62	1.6	206737	1 G3	0.03991	0.05762
Tpm2	tropomyosin 2, beta	2.16	1.82	646	4 B1	0.02405	0.03611
Tyki	thymidylate kinase family LPS-inducible member	3.46	4.2	271839	12 A1.3|12 6.0 cM	0.00531	0.00724
Usp18	ubiquitin specific protease 18	1.64	2.2	326911	6 F|6 56.0 cM	0.37210	0.00091
Vldlr	very low density lipoprotein receptor	2.25	1.68	4141	19 C1|19 20.0 cM	0.00828	0.01941
Yaf2	YY1 associated factor 2	1.72	1.69	4714	15 F1	0.00416	0.00280
Zfp313	zinc finger protein 313	2.19	2	22225	---	0.02578	0.02390
Timm44	translocator of inner mitochondrial membrane 44	1.68	1.61	195249	8 A1.1|8 2.5 cM	0.03327	0.02299

Table C.6 Genes specifically downregulated in corneal peripheral basal epithelial cells. The table includes gene symbols, names, fold changes, Welch's t-test *p*-values, unigene ID and chromosomal location of each gene.

Gene Symbol	Gene name	Fold change to		Unigene ID	ChroLocn	Welch's p-value	
		Limbus	Periphery			C-L	C-P
Slc13a2	solute carrier family 13 (sodium-dependent dicarboxylate transporter), member 2	-3.12	-1.5	20500	11 B5|11 45.03 cM	0.01925	0.01000
Col1a2	procollagen, type I, alpha 2	-2.69	-2.92	12843	6 A1|6 0.68 cM	0.04138	0.05391
Igfbp4	insulin-like growth factor binding protein 4	-3.75	-2.55	16010	11 D	0.01599	0.00887
Pcolce	procollagen C-proteinase enhancer protein	-2.11	-1.56	18542	5 G2|5 78.0 cM	0.01507	0.01955

Bibliography and References

Abdul-Manan, N., Aghazadeh, B., Liu, G.A., Majumdar, A., Ouerfelli O., Siminovich, K.A. & Rosen, M.K. (1999) Structure of Cdc42 in complex with the GTPase-binding domain of the 'Wiskott–Aldrich syndrome' protein *Nature* 399, 379 - 383

Adryan B, Schuh R. (2004)Gene-Ontology-based clustering of gene expression data.Bioinformatics. 20(16):2851-2.

Adryan, B., Schuh, R. (2004) Gene-Ontology-based clustering of gene expression data. Bioinformatics. 20(16):2851-2

Ahringer. (2003) Control of cell polarity and mitotic spindle positioning in animal cells. *Current opinion in cell biology* 15:73-81

Ajiro, K., Yoda, K., Utsumi, K., and Nishikawa, Y. (1996) Alteration of cell cycle-dependent histone phosphorylations by okadaic acid. Induction of mitosis-specific H3 phosphorylation and chromatin condensation in mammalian interphase cells. *J. Biol. Chem.* 271, 13197–13201

Alevizos, I., Mahadevappa, M., Zhang, X., Ohyama, H., Kohno, Y., Posner, M., Gallagher, G.T., Varvares, M., Cohen, D., Kim, D., Kent, R., Donoff, R.B., Todd, R., Yung, C.M., Warrington, J.A., Wong, D.T. (2001) Oral cancer in vivo gene expression profiling assisted by laser capture microdissection and microarray analysis. Oncogene 20; 6196–6204

Allen, T.D., Potten, C.S. (1974) Fine structural identiecation and organisation of the epidermal proliferative unit. J Cell Sci 15:291-319

Allis, C.D.(2000) Synergistic coupling of histone H3 phosphorylation and acetylation in response to epidermal growth factor stimulation. *Mol Cell* . 5:905-915.

Alvarez, J.d., Yasui, D.H., Niida, H., Joh, T., Loh, D.Y. and Shigematsu, K. (2000) The MAR-binding protein SATB1 orchestrates temporal and spatial expression of multiple genes during T-cell development. Genes and development 14 (5); 521-535

Barnard, Z., Apel, A.J.G., Harkin, D.G. (2001). Phenotypic analyses of limbal epithelial cell cultures derived from donor corneoscleral rims. Clin. Exp. Ophthalmol. 29, 138–142.

Barrandon, Y., Green, H. (1987).Three clonal types of keratinocyte with different capacities for multiplication. *Proc Natl Acad Sci U S A*. 84(8):2302-6.

Barratt, M. J., Hazzalin, C. A., Cano, E., and Mahadevan, L. C. (1994) Mitogen-stimulated phosphorylation of histone H3 is targeted to a small hyperacetylation-sensitive fraction.*Proc.Natl. Acad. Sci. U. S. A.* 91, 4781–4785

Barrier, A., Lemoine, A., Boelle, P.Y., Tse, C., Brault, D., Chiappini, F., Breittschneider, J., Lacaine, F., Houry, S., Huguier, M. (2005) Colon cancer prognosis prediction by gene expression profiling.Oncogene 24, 6155-6164

Bednarz, J., Herbert, A.W., Rodokanaki, A. v.S., Engelmann, K. (1995) Expression of genes coding growth factors and growth factor receptors in differentiated and de-differentiated human corneal endothelial cells. *Cornea.* 14(4); 372-81

Bertwistle, D., Sugimoto, M. & Sherr, C. J. Physical and functional interactions of the Arf tumour suppressor protein with nucleophosmin/B23.(2004) Mol. Cell. Biol.24; 985–996

Betschinger, J., Knoblich, J. A. (2004) Dare to be different: asymmetric cell division in *Drosophila*, *C. elegans* and vertebrates. *Curr. Biol.* 14: R674–R685

Bhat, M.A., Philp, A.V., Glover, D.M and Bellen, H.J. (1996) Chromatid segregation at anaphase requires the barren product, a novel chromosome-associated protein that interacts with Topoisomerase II. *Cell.* 87:1103–1114

Bhat, M.A., Philp, A.V., Glover, D.M. and Belle, H.J. (1996). Chromatid segregation at anaphase requires the barren product, a novel chromosome associated protein that interacts with Topoisomerase II. *Cell.* 87:1103–1114

Bickenbach J.R. Isolation, characterization, and culture of epithelial stem cells. In: Turksen K, editor. Epidermal cells methods and protocols. Ontario: Humana Press; 2004; p 97-102).

Bickenbach, J.R. (2004). Isolation, characterization, and culture of epithelial stem cells. *Methods Mol. Biol.* 289, 97–102.

Blanc, V., Kennedy, S., Davidson, N.O. (2003)A novel nuclear localization signal in the auxiliary domain of apobec-1 complementation factor regulates nucleocytoplasmic import and shuttling. *J Biol Chem.* 278(42);41198-204.

Blanpain, C., Lowry, W.E., Geoghegan, A., Polak, L. and Fuchs, E. (2004) SelfRenewal,Multipotency, and the existence of two cell populations within an epithelial stem cell niche. *Cell.* 118, 635–648

Bolstad, B., Irizarry, R., Strand, M. AND Speed, T. (2002). A comparison of normalization methods for high density oligonucleotide array data based on variance and bias. *Bioinformatics,* to appear.

Borgne, R., Bellaiche, L.Y. and Schweisguth, F. (2002) Drosophila E-cadherin regulates the orientation of asymmetric cell division in the sensory organ lineage. *Curr Biol* 12: 95-104

Boulton, M., Albon, J. 2004 Stem cells in the eye. *Int J Biochem Cell Biol.* 36(4):643-57

Bradbury, E. M. (1992) Reversible histone modifications and the chromosome cell cycle. *Bioessays* 14, 9–16

Bresters, D., Schipper,M.E.I., Reesink,H.W., Boeser-Nunnink,B.D.M., Cuypers, H.T.M (1994) The duration of fixation influences the yield of HCV cDNA-PCR products from formalin-fixed, paraffin-embedded liver tissue. *J. Virol. Methods*, 48, 267-272.

Britton, R.A., Lin, D.C. and Grossman, A.D. (1998). Characterization of a prokaryotic SMC protein involved in chromosome partitioning. *Genes Dev.* 12:1254–1259.

Burbelo, P. D., Drechsel, D. & Hall, A. (1995)A conserved binding motif defines numerous candidate target proteins for both Cdc42 and Rac GTPases. *J. Biol. Chem.* 270, 29071-29074

Cai, S., Han, H.J. & T Kohwi-Shigematsu, T. (2003) Tissue-specific nuclear architecture and gene expession regulated by SATB1 *Nature Genetics* 34, 42 - 51

Cairns, J. (1975): Mutation selection and the natural history of cancer. Nature 255:197-200, 1975

Cavalli, G., Paro, R. (1998)The *Drosophila* Fab-7 chromosomal element conveys epigenetic inheritance during mitosis and meiosis. *Cell* 1998, **93**:505 518.

Cayouette, M., Raff, M. (2002) Asymmetric segregation of Numb: a mechanism for neural specification from *Drosophila* to mammals. Nat Neurosci.2002;5:1265-1269.

Celli, J., Duijf, P., Hamel, B.C., Bamshad, M., Kramer, B., Smits, A.P., Newbury-Ecob, R., Hennekam, R.C., Van Buggenhout, G., van Haeringen, A., Woods, C.G., van Essen, A.J., de Waal, R., Vriend, G., Haber, D.A., Yang, A., McKeon, F., Brunner, H.G., van Bokhoven, H. Heterozygous germline mutations in the p53 homolog p63 are the cause of EEC syndrome. (1999). *Cell* 99 (2); 143-153

Celso, C.L., Prowse, D.M. and Watt, F.M. (2004) Transient activation of b-catenin signalling in adult mouse epidermis is sufficient to induce new hair follicles but continuous activation is required to maintain hair follicle tumours. *Development* 131; 1787-1799

Chaloin-Dufau, C., Sun, T. T., & Dhouailly, D. (1990). Appearance of the keratin pair K3/K12 during embryonic and adult corneal epithelial differentiation in the chick and rabbit. *Cell Differentiation and Development*, *32*, 97–108.

Chen, D., Ma, H., Hong, H., Koh, S.S., Huang, S.M., Schurter, B.T., Aswad, D.W., and Stallcup, M.R. (1999). Regulation of transcription by a protein methyltransferase. *Science* 284: 2174-2177

Chen, J.J., Tseng, S.C., (1990). Corneal epithelial wound healing in partial limbal deficiency. Invest. Ophthalmol. Vis. Sci. 31, 1301–1314.

Chen, J.J.Y., Tseng, S.C (1991).Abnormal corneal epithelial wound healing in partial thickness removal of limbal epithelium *IOVS* 32:2219-33

Chen, Z., de Paiva, C.S., Luo, L., Kretzer, F.L., Pflugfelder, S.C., Li, D.-Q. (2004). Characterization of putative stem cell phenotype in human limbal epithelia. Stem Cells 22, 355–366.

Chenn, A., McConnell, S.K.(1995) Cleavage orientation and the asymmetric inheritance of Notch1 immunoreactivity in mammalian neurogenesis. Cell. 82;631–641.

Chester, A., Somasekaram, A., Tzimina, M., Jarmuz, A., Gisbourne, J., O'Keefe, R., Scott, J., Navaratnam, N. (2003)The apolipoprotein B mRNA editing complex performs a multifunctional cycle and suppresses nonsense-mediated decay. *EMBO J.* 22(15);3971-82.

Cheung, P., Allis, C. D., and Sassone-Corsi, P. (2000) Signaling to chromatin through histone modifications. *Cell* 103, 263–271

Cheung, P., Tanner, K.G., Cheung, W.L., Sassone-Corsi, P., Denu, J.M., Allis, C.D. (2000) Synergistic coupling of histone H3 phosphorylation and

acetylation in response to epidermal growth factor stimulation. *Mol Cell* 2000, 5:905-915.

Christophers, E. (1970). Eine neue Methode zur Darstellung des Stratum Corneum. *Arch.klin. exp. Derm.* **237,** 712-721.

Christophers, E. (1971) Cellular architecture of the stratum corneum. J Invest Derm 56:165- 169

Christophers, E. (1971a). Cellular architecture of the Stratum corneum. *J. invest. Derm.* 56,165-169.

Christophers, E. (1971b). The architecture of the Stratum corneum after wounding. *J. invest.Derm.* 57, 241-246.

Christophers, E. (1971c). The columnar structure of the epidermis: Possible mechanism of differentiation. *Z. Zellforsch. mikrosk. Anat.* **114,** 441-447.

Chung, E.-H., DeGregorio, P.G., Wasson, M., Zieske, J.D. (1995). Epithelial regeneration after limbus-to-limbus debridement. Expression of a-enolase in stem and transient amplifying cells. Invest. Ophthalmol. Vis. Sci. 36, 1336–1343.

Claudinot, S., Nicolas, M., Oshima, H., Rochat, A., Barrandon, Y. (2005). *Long-term renewal of hair follicles from clonogenic multipotent stem cells.* PNAS. 102 (41):14677–14682.

Clausen, O.P.F., Aarnaes, E., Kirkhus, B., Pedersen, S., Thorud, E., Bolund, L. (1984) Subpopulations of slowly cycling cells in S and G2 phase in mouse epidermis..*Cell Tiss.Kin.*17:351-365

Clayton, A. L., Rose, S., Barratt, M. J., and Mahadevan, L. C. (2000) Phosphoacetylation of histone H3 on c-fos- and c-jun-associated nucleosomes upon gene activation*EMBO J.*19, 3714–3726

Collinson, J.M., Morris, L., Reid, Al.(2002) Clonal analysis of patterns of growth, stem cell activity and cell movement during the development and maintenance of the murine corneal epithelium. *Dev Dyn*;224:432–440.

Colombo, E., Marine, J. C., Danovi, D., Falini, B., Pelicci, P. G. (2002) Nucleophosmin regulates the stability and transcriptional activity of p53. Nature Cell Biol. 4; 529–533

Cornic M, Guidez F, Delva L, Agadir A, Degos L, Chomienne C (1992) Mechanism of action of retinoids in a new therapeutic approach to acute promyelocytic leukaemia. *Bull Cancer.* 79(7):697-704

Cotsarelis, G., Cheng, S.Z., Dong, G., Sun, T.T., Lavker, R.M. (1989) Existance of slow-cycling limbal epithelial basal cells that can be preferentially stimulated to proliferate: Implications on epithelial stem cells. *Cell* 57; 201-209.

Cotsarelis, G., Sun, T.-T., Lavker, R.M. (1990). Label-retaining cells reside in the bulge of the pilosebaceous unit: implications for follicular stem cells, hair cycle, and skin carcinogenesis. Cell 61; 1329–1337.

Cowan, C. R., Hyman, A. A. (2004)Asymmetric cell division in *C. elegans*: cortical polarity and spindle positioning. *Annu. Rev. Cell Dev. Biol.* 20: 427–453.

Cubizolles, F., Legagneux, V., Le Guellec, R., Chartrain, I., Uzbekov, R., Ford, C. and Le Guellec, K.. (1998). pEg7, a new xenopus protein required for mitotic chromosome condensation in egg extracts. *J. Cell Biol.* 143:1437–1446.

Davanger, M., Evensen, A. (1971).Role of the pericorneal papillary structure in renewal of corneal epithelium. *Nature.*229;560-561.

De Luca, L.M., Shores, R.L., Spangler, E.F. and Wenk, M.L. (1989) Inhibition of initiator-promoter-induced skin tumorigenesis in female SENCAR mice fed a vitamin A-deficient diet and reappearance of tumors in mice fed a diet adequate in retinoid or beta-carotene. Cancer Research. 49 (19) 5400-5406

De Paiva, C.S., Chen, Z., Corrales, R.M., Pflugfelder, S.C., Li, D.Q. (2005). ABCG2 transporter identifies a population of clonogenic human limbal epithelial cells. Stem Cells 23, 63–73.

Dong, Y., Roos, M., Gruijters, T., Donaldson,P.,Bullivant, S., Beyer, E. and Kistler, J. (1994).Differential expression of two gap junction proteins in corneal epithelium. *Eur.J.Cell Biol.* 64:95-100

Dua, H.S. (1995) Stem cells of the ocular surface: scientific principles and clinical applications. *Br. J. Ophth.* 79(11);968-969.

Dua, H.S. (1998).The conjuctiva in corneal epithelial wound healing. *Br.J.Opht.*82:1407-1411.

Dua, H.S., Azura-Blanco, A. (2000). Limbal stem cells of the corneal epithelium. *Surv. Of Ophth.* 44(5): 415-425.

Dua, H.S., Forrester, J.V. (1990)The corneoscleral limbus in human epithelial wound healing.*Am. J. Ophth.*110:646-656.

Dua, H.S., Gomes, J.A.P., Singh (1994) Corneal epithelial wound healing *Br.J.Opth.*78; 401-408

Dua, H.S., Joseph, A., Shanmuganathan, V.A., Jones, R.E. (2003). Stem cell differentiation and the effects of deficiency. Eye 17, 877–885.

E. M., and Roberge, M. (1995) Chromosome condensation induced by fostriecin does not require p34cdc2 kinase activity and histone H1 hyperphosphorylation, but is associated with enhanced histone H2A and H3 phosphorylation. *EMBO J.* 14, 976–985

Ebato B., Friend J., Thoft R.A. Comparison of limbal and peripheral human corneal epithelium in tissue culture. (1988)*IOVS* 29 1533-1537.

Eberharter, A and Becker, P.B., (2002)Histone acetylation: a switch between repressive and permissive chromatin *EMBO Reports* 3(3); 224-229

Eberwine, J., Yeh, H., Miyashiro, K., Cao, Y., Nair, S., Finnell, R., Zettel, M., Coleman, P.(1992) Analysis of gene expression in single live neurons. *Proc Natl Acad Sci U S A.* 89:3010-3014

Elgin, S.C. (1996) Heterochromatin and gene regulation in *Drosophila. Curr Opin Genet Dev.* **6**:193-202.

Emmert-Buck, M.R., Bonner, R.F., Smith, P.D.(1996) Laser capture microdissection. *Science.* **274;** 998–1001.

Ercolani, L., Florence, B., Denaro, M., Alexander, M. (1988) Isolation and complete sequence of a functional human glyceraldehyde-3-phosphate dehydrogenase gene. *J Biol Chem.* 263(30):15335-41

Etienne-Manneville and Hall, A. (2003) Cdc42 regulates GSK-3β and adenomatous polyposis coli to control cell polarity *Nature* 421; 753 - 756

Falini, B., Mecucci, C., Tiacci, E., Alcalay, M., Rosati, R., Pasqualucci, L., La Starza, R., Diverio, D., Colombo, E., Santucci, A., Bigerna, B., Pacini, R., Pucciarini, A., Liso, A., Vignetti, M., Fazi, P., Meani, N., Pettirossi, V., Saglio, G., Mandelli, F., Lo-Coco, F., Pelicci, P.G., Martelli, M.F.; GIMEMA Acute Leukemia Working Party. (2005) Cytoplasmic nucleophosmin in acute myelogenous leukemia with a normal karyotype. *N. Engl. J. Med.* 352; 254—266

Fend F, Emmert-Buck MR, Chuaqui R, Cole, K., Lee, J., Liotta, L.A., Raffeld, M. (1999) Immuno-LCM: laser capture microdissection of immunostained frozen sections for mRNA analysis. *Am J Pathol* . 154; 61–66.

Festing, M.F.W., Blackmore, D.K.(1971) Life span of specified-pathogen-free (MRC category 4) mice and rats. Lab Anim 5:179–192

Finke, J., Fritzen,R., Ternes,P., Lange,W. and Dölken,G (1993) An improved strategy and a useful housekeeping gene for RNA analysis from formalin-fixed, paraffin-embedded tissues by PCR. *BioTechniques*, 14, 448-453.

Fisher, G.J., Reddy, A.P., Datta, S.C., Kang, S., Yi, J.Y., Chambon, P.,

Voorhees, J.J. (1995) .All-trans retinoic acid induces cellular retinol-binding protein in human skin in vivo. J Invest Dermatol. 105(1):80-6.

Fisher, G.J., Reddy, A.P., Datta, S.C., Kang, S., Yi, J.Y., Chambon, P., Voorhees, J.J. (1995) All-trans retinoic acid induces cellular retinol-binding protein in human skin in vivo. *J Invest Dermatol.*105(1):80-6.

Fodor, S. P. A., Read, J. L., Pirrung , M. C., Stryer, L., Tsai Lu, A. and Solas, D. (1991) Light-directed, spatially addressable parallel chemical synthesis. *Science.* 251(4995);767-73

Foreman, D.M., Pancholi, S., Jarvis-Evans, J. McLeod, D., Boulton, .M.E. (1996) A simple organ culture model for assessing the effects of growth factors on corneal re-epithelialisations. *Exp. Eye. Res.* 62;555-564.

Forslund, K.O. and Nordqvist, K. (2001) The Melanoma Antigen Genes—Any Clues to Their Functions in Normal Tissues? Experimental Cell Research. 265(2);185-194

Freeman, L., Aragon-Alcaide, L. and Strunnikov, A. (2000) The Condensin Complex Governs Chromosome Condensation and Mitotic Transmission of rDNA The Journal of Cell Biology.149 (4)811–824

Fuchs, E., Green, H., (1981) Regulation of terminal differentiation of cultured human keratinocytes by Vitamin A. *Cell.* 25 (3):617-625.

Fukui, T., Kondo, M., Ito, G., Maeda, O., Sato, N., Yoshioka, H., Yokoi, K., Ueda, Y., Shimokata, K., Seki, Y. (2005) Transcriptional silencing of secreted

frizzled related protein 1 (SFRP1) by promoter hypermethylation in non-small-cell lung cancer Oncogene 24, 6323-6327

Gachon, F., Fonjallaz' P., Damiola, F., Gos, P., Kodama, T., Zakany, J., Duboule, D., Petit, B., Tafti' M., Schibler, U. (2004). The loss of circadian PAR bZip transcription factors results in epilepsy. *Genes & Development* 18;1397-1412

Galvin, S., Loomis, C., Manable, M., Dhouailly, D., Sun, T.T. (1989) The major pathways of keratinocyte differentiation as defined by keratin expression: an overview..*Adv.Dermatol.*4;277-299

Gambardella, L., and Barrandon,Y. (2003)The multifaceted adult epidermal stem cell.Current Opinion in Cell Biology 15:771–777

Garcia, V., Furuya, K., Carr, A.M. (2005) Identification and functional analysis of TopBP1 and its homologs. *DNA Repair* (Amst) (e publication ahead of print)

Garrard, S.M., Capaldo, C.T., Gao, L., Rosen, M.K., Macara, I.G. and Tomchick, D.R. (2003) Structure of Cdc42 in a complex with the GTPase-binding domain of the cell polarity protein, Par6*The EMBO Journal* 22; 1125–1133,

Giagounidis, A. A. N., Germing, U., Haase, S., Hildebrandt, B., Schlegelberger, B., Schoch, C., Wilkens, L., Heinsch, M., Willems, H., Aivado, M., Aul, C. (2004). Clinical, morphological, cytogenetic, and

prognostic features of patients with myelodysplatic syndromes and del(5q) including band

Gipson, I.K., Spurr-Michaud, S.J., Tisdale, A.S. (1987).Anchoring fibrils form a complex network in human and rabbit cornea. *IOVS* 28:212

Glanzer, J.G., Eberwine, J.H. (2004) Expression profiling of small cellular samples in cancer: less is more British Journal of Cancer 90; 1111-1114

Goldstein SR, McQueen PG, Bonner RF. (1998) Thermal modeling of laser capture microdissection. *Appl Opt.* 37; 7378–7391

Goodell, M.A., McKinney-Freeman, S., Camargo, F.D. (2004). Isolation and characterization of side-population cells. Methods Mol. Biol. 290, 343–352.

Goodrick, C.L.(1975) Life span and the inheritance of longevity of inbred mice. J Gerontol 30:257–263

Graumann, P.L., Losick, R. and Strunnikov, A.V. (1998). Subcellular localization of *Bacillus subtilis* SMC, a protein involved in chromosome condensation and segregation. *J. Bacteriol.* 180:5749–5755.

Graumann, P.L., R. Losick, and A.V. Strunnikov. (1998). Subcellular localization of *Bacillus subtilis* SMC, a protein involved in chromosome condensation and segregation. *J. Bacteriol.* 180:5749–5755.

Graven KK Yu, Q., Pan, D., Roncarati, J.S., Farber, H.W. (1999) Identification of an oxygen responsive enhancer element in the glyceraldehyde-3-phosphate dehydrogenase gene.Biochim Biophys Acta. 1447(2-3);208-18

Grewal, S.I., Klar, A.J.(1996) Chromosomal inheritance of epigenetic states in fission yeast during mitosis and meiosis. *Cell.* 86:95-101.

Grisendi, S. & Pandolfi, P. P. (2005).NPM mutations in acute myelogenous leukemia. *N. Engl. J. Med.* 352, 291–292

Grueterich, M., Espana, E.M., Tseng, S.C.G. (2003). Ex vivo expansion of limbal epithelial stem cells: amniotic membrane serving as a stem cell niche. Surv. Ophthalmol. 48, 631–646

Guacci, V., Koshland, D. and Strunnikov, A. (1997). A direct link between sister chromatid cohesion and chromosome condensation revealed through the analysis of MCD1 in *S. cerevisiae. Cell* 91,47 -57.

Guo, J., Sax, C.M., Piatigorsky, J., Xu, F.X. (1997). Heterogenous expression of transketolase in ocular tissues. Curr. Eye Res. 16, 467–474.

Guo, X. W., Th'ng, J. P., Swank, R. A., Anderson, H. J., Tudan, C., Bradbury, Gurley, L. R., D'Anna, J. A., Barham, S. S., Deaven, L. L., and

Tobey, R. A. (1978) Histone phosphorylation and chromatin structure during mitosis in Chinese hamster cells. *Eur J Biochem.* 84(1);1–15

Gurley, L. R., Walters, R. A., and Tobey, R. A. (1973) Histone phosphorylation in late interphase and mitosis *Biochem. Biophys. Res. Commun.* 50, 744–750

Haan, G., Nijhof, W., Van Zant, G. (1997) Mouse strain-dependent changes in frequency and proliferation of hematopoietic stem cells during aging: Correlation between lifespan and cycling activity. Blood 89:1543–1550

Hall, A. Rho GTPases and the actin cytoskeleton. *Science* 279, 509-514 (1998)

Hall, P.A., Watt, F.M. (1989) Stem cells: the generation and maintenance of cellular diversity. Development 109; 619-623

Hanada, K.; Kumagai, K.; Yasuda, S.; Miura, Y.; Kawano, M.; Fukasawa, M.; Nishijima, M. (2003) Molecular machinery for non-vesicular trafficking of ceramide. *Nature* 426: 803-809, 2003

Hanna, M. C., Turner, A. J., Kirkness, E. F. (1997). Human pyridoxal kinase: cDNA cloning, expression, and modulation by ligands of the benzodiazepine receptor. *J. Biol. Chem.* 272; 10756-10760

Hashimoto, T., Dykes, P.J., Marks, R. (1985) Retinoic acid-induced inhibition of growth and reduction of spreading of human epidermal cells in culture. *Br.J.Dermat.*112;637

Hashimoto, T., Dykes, P.J., Marks, R. (1985) Retinoic acid-induced inhibition of growth and reduction of spreading of human epidermal cells in culture. *Br.J.Dermat.*112:637

Hayashi, K., Kenyon, K.R. (1988). Increased cytochrome oxidase activity in alkali-burned corneas. Curr. Eye Res. 7, 131–138.

Heck, M. M. S., Hittelman, W. N., and Earnshaw, W. C. (1989) In vivo phosphorylation of the 170-kDa form of eukaryotic DNA topoisomerase II. Cell cycle analysis *J. Biol. Chem.* 264, 15161–15164

Heck, M.M., Hittelman, W.N., Earnshaw, W.C.(1989) In vivo phosphorylation of the 170-kDa form of eukaryotic DNA topoisomerase II. Cell cycle analysis. J Biol Chem. 264(26):15161-4

Hendzel, M. J., Wei, Y., Mancini, M. A., Van Hooser, A., Ranalli, T., Brinkley, B. R., Bazett-Jones, D. P., and Allis, C. D. (1997) Mitosis-specific phosphorylation of histone H3 initiates primarily within pericentromeric heterochromatin during G2 and spreads in an ordered fashion coincident with mitotic chromosome condensation. *Chromosoma* 106, 348–360

Hennig, S., Groth, D., Lehrach, H. (2003) Automated Gene Ontology annotation for anonymous sequence data. *Nucleic Acids Res.* 31(13); 3712-5.

Hennig, W.(1999) Heterochromatin. *Chromosoma.*108:1-9.

Hingorani, K., Szebeni, A. & Olson, M. O. (2000) Mapping the functional domains of nucleolar protein B23. J. Biol. Chem. 275, 24451—24457

Hirakata, A., Gupta, A.G., Proia, A.D. (1992) Effect of protein Kinase C Inhibitors and Activators and corneal re-epithelialisation in the rat. *IOVS*, 34;216-221.

Hirakata, A., Gupta, A.G., Proia. (1992) Effect of protein Kinase C Inhibitors and Activators an corneal re-epithelialisation in the rat. (1992) *IOVS*, 34:216-221.

Hirano, M., and Hirano, T. (1998). ATP-dependent aggregation of singlestranded DNA by a bacterial SMC homodimer. *EMBO (Eur. Mol. Biol. Organ.) J.* 17:7139 7148

Hirano, T., and T. Mitchison. (1994). A heterodimeric coiled-coil protein required for mitotic chromosome condensation in vitro. *Cell.* 79:449–458.

Hirano, T., Kobayashi, R. and Hirano, M. (1997). Condensins, chromosome condensation protein complexes containing XCAP-C, XCAP-E and a *Xenopus* homolog of the *Drosophila* Barren protein. *Cell.* 89:511–521.

Hirate, J., Nakagoshi, H., Nabeshima, Y., Matsuzaki, F. (1995) Asymmetric segregation of the homeodomain protein Prospero during *Drosophila* development. Nature. 1995;377:627–630.

Ho A.D. (2005) Kinetics and symmetry of divisions of hematopoietic stem cells. Experimental Hematology 33 (2005) 1–8

Hogan, W., J. Alvarado, and J. Weddell. (1971). Histology of the Human Eye. Saunders, Philadelphia

Hoheusel, J.D.(1997). *Trends in Biotechn.* 15:465-472 (removed temporarily)

Holland, E.J., Schwartz, G.S. (1996). The evolution of epithelial transplantation for severe ocular surface disease and a proposed classification system. Cornea 15, 549–556.

Hsu, J.Y., Sun, Z.W., Li, X., Reuben, M., Tatchell, K., Bishop, D.K., Grushcow, J.M., Brame, C.J., Caldwell, J.A., Hunt, D.F., Lin, R., Smith, M. M., and Allis, C. D. (2000). Mitotic phosphorylation of histone H3 is governed by Ipl1/aurora kinase and Glc7/PP1 phosphatase in budding yeast and nematodes. *Cell* 102: 279-291

Hsueh, Y.-J., Wang, D.-Y., Cheng, C.-C., Chen, J.-K. (2004). Age-related expressions of p63 and other keratinocyte stem cell markers in rat cornea. J. Biomed. Sci. 11, 641–651.

Huang, A.J.W., Tseng S.C. (1991) Corneal epithelial wound healing in the absence of limbal epithelium. *IOVS* 32;96-105

Iismaa, S.E. (2000) GTP binding and signaling by G_h/transglutaminase II involves distinct residues in a unique GTP-binding pocket. *J. Biol. Chem.* 275;18259-18265.

Irizzary, R., Hobbs, B., Collin, F, Beazer-Barclay, Y, Amtonellis, K.J., Scherph, U., Speed, T. Exploration, (2003) Normalization, and summaries of high density oligonucleotide array probe level data. *Biostatistics*, 4, (2); 249–264

Irwin, M.S., Kaelin, W.G. (2001) p53 Family Update: p73 and p63 Develop Their Own Identities. *Cell Growth Differ* 12(7):337-349

Irwin, M.S., Kaelin, W.G.Jr. (2001) Role of the newer p53 family proteins in malignancy.. *Apoptosis* 6(1-2); 17-29

Irwin, M.S., Kondo, K., Marin, M.C., Cheng, L.S., Hahn, W.C., Kaelin, W.G. Jr . (2003) Chemosensitivity linked to p73 function. Cancer Cell. 3 (4):403-10.

Ivanova, N.B., Dimos, J.T., Schaniel, C., Hackney, J.A., Moore, K.A., Lemischka, I.R. (2002) A stem cell molecular signature. Science. 18;298(5593):601-4.

Iwama, A., Oguro, H., Negishi, M., Kato, Y., Morita, Y., Tsukui, H., Ema, H., Kamijo, T., Katoh-Fukui, Y., Koseki, H., van Lohuizen, M., Nakauchi, H. (2004). Enhanced self-renewal of hematopoietic stem cells mediated by the polycomb gene product Bmi-1.Immunity. 21(6):843-51.

Jensen, P.K.A., Pedersen S., Bolund, L. (1985) Basal-cell subpopulations of slowly cycling cells in S and G2 phase in mouse epidermis. *Cell Tiss.Kin.*18;201-215.

Jessberger, R., Riwar, B., Baechtold, H. and Akhmedov, A. T. (1996) SMC proteins constitute two subunits of the mammalian recombination complex RC-1. *EMBO J.* 15,4061 -4068.

Joyce, N.C., Meklir, B., Joyce, S.J., Zieske,J.D. (1996) Cell cycle protein expression and proliferative status in human corneal cells..*IOVS.*37:645-655.

Joyce, N.C., Zieske, J.D., .(1997)Transforming growth factor-β receptor Expression in Human Cornea. *IOVS.* 38;1922-1928.

Karpen, G.H. (1994) Position-effect variegation and the new biology of heterochromatin. *Curr Opin Genet Dev*, 4:281-291.

Karthikeyan, S., Zhou, Q., Mseeh, F., Grishin, N.V., Osterman, A.L., Zhang, H.(2003). Crystal structure of human riboflavin kinase reveals a beta barrel fold and a novel active site arch. *Structure*. 3; 265-73.

Kasper, M. (1992). Patterns of cytokeratins and vimentin in guinea pig and mouse eye tissue: evidence for regional variations in intermediate filament expression in limbal epithelium. Acta Histochem. 93, 319–332.

Kasper, M., Moll, R., Stosiek, P., Karsten, U. (1988). Patterns of cytokeratin and vimentin expression in the human eye. Histochemistry 89, 369–377.

Kasper, M., Moll, R., Stosiek, P., Karsten, U. (1988). Patterns of cytokeratin and vimentin expression in the human eye. Histochemistry 89, 369–377.

Katayama I., OtoyamaK., Yokozeki H., Nishioka K. (1994) Retinoic acid upregulates c-kit ligand production by murine keratinocyte, in vitro and increases cutaneous mast cell in vivo. *J. Dermatol. Sci.* 9; 27-35

Kays, W.T., Piatigorsky, J. (1997).Aldehyde dehydrogenase class 3 expression: Identification of a cornea-preferred gene promoter in transgenic mice. *PNAS*.94;13594-13599

Kenyon K.R., Tseng S.C. (1989) Limbal autograft transplantation for ocular surface disorders. Ophthalmology 98:709-22

Kenyon, K.R. (1979) Anatomy and pathology of the ocular surface (In Thoft and Boston Little and Brown,:pp3-36 as cited in Corneal Wound healing by Boulton, M.

Kielman, M.F., Rindapää1, M., Gaspar, C., van Poppel, N., Breukel, C., van Leeuwen, S., Taketo, M.M, Roberts, S., Smits, R. & Fodde, R. (2002) *Apc* modulates embryonic stem-cell differentiation by controlling the dosage of β-catenin signaling Nature genetics 32; 594-605

Kim, J.C., Park, G.S., Kim, J.K., Kim, Y.M.(2002).The Role of Nitric Oxide in Ocular Surface Cells. *J Korean Med Sci; 17: 389-94*

Kimura, K., and Hirano, T. (1997). ATP-dependent positive supercoiling of DNA by 13S condensin: a biochemical implication for chromosome condensation. *Cell.* 90:625–634.

Kimura, K., Hirano, M., Kobayashi, R., and Hirano, T. (1998) Phosphorylation and activation of 13S condensin by Cdc2 in vitro. *Science* 282, 487–490

Kimura, K., Rybenkov, V.V., Crisona, N.J., Hirano, T. and Cozzarelli, N.R. (1999) 13S condensin actively reconfigures DNA by introducing global positive writhe: implications for chromosome condensation. *Cell.* 98:239–248.

Kinoshita s., Friend J., Thoft A. (1983) Biphasic cell proliferation in transdifferentiation of conjunctival to corneal epithelium in rabbits. *IOVS.* 24:1008-1014

Kiritoshi, A., SundarRaj, N., Thoft, R.A. (1991). Differentiation in cultured limbal epithelium as defined by keratin expression. Invest. Ophthalmol. Vis. Sci. 32, 3073–3077

Kobayashi, K., Nishioka, M., Kohno, T., Nakamoto, M., Maeshima, A., Aoyagi, K., Sasaki, H., Takenoshita, S., Sugimura, H., Yokota, J. (2004) Identification of genes whose expression is upregulated in lung adenocarcinoma cells in comparison with type II alveolar cells and bronchiolar epithelial cells in vivo Oncogene 23, 3089-3096

Kobayashi, M., Taniura, M. and Yoshikawa, K. (2002) Ectopic Expression of Necdin Induces Differentiation of Mouse Neuroblastoma Cells* J. Biol. Chem., 277 (44); 42128-42135

Koizumi, N., Inatomi, T., Suzuki, T., Sotozono, C., Kinoshita, S., (2001). Cultivated corneal epithelial stem cell transplantation in ocular surface disorders. Ophthalmology 108, 1569–1574.

Kolega, J., Manabe M., Sun, T.T. (1989) Basement membrane heterogeneity and variation in corneal epithelial differentiation. *Differentiation.*42;54-63

Kolesnichenko, T.S., Popova, N.V. (1979) Growth-stimulating effect of some nitroso-compounds on organ cultures of embryonic liver of mice and rats. Bull Exp Biold Med 12:716–719

Kolodka TM, Garlick JA, Taichman LB: Evidence for keratinocyte stem cells in vitro: long term engraftment and persistence of transgene expression from retrovirustransduced keratinocytes. Proc Natl Acad Sci USA 95:4356-4361

Kondo, T., Minamino, N., Nagamura-Inoue, T., Matsumoto, M., Taniguchi, T., Tanaka, N. (1997) Identification and characterization of nucleophosmin/B23/ numatrin which binds the anti-oncogenic transcription factor IRF-1 and manifests oncogenic activity. Oncogene 15; 1275—1281

Korinek, V., Barker, N., Moerer, P., Van Donselaar, E., Huls, G., Peters, P. & Clevers, H. (1998) Depletion of epithelial stem-cell compartments in the small intestine of mice lacking Tcf-4 *Nature Genetics* 19, 379 - 383

Koshland, D., and A. Strunnikov. 1996. Mitotic chromosome condensation. *Annu. Rev. Cell Dev. Biol.* 12:305–333.

Kruse FE, Tseng SC. (1994) Retinoic acid regulates clonal growth and differentiation of cultured limbal and peripheral corneal epithelium. *Invest Ophthalmol Vis Sci.*35(5):2405-20

Kruse, F.E., Reinhard, T., (2001). Limbal transplantation for ocular surface

Kruse, F.E., Tseng, S.C. (1993) Growth factors modulate clonal growth and differentiation of cultured rabbit limbal and corneal epithelium.*IOVS.*34:1963-

Kruse, F.E., Tseng, S.C. (1993) Serum differentialy modulates clonal growth and differentiation of cultured limbal and corneal epithelium..*IOVS.*34;2976-2982

Kruse,F.E. (1994) Stem cells and corneal epithelial regeneration *Eye* 8;170-183

Kurki, S., Peltonen, K., Latonen, L., Kiviharju, T.M., Ojala, P.M., Meek, D., Laiho, M. (2004) Nucleolar protein NPM interacts with HDM2 and protects tumour suppressor protein p53 from HDM2-mediated degradation. Cancer Cell 5; 465–475

Kurpakus, M.A., Maniaci, M.T., Esco, M.(1994). Expression of keratins K12, K4 and K14 during development of ocular surface epithelium. Çurr. Eye Res. 13, 805–814.

Kurpakus, M.A., Stock, E.L., Jones, J.C. (1990) Expression of the 55- kD/64 kD corneal keratins in ocular surface epithelium. Invest. Ophthalmol. Vis. Sci. 31, 448–456.

Kurse, F.E., Scheffer, C.G., Tseng. (1991) A serum free asssay for limbal, peripheral, and central corneal epithelium. *IOVS.*32(7); 2086-2095

Kurse, F.E., Scheffer, C.G., Tseng. (1991) Growth factors modulate clonal growth and differentiation of cultured rabbit limbal and corneal epithelium. *IOVS.*34;1963-1976

Lai, T.S., Hausladen, A., Slaughter, T.F., Eu, J.P., Stamler, J.S., Greenberg C.S. (2001)Biochemistry Calcium regulates S-nitrosylation, denitrosylation, and activity of tissue transglutaminase 40(16); 4904-4910

Lajtha, L.G. (1967). In canadian cancer conference, pp 31-39. Toronto: Pergamon Press.(in, Stem Cells, Potten(eds),1997, pp1-27.

Lajtha, L.G. (1979) Haemopoietic stem cells: concept and definitions. *Blood Cells* 5 ; 447-455.

Lajtha, L.G. (1979) Stem cell concepts*Differentiation* 14;23-34

Lajtha, L.G. (1979).Stem cell Concepts *Nouv. Rev. Fr. Hematol.*21;59-65

Lauweryns, B., van den Oord, J.J., Missotten, L., (1993b). The transitional zone between limbus and peripheral cornea. An immunohistochemical study. Invest. Ophthalmol. Vis. Sci. 34, 1991–1999.

Lauweryns, B., van der Oord, J. J., De Vos, R., & Missotten, L. (1993a). A new epithelial cell type in the human cornea. *Investigative Ophthalmology & Visual Science*, *34*, 1983–1990.

Lavker, R.M., Dong, G., Cheng, S.Z., Kudoh, K., Cotsarelis, G., Sun, T.T. (1991) Relative proliferative rates of limbal and corneal epithelia. Implications of corneal epithelial migration, circadian rhythm, and suprabasally located DNA synthesizing keratinocytes. Invest. Ophthalmol. Vis. Sci. 32, 1864–1875.

Lavker, R.M., Dong, G., Cheng, S.Z., Kudoh, K., Cotsarelis, G., Sun, T.T., (1991). Relative proliferative rates of limbal and corneal epithelia. Implications of corneal epithelial migration, circadian rhythm, and suprabasally located DNA synthesizing keratinocytes. Invest. Ophthalmol. Vis. Sci. 32, 1864–1875.

Lavker, R.M., Tseng, S.C.G., Sun, T.-T. (2004). Corneal epithelial stem cells at the limbus: looking at some old problems from a new angle. Exp. Eye Res. 78, 433–446.

Lavker, R.M., Wei, Z.-G., Sun, T.-T. (1998). Phorbol ester preferentially stimulates mouse fornical conjunctival and limbal epithelial cells to proliferate in vivo. Invest. Ophthalmol. Vis. Sci. 39, 301–307.

Lavker,R.M., Scheffer C.G. Tseng, Tung-Tien Sun (2004) Corneal epithelial stem cells at the limbus: looking at some old problems from a new angle Experimental Eye Research 78 433–446

Leblond, C.P., Walker, B.E. (1956) Renewal of cell populations. *Physiol Rev.* 36:255–79.

Leblond,C.W. (1981) The life history of cells in renewing systems. *Am.J.Anat.*160;114-158

Lechler, T. and Fuchs, E. (2005) Asymmetric cell divisions promote stratification and differentiation of mammalian skin. Nature. ahead of print doi:10.1038/nature03922

Lee, R., Davison, P., Cintron, C. (1982) The healing non linear non proliferating wounds in rabbit corneas of different ages..*IOVS.* 23 :660-665.

Leethanakul, C., Patel, V., Gillespie, J., Pallente, M., Ensley, J.F., Koontongkaew, S., Liotta, L.A., Emmert-Buck, M., Gutkind, J.S. (2000) Distinct pattern of expression of differentiation and growth-related genes in squamous cell carcinomas of the head and neck revealed by the use of laser capture microdissection and cDNA arrays. Oncogene, 19: 3220–3224

Lehrer, M.S., Sun, T.-T., Lavker, R.M. (1998) Strategies of epithelial repair: modulation of stem cell and transit amplifying cell proliferation. J. Cell Sci. 111; 2867–2875

Levine, A., Topp, W., Vande Woude, G., Watson, J.D. (Eds.), The Cancer Cell: The Transformed Phenotype, Cold Spring Harbor Lab., New York, pp. 169–176.

Levrero, M., De Laurenzi, V., Costanzo, A., Gong, J., Melino, G., Wang, J.Y. (1999) Structure, function and regulation of p63 and p73.*Cell Death Differ* 6(12);1146-53

Li, C. and Wong, W. (2001). Model-based analysis of oligonucleotide arrays: Expression index computation and outlier detection. *Proceedings of the National Academy of Science U S A* 98, 31–36.

Li, D.Q., Lee, S.B., Scheffer, C.G., Tseng, S.C. (1999) Differential expression and regulation of TGF-β1, TGF-β2 , TGF-β3 , TGF-βRI , TGF-βR2, TGF-βRIII in cultured human corneal, limbal, and conjuctival fibroblasts. *Curr. Eye. Re.* 19(2);154-161

Li, D.Q., Scheffer, C.G., Tseng. (1996) Differentialregulation of cytokine and receptor transcript expression in human corneal and limbal fibroblasts by epidermal growth factor, transforming growth factor-α, platelet-derived growth factor B, and Interleukin-1β. *IOVS.* 37;2068-2080

Li, D.Q., Tseng, S.C. (1995) Three patterns of cytokine expression potentially involved in epithelial-fibroblast intercactions of human ocular surface..*J.Cell.Physiol.*163;61-79.

Lichti, U., Weinberg, W.C., Goodman, L., Ledbetter, S., Dooley, T.,Morgan, D., and Yuspa, S.H. (1993). In vivo regulation of murine hair.

Growth: insights from grafting defined cell populations onto nudemice. J. Invest. Dermatol. 101; 124S–129S.

Lieb, J. D., Albrecht, M. R., Chuang, P. T. and Meyer, B. J. (1998). MIX-1: an essential component of the *C. elegans* mitotic machinery executes X chromosome dosage compensation. *Cell* 92,265 -277.

Lindberg, K., Brown, M.E., Chaves, H.V., Kenyon, K.R., Rheinwald, J.G., (1993). In vitro propagation of human ocular surface epithelial cells for transplantation. Invest. Ophthalmol. Vis. Sci. 34, 2672–2679

List, A. F., Vardiman, J., Issa, J. P. & DeWitte, T. M. Myelodysplastic syndromes. Hematology (Am. Soc. Hematol. Educ. Program), 297—317 (2004).

Liu, A., Stadelmann, C., Moscarello, M., Bruck, W., Sobel, A., Mastronardi, F.G., Casaccia-Bonnefil, P. (2005) Expression of stathmin, a developmentally controlled cytoskeleton-regulating molecule, in demyelinating disorders.
J Neurosci.19;25(3):737-47.

Liu, C.Y., Zhu, G., Westerhausen-Larson, A., Converse, R., Kao, C.W., Sun, T.T., Kao, W.W. (1993). Cornea-specific expression of K12 keratin during mouse development. Curr. Eye Res. 12, 963–974.

Liu,S.T., Chan,G.K., Hittle,J.C., Fujii,G., Lees,E. and Yen,T.J. (2003) Human MPS1 kinase is required for mitotic arrest induced by the loss of CENP-E from kinetochores *JOURNAL Mol. Biol. Cell* 14 (4); 1638-1651

Livak, K.J. and T.D. Schmittgen. (2001). Analysis of relative gene expression data using real-time quantitative PCR and the 2(-Delta Delta C(T)) method. *Methods* 25:402-408.

Lockhart, D. J., Dong, H., Byrne, M. C., Folletie, M. T., Gallo, M. V., Chee, M.S.,Mittimann, M., Wang, C., Kobayashi, M., Horton, H. and Brown, E. L. (1996). Expression monitoring by hybridization to high-density oligonucleotide arrays. *Nature Biotechnology* **14**, 1675–1680.

Losada, A., Hirano, M. and Hirano, T. (1998). Identification of Xenopus SMC protein complexes required for sister chromatid cohesion. *Genes Dev.* 12,1986 -1997

Lu¨tjen-Drecoll, E., Steuhl, P., Arnold, W.H., (1982). Morphologische Besonderheiten der Conjunctiva bulbi. In: Marquardt, R. (Ed.), Chronische Conjunctivitis – Trockenes Auge. Springer, Berlin, 25–34.

Luo, L., Salunga, R.C., Guo, H., Bittner, A., Joy, K.C., Galindo, J.E,, Xiao, H., Rogers, K.E., Wan, J.S., Jackson, M.R., Erlander, M.G. (1999) Gene expression profiles of laser-captured adjacent neuronal subtypes. Nat Med. 5:117–122

Luzzi, V., Holtschlag, V., Watson, M.A. (2001) Expression profiling of ductal carcinoma in situ by laser capture microdissection and high density oligonucleotide arrays. *Am J Pathol*, 158; 2005–2010

Ma, X., Bazan, H.E.P. (2000) Increased platelet-Activating factor receptor gene expression by corneal epithelial wound healing. 41;1696-1702.

MacKenzie, I.C. (1970) Relationship between mitosis and the ordered structure of the stratum corneum in mouse epidermis. Nature 226:653-655

Mackenzie, I.C. (1975) Ordered structure of the epidermis. *Journal of Investigative Dermatology*. 65: 45–51.

MacKenzie, I.C.(1997) Retroviral transduction of murine epidermal stem cell demonstrates clonal units of epidermal structure. J Inv Dermatol 109;377-383

Mahadevan, L. C., Willis, A. C., and Barratt, M. J. (1991) Rapid histone H3 phosphorylation in response to growth factors, phorbol esters, okadaic acid, and protein synthesis inhibitors. *Cell* 65, 775–783

Mäkiniemi, M., Hillukkala, T., Tuusa, J.,, Rein, K., Vaara, M., Huang, D., Pospiech, H., Majuri, I., Westerling, T., P. Mäkelä, T, and. Syväoja, J.E. *(2001) BRCT Domain-containing Protein TopBP1 Functions in DNA Replication and Damage Response. J. Biol. Chem. 276 (32), 30399-30406*

Marin, M.C., Kaelin, W.G. Jr. (2000) p63 and p73: old members of a new family. *Biochim Biophys Acta* 1470(3); M93-M100

Marshman, E., Booth, C., Potten, C.S. (2002) Our favourite cell: the intestinal epithelial stem cell. Bioessays 24:91-98

Masuda, N., Ohnishi, T., Kawamoto, S., Monden, M., Okubo, K. Analysis of chemical modification of RNA from formalin-fixed samples and optimization of molecular biology applications for such samples. *Nuc Ac Res*, 4436-4443

Matic, M., Petrov, I.N., Chen, S., Wang, C., Dimitrijevich, S.D., Wolosin, J.M. (1997). Stem cells of the corneal epithelium lack connexins and metabolite transfer capacity. Differentiation 61, 251–260.

McCartney, B.M., McEwen, D.G. and Grevengoed, E. (2001) Drosophila APC2 and Armadillo participate in tethering mitotic spindles to cortical actin. *Nat Cell Biol.* 3: 933-938.

Meyer, B. J. (2000). Sex in the worm: counting and compensating X-chromosome dose. *Trends Genet.* 16,247 -253

Michaelis, C., Ciosk, R. and Nasmyth, K. (1997). Cohesins: chromosomal proteins that prevent premature separation of sister chromatids. *Cell.* 91:35–45.

Michel, M., Torok, N., Godbout, M.J., Lussier, M., Gaudreau, P., Royal, A., Germain, L. (1996). Keratin 19 as a biochemical marker of skin stem cells in vivo and in vitro: keratin 19 expressing cells are differentially localized in function of anatomic sites, and their number varies with donor age and culture stage. J. Cell Sci. 109, 1017–1028.

Mishima T, Hamada T, Ui-Tei K, Takahashi F, Miyata Y, Imaki J, Suzuki H, Yamashita K.(2004).Expression of DDAH1 in chick and rat embryos.*Brain Res Dev Brain Res.* 148(2):223-32.

Miyoshi, Y., Uemura, H., Ishiguro, H., Kitamura, H., Nomura, N., Danenberg, P.V., Kubota, Y. (2005) Expression of thymidylate synthase, dihydropyrimidine dehydrogenase, thymidine phosphorylase, and orotate phosphoribosyl transferase in prostate cancerProstate Cancer and Prostatic Diseases 8, 260-265

Molofsky, A., Pardal, R., Iwashita, T., Park, I.K., Clarke, M.F. and Sean J. Morrison, S.J. (2003) *Bmi-1* dependence distinguishes neural stem cell self-renewal from progenitor proliferation *Nature* 425, 962-967

Molotkov, A., Ghyselinck, N.B., Chambon, P. and Duester, G. (2004) Opposing actions of cellular retinol-binding protein and alcohol dehydrogenase control the balance between retinol storage and degradation *Biochem J.*383(Pt 2): 295–302

Moore, J.E., McMullen, C.B.T., Mahon, G., Adamis, A.P. (2002). The corneal epithelial stem cell. DNA Cell Biol. 21, 443–451.

Morris, R.J., Fischer, S.M., Slaga, T.J.(1985) Evidence that the centrally and peripherally located cells in the murine epidermal proliferative unit are two distinct cell populations. J Invest Derm 34:277-281

Morris, R.J., Potten, C.S. (1994) Slowly cycling (label-retaining) epidermal cells behave like clonogenic stem cells in vitro. Cell Prolif 27:279-289

Morris, R.J., Potten, C.S. (1994) Slowly cycling (label-retaining) epidermal cells behave like clonogenic stem cells in vitro. *Cell Proliferation* 27(5): 279-289.

Morris, S. W. Kirstein, M.N., Valentine, M.B., Dittmer, K.G., Shapiro, D.N., Saltman, D.L., Look, A.T. (1994) Fusion of a kinase gene, ALK, to a nucleolar protein gene, NPM, in non Hodgkin's lymphoma. *Science* 263; 1281–1284

Mukhopadhyay D, Anant S, Lee RM, Kennedy S, Viskochil D, Davidson NO. (2002).C-->U editing of neurofibromatosis 1 mRNA occurs in tumors that express both the type II transcript and apobec-1, the catalytic subunit of the apolipoprotein B mRNA-editing enzyme. *Am J Hum Genet.* 70(1);38-50

Muller LJ, Vrensen GF, Pels L, Cardozo BN, Willekens B. (1997) Architecture of human corneal nerves. Invest Ophthalmol Vis Sci. 38(5):985-94.

Muller, L., Pels, L., Vrensen, G. (1996) Ultrastructural organisation of the human corneal nerves. *IOVS.* 37:476-488.

Murnion, M.E., Adams, R.R., Callister, D.M., Allis, D., Earnshaw, W.C., Swedlow, J.R. (2001). Chromatin-associated Protein Phosphatase 1

Regulates Aurora-B and Histone H3 Phosphorylation. *JBC*. 276 (28); 26656–26665.

Murthy, S.N.P., Lomasney, J.W., Mak, E.C., Lorand, L. (1999) Interactions of G(h)/transglutaminase with phospholipase Cδ1 and with GTP *Proc.Nat.Acad Scie. USA* 96(21);11815-11819

Napoli, J. L. (1999) Interactions of retinoid binding proteins and enzymes in retinoid metabolism. *Biochim. Biophys. Acta*. 1440:139–162.

Nathan, C., Sporn, M. (1991) Cytokines in context. *J.Cell.Biol.*113:981-986

Nehls, M., Pfeifer, D., Schorpp, M., Hedrich, H., and Boehm, T. (1994). New member of the winged-helix protein family disrupted in mouse and rat nude mutations. Nature 372; 103–107.

Nguyen CT, Weisenberger DJ, Velicescu M, Gonzales FA, Lin JC, Liang G, Jones PA. (2002)Histone H3-lysine 9 methylation is associated with aberrant gene silencing in cancer cells and is rapidly reversęd by 5-aza-2'-deoxycytidine. Cancer Res. 62(22);6456-61.

Nguyen, C.T., Weisenberger, D.J., Velicescu, M., Gonzales, F.A., Lin, J.C., Liang, G., Jones, P.A. (2002) Histone H3-lysine 9 methylation is associated with aberrant gene silencing in cancer cells and is rapidly reversed by 5-aza-2'-deoxycytidine. Cancer Res.;62(22):6456-61.

Ohyama, H., Zhang, X., Kohno, Y., Alevizos, I., Posner, M., Wong, D.T., Todd, R. (2000) Laser capture microdissection-generated target sample for highdensity oligonucleotide array hybridization. *Biotechniques*, 29: 530–536

Okuda, M., Horn, H.F., Tarapore, P., Tokuyama, Y., Smulian, A.G., Chan, P.K., Knudsen, E.S., Hofmann, I.A., Snyder, J.D., Bove, K.E., Fukasawa, K. (200) Nucleophosmin/B23 is a target of CDK2/cyclin E in centrosome duplication. *Cell* 103; 127–140

Olney, H. J. & Le Beau, M. M. in The Myelodysplastic Syndromes, Pathobiology and Clinical Management (ed. Bennet, J. M.) 89—120 (Marcel Dekker, New York, 2002).

P. Gonczy. (2002) Mechanisms of spindle positioning: Focus on flies and worms. *Trends Cell Biol.* 12: 332-339 .

Pancholi, V., (2001). Multifunctional a-enolase: its role in diseases. Cell. Mol. Life Sci. 58, 902–920.

Park, Y.N., Abe,K., Li,H., Hsuih,T., Thung,S.N. and Zhang,D.Y. (1996) Detection of hepatitis C virus RNA using ligation-dependent polymerase chain reaction in formalin-fixed, paraffin-embedded liver tissues *Am. J. Pathol.*, 149, 1485-1491.

Pellegrini , E., Golisano, O., Paterna P., Bondanza, S., Lambiase, A., Bonini, S., Rama. P., De Luca, M. (1999) Location and clonal analysis of stem cells and their differentiated progeny in the human ocular surface *J.Cell.Biol.*145;769-782

Pellegrini G, Dellambra E, Golisano O, Martinelli E, Fantozzi I, Bondanza S, Ponzin D, McKeon F, De Luca M: (2001)p63 identifies keratinocyte stem cells. Proc Natl Acad Sci USA 2001, 98:3156-3161

Pellegrini, G., Dallambra, E., Golisano, O., Martinelli E., Fantozzi, I., Bondanza, S., Ponzin, D., McKeon, F., De Luca, M. (2001) p63 identifies keratinocyte stem cells *PNAS*.98 (6); 3156-3161

Pellegrini, G., Traverso, C.E., Franzi, A.T., Zingirian, M., Cancedda, R., de Luca, M. (1997). Long-term restoration of damaged corneal surface with autologous cultivated corneal epithelium. Lancet 349, 990–993.

Phillips, J., Eberwine, J.H.(1996) Antisense RNA amplification: a linear amplification method for analyzing the mRNA population from single living cells. *Methods* 1996, 10:283-288

Potten, C. S., Owen, G. and Booth, D. (2002). Intestinal stem cells protect their genome by selective segregation of template DNA strands. *J. Cell Sci.* **115**; 2381-2388

Potten, C.S. (1974) The epidermal proliferative unit: The possible role of the central basal cell. *Cell Tissue Kinet.* 7: 77–88.

Potten, C.S. (eds) 1996, *Stem cells*, Academic Press, London.

Potten, C.S. and Catherine Booth, C. (2002) Keratinocyte Stem Cells: a Commentary 119(4) SKIN STEM CELLS 888-899

Potten, C.S., Hume, W.J., Reid, P., Cairns, J.(1978) The segregation of DNA in epithelial stem cells. Cell 15:899-906

Potten, C.S., Loeffler, M. (1990) Stem cells: attributes, cycles, spirals, uncertainties and pitfalls: lessons for and from the crypt. *Development* 110; 1001-1019

Potten, C.S., Morris, R. (1987) Epithelial stem cells in vivo *J.Cell Sci. supplement.* 10;45-62

Potten, C.S., Owen, G., Booth, D. (2002) Intestinal stem cells protect their genome by selective segregation of template DNA strands. J Cell Sci 115:2381-2388

Potten, C.S., Wichman, H.E., Dobek, K., Birch. J., Codd, T.M., Horroks L, Pedrik, M., Tickle, S. (1985) Cell kinetic studies in epidermis of mouse.III.The percent labelled mitosis technique. *Cell Tiss.Kin.*18:59-70.

Potten, C.S., Wichman, H.E., Loeffler, M.,Dobek,K.,Majpr,D. (1982) Evidence for discrete cell kinetic subpopulations in mouse epidermis based on mathematical analysis. 15;305-29.

Potten, C.S., Wichmann, H.E, Loefler, M., Dobek, K., Major, D.(1982) Evidence for discretecell kinetic subpopulations in mouse epidermis based on mathematical analysis. Cell Tiss Kinet 15:305-329

Puangsricharern, V., Tseng, S.C.G., (1995). Cytologic evidence of corneal diseases with limbal stem cell deficiency. Ophthalmology 102, 1476–1485.

Qian, X., Goderie, S.K., Shen,Q., Stern, J.H., Temple, S. (1998) Intrinsic programs of patterned cell lineages in isolated vertebrate CNS ventricular zone cells. Development. 125; 3143–3152.

Raemaekers, T., Ribbeck, K., Beaudouin, J., Annaert, W., Van Camp, M., Stockmans, I., Smets, N., Bouillon, R., Ellenberg, J., Carmeliet, G. (2003) NuSAP, a novel microtubule-associated protein involved in mitotic spindle organization. *J Cell Biol*. 162(6):1017-29.

Ramalho-Santos, M., Yoon, S., Matsuzaki, Y., Mulligan, R., Melton, D.A.(2002) Stemness": Transcriptional Profiling of Embryonic and Adult Stem Cells *Science*, 298 (5593) 597-600

Rambhatla, L., Bohn, S.A., Stadler, P.B. (2001) Cellular senescence: ex vivo p53-dependent asymmetric cell kinetics. J Biomed Biotech 2001;1:27-36

Raya, A.; Revert, F.; Navarro, S.; Saus, J. (1999) Characterization of a novel type of serine/threonine kinase that specifically phosphorylates the human Goodpasture antigen. *J. Biol. Chem.* 274: 12642-12649

Rea, S., Eisenhaber, F., O'Carroll, D., Strahl, B.D., Sun, Z.W., Schmid, M., Opravil, S., Mechtler, K., Ponting, C.P., Allis, C.D., Jenuwein, T.(2000) Regulation of chromatin structure by site-specific histone H3 methyltransferases. *Nature* 406:593-599.

Rea, S., Eisenhaber, F., O'Carroll, D., Strahl, B.D., Sun, Z.W., Schmid, M., Opravil, S., Mechtler, K., Ponting, C.P., Allis, C.D., Jenuwein, T. (2000) Regulation of chromatin structure by site-specific histone H3 methyltransferases. *Nature* 2000, 406:593-599.

Redner, R. L., Rush, E. A., Faas, S., Rudert, W. A. & Corey, S. J. (1996) The t(5;17) variant of acute promyelocytic leukemia expresses a nucleophosmin-retinoic acid receptor fusion. *Blood* 87; 882—886

Reuter, G., Spierer, P. (1992) Position effect variegation and chromatin proteins. *Bioessays* 14:605-612.

Rice, J.C. and Allis, D.C. (2001) Histone methylation versus histone acetylation: new insights into epigenetic regulation Current Opinion in Cell Biology 2001, 13:263–273

Robb, R., Kuwabara, T. (1962) Corneal wound healing. The movement of polymorphonuclear leukocytes into corneal wounds. *Archiv. Ophthal* 68:636-642

Rodrigues, M., Ben, Z.A., Krachmer, J., Schermer, A., Sun, T.-T., (1987). Suprabasal expression of a 64-kilodalton keratin (no. 3) in developing human corneal epithelium. Differentiation 34, 60–6

Roloff , T.C., Nuber, U.A.(2005) Chromatin, epigenetics and stem cells. Eur J Cell Biol. 84(2-3):123-35.

Ross, A. C. (1993) Cellular metabolism and activation of retinoids: Roles of cellular retinoid-binding proteins. *FASEB J.*;7:317–327.

Ross, L.L., Danehower, S.C., Proia, A.D., Sontag, M., Brown, D.M., Laurenza, A., Besterman, J.m. (1995) Coordinated activation of corneal wound response genes in vivo as observed by in situ Hybridization. *Exp. Eye. Res.*61:435-450

Roth, S.Y., Denu, J.M. and Allis, C.D. (2001) Histone acetyltransferases. *Annu. Rev. Biochem.*, 70, 81–120

Roth, S.Y., Denu, J.M. and Allis, C.D. (2001) Histone acetyltransferases. *Annu. Rev. Biochem.*, 70, 81–120

S. Etienne-Manneville and A. Hall. (2003) Cdc42 regulates GSK-3b and adenomatous polyposis coli to control cell polarity. *Nature* 2003. 421: 753-756.

S., Yuspa, S.H., and Lichti, U. (1993). Reconstitution of hair follicle development in vivo: determination of follicle formation, hair growth, and hair quality by dermal cells. J. Invest. Dermatol. 100; 229–236.

Saitoh, N., Goldberg, I.G., Wood, E.R. and Earnshaw, W.C. (1994). ScII: an abundant chromosome scaffold protein is a member of a family of putative ATPases with an unusual predicted tertiary structure. *J. Cell Biol.* 127:303–318

Saka, Y., T. Sutani, Y. Yamashita, S. Saitoh, M. Takeuchi, Y. Nakaseko, and M. Yanagida. (1994). Fission yeast cut3 and cut14, members of the ubiquitous protein family, are required for chromosome condensation and segregation in mitosis. *EMBO (Eur. Mol. Biol. Organ.) J.* 13:4938–4952.

Sakai, L.Y., Keene, D.R., Morris, N.P., Burgeson, R.E. (1986) Type VII collagen is a major structural component of anchoring fibrils. *J.Cell.Biol.* 103;1577

Sambrook ,J., Fritsch, E.F., Maniatis, T., editors. Molecular Cloning: A Laboratory Manual. New York: Cold Spring Harbor Laboratory, 1989; 2.73-2.76.

Sato, I., Murota, S.(1995) Paracrine function of endothelium-derived nitric oxide. Life Sci.;56(13):1079-87.

Sato, Y., Sagami, I., Shimizu, T. (2004) Identification of caveolin-1-interacting sites in neuronal nitric-oxide synthase. Molecular mechanism for inhibition of NO formation. J Biol Chem. 279(10):8827-36.

Savkur, R. S. & Olson, M. O.(1998) Preferential cleavage in pre-ribosomal RNA by protein B23 endoribonuclease. Nucleic Acids Res. 26, 4508—4515

Scheffer, C.G., Tseng, S.C. (1989) Concept and application of limbal stem cells. *Eye* 3:141-157.

Scheffer, C.G., Tseng, S.C., Li, D.Q. (1996) Comparison of protein kinase C subtype expression between normal and aniridic human ocular surfaces: implications for limbal stem cell dysfunction in aniridia. *Cornea* 15(2);168-178.

Schena M, Heller RA, Theriault TP, Konrad K, Lachenmeier E, Davis RW. (1998). Microarrays: biotechnology's discovery platform for functional genomics. *Trends Biotechnol.* 16(7):301-6.

Schermer a., Galvin S., Sun T.T. (1986) differentiation-related expression of a major 64K corneal keratin in vivo and in culture suggests limbal location of corneal epithelial stem cells. *JCB.* 103; 49-62.

Schlo¨tzer-Schrehardt, U. and Kruse, F.E. (2005) Identification and characterization of limbal stem cells Experimental Eye Research 81 ;247–264.

Schwab, I.R., Reyes, M., Isseroff, R.R., (2000). Successful transplantation of bioengineered tissue replacements in patients with ocular surface disease. Cornea 19, 421–426.

Segre, J.A., Nemhauser, J.L., Taylor, B.A., Nadeau, J.H., and Lander, E.S. (1995). Positional cloning of the nude locus: genetic, physical, and transcription maps of the region and mutations in the mouse and rat. Genomics *28*, 549–559.

Sennlaub, F., Courtois, Y., Goureau, O. Nitric Oxide Synthase–II Is Expressed in Severe Corneal Alkali Burns and Inhibits Neovascularization. *Investigative Ophthalmology and Visual Science.* 1999;40:2773-2779.

Sherley, J.L., Stadler, P.B., Johnson, D.R. (1995) Expression of the wildtype p53 antioncogene induces guanine nucleotide-dependent stem cell division kinetics. Proc Natl Acad Sci USA. 92:136-140.

Sherley, J.L., Stadler, P.B., Stadler, J.S. (1995) A quantitative method for the analysis of mammalian cell proliferation in culture in terms of dividing and non dividing cells. Cell Prolif. 28:137-144.

Siminovitch, L., McCulloch, E.A. & Till, J.E. (1963) The distribution of colony-forming cells among spleen colonies *J. Cell. Comp. Physiol.* 62, 327-336.

Sing, U.S., Kunar, M.T., Kao, Y.L., Baker, K.M. *(2001) Role of transglutaminase II in retinoic acid-induced activation of RhoA-associated kinase 2 EMBO Journal 20(10); 2413-2423.*

Sirivatanauksorn, Y., Drury, R., Crnogorac-jurc¡evic , T., Sirivatanauksorn, T., Lemoine, N. (1999) Laser-assisted microdissection: applications in molecular pathology *J. Pathol.* 189: 150–154.

Smith A. G. and Francis J. E. (1993) Genetic variation of iron-induced uroporphyria in mice. *Biochem. J.* 291, 29-35.

Smith, G.H. (2005) Label-retaining epithelial cells in mouse mammary gland divide asymmetrically and retain their template DNA strands *Development* 132, 681-687.

Song, P., Tonya, A., Abraham, Park, Y., Zivony, A.S., Harten, B, Edelhauser, H.F., Ward, S., Armstrong, C.A.and Ansel' J.C. (2001) The Expression of Functional LPS Receptor Proteins CD14 And Toll-Like Receptor 4 in Human Corneal Cells. *Investigative Ophthalmology and Visual Science.* 42;2867-2877.

Steuhl, K.-P., Thiel, H.J., (1987). Histochemical and morphological study of the regenerating corneal epithelium after limbus to limbus denudation. Graefes Arch. Clin. Exp. Ophthalmol. 225, 53–58.

Storer, J.B. (1966) Longevity and gross pathology and death in 22 inbred strains of mice. J Gerontol 21;404–409.

Strahl, B. D., and Allis, C. D. (2000) The language of covalent histone modifications *Nature* 403, 41–45.

Strano S, Rossi M, Fontemaggi G, Munarriz E, Soddu S, Sacchi A, Blandino G. (2001). From p63 to p53 across p73. *FEBS Lett* 16;490(3):163-70

Strunnikov ,A.V., Larionov ,V.L., Koshland ,D.(1993).SMC1: an essential yeast gene encoding a putative head-rod-tail protein is required for nuclear division and defines a new ubiquitous protein family. *J Cell Biol.*123:1635 - 1648.

Strunnikov, A. V., Larionov, V. L. and Koshland, D. (1993). SMC1: an essential yeast gene encoding a putative head-rod-tail protein is required for nuclear division and defines a new ubiquitous protein family. *J. Cell Biol.* 123,1635 -1648.

Strunnikov, A.V., Hogan, E. and Koshland, D.. (1995). *SMC2*, a *Saccharomyces cerevisiae* gene essential for chromosome segregation and condensation defines a subgroup within the SMC-family. *Genes Dev.* 9:587–599.

Strunnikov, A.V., Larionov, V.L. and Koshland, D. (1993). *SMC1*: an essential yeast gene encoding a putative head-rod-tail protein is required for nuclear division and defines a new ubiquitous protein family. *J. Cell Biol.* 123:1635– 1648.

Stursberg, S., Riwar, B. and Jessberger, R. (1999). Cloning and characterization of mammalian SMC1 and SMC3 genes and proteins, components of the DNA recombination complexes RC-1. *Gene* 228; 1 -12.

Su, L.K., Burrell, M. and Hill. D.E. (1995) APC binds to the novel protein EB1. *Cancer Res,* 1995. 55: 2972-2977.

Suarez-Quian CA, Goldstein SR, Pohida T. (1999) Laser capture microdissection of single cells from complex tissues. *BioTechniques*; 26:328–335.

Sun, L., Sun, T.T., Lavker, R.M. (2000). CLED: a calcium-linked protein associated with early epithelial differentiation. *Exp. Cell.Res.* 259:96-106.

Sun, T.-T., Eichner, R., Cooper, D., Schermer, A., Nelson, W.G., Weiss, R.A., (1984). Classification, expression, and possible mechanisms of evolution of mammalian epithelial keratins: a unifying model. In: reconstruction. Ophthalmologe 98, 818–831.

SundarRaj, N., Kinchinghton, Howard Wessel, Goldblatt, B., Hassel, J., Vergnes, J.P., Anderson, S. (1998) A Rho-associated protein kinase differentially distributed in limbal and corneal epithelia. *IOVS*.39(7):1266-1272.

Sutani, T., and Yanagida, M. (1997). DNA renaturation activity of the SMC complex implicated in chromosome condensation. *Nature.* 388:798–801.

Sutani, T., and Yanagida, M.. 1(997). DNA renaturation activity of the SMC complex implicated in chromosome condensation. *Nature.* 388:798–801.

Symons, M., Derry, J.M., Karlak, B., Jiang, S., Lemahieu, V., Mccormick, F., Francke, U., Abo, A. (1996) Wiskott-Aldrich syndrome protein, a novel effector for the GTPase CDC42Hs, is implicated in actin polymerization. *Cell* 84, 723-734

Tanudji, M., Shoemaker, J., L'Italien, L., Russell, L., Chin, G. and Schebye, X.M. (2004) Gene silencing of CENP-E by small interfering RNA in HeLa cells leads to missegregation of chromosomes after a mitotic delay *JOURNAL Mol. Biol. Cell* 15 (8); 3771-3781.

Thoft, R.A., Friend, J. (1983) The X-Y-Z- hypothesis of corneal epithelial maintenace.*IOVS*24;1442-1443.

Thoft, R.A., Friend, J., (1983). The x,y,z hypothesis of corneal epithelial maintenance. Invest. Ophthalmol. Vis. Sci. 24, 1442–1443.

Till, J.E., McCulloch, E.A. (1961) A direct measurement of the radiation sensitivity of normal mouse bone marrow cells. *Radiation Research* 14:213-22.

Tomic, M., Jiang, C.K. and Epstein, H.S. *(1990) Nuclear receptors for retinoic acid and thyroid hormone regulate transcription of keratin genes.* Cell Regul *1; 965-73*

Tomic-Canic, M., Day, D. , Samuels, H.H., Freedberg, I.M. and Blumenberg, M. (1996) Novel Regulation of Keratin Gene Expression by Thyroid Hormone and Retinoid Receptors. *JCB.* 271(3); 1416-1423

Tsai J.F., Sun T.T., Scheffer C.G., Tseng, S.C. (1990) Comparison of limbal and conjuctival autograft transplantation in corneal surface reconstruction in rabbits.*Ophthalmology.* 97(4);446-455.

Tseng SC, Farazdaghi M. (1998) Reversal of conjunctival transdifferentiation by topical retinoic acid. *Cornea*.7(4):273-9.

Tseng, S.C., Meller, D., Anderson, D.F., Touhami, A., Pires, R.T., Grueterich, M., Solomon, A., Espana, E., Sandoval, H., Ti, S.E., Goto, E. (2002) Ex vivo preservation and expansion of human limbal epithelial stem cells on amniotic membrane for treating corneal diseases with total limbal stem cell deficiency. Adv. Exp. Med. Biol. 506, 1323–1334.

Uzbekov, R., Timirbulatova, E., Watrin, E., Cubizolles, F., Ogereau, D., Gulak, P., Legagneux, V., Polyakov, V.J., Le Guellec, K. and Kireev, I. (2003) Nucleolar association of pEg7 and XCAP-E, two members of Xenopus laevis condensin complex in interphase cells Journal of Cell Science 116; 1667-1678.

Vaezi, A., Bauer, C., Vasioukhin, V., Fuchs, E. (2002) Actin cable dynamics and Rho/Rock orchestrate a polarized cytoskeletal architecture in the early steps of assembling a stratified epithelium. *Dev Cell.* 3; 367-81.

Van den Berghe, H. & Michaux, L. (1997).5q-, twenty-five years later: a synopsis. *Cancer Genet. Cytogenet.* 94; 1–7.

Van Gelder, R.N., von Zastrow, M.E., Yool, A., Dement, W.C., Barchas, J.D., Eberwine, J.H. (1990) Amplified RNA synthesized from limited quantities of heterogeneous cDNA. *Proc Natl Acad Sci U S A*, 87:1663-1667.

Velculescu, V.E., Zhang, L., Vogelstein, B. (1995) Serial analysis of gene clones. *Genomics* 1995; 29; 207–216.

Verploegen, S., Lammers, J.W., Koenderman, L., Coffer, P.J. (2000). Identification and characterization of CKLiK, a novel granulocyte Ca(++)/calmodulin-dependent kinase. *Blood*. 96(9):3215-23.

Waikel, R.L., Kawachi, Y., Waikel, P.A., Wang, X.J. & Roop, D.R. *(2001) Deregulated expression of c-Myc depletes epidermal stem cells.* Nature Genetics *28, 165 - 168 .*

Wakamatsu, Y., Maynard, T.M., Jones, S.U., Weston, J.A. (1999) NUMB localizes in the basal cortex of mitotic avian neuroepithelial cells and modulates neuronal differentiation by binding to NOTCH-1. Neuron; 23:71–81.

Wang, D.-Y., Hsueh, Y.-J., Yang, V.C., Chen, J.-K. (2003). Propagation and phenotypic preservation of rabbit limbal epithelial cells on amniotic membrane. Invest. Ophthalmol. Vis. Sci. 44, 4698–4704.

Wang, E., Miller, L.D., Ohnmacht, G.A., Liu, E.T., Marincola, F.M. (2000) High-fidelity mRNA amplification for gene profiling. Nature Biotechnol, 18: 457–459.

Wei, Y., Yu, L., Bowen, J., Gorovsky, M. A., and Allis, C. D. (1999) Phosphorylation of histone H3 is required for proper chromosome condensation and segregation *Cell* 97, 99–109.

Weinberg, W.C., Goodman, L.V., George, C., Morgan, D.L., Ledbetter, S., Yuspa, S.H., and Lichti, U. (1993). Reconstitution of hair follicle development in vivo: determination of follicle formation, hair growth, and hair quality by dermal cells. J. Invest. Dermatol. 100; 229–236.

Westbrook, C. A. Hsu, W.T., Chyna, B., Litvak, D., Raza, A., Horrigan, S.K. (2000) Cytogenetic and molecular diagnosis of chromosome 5 deletions in myelodysplasia. *Br. J. Haematol.* 110, 847—855.

Wigler, M.H. and Axel, R. (1976) Nucleosomes in metaphase chromosomes Nucleic Acids Research. 3(6) 1463-1471.

Wiley, L., SunderRaj, N., Sun, T. T., & Thoft, R. A.(1991). Regional heterogeneity in human corneal and limbalepithelia: An immunohistochemical evaluation. *Investigative Ophthalmology & Visual Science*, *32*, 594–602.

Wilfinger, W.W., Mackey, M., and Chomczynski, P. (1997) Effect of pH and ionic strength on the spectrophotometric assessment of nucleic acid purity. BioTechniques. 22; 474.

Wolffe, A.P. and Hayes, J.J. (1999) Chromatin disruption and modification. *Nucleic Acids Res.*, 27, 711–720.

Wolosin, J. M., Xiong, X., Shutte, M., Stegman, Z., Tieng, A. (2000) Stem cells and differentiation stages in the limbo-corneal epithelium.. *Progr in Ret. Eye Res* 19 (2) 223-255.

Wolosin, J.M., Wang, Y. (1995) Alpha-2,3 sialylation differentiate the limbal and corneal epithelial cell phenotypes. Invest. Ophthalmol. Vis. Sci. 36; 2277–2286.

Wright, N.A., Alison, M. (1984). The biology of epithelial cell population, vol 1p 536, Clarendon press oxford (in Potten Stem Cells)1997.pp5.

Wu, M.H., Yung, B.Y.*(2002) UV stimulation of nucleophosmin/B23 expression is an immediate-early gene response induced by damaged DNA. J Biol Chem. 277(50):48234-40.*

Wu, R., Zhu, G., Galvin, S., Xu, C., Haseba, T., Chaloin-Dufou,C., Dhouailly, D., Wei, Z. G., Lavker, R. M., Kao, W. Y., &Sun, T. T. (1994). Lineage specific and differentiation-dependentexpression of K12 keratin in rabbit corneal/limbal epithelialcells: cDNA cloning and Northern blot analysis. *Differentiation*,*55*, 137–144.

Yang A, Kaghad M, Wang Y, Gillett E, Fleming MD, Dotsch V, Andrews NC, Caput D, McKeon F. (1998) *p63*, a *p53* Homolog at 3q27–29, Encodes Multiple Products with Transactivating, Death-Inducing, and Dominant-Negative Activities. *Mol. Cell* 2 (3), 305-316.

Yang, A., Kaghad, M., Wang, Y. (1998) p63, a p53 homolog at 3q27-29, encodes multiple products with transactivating, death-inducing, and dominant-negative activities. Mol Cell. 2:305-316.

Yang, A., McKeon, F. (2000) P63 and P73: P53 mimics, menaces and more. Nat Rev Mol Cell Biol 2000;1:199-207.

Yen,T.J., Compton,D.A., Wise,D., Zinkowski,R.P., Brinkley,B.R., Earnshaw,W.C. and Cleveland,D.W. (1991) CENP-E, a novel human

centromere-associated protein required for progression from metaphase to anaphase *EMBO J.* 10 (5); 1245-1254.

Yen,T.J., Li,G., Schaar,B.T., Szilak,I. and Cleveland,D.W. (1992) CENP-E is a putative kinetochore motor that accumulates just before mitosisJOURNAL *Nature* 359 (6395); 536-539.

Yoneda-Kato , N. Look, A.T., Kirstein, M.N., Valentine, M.B., Raimondi, S.C., Cohen, K.J., Carroll, A.J., Morris, S.W. (1996) The t(3;5)(q25.1;q34) of myelodysplastic syndrome and acute myeloid leukemia produces a novel fusion gene, NPM-MLF1. *Oncogene* 12; 265—275.

Zhang, H. Shi, X., Paddon, H., Hampong, M., Dai, W., Pelech, S.(2004) B23/nucleophosmin serine 4 phosphorylation mediates mitotic functions of polo-like kinase 1. *J. Biol. Chem.* 279; 35726—35734.

Zhao, X., Das, A. V., Thoreson, W. B., James, J., Wattman, T. E., Rodriguez-Sierra, J., & Ahmed, I. (2002). Adult corneal limbal epithelium: A model for studying neural potential of non-neural stem cells/progenitors. *Developmental Biology*, *250*, 317–331.

Zhong, W., Feder, J.N., Jian, M.M., Jan, L.Y., Jan, Y.N. (1996) Asymmetric localization of a mammalian numb homolog during mouse cortical neurogenesis. Neuron.17:43–53.

Zhong, W., Jiang, M.M., Schonemann, M.D. (2000) Mouse numb is an essential gene involved in cortical neurogenesis. Proc Natl Acad Sci USA.97:6844–6849.

Zieske, J.D. (1994) Perpetuation of stem cells in the eye. *Eye.*8:163-69.

Zieske, J.D., Bukusoglu G., Yankauckas M.A. (1992) Characterization of a potential marker of corneal epithelial stem cells. *IOVS.* 33:143-52.

Zieske, J.D., Bukusoglu G., Yankauckas M.A. Wasson. (1992) A-enolase is resrticted to basal cells of stratified squamous epithelium *Dev. Biol.* 151:18-26.